

Equilibrium Adsorption of Light Alkanes and their Mixtures at High Pressure on 5A, 13X and S-115 Adsorbents

by

Hassan Bin Abdul Rehman

A Thesis Presented to the

FACULTY OF THE COLLEGE OF GRADUATE STUDIES

KING FAHD UNIVERSITY OF PETROLEUM & MINERALS

DHAHRAN, SAUDI ARABIA

In Partial Fulfillment of the
Requirements for the Degree of

MASTER OF SCIENCE

In

CHEMICAL ENGINEERING

June, 1988

INFORMATION TO USERS

This manuscript has been reproduced from the microfilm master. UMI films the text directly from the original or copy submitted. Thus, some thesis and dissertation copies are in typewriter face, while others may be from any type of computer printer.

The quality of this reproduction is dependent upon the quality of the copy submitted. Broken or indistinct print, colored or poor quality illustrations and photographs, print bleedthrough, substandard margins, and improper alignment can adversely affect reproduction.

In the unlikely event that the author did not send UMI a complete manuscript and there are missing pages, these will be noted. Also, if unauthorized copyright material had to be removed, a note will indicate the deletion.

Oversize materials (e.g., maps, drawings, charts) are reproduced by sectioning the original, beginning at the upper left-hand corner and continuing from left to right in equal sections with small overlaps. Each original is also photographed in one exposure and is included in reduced form at the back of the book.

Photographs included in the original manuscript have been reproduced xerographically in this copy. Higher quality 6" x 9" black and white photographic prints are available for any photographs or illustrations appearing in this copy for an additional charge. Contact UMI directly to order.

UMI

A Bell & Howell Information Company
300 North Zeeb Road, Ann Arbor MI 48106-1346 USA
313/761-4700 800/521-0600

**EQUILIBRIUM ADSORPTION OF LIGHT ALKANES
AND THEIR MIXTURES AT HIGH PRESSURE
ON 5A, 13X AND S-115 ADSORBENTS**

BY

HASSAN BIN ABDUL REHMAN

**A Thesis Presented to the
FACULTY OF THE COLLEGE OF GRADUATE STUDIES
KING FAHD UNIVERSITY OF PETROLEUM & MINERALS
DHAHRAN, SAUDI ARABIA**

**LIBRARY
KING FAHD UNIVERSITY OF PETROLEUM & MINERALS
Dhahran - 31261. SAUDI ARABIA**

**In Partial Fulfillment of the
Requirements for the Degree of**

**MASTER OF SCIENCE
In
CHEMICAL ENGINEERING**

JUNE 1988

UMI Number: 1381125

UMI Microform 1381125
Copyright 1997, by UMI Company. All rights reserved.

**This microform edition is protected against unauthorized
copying under Title 17, United States Code.**

UMI
300 North Zeeb Road
Ann Arbor, MI 48103

KING FAHD UNIVERSITY OF PETROLEUM & MINERALS

DHAHRAN, SAUDI ARABIA

This thesis, written by

HASSAN BIN ABDUL REHMAN

under the direction of his thesis committee, and approved by all the members, has been presented to and accepted by the Dean, College of Graduate Studies, in partial fulfillment of the requirements for the degree of

MASTER OF SCIENCE IN CHEMICAL ENGINEERING

Thesis Committee

Kevin F. Loughlin
Chairman (Dr. Kevin F. Loughlin)

[Signature]
Member (Dr. Mohammad A. Hasanain)

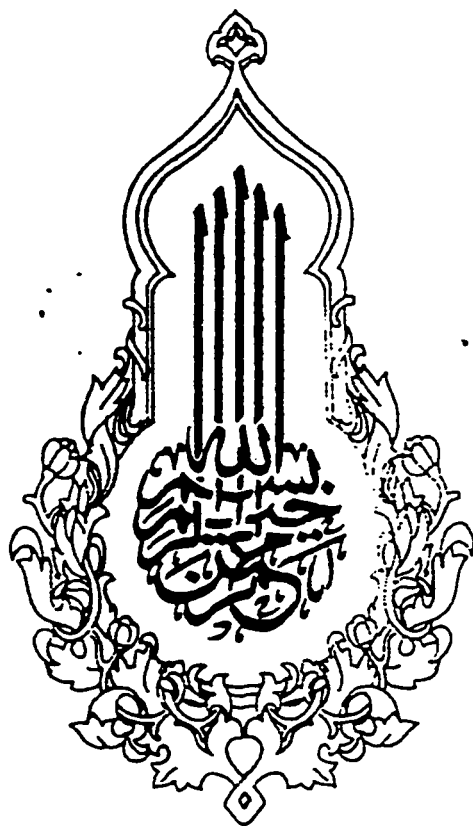
Mirza Manirul Hassan
Member (Dr. Mirza M. Hassan)

MA Saleh 14/6/88
Dr. Mohammad A. Al-Saleh
Department Chairman

Abdullah S. Al-Zakri
Dr. Abdullah S. Al-Zakri
Dean College of Graduate Studies

Date: June 14, 1988





Dedicated To My Parents

ACKNOWLEDGEMENT

I am most grateful to ALLAH the Almighty for providing me an opportunity and capability to complete this thesis. Acknowledgement is due to King Abdul Aziz City for Science & Tecnology (KACST) for the financial support for this research.

I am greatly indebted to my supervisor Dr. Revin F. Loughlin for his careful guidance throughout the completion of this research.

Appreciation and special thanks are also extended to the other members of committee, Dr. M. A. Hasanain and Dr. M. M. Hassan for their helpful comments when reviewing the thesis.

I would like to thank the King Fahd University of Petroleum & Minerals for supporting my program of study. The cooperation and help from the Chemical Engineering faculty, staff and technicians is greatly appreciated.

Finally, I would like to express my profound gratitude to my parents, brothers and sisters for all their love and affection, and for enduring the geographical distance from me during my graduate studies. Their sacrifices and foresightedness made this work possible.

Last, but not least, I would like to thank many of my other friends for their support in different phases of this investigation.

TABLE OF CONTENTS

	PAGE
Acknowledgement	iii
List of Tables	viii
List of Figures	xv
Nomenclature	xxiv
Thesis Abstract	xxvii
Arabic Abstract	xxix
CHAPTER	
<i>1 Introduction</i>	
1.1 Definition of Problem	1
1.2 Description of Adsorbents Used	3
1.3 Properties of Gases Used	7
1.4 Objectives of This Study	8
Literature Cited	21
<i>2 Literature Survey.</i>	
2.1 Introduction	25
2.2 Thermodynamic Aspects	26
2.2.1 Heat of Adsorption	26
2.2.2 The Differential Molar Entropy	27
2.2.3 Henry Constant and Saturation Concentration	28
2.2.4 Thermodynamic Consistency	31
2.3 The Simple Isotherm Models	32
2.3.1 The Langmuir Isotherm Model	32
2.3.2 The BET Isotherm Model	33

2.3.3 The Dubinin-Polanyi Theory	34
2.3.4 The LRC Isotherm Model	35
2.3.5 The Mathews and Weber Isotherm Model	36
2.3.6 The Generalised Isotherm Model	37
2.4 Statistical Isotherm Models	41
2.4.1 The Ruthven Isotherm Model	42
2.4.2 The Shirmer et al. Isotherm Model	44
2.5 Multicomponent Isotherm Models	46
2.5.1 Langmuir Binary Model	46
2.5.2 The LRC Multicomponent Model	47
2.5.3 Ruthven's Binary Model Isotherm	49
2.5.4 Binary Model of Shirmer et al's Isotherm	50
2.5.5 The Generalised Jaroniec Model	51
Literature Cited	53
3 Apparatus and Procedure	58
3.1 Choice of Experimental Methods	58
3.2 The Apparatus	59
3.3 Procedure	60
3.3.1 Determination of Dry Weight of Adsorbent	61
3.3.2 Calibration of Different Volumes	61
3.3.3 Pure Component Adsorption Isotherm Determination	62
3.3.4 Binary and Multicomponent Adsorption Isotherm Determination	63
Literature Cited	66

4	Pure and Multicomponent Equilibrium Results on Linde 5A zeolite Pellets	67
4.1	Non Ideality of the Gas Phase	68
4.2	Evaluation of Intrinsic Henry Constant	68
4.3	Determination of Saturation Concentration	70
4.4	Modelling of Pure Component Data	71
4.5	Fit of the Data Using Theoretical N_0 , β and Intrinsic K	72
4.6	Fit of the Data Using Optimized Parameters	73
4.6.1	Fit of LRC Model Using Optimized Parameters	73
4.6.2	Fit of Toth Model Using Optimized Parameters	73
4.6.3	Fit of Mathews and Weber Model Using Optimized Parameters	74
4.6.4	Fit of Jaroniec Model Using Optimized Parameters	74
4.6.5	Fit of Ruthven Model Using Optimized Parameters	75
4.7	Derivation of Multicomponent Ruthven Model	76
4.7.1	Fit of Multicomponent Ruthven Model	79
	Literature Cited	130
5	Pure and Multicomponent Equilibrium Results on Linde S-115 zeolite Pellets	131
5.1	Fit of LRC Model to Silicalite Pure Component Data	132
5.2	Fit of Toth Model to Silicalite Pure Component Data	134
5.3	Fit of Mathews and Weber Model to Silicalite Pure Component Data	135
5.4	Fit of Jaroniec Model to Silicalite Pure Component Data	136

5.5	Fit of Ruthven Model to Silicalite Pure Component Data	137
5.6	Derivation of Multicomponent Toth Model	138
5.7	Fit of Multicomponent Toth Model	139
6	Pure and Multicomponent Equilibrium Results on Linde 13X zeolite Pellets	232
6.1	Fit of LRC Model to 13X Pure Component Data	233
6.2	Fit of Toth Model to 13X Pure Component Data	234
6.3	Fit of Mathews and Werber Model to 13X Pure Component Data	235
6.4	Fit of Jaroniec Model to 13X Pure Component Data	236
6.5	Fit of Ruthven Model to 13X Pure Component Data	238
6.6	Fit of Multicomponent Ruthven Model	238
	Literature Cited	276
7	Conclusions and Recommendations	
7.1	Conclusions	277
7.2	Recommendations	282
	Literature Cited	284

APPENDICES

A	Soave-Redlich-Kwong Equation of States	I
B	Computer Programs for Pure and Multicomponent Data	IV
	VITA	XXXII

LIST OF TABLES

	PAGE
1.1 Properties of Linde 5A Zeolite Crystals.	10
1.2 Properties of Linde 13X Zeolite Crystals.	11
1.3 Properties of Linde S-115 Silicalite Crystals.	12
1.4 Commercial Forms of Linde 5A, 13X and Linde S-115 Adsorbents.	13
1.5 Properties of First Four n-Alkanes.	14
2.1 Presentation of different isotherms in Langmuir's form given by Equation (2.20)	38
4.1 Intrinsic Henry Constant (K'), Pre-Exponential Factor (K_0) and Heat of Adsorption ($-\Delta U_0$) for Linde 5A Pellets.	81
4.2 Theoretical Saturation Concentration (N_0), Molecular Volume β and Intrinsic Equilibrium Constant ($K=K'/N_0$) for Linde 5A Pellets.	82
4.3 Optimised Parameters (K , n and m) of Methane for Different Models with Theoretical (N_0) for Linde 5A Pellets.	83
4.4 Optimised Parameters (K , n and m) of LRC Model for Linde 5A Pellets.	84
4.5 Optimised Parameters (N_0 , K & n) of Toth Model for Linde 5A Pellets.	85
4.6 Optimised Parameters (N_0 , K & n) of Mathews and Weber Model for Linde 5A Pellets.	86
4.7 Optimised Parameters (N_0 , K , m & n) of Jaroniec Model for Linde 5A Pellets.	87
4.8 Optimised Parameters (β & K') of Ruthven Model for Linde 5A Pellets.	88

4.9	Binary Adsorption of Methane and Ethane on Linde 5A Pellets at 300 °K and 50 PSIA Total Pressure.	89
4.10	Binary Adsorption of Methane and Propane on Linde 5A Pellets at 300 °K and 50 PSIA Total Pressure.	90
4.11	Binary Adsorption of Ethane and Propane on Linde 5A Pellets at 300 °K and 50 PSIA Total Pressure.	91
4.12	Ternary Adsorption of Methane-Ethane-Propane on Linde 5A Pellets at 300 °K and 50 PSIA Total Pressure (Mole Fraction).	92
4.13	Ternary Adsorption of Methane-Ethane-Propane on Linde 5A Pellets at 300 °K and 50 PSIA Total Pressure (Concentration).	93
4.14	Ternary Adsorption of Methane-Ethane-n-Butane on Linde 5A Pellets at 300 °K and 50 PSIA Total Pressure (Mole Fraction).	94
4.15	Ternary Adsorption of Methane-Ethane-n-Butane on Linde 5A Pellets at 300 °K and 50 PSIA Total Pressure (Concentration).	95
4.16	Quaternary Adsorption of Methane-Ethane-Propane-n-Butane on Linde 5A Pellets at 300 °K and 50 PSIA Total Pressure (Mole Fraction).	96
4.17	Quaternary Adsorption of Methane-Ethane-Propane-n-Butane on Linde 5A Pellets at 300 °K and 50 PSIA Total Pressure (Concentration).	97
5.1	Intrinsic Henry Constant K' , Theoretical Saturation Concentration (N_0), Pre-Exponential Factor (K_0) and Heat of Adsorption ($-\Delta U_0$) for Linde S-115 Pellets.	141
5.2	Optimised Parameters of LRC Model (Intrinsic K) for Linde S-115 Pellets.	142
5.3	Optimised Parameters of LRC Model (Theoretical N_0) for Linde S-115 Pellets.	143
5.4	Optimised Parameters (N_0 , K & n) of LRC Model for Linde S-115 Pellets.	144

5.5	Intrinsic Equilibrium Constant K , Theoretical Saturation Concentration (N_0), and Optimised n 's for LRC Model at Different Range of Concentrations for Linde S-115 Pellets.	145
5.6	Optimised Parameters of Toth Model (Intrinsic K & Theoretical N_0) for Linde S-115 Pellets.	146
5.7	Optimised Parameters of Toth Model (Intrinsic K) for Linde S-115 Pellets.	147
5.8	Optimised Parameters of Toth Model (Theoretical N_0) for Linde S-115 Pellets.	148
5.9	Optimised Parameters (N_0 , K & n) of Toth Model for Linde S-115 Pellets.	149
5.10	Intrinsic Equilibrium Constant K , Theoretical Saturation Concentration (N_0), and Optimised n 's for Toth Model at Different Range of Concentrations for Linde S-115 Pellets.	150
5.11	Optimised Parameters of Mathews and Weber Model (Intrinsic K) for Linde S-115 Pellets.	151
5.12	Optimised Parameters (n_0 , K & n) of Mathews & Weber Model for Linde S-115 Pellets.	152
5.13	Intrinsic Equilibrium Constant K , Theoretical Saturation Concentration (N_0), and Optimised n 's for Mathews and Weber Model at Different Range of Concentrations for Linde S-115 Pellets.	153
5.14	Optimised Parameters of Jaroniec Model (Intrinsic K & Theoretical N_0) for Linde S-115 Pellets.	154
5.15	Optimised Parameters of Jaroniec Model (Intrinsic K) for Linde S-115 Pellets.	155
5.16	Optimised Parameters of Jaroniec Model (Theoretical N_0) for Linde S-115 Pellets.	156
5.17	Optimised Parameters (N_0 , K & n) of Jaroniec Model for Linde S-115 Pellets.	157

5.18	Intrinsic Equilibrium Constant K, Theoretical Saturation Concentration N_0 and Optimised n's and m's for Jaroniec Model at Different Range of Concentrations for Linde S-115 Pellets.	158
5.19	Binary Adsorption of Methane and Ethane on Linde S-115 Pellets at 300 °K and 50 PSIA Total Pressure Using Optimised K.	159
5.20	Binary Adsorption of Methane and Ethane on Linde S-115 Pellets at 300 °K and 50 PSIA Total Pressure Using Intrinsic K.	159
5.21	Binary Adsorption of Methane and Ethane on Linde S-115 Pellets at 300 °K and 95 PSIA Total Pressure Using Optimised K.	160
5.22	Binary Adsorption of Methane and Ethane on Linde S-115 Pellets at 300 °K and 95 PSIA Total Pressure Using Intrinsic K.	160
5.23	Binary Adsorption of Methane and Propane on Linde S-115 Pellets at 300 °K and 50 PSIA Total Pressure Using Optimised K.	161
5.24	Binary Adsorption of Methane and Propane on Linde S-115 Pellets at 300 °K and 50 PSIA Total Pressure Using Intrinsic K.	161
5.25	Binary Adsorption of Methane and n-Butane on Linde S-115 Pellets at 300 °K and 50 PSIA Total Pressure Using Optimised K.	162
5.26	Binary Adsorption of Methane and n-Butane on Linde S-115 Pellets at 300 °K and 50 PSIA Total Pressure Using intrinsic K.	162
5.27	Binary Adsorption of Ethane and Propane on Linde S-115 Pellets at 300 °K and 50 PSIA Total Pressure Using Optimised K.	163
5.28	Binary Adsorption of Ethane and Propane on Linde S-115 Pellets at 300 °K and 50 PSIA Total Pressure Using Intrinsic K.	163
5.29	Ternary Adsorption of Methane-Ethane-Propane on Linde S-115 Pellets at 300 °K and 50 PSIA Total Pressure (Mole	

	Fraction).	164
5.30	Ternary Adsorption of Methane-Ethane-Propane on Linde S-115 Pellets at 300 °K and 50 PSIA Total Pressure (Concentration).	164
5.31	Ternary Adsorption of Methane-Ethane-n-Butane on Linde S-115 Pellets at 300 °K and 50 PSIA Total Pressure (Mole Fraction).	165
5.32	Ternary Adsorption of Methane-Ethane-n-Butane on Linde S-115 Pellets at 300 °K and 50 PSIA Total Pressure (Concentration).	165
5.33	Ternary Adsorption of Methane-Propane-n-Butane on Linde S-115 Pellets at 300 °K and 50 PSIA Total Pressure (Mole Fraction).	166
5.34	Ternary Adsorption of Methane-Propane-n-Butane on Linde S-115 Pellets at 300 °K and 50 PSIA Total Pressure (Concentration).	166
5.35	Quaternary Adsorption of Methane-Propane-n-Butane on Linde S-115 Pellets at 300 °K and 50 PSIA Total Pressure (Mole Fraction).	167
5.36	Quaternary Adsorption of Methane-Propane-n-Butane on Linde S-115 Pellets at 300 °K and 50 PSIA Total Pressure (Concentration).	167
6.1	Intrinsic Henry Constant K' , Theoretical Saturation Concentration (N_0), and Pre-exponential Factor (K_0) and Heat of Adsorption ($-\Delta U_0$) for Linde 13X Pellets.	240
6.2	Optimised Parameters of LRC Model (Intrinsic K & Theoretical N_0) for Linde 13X Pellets.	241
6.3	Optimised Parameters of LRC Model (Intrinsic K) for Linde 13X Pellets.	241
6.4	Optimised Parameters of LRC Model (Theoretical N_0) for Linde 13X Pellets.	242
6.5	Optimised Parameters (N_0 , K & n) of LRC Model for Linde 13X Pellets.	242

6.6	Optimised Parameters of Toth Model (Intrinsic K & Theoretical N_0) for Linde 13X Pellets.	243
6.7	Optimised Parameters of Toth Model (Intrinsic K) for Linde 13X Pellets.	243
6.8	Optimised Parameters of Toth Model (Theoretical N_0) for Linde 13X Pellets.	244
6.9	Optimised Parameters (N_0 , K & n) of Toth Model for Linde 13X Pellets.	244
6.10	Optimised Parameters of Mathews and Weber Model (Intrinsic K and Theoretical N_0) for Linde 13X Pellets.	245
6.11	Optimised Parameters of Mathews and Weber Model (Intrinsic K) for Linde 13X Pellets.	245
6.12	Optimised Parameters of Mathews and Weber Model (Theoretical N_0) for Linde 13X Pellets.	246
6.13	Optimised Parameters (N_0 , K & n) of Mathews and Weber Model for Linde 13X Pellets.	246
6.14	Optimised Parameters of Jaroniec Model (Intrinsic K & Theoretical N_0) for Linde 13X Pellets.	247
6.15	Optimised Parameters of Jaroniec Model (Intrinsic K) for Linde 13X Pellets.	247
6.16	Optimised Parameters of Jaroniec Model (Theoretical N_0) for Linde 13X Pellets.	248
6.17	Optimised Parameters (N_0 , K & n) of Jaroniec Model for Linde 13X Pellets.	248
6.18	Optimised Parameter K' (Theoretical β) of Ruthven Model for Linde 13X Pellets.	249
6.19	Optimised Parameters (β & K') of Ruthven Model for Linde 13X Pellets.	249

6.20	Binary Adsorption of Methane and Ethane on Linde 13X Pellets at 300 °K and 50 PSIA Total Pressure.	250
6.21	Binary Adsorption of Methane and Ethane on Linde 13X Pellets at 300 °K and 95 PSIA Total Pressure.	250
6.22	Binary Adsorption of Methane and Propane on Linde 13X Pellets at 300 °K and 50 PSIA Total Pressure.	251
6.23	Binary Adsorption of Methane and Propane on Linde 13X Pellets at 300 °K and 95 PSIA Total Pressure.	251
6.24	Ternary Adsorption of Methane-Ethane-Propane on Linde 13X Pellets at 300 °K and 50 PSIA Total Pressure (Mole Fraction).	252
6.25	Ternary Adsorption of Methane-Ethane-Propane on Linde 13X Pellets at 300 °K and 50 PSIA Total Pressure (Concentration).	252
6.26	Ternary Adsorption of Methane-Ethane-n-Butane on Linde 13X Pellets at 300 °K and 50 PSIA Total Pressure (Mole Fraction).	253
6.27	Ternary Adsorption of Methane-Ethane-n-Butane on Linde 13X Pellets at 300 °K and 50 PSIA Total Pressure (Concentration).	253
6.28	Ternary Adsorption of Methane-Propane-n-Butane on Linde 13X Pellets at 300 °K and 50 PSIA Total Pressure (Mole Fraction).	254
6.29	Ternary Adsorption of Methane-Propane-n-Butane on Linde 13X Pellets at 300 °K and 50 PSIA Total Pressure (Concentration).	254
6.30	Quaternary Adsorption of Methane-Ethane-Propane-n-Butane on Linde 13X Pellets at 300 °K and 50 PSIA Total Pressure (Mole Fraction).	255
6.31	Quaternary Adsorption of Methane-Ethane-Propane-n-Butane on Linde 13X Pellets at 300 °K and 50 PSIA Total Pressure (Concentration).	255
7.1	Calculated Heats of Adsorption for Light Alkanes on Different Adsorbents	278

LIST OF FIGURES

		PAGE
1.1	Sodalite Cage.	15
1.2	Unit Cell of Type A Zeolite.	16
1.3	Unit Cell of Type X Zeolite.	17
1.4	Crystal Structure of Silicalite S-115 (a) Secondary Building Unit (b) Chain-Type Building Block.	18
1.5	Idealised Channel System in Silicalite S-115.	19
1.6	Schematic Diagram of Unit Cell of a Silicalite S-115 Structure Showing how the Framework is Built up from the D5R Units.	20
3.1	Schematic Diagram of High Pressure Multicomponent Equilibrium (HPME) Adsorption Apparatus.	65
4.1	Virial Isotherms of Methane on Linde 5A Pellets.	98
4.2	Virial Isotherms of Ethane on Linde 5A Pellets.	99
4.3	Virial Isotherms of Propane on Linde 5A Pellets.	100
4.4	Virial Isotherms of n-Butane on Linde 5A Pellets.	101
4.5	Van't Hoff Plot For Light Alkanes on Linde 5A Pellets.	102
4.6	Methane Isotherms on Linde 5A Pellets: Fit of LRC Model with Theoretical N_0 and Optimized K.	103
4.7	Methane Isotherms on Linde 5A Pellets: Fit of Toth Model with Theoretical N_0 and Optimized K.	104
4.8	Methane Isotherms on Linde 5A Pellets: Fit of Mathews and Weber Model with Theoretical N_0 and Optimized K.	105
4.9	Methane Isotherms on Linde 5A Pellets: Fit of Jaroniec Model with Theoretical N_0 and Optimized K.	106

4.10	Methane Isotherms on Linde 5A Pellets: Fit of LRC Model with Optimized N_o , and K	107
4.11	Ethane Isotherms on Linde 5A Pellets: Fit of LRC Model with Optimized N_o , and K.	108
4.12	Propane Isotherms on Linde 5A Pellets: Fit of LRC Model with Optimized N_o , and K.	109
4.13	n-Butane Isotherms on Linde 5A Pellets: Fit of LRC Model with Optimized N_o , and K.	110
4.14	Methane Isotherms on Linde 5A Pellets: Fit of Toth Model with Optimized N_o , and K.	111
4.15	Ethane Isotherms on Linde 5A Pellets: Fit of Toth Model with Optimized N_o , and K.	112
4.16	Propane Isotherms on Linde 5A Pellets: Fit of Toth Model with Optimized N_o , and K.	113
4.17	n-Butane Isotherms on Linde 5A Pellets: Fit of Toth Model with Optimized N_o , and K.	114
4.18	Methane Isotherms on Linde 5A Pellets: Fit of Mathews and Weber Model with Optimized N_o , and K.	115
4.19	Ethane Isotherms on Linde 5A Pellets: Fit of Mathews and Weber Model with Optimized N_o , and K.	116
4.20	Propane Isotherms on Linde 5A Pellets: Fit of Mathews and Weber Model with Optimized N_o , and K.	117
4.21	n-Butane Isotherms on Linde 5A Pellets: Fit of Mathews and Weber Model with Optimized N_o , and K.	118
4.22	Methane Isotherms on Linde 5A Pellets: Fit of Jaroniec Model with Optimized N_o , and K.	119
4.23	Ethane Isotherms on Linde 5A Pellets: Fit of Jaroniec Model with Optimized N_o , and K.	120

4.24	Propane Isotherms on Linde 5A Pellets: Fit of Jaroniec Model with Optimized N_0 , and K .	121
4.25	n-Butane Isotherms on Linde 5A Pellets: Fit of Jaroniec Model with Optimized N_0 , and K .	122
4.26	Methane Isotherms on Linde 5A Pellets: Fit of Ruthven Model with Optimized β and K' .	123
4.27	Ethane Isotherms on Linde 5A Pellets: Fit of Ruthven Model with Optimized β and K' .	124
4.28	Propane Isotherms on Linde 5A Pellets: Fit of Ruthven Model with Optimized β and K' .	125
4.29	n-Butane Isotherms on Linde 5A Pellets: Fit of Ruthven Model with Optimized β and K' .	126
4.30	X-Y Plot of Methane-Ethane Binary on Linde 5A Pellets: Fit of Ruthven Model with Theoretical β and Intrinsic K' .	127
4.31	X-Y Plot of Methane-Propane Binary on Linde 5A Pellets: Fit of Ruthven Model with Theoretical β and Intrinsic K' .	128
4.32	X-Y Plot of Ethane-Propane Binary on Linde 5A Pellets: Fit of Ruthven Model with Theoretical β and Intrinsic K' .	129
5.1	Virial Isotherms of Methane on Linde S-115 Pellets.	168
5.2	Virial Isotherms of Ethane on Linde S-115 Pellets.	169
5.3	Virial Isotherms of Propane on Linde S-115 Pellets.	170
5.4	Virial Isotherms of n-Butane on Linde S-115 Pellets.	171
5.5	Van't Hoff Plot For Light Alkanes on Linde S-115 Pellets.	172
5.6	Methane Isotherms on Linde S-115 Pellets: Fit of LRC Model with Optimized N_0 and Intrinsic K .	173
5.7	Ethane Isotherms on Linde S-115 Pellets: Fit of LRC Model with Optimized N_0 and Intrinsic K .	174
5.8	Propane Isotherms on Linde S-115 Pellets: Fit of LRC	

	Model with Optimized N_0 and Intrinsic K.	175
5.9	n-Butane Isotherms on Linde S-115 Pellets: Fit of LRC Model with Optimized N_0 and Intrinsic K.	176
5.10	Methane Isotherms on Linde S-115 Pellets: Fit of LRC Model with Theoretical N_0 and Optimized K.	177
5.11	Ethane Isotherms on Linde S-115 Pellets: Fit of LRC Model with Theoretical N_0 and optimized K.	178
5.12	Propane Isotherms on Linde S-115 Pellets: Fit of LRC Model with Theoretical N_0 and optimized K.	179
5.13	n-Butane Isotherms on Linde S-115 Pellets: Fit of LRC Model with Theoretical N_0 and optimized K.	180
5.14	Methane Isotherms on Linde S-115 Pellets: Fit of LRC Model with Optimized N_0 and K.	181
5.15	Ethane Isotherms on Linde S-115 Pellets: Fit of LRC Model with Optimized N_0 and K.	182
5.16	Propane Isotherms on Linde S-115 Pellets: Fit of LRC Model with Optimized N_0 and K.	183
5.17	n-Butane Isotherms on Linde S-115 Pellets: Fit of LRC Model with Optimized N_0 and K.	184
5.18	Methane Isotherms on Linde S-115 Pellets: Fit of Toth Model with Theoretical N_0 and Intrinsic K.	185
5.19	Ethane Isotherms on Linde S-115 Pellets: Fit of Toth Model with Theoretical N_0 and Intrinsic K.	186
5.20	Propane Isotherms on Linde S-115 Pellets: Fit of Toth Model with Theoretical N_0 and Intrinsic K.	187
5.21	n-Butane Isotherms on Linde S-115 Pellets: Fit of Toth Model with Theoretical N_0 and Intrinsic K.	188

5.22	Methane Isotherms on Linde S-115 Pellets: Fit of Toth Model with Optimized N_0 and Intrinsic K.	189
5.23	Ethane Isotherms on Linde S-115 Pellets: Fit of Toth Model with Optimized N_0 and Intrinsic K.	190
5.24	Propane Isotherms on Linde S-115 Pellets: Fit of Toth Model with Optimized N_0 and Intrinsic K.	191
5.25	n-Butane Isotherms on Linde S-115 Pellets: Fit of Toth Model with Optimized N_0 and Intrinsic K.	192
5.26	Methane Isotherms on Linde S-115 Pellets: Fit of Toth Model with Theoretical N_0 and Optimized K.	193
5.27	Ethane Isotherms on Linde S-115 Pellets: Fit of Toth Model with Theoretical N_0 and optimized K.	194
5.28	Propane Isotherms on Linde S-115 Pellets: Fit of Toth Model with Theoretical N_0 and optimized K.	195
5.29	n-Butane Isotherms on Linde S-115 Pellets: Fit of Toth Model with Theoretical N_0 and optimized K.	196
5.30	Methane Isotherms on Linde S-115 Pellets: Fit of Toth Model with Optimized N_0 and K.	197
5.31	Ethane Isotherms on Linde S-115 Pellets: Fit of Toth Model with Optimized N_0 and K.	198
5.32	Propane Isotherms on Linde S-115 Pellets: Fit of Toth Model with Optimized N_0 and K.	199
5.33	n-Butane Isotherms on Linde S-115 Pellets: Fit of Toth Model with Optimized N_0 and K.	200
5.34	Methane Isotherms on Linde S-115 Pellets: Fit of Mathews and Weber Model with Optimized N_0 and Intrinsic K.	201
5.35	Ethane Isotherms on Linde S-115 Pellets: Fit of Mathews and Weber Model with Optimized N_0 and Intrinsic K.	202

5.36	Propane Isotherms on Linde S-115 Pellets: Fit of Mathews and Weber Model with Optimized N_0 and Intrinsic K.	203
5.37	n-Butane Isotherms on Linde S-115 Pellets: Fit of Mathews and Weber Model with Optimized N_0 and Intrinsic K.	204
5.38	Methane Isotherms on Linde S-115 Pellets: Fit of Mathews and Weber Model with Optimized N_0 and K.	205
5.39	Ethane Isotherms on Linde S-115 Pellets: Fit of Mathews and Weber Model with Optimized N_0 and K.	206
5.40	Propane Isotherms on Linde S-115 Pellets: Fit of Mathews and Weber Model with Optimized N_0 and K.	207
5.41	n-Butane Isotherms on Linde S-115 Pellets: Fit of Mathews and Weber Model with Optimized N_0 and K.	208
5.42	Methane Isotherms on Linde S-115 Pellets: Fit of Jaroniec Model with Theoretical N_0 and Intrinsic K.	209
5.43	Ethane Isotherms on Linde S-115 Pellets: Fit of Jaroniec Model with Theoretical N_0 and Intrinsic K.	210
5.44	Propane Isotherms on Linde S-115 Pellets: Fit of Jaroniec Model with Theoretical N_0 and Intrinsic K.	211
5.45	n-Butane Isotherms on Linde S-115 Pellets: Fit of Jaroniec Model with Theoretical N_0 and Intrinsic K.	212
5.46	Methane Isotherms on Linde S-115 Pellets: Fit of Jaroniec Model with Optimized N_0 and Intrinsic K.	213
5.47	Ethane Isotherms on Linde S-115 Pellets: Fit of Jaroniec Model with Optimized N_0 and Intrinsic K.	214
5.48	Propane Isotherms on Linde S-115 Pellets: Fit of Jaroniec Model with Optimized N_0 and Intrinsic K.	215
5.49	n-Butane Isotherms on Linde S-115 Pellets: Fit of Jaroniec Model with Optimized N_0 and Intrinsic K.	216

5.50	Methane Isotherms on Linde S-115 Pellets: Fit of Jaroniec Model with Theoretical N_0 and Optimized K.	217
5.51	Ethane Isotherms on Linde S-115 Pellets: Fit of Jaroniec Model with Theoretical N_0 and optimized K.	218
5.52	Propane Isotherms on Linde S-115 Pellets: Fit of Jaroniec Model with Theoretical N_0 and optimized K.	219
5.53	n-Butane Isotherms on Linde S-115 Pellets: Fit of Jaroniec Model with Theoretical N_0 and optimized K.	220
5.54	Methane Isotherms on Linde S-115 Pellets: Fit of Jaroniec Model with Optimized N_0 and K.	221
5.55	Ethane Isotherms on Linde S-115 Pellets: Fit of Jaroniec Model with Optimized N_0 and K.	222
5.56	Propane Isotherms on Linde S-115 Pellets: Fit of Jaroniec Model with Optimized N_0 and K.	223
5.57	n-Butane Isotherms on Linde S-115 Pellets: Fit of Jaroniec Model with Optimized N_0 and K.	224
5.58	X-Y Plot of Methane-Ethane Binary on Linde S-115 Pellets: Fit of Toth Model with Optimized N_0 and Intrinsic K at 50.00 PSIA.	225
5.59	X-Y Plot of Methane-Ethane Binary on Linde S-115 Pellets: Fit of Toth Model with Optimized N_0 and Intrinsic K at 95.00 PSIA.	226
5.60	X-Y Plot of Methane-Propane Binary on Linde S-115 Pellets: Fit of Toth Model with Optimized N_0 and Intrinsic K.	227
5.61	X-Y Plot of Methane-n-Butane Binary on Linde S-115 Pellets: Fit of Toth Model with Optimized N_0 and Intrinsic K.	228
5.62	X-Y Plot of Ethane-Propane Binary on Linde S-115 Pellets: Fit of Toth Model with Optimized N_0 and Intrinsic K.	229

5.63	X-Y Plot of Methane-Ethane Binary on Linde S-115 Pellets: Fit of Toth Model with Optimized N_0 and K.	230
5.64	X-Y Plot of Methane-Ethane Binary on Linde S-115 Pellets: Fit of Toth Model with Optimized N_0 and K.	231
6.1	Virial Isotherms of Methane on Linde 13X Pellets.	256
6.2	Virial Isotherms of Propane on Linde 13X Pellets.	257
6.3	Van't Hoff Plot For Light Alkanes on Linde 13X Pellets.	258
6.4	Methane Isotherms on Linde 13X Pellets: Fit of LRC Model with Theoretical N_0 and Optimized K.	259
6.5	Propane Isotherms on Linde 13X Pellets: Fit of LRC Model with Theoretical N_0 and Optimized K.	260
6.6	Propane Isotherms on Linde 13X Pellets: Fit of LRC Model with Optimized N_0 and K.	261
6.7	Methane Isotherms on Linde 13X Pellets: Fit of Toth Model with Theoretical N_0 and Optimized K.	262
6.8	Propane Isotherms on Linde 13X Pellets: Fit of Toth Model with Optimized N_0 and K.	263
6.9	Methane Isotherms on Linde S-115 Pellets: Fit of Mathews and Weber Model with Optimized N_0 and Intrinsic K.	264
6.10	Propane Isotherms on Linde 13X Pellets: Fit of Mathews and Weber Model with Optimized N_0 and K.	265
6.11	Methane Isotherms on Linde 13X Pellets: Fit of Jaroniec Model with Theoretical N_0 and Intrinsic K.	266
6.12	Propane Isotherms on Linde 13X Pellets: Fit of Jaroniec Model with Optimized N_0 and Intrinsic K.	267
6.13	Propane Isotherms on Linde 13X Pellets: Fit of Jaroniec Model with Optimized N_0 and K.	268

6.14	Propane Isotherms on 13X Pellets: Fit of Ruthven Model with Theoretical β and optimised Henry Constant K' .	269
6.15	Methane Isotherms on 13X Pellets: Fit of Ruthven Model with Optimized β and Henry Constant K' .	270
6.16	Propane Isotherms on 13X Pellets: Fit of Ruthven Model with Optimized β and Henry Constant K' .	271
6.17	X-Y Plot of Methane-Ethane Binary on Linde 13X Pellets: Fit of Ruthven Model with Optimized and Theoretical Henry Constant at 50 PSIA.	272
6.18	X-Y Plot of Methane-Ethane Binary on Linde 13X Pellets: Fit of Ruthven Model with Optimized and Theoretical Henry Constant at 95 PSIA.	273
6.19	X-Y Plot of Methane-Propane Binary on Linde 13X Pellets: Fit of Ruthven Model with Optimized and Theoretical Henry Constant at 50 PSIA.	274
6.20	X-Y Plot of Methane-Propane Binary on Linde 13X Pellets: Fit of Ruthven Model with Optimized and Theoretical Henry Constant at 95 PSIA.	275

NOMENCLATURE

- A : Zeolite family type
 \bar{A} : Analogous to Equilibrium K , Defined in Table 2.1
 $A_{1..4}$: Coefficients for LRC Model
 A_i : Coefficient for Barrer and Lee Equation
 b : Van der Waal's b
 C : Adsorbed phase concentration, (molecules/cavity or millimoles/gm pellet)
 $C_{1..4}$: Adsorbed phase concentration for 1..4 component (molecules/cavity or millimoles/gm pellet)
 C_{exp} : Experimental concentration
 C_o : Maximum attainable loading
 C_{pre} : Predicted concentration from theoretical model
 C_s : Maximum adsorbed phase concentration (molecules/cavity or millimoles/gm pellet)
 C_{si} : Maximum adsorbed phase concentration for component i (molecules/cavity or millimoles/gm pellet)
 E_i, E_k : Difference in energy between gas and sorbed phases
 f : Fugacity
 f_i : Fugacity for component i in a mixture
 K' : Henry constant (molecules/cavity/psia)
 K : Equilibrium constant (1/psia)
 $K'_{1..4}$: Henry constant for component 1..4 (molecules/cavity/psia)

K_{i1}	: Ratio of Equilibrium constants K_i and K_1
K_0	: Pre-exponential factor for Van't Hoff Relation
m	: Parameter power or maximum no molecules/cavity
n	: Parameter power or maximum no molecules/cavity
o	: maximum no molecules/cavity
p	: maximum no molecules/cavity
P	: Pressure, psia
$P_{1..4}$: Partial Pressure for component 1..4
P_c	: Critical Pressure, atm
P_0	: Standard state pressure
P_s	: Saturated Vapour Pressure
p^0	: Vapour Pressure, atm
q^0	: Heat of Adsorption
S_i, S_k	: Difference in entropy between gas and sorbed phases
R	: Universal gas constant
R	: Loading ratio
R_i	: Loading ratio for i^{th} component
T	: Temperature °K
T_B	: Boiling point °K
T_C	: Critical temperature °K
T_0	: Standard state temperature

$-\Delta U_o$: Heat of Adsorption

V_p : Pore volume ccm/gm

X_i : Mole fraction of species i in sorbed phase

X : Zeolite family type

Y_i : Mole fraction of species i in gas phase

Z_C : Critical compressibility

Greek Symbols

α : Cage type

β : Cage type

β : Molecular volume

$\beta_{1..4}$: Molecular volume for 1..4 component

γ : Activity coefficient

η : Adsorbed phase interactions

θ : Fractional coverage

ρ : Liquid density

v_B : Molar volume at the boiling point

v^* : Molar volume at the temperature T

ω : Interaction between adjacent molecules

ω : Acentric Factor

THESIS ABSTRACT

NAME OF STUDENT : HASSAN BIN ABDUL REHMAN

**TITLE OF STUDY : EQUILIBRIUM ADSORPTION OF LIGHT ALKANES
AND THIER MIXTURES AT HIGH PRESSURE
ON 5A, 13X, AND S-115 ADSORBENTS**

MAJOR FIELD : CHEMICAL ENGINEERING

DATE OF DEGREE : MAY 29, 1988

Pure and Multicomponet equilibrium data are reported for Linde 5A, 13X and S-115 adsorbents at pressures up to 250 psia and in the temperature range of 275 to 350°K. The intrinsic Henry constants are extracted from the data using virial isotherm techniques. The pure component data are modelled by four simple isotherm (LRC, Toth, Mathews and Weber, Jaroniec) and one statistical thermodynamic isotherm (Ruthven). The multicomponent form of Ruthven's isotherm is developed, and used to model 5A and 13X data. The multicomponent Toth model is used to model the S-115 data.

For the 5A pellets, the Toth model fits the data for all four components. The Ruthven model is best for methane, ethane and propane. The four simple isotherms (LRC, Toth, Mathews and Weber, Jaroniec) fit

the data for silicalite (S-115) but the Ruthven model is not applicable. Only isotherms of methane and propane have been measured for 13X zeolite. All models fit the methane data but the propane data is not well fitted by any models. Toth, Mathews and Weber and Ruthven model are the best.

Binary, ternary and quaternary data are reported at 300°K and at 50 and 95 psia. For the 5A and 13X pellets these data are analysed and modelled with the multicomponent form of Ruthven's model and the fit is reasonable with intrinsic Henry constant for 5A and with optimized Henry constant for 13X pellets. The multicomponent Toth model is used to fit the multicomponent data for the silicalite pellets and the fit is reasonable. Considering equilibrium only the separation of methane is greater in silicalite than in 13X or in 5A pellets.

MASTER OF SCIENCE DEGREE

KING FAHD UNIVERSITY OF PETROLEUM & MINERALS

DHAHRAN, SAUDI ARABIA.

June, 1988.

ملامعة الرسالة

اسم الطالب الكامل : حسن بن عبد الرحمن

منوان الدراسة : العز الاتزانى للألكانات الخفيفة ومخاليطها فى
فغوط عالية على كل من المازات 5A 13X S-115

التخصص : الهندسة الكىماوية

تارىخ الشهادة : ١٩٨٨ / ٥ / ٢٩ م

يعرفى هذا البحث معلومات اتزانىة فى حالة النقاوة والخلط لكل من 5A , 13X و S-115 فى فغوط تعل الى 250 psia ودرجات حرارة تتراوح بين 275-350 K. تم استخلاى قيم هنرى الحقيقىة باستخدام طرىقة المنحنىات المتساوىة فى درجة الحرارة . مثلت معطىات النقاوة بأربعة نماذج مبسطة وبنموذج احصائى شرمودىنامىكى . ومثلت معطىات الخلط بنموذج رذفن حىث مثلت 5A , 13X , فى حىن مثلت معطىات S-115 بنموذج توث .

تبىن أن نموذج توث يلائم معطىات كل المكونات الأربعة على الماز 5A . أما نموذج رذفن فهو الافضل لكل من المىشان , الايشان والبروبان . وأما النموذج الرباعى فقد لائم معطىات S-115 ولم يكن نموذج رذفن كذلك . بالنسبة للماز 13X فقد أخذت منحنىات المىشان والبروبان فقط . كل النماذج لائم المىشان . أما البروبان فلم يعثل جيدا بأي نموذج . أحسن النماذج هى نماذج توث , رذفن , ماشيو ووبر .

يعطى هذا البحث معلومات عن المكونات الشائفة والثلاشىة والرباعىة فى درجة 300k وغط من 95psia 50 بالنسبة للمازات 5A , 13X حطت النتاىج ومثلت باستخدام نموذج رذفن وتم اىجاد قىمة ثابت هنرى الحقيقى والافضل . فى حىن استخدم نموذج توث لتمشىل ماز السلىكسات وكان ملائما .

ان فعل المىشان أكبر فى السلىكسات عنه فى 13X وفى 5A .

درجة الماجستير فى العلوم

جامعة الملك فهد للبترول والمعادن
الطهران - المملكة العربىة السعودىة

يونىو ١٩٨٨

CHAPTER 1

INTRODUCTION

1.1: DEFINITION OF THE PROBLEM

Natural gas is fractionated to produce a methane rich stream and natural gas liquids (C_2, C_3, C_4 etc..). Since the boiling point of methane is very low this requires very low temperatures in order to separate the methane from the natural gas. To reach these low temperatures expensive refrigeration units are required and even still the methane produced is only about 92% pure. If 90% of the methane can be removed by other means the refrigeration units required for separation will be substantially reduced, and hence the cost of production will decrease.

Pressure swing adsorption (PSA), which is also known as heatless adsorption or adiabatic adsorption process, is a cyclic process used for separation of gas mixtures into two different main streams. The PSA cycle operates between two pressures, adsorbing at higher pressure and desorbing at the lower pressure, on the same equilibrium isotherm, with a minimal change in temperature resulting from the heat of adsorption.

If a pressure swing adsorption (PSA) unit is installed before the fractionator such that 90% of the methane from the natural gas stream can be recovered at atmospheric temperatures, the size of gas stream is reduced by 50% and consequently the size of the fractionation and refrigeration units will be reduced. The energy savings in refrigeration would be substantial; also it is possible to produce 99% pure methane which is difficult to reach at present.

To successfully separate methane from other hydrocarbons by PSA in large quantities, high pressures such as 100 to 200 psia may be required. Knowledge of the equilibrium and dynamic processes occurring at these high pressures are also required.

Equilibrium adsorption of C_1 to C_4 hydrocarbons on 5A and 13X zeolites are well documented (2,13,15,18,21,32) but are mostly limited to atmospheric pressure. Isotherms are of Langmuir shape and may be modelled using the Toth model (30), the Loading Ratio Correlation (LRC) model (31), Langmuir-Freundlich model (27), Ruthven's or Schirmer et al's statistical isotherm models (19,26), virial isotherm of Barrer and Lee(1), the vacancy solution theory of Suwanayuen and Danner (28), or using the Dubinin-Polyani potential theory of Cook and Basmadjian (5). Papers by Zuech et al. (32) and Suwanayuen and Danner (28) contain high pressure equilibrium adsorption data for methane, nitrogen and carbon dioxide, but for other hydrocarbons and their mixtures data at high pressures are scarce to non-existent.

Binary models for the Ruthven isotherm (25), Schirmer et al. (14), vacancy solution theory (29), ideal adsorbed solution theory (17) and the potential theory (12) have appeared and been successfully applied at atmospheric pressure. Only Ruthven's and the potential theory appear to have been applied to high pressures successfully (12,17). It is desirable to measure pure, binary and multicomponent adsorption isotherms at high pressures and test the various models. The appropriate model needs then to be incorporated into the design of a demethanizer for the PSA unit.

1.2: DESCRIPTION OF ADSORBENTS USED :

Three adsorbents are used in this work namely Linde 5A, Linde S-115 and Linde 13X in pelleted form. The 5A and 13X zeolites are synthetically produced crystalline metal alumino-silicates having a basic formula of $M_{2/n}O \cdot Al_2O_3 \cdot xSiO_2 \cdot yH_2O$, where M is an n valence cation and x and y are stoichiometric constants. The zeolites can be activated for adsorption by removing the water of hydration. Because little or no change in structure occurs during this dehydration, unusually high porous adsorbents are formed that have strong affinity for water and certain other gases and liquids.

In contrast to other adsorbents, pores of any particular type of zeolite are precisely uniform in size and of molecular dimensions.

Depending on the size of these pores, molecules may be readily adsorbed, slowly adsorbed or completely excluded. This sieve-like selectivity, based on molecule size, plus a selective preference for polar or polarizable molecules and a high capacity over a wide range of operating conditions, give zeolites a high level of adsorption efficiency and have made possible the development of large-scale separation processes.

The fundamental building-block of the zeolite crystal structure is a tetrahedron of four oxygen anions surrounding smaller silicon (SiO_4) or aluminum (AlO_4) cations. Sodium ions or other cations serve to make up the positive charge deficit in the alumina tetrahedra; these cations are quite mobile and may usually be exchanged, to varying degrees by other cations. Each of the four oxygen anions is shared, in turn, with another silica or alumina tetrahedron to extend the crystal lattice in three dimensions.

Zeolites are distinguished on the basis of chemical composition, structure and their physical and chemical properties. The crystal structure of 5A and 13X zeolites can be better described in terms of somewhat larger 'Secondary building units', the sodalite unit which is shown diagrammatically in Figure 1.1. This consists of a truncated octahedron with eight hexagonal and six square faces. Each edge represents an oxygen ion located at or near the center of the line, while the small silicon or aluminium ions are located at the corners. The interior of the

sodalite unit, called the β cage, has an interior diameter of 6.6 Å with free volume of 150 Å³. The six-membered oxygen rings, which make up the hexagonal faces, have a large enough free diameter (≈ 2.2 Å) to admit very small molecules such as water and ammonia but larger molecules cannot penetrate the sodalite cage.

The structures of 5A and 13X zeolites are assembled by combining these sodalite units in different arrangements. In 5A zeolite, the sodalite cages are joined at the square faces, called the double 4 ring (D4R) connection, to form an open symmetrical cubic structure as in Figure 1.2. Eight sodalite cages enclose a cavity called the α cage, of 11.4 Å diameter, and of volume 776 Å³, in which adsorption of hydrocarbons occur. The cavities are connected by octagonal windows of free apertures of 4.2 Å. These apertures contain cations which restrict the size of molecules that can penetrate into the zeolite. The properties of the 5A zeolite are presented in Table 1.1. The elasticity and kinetic energy of incoming molecules allows easy passage of molecules which are slightly larger than the free diameter of the aperture e.g. n-butane, which has a kinetic diameter of 4.3 Å.

The 13X zeolite is formed when the sodalite cages are joined by hexagonal faces forming double 6-ring (D6R) bonds, to form one of the most open structures in zeolites, shown diagrammatically in Figure 1.3. The 13X zeolite used for this study is the sodium cationic form of the

X type whose properties are presented in Table 1.2. The 13X zeolite can adsorb much larger molecules than the 5A zeolite (3).

S-115 silicalite is a new, crystalline, siliceous material. S-115 does not have ion-exchange properties similar to aluminosilicate zeolites because its structure is composed entirely of silica. S-115 silicalite is a hydrophobic, organophilic material.

The structure of S-115, shown diagrammatically in Figures 1.4 to 1.6, is a new topological type of tetrahedral framework, which contains a large fraction of five-membered rings of silicon-oxygen tetrahedra. Its channel system is composed of near-circular zig-zag channels of free cross-section 5.4 \AA^2 , cross-linked by elliptical straight channels with a free cross-section of $5.75 \times 5.15 \text{ \AA}^2$. Both channels are defined by ten-membered rings.

At ambient temperature S-115 will adsorb molecules as large as benzene (kinetic diameter 5.85 \AA), but rejects molecules larger than 6 \AA (e.g., neopentane 6.2 \AA). In contrast to the extremely high preference of aluminosilicate zeolite surfaces for water and other polar molecules, S-115 has a very low selectivity for the adsorption of water, and a very high preference for the adsorption of organic molecules smaller than its limiting pore size. S-115 silicalite is stable in air to over $1,000^\circ\text{C}$ and only slowly converts to an amorphous glass at $1,300^\circ\text{C}$. The properties of S-115 silicalite are given in Table 1.3. (7).

After dehydration, the zeolite is a crystalline solid permeated by micropores. These micropore volume depend on the framework of zeolite, and for 5A the pore volume is 0.268 cc/gm, for 13X it is 0.296 cc/gm and for silicalite it is 0.19 cc/gm. The properties of the commercial forms of Linde 5A, S-115, and 13X adsorbents are given in Table 1.4.

1.3: PROPERTIES OF GASES USED :

The thermodynamic properties of methane, ethane, propane and n-butane are given in the texts by Maxwell(16) and Gallant(8). The important physical properties as relevant for this thesis are tabulated in Table 1.5.

One property that should be noted is the saturation pressure at room temperature of 25°C. This varies from 2.48 bar for n-butane, 10 bar for propane, to 43.4 bar for ethane. For methane the gas is supercritical at room temperature. For the studies at higher pressure the temperature should be raised to achieve higher pressures with propane and n-butane.

The adsorbed substance (in the form of a liquid) is in the adsorption-force field in a highly compressed state; hence the temperature dependency of molar volume of a substance in the adsorbed state may be expressed, in the interval from normal boiling point to the critical point, by a linear relationship given by (6)

$$v^* = v_B + \left\{ \frac{T - T_B}{T_C - T_B} \right\} \times (b - v_B) \quad (1.1)$$

where v^* is molar volume at temperature T

v_B is molar volume at boiling point T_B

T_C is the critical temperature and

b is the van der Waals constant.

For temperature above the critical Dubinin assume that the effective molar volume becomes independent of temperature (6). However Ruthven and coworkers have used Equation 1.1 above the critical temperature (24).

1.4: OBJECTIVES OF THIS STUDY.

The objectives of this study is to construct and measure high pressure pure, binary and multicomponent equilibrium adsorption data for the selective adsorption of the simulated natural gas constituents on three typical zeolite adsorbents (5A, 13X & S-115). Such data is not available in the literature for high pressures.

The experimental data will be modelled with existing models, for the high pressure pure and binary equilibrium adsorption. A further

objective is to develop a model for the ternary and quaternary equilibrium adsorption. The results can be used to design a PSA unit.

Table 1.1 Properties of Linde 5A Zeolite Crystals.

Chemical Composition.

Typical unit cell contents : $\text{Ca}_6(\text{AlO}_2)_{12}(\text{SiO}_2)_{12} \cdot 30\text{H}_2\text{O}$

Variations, Si/Al ratio : 0.7 to 1.2

Crystallographic Data.

Symmetry : Cubic

Dehydrated density : 1.57 gm/cc

Unit cell volume : 1843 \AA^3 , pseudocell

Unit cell constants : $a = 12.26 \text{ \AA}$, pseudocell
 $a = 24.52 \text{ \AA}$, truecell

Pore Volume : 776 \AA^3 for α cage (puc)
 930 \AA^3 for $(\alpha + \beta)$ cage (puc)
 : 0.268 cc/gm

Structural Properties.

Cage type : One α cage, one β cage(puc)

Framework : Cubic array of β cages
 linked by D4R units

Channel system : Three dimensional

Cavity diameter : 11.4 \AA α cage, 6.6 \AA β cage

No. of unit cells/gram : 3.64×10^{20} cells/gm

Framework density : 1.27 gm/cc

Free aperture : 4.2 \AA

Kinetic diameter : 4.9 \AA

Effect of dehydration : Stable and reversible
 up to 800°C

puc = per unit cell

Table 1.2 Properties of Linde 13X Zeolite Crystals:

11

Chemical Composition.

Typical unit cell contents : $\text{Na}_{86}(\text{AlO}_2)_{86}(\text{SiO}_2)_{106} \cdot 26\text{H}_2\text{O}$

Variations, Si/Al ratio : 1.0 to 1.5

Crystallographic Data.

Symmetry : Cubic

Dehydrated density : 1.43 gm/cc

Unit cell volume : 15,362 - 15,670 \AA^3 ,pseudocell

Unit cell constants : $a = 24.86 - 25.02 \text{ \AA}$,pseudocell

Pore Volume : 6576 \AA^3 (puc) (for large voids)

: 7832 \AA^3 (puc) (for total voids)

: 0.296 cc/gm

Structural Properties.

Cage type : One β ,26 hedron(11) (puc)

Framework : Truncated octahedra, β cages,
linked by D6R units

Channel system : Three dimensional

Cavity diameter : 13.0 \AA α cage, 6.6 \AA β cage

No of cavities puc: 8

No. of unit cells/gram : 0.45×10^{20} cells/gm

Framework density : 1.31 gm/cc

Free aperture : 7.4 \AA

Kinetic diameter : 8.1 \AA

Effect of dehydration : Stable and reversible
up to 700°C

puc = per unit cell

Table 1.3 Properties of S-115 Zeolite Crystals.

Chemical Composition.

Typical unit cell contents : > 99% (SiO₂)

Crystallographic Data.

Symmetry : Apparently orthorhombic

Dehydrated density : 1.76 gm/cc

Unit cell volume : (*) A°³, pseudocell

Unit cell constants : a = 20.06 A°
b = 19.80 A°
c = 13.36 A°

Pore Volume : (*) A°³ (puc)

: 0.190 cc/gm

Structural Properties.

Cage type : Chains

Framework : Topological type of tetrahedral channels linked by D5R units.

Channel system : Three dimensional zig-zag & straight

Free aperture : Circular 5.4 A°
Elliptical 5.75 x 5.15 A°

Kinetic diameter : 6.0 A°

Effect of dehydration : Stable and reversible in air up to 1000°C

puc = per unit cell

(*) not available

Table 1.4 Commercial Forms of 5A, 13X and S-115 Zeolites.

13

	Linde 5A	Linde 13X	Linde S-115
Micropore Size A°	5.0	10.0	5.4
Macropore Size A°	10,000	(*)	(*)
Particle Size 1/16" pellet 1/8" pellet	.0575 - .0775"	.0575 - .0775"	.0575 - .0775"
Bulk Density (lbm/ft ³)	45.0	38.0	(*)
Pellet Density (lbm/ft ³)	70.0	(*)	(*)
Crush Strength (lb)	5.8	12.0	(*)
Water capacity (wt%)	21.5	28.5	(*)
Binder (wt%)	20.0	20.0	20.0

(*) not available

Table 1.5 Properties of First Four n-Alkanes.

Property	Methane	Ethane	Propane	n-Butane
Molecular Weight	16.04	30.07	44.09	58.12
Critical Temperature (K)	191.0	305.4	370.0	425.1
Critical Pressure (bar)	46.40	48.90	42.60	38.00
Critical Volume (cc/g-mole)	99.00	148.0	203.0	255.0
Boiling Point (K)	111.7	184.6	231.1	272.7
Critical Compressibility Z_c	0.288	0.285	0.281	0.274
Acentric Factor	0.008	0.098	0.152	0.193
Van der Waal's b :				
(cc/gmole)	42.78	63.80	84.45	122.6
A^0 ³ /molecule	71.04	105.9	140.2	203.6
Molar Volume at Boiling Point V_m :				
(cc/gmole)	37.31	53.69	76.02	96.07
A^0 ³ /molecule	61.95	89.16	126.2	159.5
Lennard Jones Potentials :				
σ (A^0)	3.758	4.443	5.118	4.687
$\frac{\epsilon_0}{\kappa}$ (K)	148.6	215.7	237.1	531.4
Vapor Pressure at 25 °C (bar)	supercritical	43.40	10.00	2.480

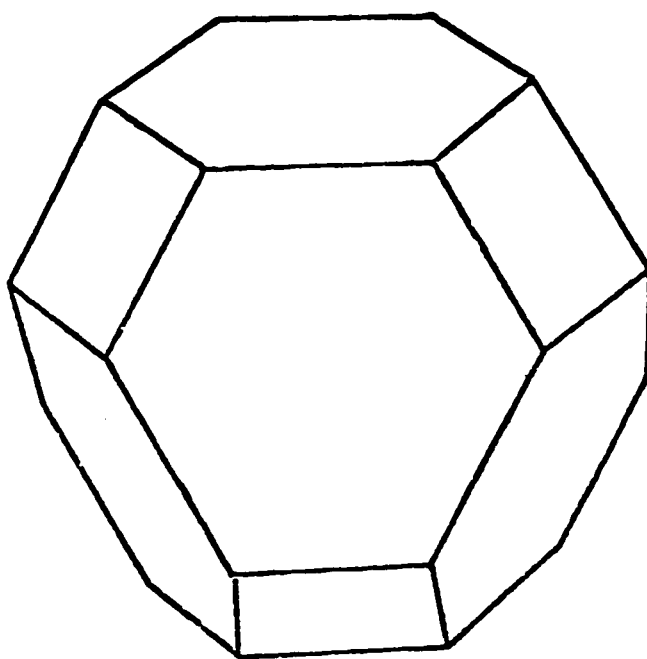


Figure 1.1. Sodalite Cage.

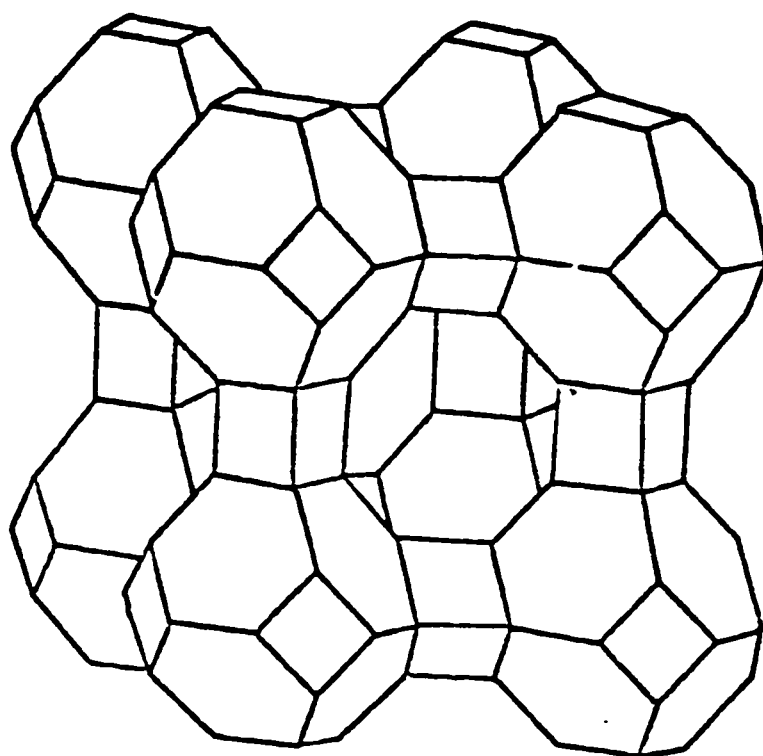


Figure 1.2. Unit cell of Type A Zeolite.

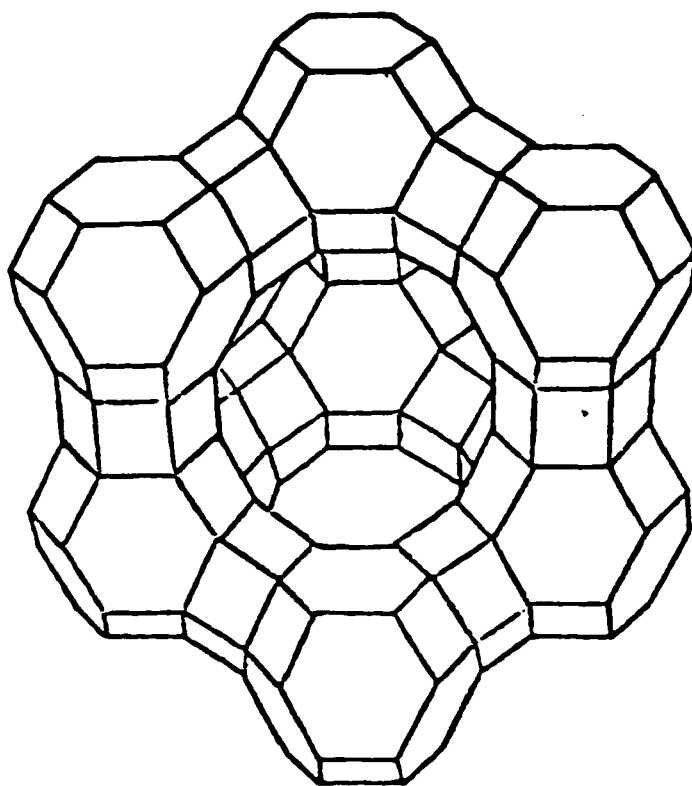


Figure 1.3. Unit cell of Type X Zeolite.

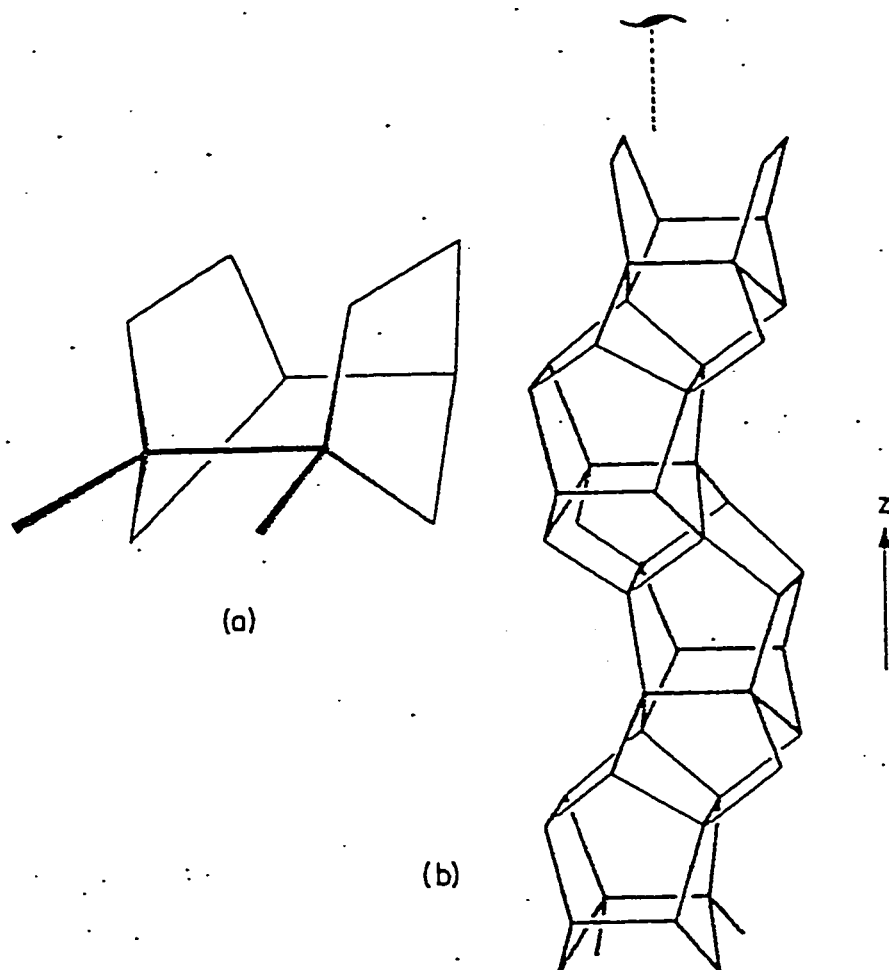


Figure 1.4. Crystal structure of Silicalite S-115 (a) Secondary building unit (b) Chain-type building block.

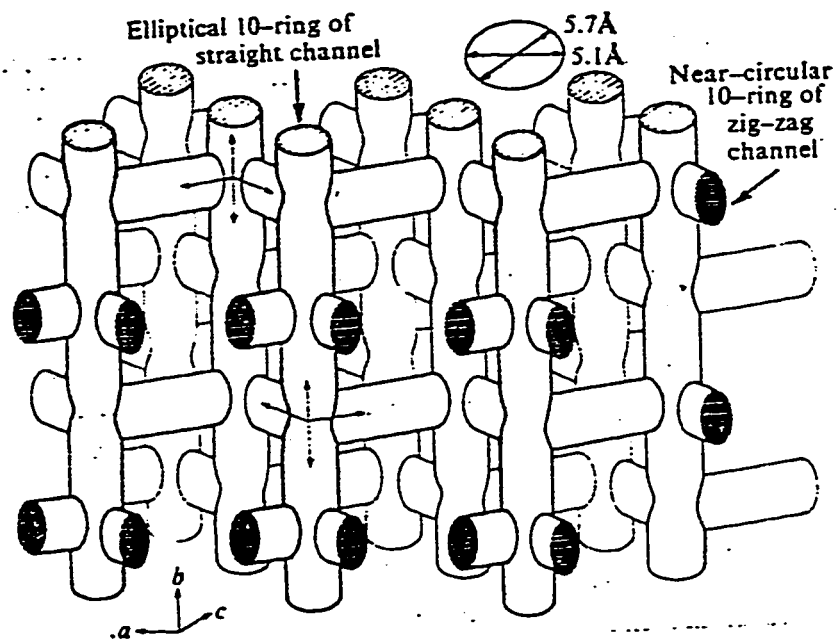


Figure 1.5. Idealised Channel System in Silicalite S-115.

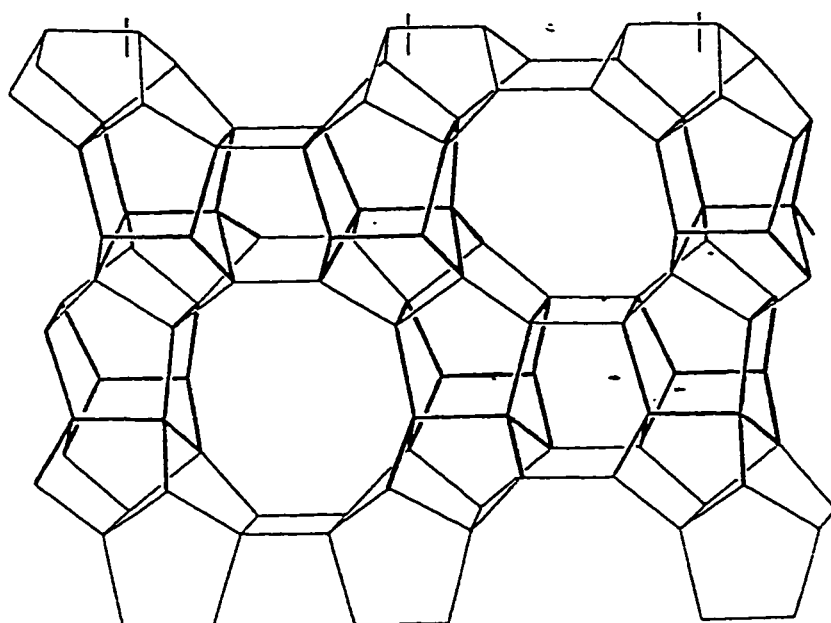


Figure 1.6. Schematic diagram of Unit Cell of a Silicalite S-115 structure showing how the framework is built up from the D5R units.

LITERATURE CITED

1. Barrer, R.M. and J.A. Lee, Surface Sci., 12, 354 (1968).
2. Barrer, R.M. and J.W. Sutherland, "Inclusion Complexes of Faujasite With Paraffins and Permanent Gases", Proc. Roy. Soc., Ser. A., 237, 439 (1956).
3. Breck, D.W., "Zeolite Molecular Sieves", Wiley-Interscience, New York, (1974).
4. Campbell, J.M., "Gas Conditioning and Processing", Published by Campbell Petroleum Series, Inc., Oklahoma, (1979).
5. Cook, W.H. and D. Basmadjian, Can. J. Chem. Eng., 42, 146 (1964).
6. Dubinin, M.M., Chem. Rev., 60, 235 (1960).
7. Flanigen, E.M., J.M. Bennett, R.W. Grose, J.P. Cohen, R.L. Patton, and R.M. Kirchner, "Silicalite, a New Hydrophobic Crystalline Silica Molecular Sieve", Nature, 271, 512-516, (1978).
8. Gallant, R.W., "Physical Properties of Hydrocarbons", Vol 1., Gulf Pub. Co., Houston, (1974).
9. Hasanain, M.A. and K.F. Loughlin, "Demethanization of Natural Gas by Pressure Swing Adsorption", KACST Project Report # 1, July 16th, (1985).
10. Jaroniec, M., "Physical Adsorption on Heterogeneous Solids", Fundamentals of Adsorption, Edited by Myers, A.L. and G. Belfort, 239-248, published by AIChE, New York, (1984).

11. Khaleeq, M., "Adsorption of Xylenes on Ba-X Zeolite Pellets", M.S. Thesis, KFUPM, (1984).
12. Lederman, P.D. and B. Williams, "The Adsorption of Nitrogen-Methane on Molecular Sieves", *AIChE J.*, 10, 30, (1964).
13. Linde Data Sheets for Hydrocarbons, Supplied by Linde Division of Union Carbide Corp., Tarrytown, N.Y.
14. Loughlin, K.F. and G.D. Roberts, "A New Binary Sorption Equilibrium Isotherm for Molecular Sieves Zeolite", *AIChE J.*, Accepted for Publication.
15. Loughlin, K.F. and D.M. Ruthven, "A Generalized Correlation of Equilibrium Data for the Sorption of Light Paraffins in Linde 5A Zeolite", *J. Coll. Interfacial Sci.*, 30(2), 331 (1972).
16. Maxwell, J.B., "Data Book on Hydrocarbons", Van Nostrand, N.Y., (1968).
17. Myers, A.L. and J.M. Prauznitz, "Thermodynamics of Mixed Gas Adsorption", *AIChE J.*, 11, 121 (1965).
18. Richards, E.R., H.J.F. Stroud, and N.G. Parsonage, "Thermodynamic Study of the Linde Sieve 5A + Ethane System", *J. Chem. Soc., Faraday Trans. 1*, 72, 1759 (1976).
19. Ruthven, D.M., "Simple Theoretical Adsorption Isotherm for Zeolites", *Nature Phys. Sci.*, 232, 70 (1970).
20. Ruthven, D.M. and R.I. Derrah, "Sorption in Davison 5A Molecular Sieves", *Can. J. Chem. Eng.*, 50, 743, (1972).

21. Ruthven, D.M. and K.F. Loughlin, "Sorption of Light Paraffins in Type A Zeolites: Analysis and Interpretation of Equilibrium Isotherms", J. Chem. Soc., Faraday Trans. 1, 68, 696 (1972).
22. Ruthven, D.M. and K.F. Loughlin, "The Sorption and Diffusion of n-Butane in Linde 5A Molecular Sieves", Chem. Eng. Sci., 26, 1145-1154, (1971).
23. Ruthven, D.M. and K.F. Loughlin, "Correlation and Interpretation of Zeolitic Diffusion Coefficients", Trans. Far. Soc., 67, 1661-1671 (1971).
24. Ruthven, D.M., K.F. Loughlin, and R.I. Derrah, "Sorption and Diffusion of Light Hydrocarbons and Other Simple Nonpolar Molecules in Type A Zeolites", Adv. Chem. Ser., 121, 330-344 (1973).
25. Ruthven, D.M., K.F. Loughlin, and K.A. Holborow, "Multicomponent Sorption Equilibrium in Molecular Sieves Zeolites", Chem. Eng. Sci., 28, 701-709 (1973).
26. Schirmer, W., K. Fiedler, and H. Stach, "Thermodynamics of Adsorption on Zeolites", A.C.S. Symposium Ser., 40, 305 (1977).
27. Sips, J.R., J. Chem. Phys., 16, 420 (1948); 18, 1024 (1950).
28. Suwanayuen, S. and R.P. Danner, "A Gas Adsorption Isotherm Based on Vacancy Solution Theory", AIChE J., 26, 68-76 (1980).
29. Suwanayuen, S. and R.P. Danner, "Vacancy Solution Theory of Adsorption from Gas Mixtures", AIChE J, 26, 76-82 (1980).

30. Toth, J., "Isotherm Equations for Monolayer Adsorption of Gases on Heterogeneous Solid Surfaces", Fundamentals of Adsorption, Edited by Myers, A.L. and G. Belfort, published by AIChE, New York, 657-665 (1984).
31. Yon, C.M. and P.H. Turnock, "Multicomponent Adsorption Equilibria on Molecular Sieves", AIChE J. Symp. Ser., 67(117), 75 (1971).
32. Zuech, J.L., A.L. Hines, and E.D. Sloan, "Methane Adsorption on 5A Molecular Sieves in the Pressure Range 4 to 690 kPa", Ind. Eng. Chem. Process Des. Dev., 22, 172-174 (1983).

CHAPTER 2

LITERATURE SURVEY

2.1: INTRODUCTION

For successful design of processes where zeolites are used, there exists a need for suitable techniques for predicting equilibrium multi-component adsorption data. In addition to the standard isotherm equations (e.g. Henry's Law, Langmuir isotherm, BET equation, etc.), many equations have been proposed on physical adsorption of pure gases which would apply to the adsorbed phase in zeolites under all conditions. Although the majority of the equations have some degree of broad applicability, no universal adsorption equation exists. As it is easier to obtain data for pure component than for multicomponent, a reliable method for predicting equilibrium data for mixtures from the isotherms of pure components is needed for process design.

The property of zeolites to preferentially adsorb certain compounds depends upon polarity (permanent dipole moments), molecular weights and dimensions (size) of adsorbate molecules. This last seems to be the most important parameter, as almost all sorption is accomplished by cavity filling. Octahedral cavities of specific sizes comprise the basic units of zeolites which are repeated regularly all over the crystal lat-

tice. These cavities are interconnected via windows of specific sizes, and in order to sorb molecules within zeolites, molecules must be able to pass through these windows. If the sorbate consists of several components that can enter the cavities of zeolites, there is competition for the limited space (volumes of cavities), and hence at equilibrium the amount and composition of the sorbed phase is governed by sorbent - sorbate and sorbate - sorbate interactions.

2.2: THERMODYNAMIC ASPECTS:

2.2.1 Heat of Adsorption:

Thermodynamically the process of equilibrium adsorption involves a decrease in free energy. Therefore the change in enthalpy, ΔH must be negative, since the entropy is negative. The adsorption process consists of a loss in degrees of freedom by the adsorbate molecules due mainly to elimination of the translation energy. The result is the formation of a more ordered configuration in the intra-zeolite state causing the entropy change, ΔS , to be negative. Hence the process of adsorption is exothermic and heat is liberated during the adsorption.

Many terms are used in describing the heat of adsorption. The three in most general use are

1. The Isothermal Integral Heat of Adsorption: this is the total heat attributed to the adsorption process from zero adsorbate loading to some final adsorbate loading at a constant temperature.
2. The Differential Heat of Adsorption, ΔH_s : this is the change in integral heat of adsorption with a change in adsorbate loading. It is defined as

$$\Delta H_s = \bar{H}_s - H_g \quad (2.1)$$

where H_g is the molar enthalpy of the adsorbate gas and \bar{H}_s is the partial molar enthalpy of the adsorbate. The differential heat of adsorption is dependent upon pressure, temperature and adsorbate coverage or loading.

3. The Isosteric Heat of adsorption, q_{st} : this is derived from adsorption isosteres and is defined by the relation

$$q_{st} = H_g - \bar{H}_s \equiv - \Delta H_s \quad (2.2)$$

2.2.2 The Differential Molar Entropy:

For an adsorbate this is given by

$$\bar{S}_s = S_g^0 + R \ln \left\{ \frac{P^0}{P} \right\} + \frac{\Delta H}{T} \quad (2.3)$$

where S_g^0 is the molar entropy of the gas at standard pressure P^0 , and temperature T , assuming a perfect gas.

2.2.3 Henry Constant and Saturation Concentration:

Henry's Law is an equilibrium constant between the sorbed phase and gas phase molecules; it is defined as

$$K' = \lim_{P \rightarrow 0} \frac{C}{P} \quad (2.4)$$

where K' = Henry constant

C = Adsorbed phase concentration, and

P = Pressure.

The saturation concentration is defined as

$$C_s = \lim_{P \rightarrow P_s} C \quad (2.5)$$

where C_s is the maximum concentration that the adsorbent will adsorb and P_s is the saturation vapor pressure. Any practical isotherm model should include these two parameters as they are asymptotic limits of the isotherm.

The dependency of K' , the Henry Constant, on temperature can be derived from thermodynamic considerations, and is known as the Van't Hoff relationship

$$K' = K'_0 \exp \left\{ \frac{q_0}{RT} \right\} \quad (2.6)$$

where q_0 = The heat of adsorption at zero concentration

T = Absolute temperature

R = Ideal gas constant, and

K'_0 = pre-exponential constant.

A secondary parameter often required is ω the energy of interaction of two adsorbate molecules at high loading.

The ratio $\frac{C}{C_s}$ is known as the partial coverage or loading and is represented by θ

$$\theta = \frac{C}{C_s} \quad (2.7)$$

As $\frac{P}{P_s} \rightarrow 1$ the quantity of material adsorbed C_s at this point of saturation is assumed to fill the micropores of the solid as a compressed liquid having density ρ_t of the liquid at the particular temperature of the isotherm.

The pore volume is given by

$$V_p = \frac{C_s}{\rho_t} \quad (2.8)$$

For zeolites the micropore volume V_p can be accurately estimated from crystallographic information, so we can calculate C_s as

$$C_s = \rho_t \times V_p \quad (2.9)$$

Thus C_s for methane varies from 12.6 molecules/cavity at the normal boiling point to 10.85 molecules/cavity at the critical temperature for 5A crystals. It was found that the saturation concentrations C_s for the first four alkanes was the same for both zeolite crystals and pellets (19). This shows that there is no adsorption of adsorbate on binder

used in pellets.

Schirmer et al. (39) have experimentally measured the heats of adsorption of the first four alkanes on CaA and NaA zeolite, equivalent to 5A and 4A, over the entire range of coverage, and found that the heats of sorption to be invariant with the possible exception of the range $0.9 < \theta < 1.0$

2.2.4 Thermodynamic Consistency:

Barrer and Lee (1) have proposed a virial isotherm in terms of osmotic pressure to describe adsorption phenomena. The isotherm is

$$P = \frac{C}{K'} \exp\{A_1 C + A_2 C^2 + \dots + A_i C^i\} \quad (2.10)$$

where P = Pressure.

C = Adsorbed phase concentration,

K' = Henry constant

and A_i are virial coefficients. These A_i have been given physical significance by both Barrer & Lee (1) and Kiselev & Lopatkin (15) but the values obtained by curve fitting techniques depend to some extent upon the degree, i , of polynomial used in fitting the experimental data and upon the concentration range upon which the data are gathered. This

virial isotherm is at present the best practical method for estimating the intrinsic Henry constant from equilibrium data as demonstrated by Barrer & Lee (1) and Ruthven et al. (35).

2.3: THE SIMPLE ISOTHERM MODELS

From an examination of experimental sorption isotherm data for several gases on zeolites, it becomes evident that the simple isotherm models of Langmuir, BET, Volmer, Freundlich, etc..., do not adequately or universally explain all the data. Efforts have been made to reduce the experimental data to modified Langmuir or Freundlich isotherm models. These models, when applied to zeolites systems, serve little more than curve fitting as the regression parameters of these models do not convey any meaningful information. This is because these classical models assume that sorbate - sorbate interactions are absent as the adsorption occurs on isolated sites. The reality of sorption by cavity filling in zeolites makes any such assumption or interpretation meaningless.

Many isotherm models have only been applied to systems of approximately one bar pressure, and have not been tested at higher pressures.

2.3.1 The Langmuir Isotherm model:

The simplest isotherm model which has been successfully employed for low coverage on zeolites is the Langmuir isotherm (16). The assumptions for the Langmuir adsorption model are

1. The adsorbate in the bulk gas phase behaves as an ideal gas.
2. The amount adsorbed is confined to a monolayer.
3. Every position of the surface has the same energy of adsorption.
4. No adsorbate - adsorbate interaction.
5. The adsorbate molecules are localized.

With these assumptions the Langmuir Isotherm is given by

$$\theta = \frac{C}{C_s} = \frac{KP}{\{1+KP\}} \quad (2.11)$$

where C = Coverage (molecules/cavity) or (mmoles/gm),

C_s = Saturation coverage, "

K = Equilibrium constant (pressure)⁻¹

P = Pressure

2.3.2 The BET Isotherm model:

The adsorption equation of Brunauer, Emmett and Taylor (4), the BET equation, has been applied to zeolites to determine the internal surface area. The BET equation has been derived for multilayer adsorp-

tion with the assumption that the surface is homogeneous and that there is no lateral interaction among the molecules. For an infinite number of adsorbing layers and also for L layers of adsorbate, the BET equations are respectively

$$\frac{C}{C_s} = \frac{K\chi}{(1-\chi)\{1-(1-K)\chi\}} \quad (2.12)$$

where $\chi = \frac{P}{P^0}$ and

$$\frac{C}{C_s} = \frac{K\chi\{1-(L-1)\chi^L + L\chi^{L+1}\}}{(1-\chi)\{1-(1-K)\chi^L - K\chi^{L+1}\}} \quad (2.13)$$

2.3.3 The Dubinin-Polanyi Theory:

A popular adsorption theory has been proposed by Dubinin-Polanyi. This theory does not incorporate the Henry constant and is more applicable to the saturation end of the isotherm. It states that

$$CV = \overline{CV} \left\{ \frac{T}{V} \ln (P/P^0) \right\} \quad (2.14)$$

should be a unique function of the adsorbent and independent of the temperature of the adsorbate. The term V in above equation has been

assumed, by various investigators, to be the molar volume of saturated liquid at either the normal boiling point, the adsorption temperature or the adsorption pressure (7,9).

2.3.4 The LRC Isotherm Model:

Yon & Turnock (46) proposed a Loading Ratio Correlation (LRC) model to account for adsorption on molecular sieves. The LRC model is actually an extension of the Langmuir isotherm in which the concept of monolayer capacity C_s is replaced by a maximum attainable loading C_o for a molecular sieve. The basic LRC equation can be expressed for a pure component in terms of a loading ratio R and is given by

$$R = \frac{C}{C_o} = \frac{(KP)^{1/n}}{[1+(KP)^{1/n}]} \quad (2.15)$$

Rearranging gives

$$\ln (P) = -\ln (K) + n \ln \left\{ \frac{R}{(1-R)} \right\} \quad (2.16)$$

Substituting for K in accordance with Van't Hoff expression gives

$$\ln (P) = A_1 + A_2/T + n \ln \left\{ \frac{C}{(C_0 - C)} \right\} \quad (2.17)$$

where $A_1 = -\ln (K_0)$

$$A_2 = -\Delta H/R$$

Yon & Turnock also suggest that the values of n may be described by a temperature dependent function $n(T)$ such as

$$n(T) = A_3 + \frac{A_4}{T} \quad (2.18)$$

or other suitable relationship but in their work for pressure up to 500 psig, they apply appropriate constant parameters A_1 , A_2 , n and C_0 . They recommend that the LRC constants, which are specific to each adsorbate-adsorbent combination, should be evaluated by correlation of the data, rather than from intrinsic evaluation of the Henry constants and the saturation concentration.

2.3.5 Mathews and Weber Isotherm Model :

Mathews & Weber (24) proposed another new isotherm model with three parameters and it is given by

$$\frac{C}{C_s} = \frac{KP}{[1+(KP)^n]} \quad (2.19)$$

The three parameters are C_s , K and n and these parameters are evaluated from the regression analysis of experimental data.

2.3.6 The Generalised Isotherm Model :

Jaroniec (13) postulates that many isotherm equations describing different models of adsorption from gaseous and liquid phases on homogeneous surfaces can be represented mathematically by

$$Y(x) = \left\{ \frac{\bar{A}X}{(1+\bar{A}X)} \right\} \quad (2.20)$$

where $Y(x)$ is the adsorption loading, $\bar{A} = A_0 \exp(E/RT)$ is defined analogous to Henry's constant K and X is pressure. The definition of Y , X and A for different models of physical adsorption on homogeneous surfaces are presented in Table 2.1. These isotherm equations can be used as local isotherms in the integral equation, given by

$$Y_t(X) = \int Y(X,E)F(E)dE \quad (2.21)$$

Table 2.1 Presentation of different Isotherms in Langmuir's form given by Equation (2.20) (13).				
S. No	Adsorption Model	Y	X	A
1	Monolayer single-gas adsorption without lateral interactions	θ	P	K
2	Monolayer single-gas adsorption with lateral interactions on "random" heterogeneous surfaces	θ	$P \exp(\alpha \theta_t)$	K
3	Multilayer single-gas adsorption occurring according to the BET model	$\frac{\theta^M}{G(h)}$	$y(h)$	$K=C/P_s$
4	Monolayer adsorption from multicomponent gas mixture without lateral interactions	$\theta_{(r)}$	$P_1 + \sum_{i=2}^r K_{i1} P_i$	K_1

θ, θ^M = relative monolayer and multilayer surface coverages

$\theta_{(r)}$ = total quantity for r components

$y(h) = h/(1-h)$ and h = relative pressure

$G(h) = 1/(1-h)$

where $Y_t(X)$ and $Y(X,E)$ denote the overall and local adsorption isotherms respectively and $F(E)$ is the distribution function of E normalized to unity.

The Equation (2.21) along with Table 2.1 for local isotherms can be integrated over the energy field of adsorption to obtain heterogeneous isotherm equations. The analytical solution of Equation (2.21) is given by

$$Y_t(X) = \left\{ \frac{(\bar{A}X)^n}{[1 + (\bar{A}X)^n]} \right\}^{m/n} \quad (2.22)$$

where m and n are heterogeneity parameters.

In general Equation (2.21) describes single gas adsorption on heterogeneous surfaces by quasi-Gaussian energy distributions. These distributions are symmetrical for $n = m$, and assymmetrical for other sets of parameter n and m . If $n > m$, they show a widening to the right hand side, whereas for $n < m$ this widening appears on the left hand side.

Four specific well known isotherm equations can be derived from Equation (2.22).

Case 1. For $n = m = 1$: Equation (2.22) becomes the Langmuir Isotherm (16)

$$Y_t(X) = \frac{(\bar{A}X)}{(1 + \bar{A}X)} \quad (2.23)$$

Case 2. For $n = 1, 0 < m < 1$, the generalised Freundlich isotherm is obtained (42)

$$Y_t(X) = \left\{ \frac{(\bar{A}X)}{(1 + \bar{A}X)} \right\}^m, \quad (2.24)$$

Case 3. For $n = m, 0 < n, m < 1$, the Langmuir - Freundlich isotherm is obtained (25,42)

$$Y_t(X) = \frac{(\bar{A}X)^n}{[1 + (\bar{A}X)^n]} \quad (2.25)$$

Note that this is identical to the LRC model Equation (2.15).

Case 4. For $m = 1$ and $0 < n < 1$, the Toth isotherm is obtained (45)

$$Y_t(X) = \left\{ \frac{(\bar{A}X)^n}{\{1 + (\bar{A}X)^n\}} \right\}^{1/n} \quad (2.26)$$

2.4: STATISTICAL ISOTHERM MODELS

The statistical approach to adsorption, which was developed largely by Fowler & Guggenheim and Hill (8,12), depends on representing the adsorbed species in terms of a simplified physical model for which the appropriate expression for the position function may be derived. The thermodynamic properties are then obtained using the established relationship between the partition functions and the classical thermodynamic properties.

The general isotherm equation for average number of molecules per cavity is given by

$$C = \frac{\sum_{s=0}^m sZ(s)a^s}{\sum_{s=0}^m Z(s)a^s} \quad (2.27)$$

where 'a' is the activity and for gases equals to $\frac{P}{kT}$, and $Z(s)$ is the configuration integral for 's' molecules in a cavity and is given by

$$Z(s) = \frac{1}{s!} \int_V \exp\{-(r_1, r_2, \dots, r_s U_s)kT\} dr_1 \dots dr_s \quad (2.28)$$

2.4.1 Ruthven Isotherm Model:

Ruthven (29) presented an isotherm based on statistical mechanics, where the sorbate - sorbent interaction was accounted for by Henry's constant (slope of the earlier part of sorption isotherm), sorbate - sorbate interaction by force constant (Lennard - Jones type) and by a reduction in the free volume of cavity due to the finite size of the occluded molecules. In his original formulation he suggested that the Henry's constant may be derived by curve fitting his model to experimental data, that the force constant may be determined from viscosity data or by virial coefficients, and molecular volumes from liquid densities at appropriate temperature and pressure conditions. For temperatures above critical temperature, he recommended the use of Van der Waal's covolumes as the molecular volumes of the sorbed phases. The Ruthven isotherm model equation is derived with the following assumptions and approximations to the configuration integral:

1. The molecules within a given cavity move randomly and independently in the potential field resulting from the sorbate - sorbent interactions.
2. The potential is uniform throughout the cavity even when more than one molecule is present but the effective volume of the cavity is reduced.
3. The effect of sorbate molecules in neighbouring cavities is neglected.

With these assumptions the configuration integral becomes

$$Z(0) = 1$$

$$Z(1)a = K'P$$

$$Z(s) = \frac{Z(1)^s}{s!} \left\{1 - \frac{s\beta}{v}\right\}^s \exp\left\{\frac{s\beta\epsilon}{vKT}\right\}$$

Therefore the isotherm equation becomes:

$$C = \frac{K'P + \sum_{n=2}^m \frac{(K'P)^n}{(n-1)!} \left(1 - \frac{n\beta}{v}\right)^n \exp\left\{\frac{n\beta\epsilon}{vKT}\right\}}{1 + K'P + \sum_{n=2}^m \frac{(K'P)^n}{n!} \left(1 - \frac{n\beta}{v}\right)^n \exp\left\{\frac{n\beta\epsilon}{vKT}\right\}} \quad (2.29)$$

where C is molecules adsorbed per cavity

K' is Henry's constant (molecules/cavity/pressure)

P is pressure

β is molecular volume (Angstrom)³

v is volume of cavity (Angstrom)³

$\frac{\epsilon}{\kappa}$ is Lennard Jones potential °K

T is temperature °K

m is the saturation limit (integer) $\leq \frac{v}{\beta}$

If the attraction forces between sorbate molecules are neglected then the isotherm equation becomes

$$C = \frac{K'P + \sum_{n=2}^m \frac{(K'P)^n}{(n-1)!} \left(1 - \frac{n\beta}{v}\right)^n}{1 + K'P + \sum_{n=2}^m \frac{(K'P)^n}{n!} \left(1 - \frac{n\beta}{v}\right)^n} \quad (2.30)$$

2.4.2 The Schirmer et al. Isotherm Model:

Schirmer et al. (38) proposed another isotherm model based on statistical thermodynamics in which they replace the configuration integral expression of $Z(s)$ by finite sums, whose n summations corresponds to different energy levels. Hence it is possible to describe different states

of energy and their transitions. For a cavity which, for a given coverage, is energetically homogeneous $n = 1$; in other cases $n = 2$ different states may be regarded as sufficient. The sums are represented by

$$Z(0) = 1$$

$$Z(i) a^i = \left[\frac{P/P_0}{T/T_0} \right]^i \sum_{j=1}^n \exp \{ i(S_{ji}T - E_{ji})/RT \}$$

where S_{ij} are constants for the standard difference of entropy, and E_{ij} are energy constants of the corresponding levels.

For $n = 1$ the isotherm equation becomes

$$C = \frac{\sum_{i=1}^m \left[\frac{P/P_0}{T/T_0} \right]^i \exp \left\{ \frac{(iS_i T - E_i)}{RT} \right\}}{1 + \sum_{i=1}^m \left[\frac{P/P_0}{T/T_0} \right]^i \exp \left\{ \frac{(iS_i T - E_i)}{RT} \right\}} \quad (2.31)$$

where m is the maximum number of molecules occluded per cavity.

Equation (2.31) depends on the constants, S_i and E_i , which are superior to virial coefficients in that the form of their dependence on pressure and temperature is known. The values of S_i and E_i are determined by means of a method of parameter determination using the meas-

ured equilibrium data.

2.5: MULTICOMPONENT ISOTHERM MODELS

2.5.1 Langmuir Binary Model:

For binary adsorption Butler and Ockrent,(5) on the basis of kinetic consideration alone, derived the binary Langmuir isotherm as

$$\frac{C_i}{C_{is}} = \frac{K_i P_i}{1 + \sum_{i=1}^2 K_i P_i} \quad (2.32)$$

This isotherm has been criticized (17) because it is thermodynamically inconsistent with the Gibbs adsorption isotherm for an ideal adsorbed solution, unless the saturation monolayer capacities of each of the binary components are equal. However, LeVan and Vermeulan (17) were able to derive explicit and thermodynamically consistent isotherm as follows; for component number 1.

$$C_1 = \frac{C_s K_1 P_1}{1 + \sum_{i=1}^2 K_i P_i} + (C_{s1} - C_{s2}) \frac{\ln \left(1 + \sum_{i=1}^2 K_i P_i \right)}{\sum_{i=1}^2 K_i P_i} \quad (2.33)$$

where

$$C_s = \frac{C_{s1} K_1 P_1 + C_{s2} K_2 P_2}{K_1 P_1 + K_2 P_2}$$

For multicomponent models, the Langmuir equation is written as

$$C_i = \frac{C_{si} K_i P_i}{1 + \sum_{i=1}^n K_i P_i} \quad (2.34)$$

Schay and co-workers (36,37) have extended the above equation by accommodating molecular interactions in the adsorbed phase as follows

$$\frac{C_i}{C_{si}} = \frac{K_i P_i / \eta_i}{1 + \sum_{i=1}^n K_i P_i / \eta_i} \quad (2.35)$$

where the η describe the adsorbed phase interactions between different molecular species.

2.5.2 Loading Ratio Correlation Model:

Using the method of Markham and Benton (23) the Loading Ratio Correlation proposed by Yon and Turnock (46) can be extended for

multicomponent systems to give the equation

$$R_i = \frac{C_i}{C_{oi}} = \frac{(K_i P_i)^{1/n_i}}{\{1 + \sum_{j=1}^r (K_j P_j)^{1/n_j}\}} \quad (2.36)$$

or

$$\ln (P_i) = A_{1i} + A_{2i}/T + n_i \ln \frac{R_i}{\{1 - \sum_{j=1}^r R_j\}} \quad (2.37)$$

The constants in the latter two equations can often remain associated with only the pure component adsorption data. However, for highly polar adsorption data there is interaction due to the presence of other adsorbates promoting strong attractive forces due to the polarizable molecules. For this reason the LRC constants should be modified by the method of Schay et al. (36,37) to yield.

$$R_i = \frac{(K_i P_i / \eta_i)^{1/n_i}}{1 + \sum_{j=1}^n (K_j P_j / \eta_j)^{1/n_j}} \quad (2.38)$$

or

$$\ln (P_i) = \ln (\eta_i) + A_{1i} + A_{2i}/T + n_i \ln \frac{R_i}{\{1 - \sum_{j=1}^r R_j\}} \quad (2.39)$$

2.5.3 Ruthven's Binary Isotherm Model:

Ruthven et al. (31,35) extended the pure component model to binary system to give the isotherm equation as

$$C_1 = \frac{K'_1 P_1 + \sum_{j=0}^n \sum_{i=0}^m \frac{(K'_1 P_1)^i (K'_2 P_2)^j}{(i-1)! j!} \left(1 - \left(\frac{i\beta_1 + j\beta_2}{v}\right)\right)^{i+j}}{1 + K'_1 P_1 + K'_2 P_2 + \sum_{j=0}^n \sum_{i=0}^m \frac{(K'_1 P_1)^i (K'_2 P_2)^j}{i! j!} \left(1 - \left(\frac{i\beta_1 + j\beta_2}{v}\right)\right)^{i+j}} \quad (2.40)$$

with the restriction that $i\beta_A + j\beta_B < v$ and $i+j \geq 2$ for maximum loading in the cavity. This equation has been successfully applied to various binary adsorbate systems on 5A and 13X zeolites. Rolniak and Kobayashi (27) applied this equation to the high pressure sorption of methane and carbon dioxide mixtures in the form

$$C_1 = \frac{K'_1 f_1 + \sum_{j=0}^n \sum_{i=0}^m \frac{(K'_1 f_1)^i (K'_2 f_2)^j}{(i-1)! j!} \left(1 - \left(\frac{i\beta_1 + j\beta_2}{v}\right)\right)^{i+j} \exp\left\{-\frac{i\beta_1 \varepsilon_1 + j\beta_2 \varepsilon_2}{v k T}\right\}}{1 + K'_1 f_1 + K'_2 f_2 + \sum_{j=0}^n \sum_{i=0}^m \frac{(K'_1 f_1)^i (K'_2 f_2)^j}{i! j!} \left(1 - \left(\frac{i\beta_1 + j\beta_2}{v}\right)\right)^{i+j} \exp\left\{-\frac{i\beta_1 \varepsilon_1 + j\beta_2 \varepsilon_2}{v k T}\right\}} \quad (2.41)$$

where fugacities replace pressures. Good agreement was found with the data using this model.

2.5.4 Binary Model of Schirmer et al's Isotherm :

Loughlin and Roberts (20,21) extended the Schirmer et al. pure component isotherm to multicomponent adsorption and presented the binary isotherm equation as

$$C_A = \frac{\sum_{j=0}^n \sum_{i=1}^m i \left\{ \frac{P_A/P_0}{T/T_0} \right\}^i \left\{ \frac{P_B/P_0}{T/T_0} \right\}^j \exp\{(kS_k T - E_k)/RT\}}{\sum_{j=0}^n \sum_{i=0}^m i \left\{ \frac{P_A/P_0}{T/T_0} \right\}^i \left\{ \frac{P_B/P_0}{T/T_0} \right\}^j \exp\{(kS_k T - E_k)/RT\}} \quad (2.42)$$

where k is the sum of molecules ($i+j$)

S is the standard difference of entropy constant

E is the energy constant for corresponding levels

$$S_k = \frac{1}{k} [iS_{Ak} + jS_{Bk} + R \ln \frac{kl}{iljl}] \quad (2.43)$$

$$E_k = \frac{1}{k} [iE_{Ak} + jE_{Bk} + E_m] \quad (2.44)$$

2.5.5 The Generalized Jaroniec Model:

The multicomponent generalized isotherm proposed by Jaroniec (13) is given by

$$Y_1 = \left\{ \frac{(\bar{A}P_1)^n}{1 + \{\bar{A} [P_1 + \sum_{i=2}^r (K_{i1} P_i)]\}^n} \right\}^{m/n} \quad (2.45)$$

where $\bar{A} = K_1$ and

K_{i1} = Ratio of constants K_i and K_1

These various isotherm models can be applied to the study of pure, binary, ternary and quaternary mixtures of the first four hydrocarbons. For fundamental adsorption behavior, the models of Ruthven et al., Schirmer et al., and Danner et al., are probably best but these are very complicated for the design of a PSA unit which needs simple

isotherm models e.g. Jaroniec, LRC, Toth, etc...

Hamad (10) studied four models namely Schirmer et al., Ruthven, Vacancy Solution model of Suwanayuen and Danner. and virial for pure and binary adsorption of propane and n-butane on 5A and 13X zeolites, and indicates that the Schirmer et al. model best fits the data in general; the Ruthven model gives better fit for 5A zeolite than for 13X zeolite. Hamad explains that the better fit of the Schirmer et al. model is probably due to the fact that in the Schirmer et al. model the canonical partition function is evaluated from experimental data in nearly its exact form, while in the Ruthven model it is approximated on the basis of a very good crude assumption.

LITERATURE CITED

1. Barrer, R.M., and J.A. Lee, Surface Sci., 12, 354 (1968).
2. Barrer, R.M., and J.W. Sutherland, "Inclusion Complexes of Faujasite With Paraffins and Permanent Gases", Proc. Roy. Soc., Ser. A., 237, 439 (1956).
3. Breck, D.W., "Zeolite Molecular Sieves", Wiley-Interscience, New York, (1974).
4. Brunauer, S., P.H. Emmett, and E. Teller, J. Am. Chem. Soc., 60, 309 (1938).
5. Butler, J.A.V., and C. Ockrent., J. Phys. Chem. 85, 22 (1930)
6. Cook, W.H. and D. Basmadjian, Can. J. Chem. Eng., 42, 146 (1964).
7. Dubinin, M.M., and L.V. Radushkevich, Comp. Rend. Acad. Sci., U.S.S.R., 55, 327, (1947).
8. Fowler, R.H. and E.A. Guggenheim, "Statistical Thermodynamics", Cambridge University Press, p 431, (1949).
9. Grant, R.J. and M. Manes, Ind. Eng. Chem. Fund., 3, 221, (1964).
10. Hamad, E.D.K., "Comparision of Binary Adsorption of Propane and n-Butane on 5A and 13X Molecular sieves", M.S Thesis, KFUPM (1984).
11. Hasanain, M.A. and K.F. Loughlin, "Demethanization of Natural Gas by Pressure Swing Adsorption", KACST Project No AR-6-147 Report # 1, July 16th (1985) and Report # 2, March 16th (1986).

12. Hill, T.L., "Introduction to Statistical Thermodynamics", Addison Wesley, Massachusetts, (1960).
13. Jaroniec, M., "Physical Adsorption on Heterogeneous Solids", Fundamentals of Adsorption, Edited by Myers, A.L. and G. Belfort, 239-248, published by AIChE, New York, (1984).
14. Khaleeq, M., "Adsorption of Xylenes on Ba-X Zeolite Pellets", M.S. Thesis, KFUPM, (1984).
15. Kiselev, A.V., and A.A. Lopatkin, In Molecular Sieves, London Soc. Chem. Ind., 252 (1968).
16. Langmuir, I., J. Am. Chem. Soc., 40, 1361 (1918).
17. LeVan, M. and T. Vermeulan, J. Phys. Chem. 85, 22 (1981).
18. Lederman, P.D. and B. Williams, "The Adsorption of Nitrogen-Methane on Molecular Sieves", AIChE J., 10, 30, (1964).
19. Loughlin, K.F., Ph.D Thesis, University of New Brunswick, 1970.
20. Loughlin, K.F. and G.D. Roberts, "A New Binary Sorption Equilibrium Isotherm for Molecular Sieves Zeolite", AIChE J, Accepted for Publication.
21. Loughlin, K.F. and G.D. Roberts, "Study of Mixture Equilibria of Methane and Krypton on 5A Zeolite", ACS Sym. Ser. No 105, (1980).
22. Loughlin, K.F. and D.M. Ruthven, "A Generalized Correlation of Equilibrium Data for the Sorption of Light Paraffins in Linde 5A Zeolite", J. Coll. Interfacial Sci., 30(2), 331 (1972).

23. Markham, E.D. and A.F. Benton, *J. Am. Chem. Soc.*, 53, 497 (1931).
24. Mathews, A.P. and W.J. Weber, Jr, "Mathematical Modeling of Adsorption in Multicomponent System", *Adsorption and Ion Exchange with Synthetic Zeolites*, ACS Symposium Series, 135, 27 (1980).
25. Misra, D.N., *J. Chem. Phys.*, 52, 5499 (1970).
26. Myers, A.L. and J.M. Prauznitz, "Thermodynamics of Mixed Gas Adsorption", *AIChE J.*, 11, 121 (1965).
27. Rolniak, P., and R. Kobayashi, "Adsorption of Methane and Several Mixtures of Methane and Carbon Dioxide at Elevated Pressures and Near Ambient Temperatures on 5A and 13X Molecular Sieves by Tracer Perturbation Chromatography ", *AIChE J.*, 26, 4, 616 (1980).
28. Ruthven, D.M., "Principles of Adsorption and Adsorptive Separative Process", Wiley-Interscience, New York, (1984).
29. Ruthven, D.M., "Simple Theoretical Adsorption Isotherm for Zeolites", *Nature Phys. Sci.*, 232, 70 (1970).
30. Ruthven, D.M. and R.I. Derrah, "Sorption in Davison 5A Molecular Sieves", *Can. J. Chem. Eng.*, 50, 743, (1972).
31. Ruthven, D.M. and K.F. Loughlin, "Sorption of Light Paraffins in Type A Zeolites : Analysis and Interpretation of Equilibrium Isotherms", *J. Chem. Soc., Faraday Trans. 1*, 68, 696 (1972).

32. Ruthven, D.M. and K.F. Loughlin, "The Sorption and Diffusion of n-Butane in Linde 5A Molecular Sieves", Chem. Eng. Sci., 26, 1145-1154, (1971).
33. Ruthven, D.M. and K.F. Loughlin, "Correlation and Interpretation of Zeolitic Diffusion Coefficients", Trans. Far. Soc., 67, 1661-1671 (1971).
34. Ruthven, D.M., K.F. Loughlin, and R.I. Derrah, "Sorption and Diffusion of Light Hydrocarbons and Other Simple Nonpolar Molecules in Type A Zeolites", Adv. Chem. Ser., 121, 330-344 (1973).
35. Ruthven, D.M., K.F. Loughlin, and K.A. Holborow, "Multicomponent Sorption Equilibrium in Molecular Sieves Zeolites", Chem. Eng. Sci., 28, 701-709 (1973).
36. Schay, G.J., Chem. Phys. Hungary, 53, 691 (1956).
37. Schay, G.J., P. Fejes, and J. Szethmary, Acta. Chem. Acad. Sci., Hungary, 12, 299 (1957).
38. Schirmer, W., K. Fiedler, and H. Stach, "Thermodynamics of Adsorption on Zeolites", A.C.S. Symposium Ser., 40, 305 (1977).
39. Schirmer, W., G. Fiedrich, and H. Stach, "1st Int. Conf. on Molecular Sieve Zeolites (London 1967); Proc. Soc. Chem. Ind., 276 (1968).
40. Singhal, A.K, "Multicomponent Sorption Equilibria of Hydrocarbon Mixtures in Zeolite Molecular Sieves", AIChE Sym. Ser., 179, 74, 41 (1978).
42. Sips, J.R., J. Chem. Phys., 16, 420 (1948); 18, 1024 (1950).

43. Suwanayuen, S. and R.P. Danner, "A Gas Adsorption Isotherm Based on Vacancy Solution Theory", *AIChE J.*, 26, 68-76 (1980).
44. Suwanayuen, S. and R.P. Danner, "Vacancy Solution Theory of Adsorption from Gas Mixtures", *AIChE J.*, 26, 76-82 (1980).
45. Toth, J., "Isotherm Equations for Monolayer Adsorption of Gases on Heterogeneous Solid Surfaces", *Fundamentals of Adsorption*, Edited by Myers, A.L. and G. Belfort, 657-665, published by AIChE, New York, (1984).
46. Yon, C.M. and P.H. Turnock, "Multicomponent Adsorption Equilibria on Molecular Sieves", *AIChE J. Symp. Ser.*, 67(117), 75 (1971).
47. Zuech, J.L., A.L. Hines, and E.D. Sloan, "Methane Adsorption on 5A Molecular Sieves in the Pressure Range 4 to 690 kPa", *Ind. Eng. Chem. Process Des. Dev.*, 22, 172-174 (1983).

CHAPTER 3

APPARATUS AND PROCEDURE

3.1: Choice of Experimental Method:

Adsorption isotherms are generally determined by one of the two direct methods:

1. The Volumetric Method or
2. The Gravimetric Method

In the volumetric method the moles of gas added is determined from measurement of known volumes, pressure and temperature and the moles of gas adsorbed is determined from the knowledge of moles present in the gas phase.

In gravimetric method the amount of gas adsorbed is measured by weighing the sample in a closed system on a balance, generally of the Quartz Spring type. In the measurement of multicomponent equilibrium adsorption by the gravimetric method it is difficult to measure separately the amount of each species adsorbed in the adsorbed phase and it is difficult to provide good mixing in the gas phase; hence it is not suitable for high pressure and multicomponent adsorption. Hence the volumetric method is preferred where there is a need to know the amount of each species adsorbed.

3.2: THE APPARATUS

The apparatus for the high pressure equilibrium adsorption was constructed using stainless steel vessels, tubes and a calibrated volume glass chamber, which is used only for the calibration of volumes. The main parts of the apparatus consists of the adsorption cell D, storage chamber B and the mixing chamber C. The ancillary parts consists of a furnace, temperature controller, temperature indicator, water bath, differential pressure gauges, electronic manometer, recirculating magnetic pump and a vacuum pump. The apparatus is shown schematically in Figure 3.1.

The chamber A was calibrated by filling with mercury three times and was found to have a volume of 125.00 ccms (1). This was used to calibrate the other volumes (B, C and D) and was removed after calibration since it was not designed for high pressure use.

Chamber B (982.47 ccms) is connected to chamber C (396.62 ccms) and adsorption cell D (whose gas phase volume changes whenever a new adsorbent sample is used) by the control valve (type Brooks 5835N), to the gas inlet line, to a 0-200 psig differential barocell pressure transducer (Model No 570 D-200 P-2A1-VIX), to calibrated volume A and to the vacuum pump. Chamber C which was the recirculation loop, was connected to the pressure control valve, sampling valve, vacuum pump and by two on-off valves to the adsorption cell D. It also incorporates

the Ruska 0 - 1200 psia recirculating magnetic pump (Model No 2330-802) which recirculates the gas mixture through the system until constant composition is attained.

The composition of the gas phase for multicomponent adsorption was measured using a Gow-Mac gas chromatograph (Model No 69-150) with a Hewlett-Packard integrater (Model No 3390A). Two vacuum pumps were used due to breakdown, one was type KC-3 and the other was a replacement Edwards which gives an ultimate vacuum of 2×10^{-4} torr. The waterbath used was a Lauda type (Model No K4R) for the temperature control of the adsorption cell and the temperature was measured from the thermocouple well using a thermocouple actuated digital indicator (Model No 3750 K). The furnace for the regeneration of the adsorbents was controlled by a Thermolyne Funatrol (Model No CP-13315) temperature controller via a temperature sensor which is placed in the furnace.

The pressure was measured using two 0-200 psig differential pressure transducers (Model Nos 570 D-200 P-2AI-VIX), one reference digital pressure guage (Wallace and Tiernan Type U8 4349), and one Datametrics electronic manometer (Type 1014A) with null offset adapter (Type 1056).

3.3 PROCEDURE

3.3.1 Determination Of The Dry Weight Of Adsorbent :

A glass flask is used to determine the dry weight of adsorbent. First the empty weight of the evacuated glass flask is noted (W_1). The adsorbent sample is placed in the flask and its weight is noted (W_2). The flask is connected to the vacuum pump and is placed into the furnace; the temperature of the furnace is raised in incremental steps up to a maximum of 375 °C and kept constant at this temperature for a minimum period of 24 hours. Then the flask is sealed and cooled to the room temperature and its weight is noted (W_3). The heating step is repeated several times until a constant weight is reached (W_4). The weight of adsorbent sample is found by subtracting W_1 from W_4 . The dried adsorbent of weight ($W_4 - W_1$) is then transferred into the adsorption cell D.

3.3.2 Calibration Of Different Volumes :

The volumes of the chambers used in the study of equilibrium adsorption by the volumetric method, need to be calibrated carefully. The accuracy of adsorption equilibria depends on the accuracy of volumes and pressure measurements. The standard reference volume A was calibrated three times by filling with mercury and weighing the amount of mercury needed to fill. From the knowledge of the density of mer-

cury at room temperature the volume of chamber A was found (1).

This reference volume is used to calibrate the volume of the other chambers B,C and D by expanding helium into them. At room temperature helium is negligibly adsorbed. The helium is loaded into chamber A to approximately atmospheric pressure which is recorded and is then allowed to expand into chamber B. The final pressure is noted; this procedure is repeated several times to get a reproducible value. Volumes of chambers C and D are calibrated by expanding helium from chamber B. The volume of adsorption cell D is recalibrated whenever the adsorbent is changed. The standard deviation in the calibration of volume B was 5.532 ccms and for volume C was 6.639 ccms.

3.3.3 Pure Component Adsorption Isotherm Determination:

High pressure equilibrium adsorption data for methane, ethane, propane and n-butane at 275, 300, 325 and 350 °K on Linde 5A, 13X and S-115 pellets was measured. After regeneration the adsorbent cell is sealed, cooled and maintained at the desired isotherm temperature using a water bath. Evacuated chamber B is filled with adsorbate gas from the high purity cylinders up to a maximum pressure of 200 psia. After some time when the pressure becomes constant, the pressure is noted on the electronic manometer and the moles of gas enclosed may then be evaluated using the Soave-Redlich-Kwong equation of state.

Opening the pressure control valve allows the gas to enter chambers C and D where it is adsorbed on the adsorbent. After a suitable drop in pressure in chamber B, the control control valve is closed. When the gas is adsorbed the temperature of the adsorption bed rises due to the release of heat of adsorption. After some time, when the equilibrium pressure becomes constant at the constant isotherm temperature, the temperature and pressure of chambers B, C and D are noted. From the volumetric measurements the moles in the gas phase can be established, and by subtraction from the original moles present, the number of moles adsorbed is determined; hence from the known weight of adsorbent, the concentration can be established. Programs to perform these calculations are included in KACST reports (2).

The adsorption cell with known gas pressure is again isolated by closing the pressure control valve. Additional moles are added to the chamber B to bring its pressure back to 200 psia approximately. The increase in moles is recorded. The pressure control valve is opened and the process is repeated sequentially until the maximum desired pressure is reached.

3.3.4 Binary and Multicomponent Adsorption Determination:

For binary and multicomponent adsorption the zeolite is regenerated first and then cooled to the desired isotherm temperature (300°K) using

the water bath. The heavier gas X (i.e. n-butane or propane or ethane) is adsorbed first to the desired pressure. The moles of X in the gas phase in chambers B, C and D and on the adsorbent are recorded. The adsorption chamber is isolated and the chambers B and C are evacuated. The moles of gas X discharged are noted. Then the lighter gas Y (i.e propane or ethane or methane) is loaded into the chamber B. Chamber C is isolated from the vacuum pump and reconnected to the adsorption cell D. The pressure drops below the desired value due to gas desorption. The recirculation pump is started to pump the gas around the loop and the pressure control valve, which is set at the desired value, is turned on. Gas Y flows from chamber B to the adsorption loop (C+D) due to the difference in pressure. Equilibrium at the desired pressure occurs when no more gas Y flows from chamber B.

The pressure control valve is closed, and the adsorption cell D is isolated by closing the on-off valves. The gas from chamber C is analyzed using the gas chromatograph and integrater. This gives the composition in the gas phase, and from the knowledge of the moles of X and Y in the gas phase, the moles of X and Y in the adsorbed phase can easily be determined.

For the next point on the mixture diagram, chamber C is evacuated and the moles of X and Y discharged is noted. The lighter gas Y is added again to bring the system back to the desired pressure and the procedure is repeated.

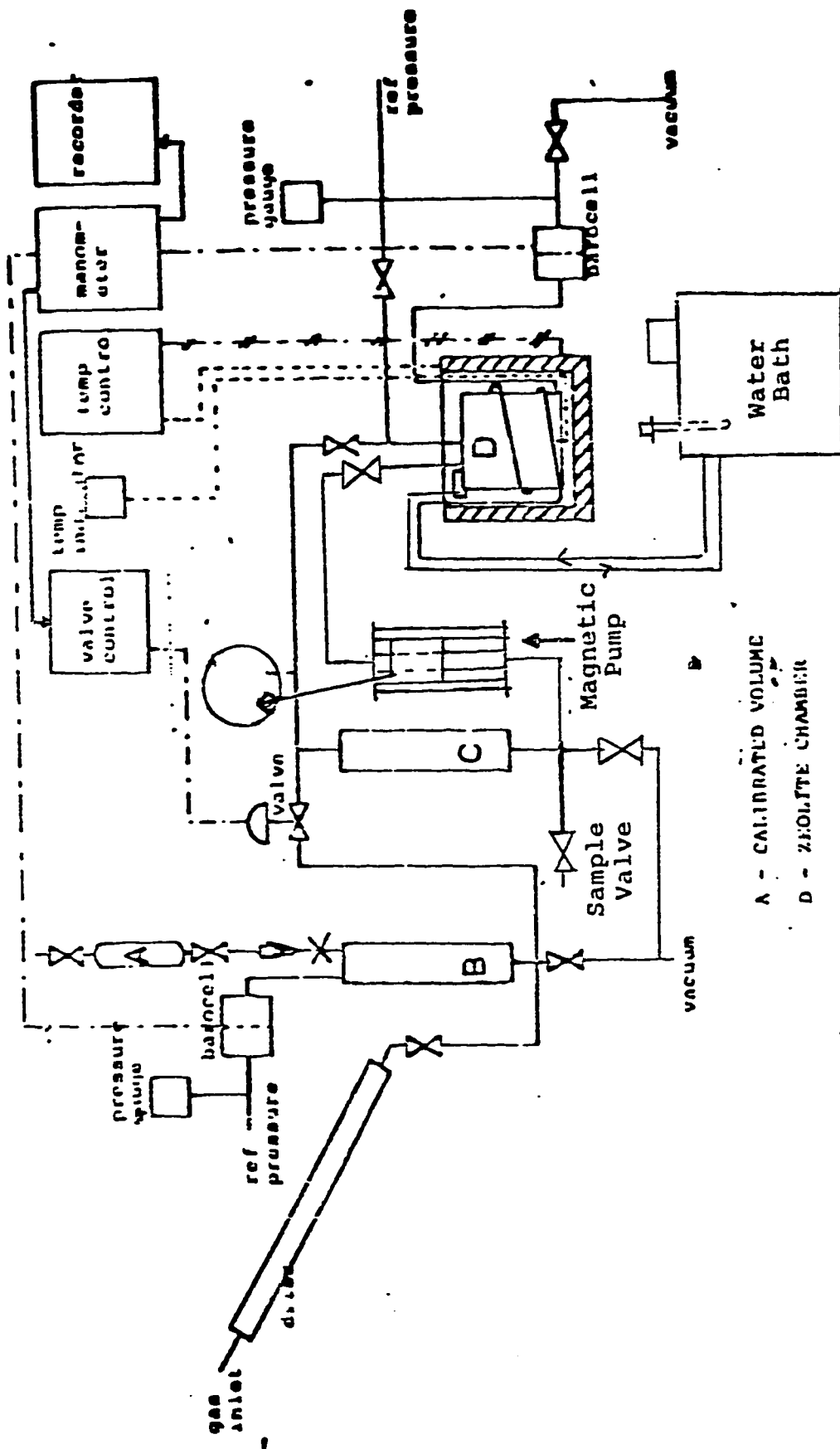


Fig. 3.1: Flow Diagram of High Pressure Multicomponent Equilibrium Adsorption Apparatus.

LITERATURE CITED

1. Hamad, E.D.K., "Comparison of Binary Adsorption of Propane and n-Butane on 5A and 13X Zeolites", M.S Thesis, KFUPM (1984).
2. Hasanain, M.A. and K.F. Loughlin, "Demethanization of Natural Gas by Pressure Swing Adsorption", KACST Project No AR-6-147 Report # 1, July 16th (1985) and Report # 2, March 16th (1986). and Report # 3, September 16th (1986).

CHAPTER 4

PURE AND MULTICOMPONENT EQUILIBRIUM RESULTS ON LINDE 5A PELLETS.

One objective of this thesis is to select a reliable simple isotherm model, from the published models, which can be recommended for the design of a Pressure Swing Adsorption unit for the separation of methane from natural gas. In order to do this first pure component equilibrium adsorption data were measured for methane, ethane, propane and n-butane on Linde 5A, 13X and SR115 adsorbents at temperatures of 275, 300, 325 and 350°K and at high pressures. Due to the low vapor pressure of propane and n-butane at room temperature, the maximum pressure reached with these components was approximately 30 and 55 psia respectively. The moles adsorbed can be calculated from the knowledge of pressure, temperature and volume and the data is presented in the KACST reports (AR-6-147) no 2,3 and 4. Binary, ternary and quaternary mixtures of methane with the other three gases were measured at a pressure of 50 psia and temperature of 300°K for the three adsorbents; the data as analysed is given in KACST reports (AR-6-147) no 3 and 4. Some binary data was also obtained at 95 psia and 300°K. In the remainder of this chapter the results are presented for adsorbent Linde 5A zeolite only.

4.1: Non-Ideality Of The Gas Phase:

Since the experimental pressures are well above atmospheric pressure, the gases especially propane and n-butane, exhibit some non-ideality; in order to determine the moles adsorbed a satisfactory equation of state must be used to describe the gas phase density. Two equation of states were tested namely the Soave-Redlich-Kwong and Peng-Robinson. It was observed that both these equations gave identical results; hence it was decided to use the Soave-Redlich-Kwong equation of state only to calculate the molar density. This equation is given in Appendix A.

4.2: Evaluation of Intrinsic Henry Constant:

The intrinsic Henry Constant is best evaluated by using the Barrer and Lee virial equation given by

$$f = \frac{C}{K'} \exp(A_1 C + A_2 C^2 + \dots + A_i C^i + \dots) \quad (4.1)$$

or

$$\ln \frac{f}{C} = \ln \frac{1}{K'} + A_1 C + A_2 C^2 + \dots + \dots$$

where A_i are virial coefficients, K' is the Henry constant, f is the fugacity and C is the concentration. At the low concentration region, a plot of $\ln(f/C)$ versus C becomes linear with a slope of A_1 and intercept $\ln(1/K')$. Hence

$$\ln \frac{1}{K'} = \ln \frac{f}{C} \quad (4.2)$$

The data is plotted as $\ln(f/C)$ versus C on semilogarithmic paper for all the components in Figures 4.1 to 4.4. The intercept reads directly $1/K'$ and the Henry constants are given in Table 4.1.

The temperature dependency of Henry constant is given by the Van't Hoff relationship i.e.

$$K' = K'_0 \exp\left(\frac{-\Delta U_0}{RT}\right) \quad (4.3)$$

where $-\Delta U_0$ is the heat of adsorption and K'_0 is the pre-exponential factor. The experimental data are plotted as $\ln(K')$ versus $1/T$ on semilogarithmic paper in Figure 4.5. The heat of adsorption ($-\Delta U_0$) is calculated from the slope $\left\{\frac{-\Delta U_0}{R}\right\}$ and the intercept K'_0 calculated from the best fit at $K' = 1$. The resulting values are given in Table 4.1 along with the values given in literature from reference (1) and are plotted in

Figure 4.5.

The Henry constant for methane, ethane and propane of this work lies within the range of the literature values and the value of K'_0 and $(-\Delta U_0)$ is calculated by regression of all the values. For n-butane the value of Henry constant calculated in this work lies well below the values given in literature, the reason for this may be in the reading of pressure at low pressures. Errors at extremely low pressure are due to the fact that the apparatus is designed for high pressure; the range of the pressure sensor is high and the vacuum pump used is not a high vacuum pump.

4.3: Determination of Saturation Concentration:

At the saturation concentration the molecules adsorbed are closely packed analogous to a liquid. The molar volumes for the four sorbates are found from Equation (2.1). The void volume of the adsorbents is reported in the literature and are given in Tables 1.1 to 1.3. If we assume that the adsorbates occupies 100 % of the void volume then the saturation concentrations may be calculated for Linde 5A pellets using the equation

$$N_o = 0.216x p_{\text{sorbate}} \quad (4.3a)$$

where 0.216 comes from multiplying the voidage of 0.27 cc/gm zeolite by 0.8 to convert to 0.216 cc/gm pellet and for Linde 5A pellets it is given in Table 4.2.

4.4: Modelling of Pure Component Data :

Five simple isotherm models are used for the analysis of pure component data. These are

1. Loading Ratio Correlation (LRC) model.
2. Toth model.
3. Mathews and Weber model.
4. Jaroniec model.
5. Ruthven model.

These models are discussed in detail in chapter 2. To account for the non-ideality, fugacity was used instead of pressure in these models.

Each of these models is described by two or more parameters that follow, namely

K , the equilibrium constant analogue of the Henry constant

N_0 , the saturation concentration

β , the sorbate molar volume and

n , m constants.

These parameters were evaluated by the least squares regression techniques using the subroutine BSOLVE given in KACST project report # 2.

The data was regressed using the equation

$$SS = \sum_{i=1}^N \left\{ \frac{C_{pre}}{C_{exp}} - 1 \right\}^2 \quad (4.3b)$$

4.5: Fit of Data Using Theoretical N_0 , β And Intrinsic K:

Using theoretical N_0 , β and intrinsic K from this work, the data was regressed using the different models mentioned above. It was observed that the data does not fit any model satisfactorily for all the four sorbates. Employing theoretical N_0 and β only to fit the data to different models along with the optimized parameters K, n and m, it was observed that the data does not fit any model satisfactorily for ethane, propane and n-butane; for methane the data fits the first four models satisfactorily. These results are plotted in Figures 4.6 to 4.9 and the value of the parameters are given in Table 4.3.

In order to fit the data of other sorbates the N_0 and β was optimized along with n and m using the intrinsic K value. It was observed that the data does not fit any of the models for ethane, propane and n-butane. For methane the fit of the first four models was somewhat reasonable and the fit of the Ruthven model was satisfactory.

4.6 FIT OF THE DATA USING OPTIMISED PARAMETERS:

4.6.1 Fit of LRC Model Using Optimized Parameters:

With optimized Equilibrium constant, saturation concentration and n the fit of LRC model was good for methane and ethane and somewhat satisfactory for propane and n -butane as shown in Figures 4.10 to 4.13 with the optimized parameters being given in Table 4.4. It was observed from Table 4.4 that the value of optimized parameter K for methane and propane is close to the intrinsic K and for ethane and n -butane it was little higher. The value of parameter n appears to increase with temperature. The value of optimized N_0 is about the maximum experimental concentration for ethane, propane and n -butane and for methane it is more than the theoretical value for two isotherms and increases with the temperature contrary to what would be expected.

4.6.2. Fit of Toth Model Using Optimized Parameters:

With optimized K , N_0 and n the fit of the Toth model was best for methane and ethane, and somewhat satisfactory for propane and n -butane except for the propane data at 275 °K. These results are plotted in Figures 4.14 to 4.17 and the value of the parameters are given in Table 4.5. The value of parameter K is higher than the intrinsic value for ethane, propane and n -butane, and for methane it is nearly the

same. The value of parameter n decreases with temperature for methane and propane but appears to be constant for ethane and n-butane. Conclusions regarding the N_0 is analogous to those in LRC model.

4.6.3. Fit of Mathews and Weber Model Using Optimized Parameters:

With optimized K , N_0 and n the fit of the model was best for all isotherms except for propane at 275°K. This can be observed from the Figures 4.18 to 4.21 and Table 4.6. It is observed that the value of optimized K is higher than the intrinsic value. The value of parameter n increases with temperature for methane and propane, whereas for ethane and n-butane it decreases with temperature. And the value of parameter N_0 is about the maximum experimental concentration for methane, ethane and propane but is slightly higher for n-butane.

4.6.4. Fit of Jaroniec Model Using Optimized Parameters:

With optimized K , N_0 , n and m the fit of Jaroniec model was best and is plotted in Figures 4.22 to 4.25 with the value of the parameters being given in the Table 4.7. The value of the parameter K is higher than the intrinsic value for all the sorbates. It was observed that for most of the cases one of the four parameters was not optimized. This indicates that three parameters are sufficient to define the pure compo-

nent isotherm.

4.6.5. Fit of Ruthven Model Using Optimized Parameters:

With optimized K' and β the fit of the Ruthven model was best for methane, ethane and propane, but for n-butane the model does not fit the data satisfactorily. This can be observed from Figures 4.26 to 4.29 with the parameters being given in Table 4.8. It was observed that the value of optimized β was close to the theoretical value for ethane, propane and n-butane, but for methane it was less. This probably reflects the fact that for this sorbate the value of β estimated originally is inaccurate due to being way above the critical temperature. A revised procedure to calculate β away above the critical temperature is probably required. Optimized β values reported here for methane are similar to those reported by Rolniak and Kobayashi (5) for this temperature range.

With all these models it was observed that the use of theoretical saturation concentration N_o was not applicable for sorbates ethane, propane and n-butane on Linde 5A pellets. Using the intrinsic Henry and Equilibrium constant the Jaroniec model fits the experimental data satisfactorily for methane, ethane and propane. The Mathews and Weber model fits the experimental data satisfactorily for n-butane better than any other model.

Using optimized K , N_0 , n and m all models fit the experimental data satisfactorily. In these models the Jaroniec model is the best for all components, but the value of K is much higher than the intrinsic Equilibrium constant and the value of N_0 for methane increases with temperature. The LRC and Toth models are second best with the value of K being closer to the intrinsic Equilibrium constant. The Mathews and Weber model is also good but again the value of K is slightly more than the LRC and Toth models and the value of N_0 for methane is lower than the other models.

The Ruthven model fits the data satisfactorily for sorbates methane, ethane and propane, but for methane the value of optimized β was less than the theoretical value. This is due to behaviour of methane which is supercritical at the room temperature.

4.7: Derivation of Multicomponent Ruthven Model:

The binary equation of Ruthven model derived by Holborow (2) can be extended to ternary and quaternary adsorption. For quaternary adsorption the partition function, with only a volume restriction upper limit on the number of molecules it contains, becomes

$$Q_{1234} = \sum_{i=0}^m \sum_{j=0}^n \sum_{k=0}^o \sum_{l=0}^p q\{i,j,k,l\} \lambda_1^i \lambda_2^j \lambda_3^k \lambda_4^l \quad (4.3)$$

where $q(i,j,k,l)$ is the partition function for a single cavity containing i molecules of species 1, j molecules of species 2, k molecules of species 3 and l molecules of species 4. The volume restriction limit requires that

$$i\beta_1 + j\beta_2 + k\beta_3 + l\beta_4 \leq v$$

Further we have that the expression for concentration is

$$C_1 = \frac{\sum_{i=0}^m \sum_{j=0}^n \sum_{k=0}^o \sum_{l=0}^p q\{i,j,k,l\} \lambda_1^i \lambda_2^j \lambda_3^k \lambda_4^l}{Q_{1234}} \quad (4.4)$$

The expression for the concentration of 1 becomes

$$C_1 = \frac{\sum_{i=0}^m \sum_{j=0}^n \sum_{k=0}^o \sum_{l=0}^p z\{i,j,k,l\} a_1^i a_2^j a_3^k a_4^l}{\sum_{i=0}^m \sum_{j=0}^n \sum_{k=0}^o \sum_{l=0}^p z\{i,j,k,l\} a_1^i a_2^j a_3^k a_4^l} \quad (4.5)$$

with similar expression for 2, 3 and 4. The configuration integrals can be given by

$$z\{0,0,0,0\} = z\{0\} = 1$$

$$z\{1,0,0,0\} a_1 = z_1 \{1\} \frac{P_1}{\kappa T} = K'_1 P_1$$

$$z\{0,1,0,0\}a_2 = z_2\{1\}\frac{P_2}{\kappa T} = K'_2 P_2$$

$$z\{0,0,1,0\}a_3 = z_3\{1\}\frac{P_3}{\kappa T} = K'_3 P_3 \quad (4.6)$$

$$z\{0,0,0,1\}a_4 = z_4\{1\}\frac{P_4}{\kappa T} = K'_4 P_4$$

$$z\{i,j,k,l\} = \frac{z\{1,0,0,0\}^i z\{0,1,0,0\}^j z\{0,0,1,0\}^k z\{0,0,0,1\}^l}{i!j!k!l!} \left(1 - \frac{\Sigma\beta}{v}\right)^{i+j+k+l}$$

where $i+j+k+l \geq 2$ and $\Sigma\beta = i\beta_1 + j\beta_2 + k\beta_3 + l\beta_4 \leq v$

Hence the isotherm equation becomes

$$C_1 = \frac{K'_1 P_1 + \frac{\sum_{i=0}^m \sum_{j=0}^n \sum_{k=0}^o \sum_{l=0}^p (K'_1 P_1)^i (K'_2 P_2)^j (K'_3 P_3)^k (K'_4 P_4)^l \left(1 - \frac{\Sigma\beta}{v}\right)^{i+j+k+l}}{(i-1)!j!k!l!}}{1 + K'_1 P_1 + K'_2 P_2 + K'_3 P_3 + K'_4 P_4 + \frac{\sum_{i=0}^m \sum_{j=0}^n \sum_{k=0}^o \sum_{l=0}^p (K'_1 P_1)^i (K'_2 P_2)^j (K'_3 P_3)^k (K'_4 P_4)^l \left(1 - \frac{\Sigma\beta}{v}\right)^{i+j+k+l}}{i!j!k!l!}} \quad (4.7)$$

This equation with the corresponding equation for C_2 , C_3 and C_4 gives the adsorption equilibria in terms of Henry's constant for the pure component and the molecular volume β , and provides a convenient means of predicting multicomponent equilibria from the data of pure components.

Equation (4.7) can be easily reduced to ternary and binary isotherm equations. The programs for calculation of concentrations are given in Appendix B.

4.7.1: *Fit Of Multicomponent Ruthven Model:*

The multicomponent Ruthven model derived in the previous section was used to fit the quaternary, ternary and binary equilibrium adsorption data using the intrinsic Henry's constant K' calculated from the K'_0 and $-\Delta U_0$ from the Table 4.1, and with the theoretical molecular volume β from Equation (1.1) given in Table 4.2.

The fit of the binary data is plotted in Figures 4.30 to 4.32 and the calculated concentration and mole fraction are given in Tables 4.9 to 4.11. The fit of the model is good for methane-ethane and ethane-propane binary adsorption and somewhat satisfactory for methane-propane binary.

The ternary and quaternary data analysed using Equation (4.7) are given in Tables 4.12 to 4.17. The fit of the model is good for methane-

ethane-propane ternary and also satisfactory for methane-ethane-n-butane ternary adsorption. And by comparing the calculated concentration and mole fraction with the experimental concentration and mole fraction it is interesting to observe that the fit of the model to the quaternary adsorption of methane-ethane-propane-n-butane is also quite satisfactory.

For n-butane the value of l , the maximum no of molecules per cavity, is equal to 4 but with this value the model isotherm did not give good results. Since the maximum number of molecules per cavity for n-butane in the quaternary adsorption is about 2.5 molecules per cavity, we use l equals to 3 and the fit of the model was good. Practically it is not possible to have 4 molecules per cavity of n-butane in the multicomponent adsorption in the ternary and quaternary case for 5A.

Table 4.1: Intrinsic Henry Constant (K'), Pre-exponential Factor (K'_0) And Heat Of Adsorption ($-\Delta U_0$) For Linde 5A Pellets.

Sorbate	Temperature °K	K' (molecule/cavity/torr)	$K'_0 \times 10^7$	$(-\Delta U_0)$ Kcal/mole
Methane	(a)275	0.0042	2.7	5.41
	(a)300	0.0020		
	(a)325	0.0012		
	(a)350	0.0007		
	(b)230	0.0317		
	(b)230	0.0393		
	(b)273	0.0078		
Ethane	(a)275	0.0524	1.31	7.45
	(a)300	0.0330		
	(a)325	0.0089		
	(a)350	0.0025		
	(b)230	1.7100		
	(b)273	0.1140		
	(b)324	0.0234		
	(b)345	0.0093		
	(b)298	0.0440		
	(b)308	0.0610		
	(b)318	0.0204		
Propane	(a)275	1.5062	19.5	7.60
	(a)300	0.2862		
	(a)325	0.1684		
	(a)350	0.0716		
	(b)273	3.9600		
	(b)273	3.8200		
	(b)323	0.3210		
	(b)358	0.1170		
	(b)358	0.1230		
	(b)398	0.0330		
n-butane	(a)275	0.3066	8.6	10.28
	(a)300	0.1651		
	(a)350	0.0818		
	(b)323	6.2400		
	(b)358	1.8700		
	(b)358	3.1100		
	(b)398	0.3690		
	(b)398	0.3740		
	(b)423	3.1750		
	(b)498	3.0176		
	(b)318	6.5300		
	(b)328	3.8700		
	(b)308	12.4300		
	(b)323	10.2900		

(a) This Work, and (b) Ref(1)

Table 4.2: Theoretical Saturation Concentration (N_o), Molecular Volume β And Intrinsic Equilibrium Constant ($K=K'/N_o$) For Linde 5A Pellets.

Sorbate	T °K	N_o mmoles/gm pellet	β $A^{0.3}$ / molecule	K (1/psia)
Methane	275	4.446	80.67	0.0221
	300	4.294	83.54	0.0111
	325	4.152	86.40	0.0066
	350	4.018	89.27	0.0042
Ethane	275	3.526	101.72	0.3460
	300	3.410	105.19	0.2256
	325	3.301	108.66	0.0631
	350	3.198	112.14	0.0178
Propane	275	2.745	130.65	12.7825
	300	2.693	133.16	2.4754
	325	2.644	135.67	1.4834
	350	2.596	138.19	0.6420
n-Butane	275	2.239	160.18	3.1903
	300	2.142	167.41	1.7955
	350	1.972	181.87	0.9660

Table 4.3: Optimised Parameters (K, n and m) of Methane For Different Models With Theoretical (N_0) For Linde 5A Pellets.

Model	T °K	K (1/psia)	Parameters		Sum of least squares
			n	m	
LRC	275	0.0156	1.2553		0.0414
	300	0.0079	1.1943		0.0140
	325	0.0050	1.0802		0.0336
	350	0.0032	1.0989		0.0031
Toth	275	0.0292	0.7105 [*]		0.0113
	300	0.0131	0.7521		0.0085
	325	0.0062	0.8953		0.0064
	350	0.0042	0.8317		0.0040
Mathews & Weber	275	0.0175	0.8983		0.1156
	300	0.0084	0.8532		0.0769
	325	0.0055	0.9471		0.0297
	350	0.0034	0.9645		0.0266
Jaroniec	275	0.0292	0.7110	1.0000	0.0112
	300	0.0131	0.7520	1.0000	0.0085
	325	0.0044	1.0000	0.8743	0.0036
	350	0.0033	0.9008	0.9194	0.0031

Table 4.4: Optimised Parameters (N_o , K & n) Of LRC Model For Linde 5A Pellets.

Sorbate	T Temperature °K	N_o Saturation Conc mmoles/gm pellet	K Equilibrium Constant (1/(psia))	n Parameter	Sum of Least Squares
Methane	275.00	3.882	0.0219	1.0840	0.00597
	300.00	3.992	0.0094	1.1136	0.01111
	325.00	4.643	0.0042	1.1290	0.00296
	350.00	4.554	0.0025	1.1460	0.00255
Ethane	275.00	2.141	0.6591	0.9182	0.03419
	300.00	2.104	0.3835	1.0224	0.00289
	350.00	1.430	0.0604	0.8603	0.01095
Propane	275.00	2.096	11.0086	1.3990	0.13434
	300.00	1.958	3.2186	1.1845	0.08756
	325.00	1.857	1.8666	1.3018	0.04803
	350.00	1.766	0.7961	1.3721	0.02024
N-Butane	275.00	1.455	8.2980	0.6861	0.02399
	300.00	1.400	5.2500	0.6000	0.01525
	350.00	1.400	2.3247	0.7320	0.00715

Table 4.5: Optimised Parameters (N_o , K & n) Of Toth Model For Linde 5A Pellets.

Sorbate	T Temperature °K	N_o Saturation Conc mmoles/gm pellet	K Equilibrium Constant (1/(psia))	n Parameter	Sum of Least Squares
Methane	275.00	4.008	0.0268	0.8418	0.00492
	300.00	4.484	0.0131	0.7152	0.00818
	325.00	5.714	0.0054	0.6745	0.00250
	350.00	6.000	0.0033	0.6289	0.00210
Ethane	275.00	2.157	0.6374	1.0000	0.03990
	300.00	2.113	0.4071	0.9539	0.00255
	350.00	1.486	0.0571	1.0000	0.01554
Propane	275.00	2.076	12.0000	0.8600	0.28546
	300.00	1.992	5.3820	0.7354	0.08069
	325.00	1.899	4.2610	0.6470	0.03869
	350.00	1.815	2.1240	0.6118	0.01698
N-Butane	275.00	1.547	7.3665	1.0000	0.10260
	300.00	1.426	4.2645	1.0000	0.13808
	350.00	1.600	1.5812	1.0000	0.02451

Table 4.6: Optimised Parameters (N_0 , K & n) Of Mathews and Weber Model For Linde 5A Pellets.

Sorbate	T Temperature °K	N_0 Saturation mmoles/gm pellet	K Equilibrium Constant ($1/(psia)$)	n Parameter	Sum of Least Squares
Methane	275.00	3.223	0.0319	1.0727	0.00380
	300.00	2.690	0.0204	1.1724	0.00598
	325.00	2.924	0.0100	1.2444	0.00246
	350.00	2.283	0.0088	1.4130	0.00145
Ethane	275.00	2.122	0.6620	1.0040	0.03950
	300.00	2.014	0.4211	1.0130	0.00191
	350.00	1.600	0.0486	0.9690	0.01410
Propane	275.00	1.894	10.0000	1.0164	0.32545
	300.00	1.570	5.3680	1.0441	0.05004
	325.00	1.304	4.3545	1.0707	0.01506
	350.00	1.300	1.6673	1.0624	0.00995
N-Butane	275.00	1.816	5.3600	0.9506	0.07340
	300.00	1.850	2.8050	0.9218	0.05314
	350.00	1.850	1.1540	0.8000	0.01687

Table 4.7: Optimised Parameters (N_o , K , m & n) Of Jaroniec Model For Linde 5A Pellets.

Sorbate	T Temperature °K	N_o Saturation conc mmoles/gm pellet	K Equilibrium Constant (1/(psia))	n Parameters	m Parameters	Sum of least squares
Methane	275.00	4.375	0.0731	0.6599	1.4390	0.00370
	300.00	5.392	0.0526	0.5172	1.5000	0.00521
	325.00	5.499	0.0061	0.6808	1.0313	0.00261
	350.00	5.500	0.0052	0.6147	1.1101	0.00255
Ethane	275.00	2.169	4.3450	0.8373	3.0000	0.01290
	300.00	2.148	0.7286	0.8430	1.2930	0.00122
	350.00	1.481	0.3000	0.8956	3.0000	0.008316
Propane	275.00	2.182	30.7126	0.5000	0.7876	0.06135
	300.00	1.983	5.3429	0.7429	1.0000	0.01864
	325.00	1.902	4.3491	0.6417	1.0000	0.03876
	350.00	1.850	2.4718	0.5712	1.0000	0.01721
n-Butane	275.00	1.500	12.4866	1.4242	1.8585	0.02719
	300.00	1.500	5.2184	1.3834	1.6075	0.06606
	350.00	1.500	4.7265	1.0105	2.0000	0.00327

Table 4.8: Optimised Parameters (β & K') Of Ruthven Model For Linde 5A Pellets.

Sorbate	T Temperature °K	β Molecular Volume $A_{03}/\text{molecule}$	K' Henry Constant (molecules/cavity/psia)	Sum of least squares
Methane	275.00	58.69	0.2540	0.00428
	300.00	58.61	0.1171	0.00925
	325.00	55.00	0.0609	0.05336
	350.00	57.79	0.0389	0.00418
Ethane	275.00	119.61	5.6835	0.16241
	300.00	112.62	2.8097	0.04579
	350.00	150.00	0.3331	0.06836
Propane	275.00	139.36	145.7870	0.01536
	300.00	137.18	30.8711	0.07852
	325.00	141.27	16.2980	0.03593
	350.00	155.06	7.6689	0.01463
n-Butane	275.00	163.19	52.7990	0.31077
	300.00	174.04	28.5790	0.31243
	350.00	150.00	8.6472	0.07180

TABLE 4.9: BINARY ADSORPTION OF METHANE & ETHANE ON LINDE 5A PELLETS
AT 300.00 DEGREE KELVIN AND 50.00 PSIA TOTAL PRESSURE.

		HENRY CONSTANT (MOLECULES/CAVITY/PSIA)			
		HK1	HK2	HK3	HK4
		0.122	1.820	34.950	1385.000
		MOLECULAR VOLUME			
		CUBIC ANGSTROM/MOLECULE			
		BETA1	BETA2	BETA3	BETA4
		83.5344	105.1899	133.1647	167.4126
		ADSORB PHASE CONCENTRATION AND MOLE FRACTION			
PARTIAL PRESSURES	METHANE PSIA	EXPERIMENTAL		THEORETICAL	
		METHANE MMOLE/GM	ETHANE PELLET	METHANE MMOLE/GM	ETHANE PELLET
19.4072	32.1528	0.0400	2.2100	0.1086	1.8609
24.0089	36.3150	0.1300	1.9200	0.1226	1.8875
28.2757	22.8743	0.2100	1.9100	0.1950	1.6921
31.5115	18.8585	0.2900	1.8200	0.2435	1.5938
34.3395	16.1004	0.3600	1.7500	0.2897	1.5078
36.1888	13.9412	0.4100	1.6800	0.3300	1.4298
37.4644	12.3156	0.4600	1.6100	0.3646	1.3623
38.9928	11.0172	0.5200	1.5500	0.4007	1.2984
40.2383	9.9717	0.5600	1.4900	0.4334	1.2410
40.9275	10.1425	0.5600	1.4900	0.4360	1.2459
41.7129	9.3871	0.5800	1.4400	0.4605	1.2021
41.1912	8.4487	0.6200	1.3900	0.4795	1.1508
42.3286	7.8714	0.6600	1.3500	0.5070	1.1081
42.7291	7.3108	0.6900	1.3100	0.5284	1.0678
43.0923	6.8177	0.7200	1.2700	0.5486	1.0300
43.7445	6.4155	0.7400	1.2300	0.5698	0.9953
43.8230	6.4270	0.7400	1.2300	0.5702	0.9958
44.0793	6.0507	0.7700	1.1900	0.5874	0.9638
44.3027	5.7173	0.8000	1.1600	0.6034	0.9339
44.7516	5.4184	0.8300	1.1300	0.6211	0.9046
44.9856	5.1544	0.8500	1.1000	0.6356	0.8785
45.2423	4.8877	0.8800	1.0700	0.6512	0.8510
45.3187	4.6413	0.9100	1.0400	0.6643	0.8255
45.6237	4.4462	0.9400	1.0100	0.6779	0.8032
46.2267	4.2832	0.9600	0.9800	0.6935	0.7823
45.9801	4.0799	0.9800	0.9600	0.7021	0.7606
46.0900	3.9100	1.0000	0.9400	0.7132	0.7403
46.2265	3.7535	1.0100	0.9100	0.7242	0.7208
		EXPERIMENTAL		THEORETICAL	
		METHANE MMOLE/GM	ETHANE PELLET	METHANE MMOLE/GM	ETHANE PELLET
0.0551	0.9449	0.0551	0.9449	0.0551	0.9449
0.0610	0.9390	0.0610	0.9390	0.0610	0.9390
0.1033	0.8967	0.1033	0.8967	0.1033	0.8967
0.1325	0.8675	0.1325	0.8675	0.1325	0.8675
0.1612	0.8388	0.1612	0.8388	0.1612	0.8388
0.1875	0.8125	0.1875	0.8125	0.1875	0.8125
0.2111	0.7889	0.2111	0.7889	0.2111	0.7889
0.2359	0.7641	0.2359	0.7641	0.2359	0.7641
0.2588	0.7412	0.2588	0.7412	0.2588	0.7412
0.2592	0.7408	0.2592	0.7408	0.2592	0.7408
0.2770	0.7230	0.2770	0.7230	0.2770	0.7230
0.2941	0.7059	0.2941	0.7059	0.2941	0.7059
0.3139	0.6861	0.3139	0.6861	0.3139	0.6861
0.3310	0.6690	0.3310	0.6690	0.3310	0.6690
0.3475	0.6525	0.3475	0.6525	0.3475	0.6525
0.3641	0.6359	0.3641	0.6359	0.3641	0.6359
0.3787	0.6213	0.3787	0.6213	0.3787	0.6213
0.3925	0.6075	0.3925	0.6075	0.3925	0.6075
0.4071	0.5929	0.4071	0.5929	0.4071	0.5929
0.4198	0.5802	0.4198	0.5802	0.4198	0.5802
0.4335	0.5665	0.4335	0.5665	0.4335	0.5665
0.4459	0.5541	0.4459	0.5541	0.4459	0.5541
0.4577	0.5423	0.4577	0.5423	0.4577	0.5423
0.4699	0.5301	0.4699	0.5301	0.4699	0.5301
0.4800	0.5200	0.4800	0.5200	0.4800	0.5200
0.4907	0.5093	0.4907	0.5093	0.4907	0.5093
0.5012	0.4988	0.5012	0.4988	0.5012	0.4988

TABLE 4.10: BINARY ADSORPTION OF METHANE & PROPANE ON LINDE 5A PELLETS
AT 300.00 DEGREE KELVIN AND 50.00 PSIA TOTAL PRESSURE.

PARTIAL PRESSURES		ADSORB PHASE CONCENTRATION AND MOLE FRACTION		THEORETICAL		EXPERIMENTAL		THEORETICAL		EXPERIMENTAL		THEORETICAL	
METHANE PSIA	PROPANE PSIA	EXPERIMENTAL METHANE MMOLE/GM PELLETT	PROPANE MMOLE/GM PELLETT	THEORETICAL METHANE MMOLE/GM PELLETT	PROPANE MMOLE/GM PELLETT	EXPERIMENTAL METHANE MMOLE/GM PELLETT	PROPANE MMOLE/GM PELLETT	THEORETICAL METHANE MMOLE/GM PELLETT	PROPANE MMOLE/GM PELLETT	EXPERIMENTAL METHANE MMOLE/GM PELLETT	PROPANE MMOLE/GM PELLETT	THEORETICAL METHANE MMOLE/GM PELLETT	PROPANE MMOLE/GM PELLETT
14.2328	38.6772	0.0600	1.6900	0.0131	2.0605	0.0343	0.9657	0.0063	0.9937	0.0063	0.9937	0.0063	0.9937
22.5679	27.3721	0.0700	1.6300	0.0264	2.0078	0.0412	0.9588	0.0130	0.9870	0.0130	0.9870	0.0130	0.9870
31.0658	20.2742	0.0900	1.5600	0.0442	1.9556	0.0545	0.9455	0.0221	0.9779	0.0221	0.9779	0.0221	0.9779
34.9250	15.7350	0.1000	1.5100	0.0582	1.9112	0.0621	0.9379	0.0295	0.9705	0.0295	0.9705	0.0295	0.9705
37.9589	12.3911	0.1600	1.4600	0.0731	1.8676	0.0988	0.9012	0.0377	0.9623	0.0377	0.9623	0.0377	0.9623
42.7548	10.2251	0.1700	1.4100	0.0922	1.8276	0.1076	0.8924	0.0480	0.9520	0.0480	0.9520	0.0480	0.9520
42.3237	8.4363	0.1700	1.3800	0.1025	1.7926	0.1097	0.8903	0.0541	0.9459	0.0541	0.9459	0.0541	0.9459
43.5962	7.1738	0.1900	1.3400	0.1161	1.7594	0.1242	0.8758	0.0619	0.9381	0.0619	0.9381	0.0619	0.9381
43.2813	6.1887	0.2000	1.3100	0.1259	1.7303	0.1325	0.8675	0.0678	0.9322	0.0678	0.9322	0.0678	0.9322
44.5660	5.4239	0.2100	1.2900	0.1400	1.7005	0.1400	0.8600	0.0761	0.9239	0.0761	0.9239	0.0761	0.9239
45.6631	4.8268	0.2100	1.2600	0.1535	1.6730	0.1429	0.8571	0.0841	0.9159	0.0841	0.9159	0.0841	0.9159
45.5380	4.3120	0.2100	1.2400	0.1636	1.6477	0.1448	0.8552	0.0903	0.9097	0.0903	0.9097	0.0903	0.9097
45.8687	3.8912	0.2200	1.2200	0.1751	1.6229	0.1528	0.8472	0.0974	0.9026	0.0974	0.9026	0.0974	0.9026
46.3657	3.5543	0.2400	1.2000	0.1865	1.5998	0.1667	0.8333	0.1044	0.8956	0.1044	0.8956	0.1044	0.8956
47.8821	2.3878	0.2500	1.1900	0.2423	1.4903	0.1736	0.8264	0.1398	0.8602	0.1398	0.8602	0.1398	0.8602

HENRY CONSTANT
(MOLECULES/CAVITY/PSIA)
HK1 HK2 HK3 HK4
0.122 1.820 34.950 1385.000

MOLECULAR VOLUME
CUBIC ANGSTROM/MOLECULE
BETA1 BETA2 BETA3 BETA4
83.5344 105.1899 133.1647 167.4126

TABLE 4.12 TERNARY ADSORPTION OF METHANE-ETHANE-& PROPANE ON LINDE 5A PELLETS
AT 300.00 DEGREE KELVIN AND 50.0 PSIA TOTAL PRESSURE.

			HENRY CONSTANT (MOLECULES/CAVITY/PSIA)							
			HK1	HK2	HK3	HK4				
			0.122	1.8206	34.950	1385.000				
			MOLECULAR VOLUME CUBIC ANGSTROM/MOLECULE							
			BETA1	BETA2	BETA3	BETA4				
			83.5344	105.1899	133.1647	167.4126				
PARTIAL PRESSURES										
		ETHANE PSIA	PROPANE PSIA	EXPERIMENTAL MOLE FRACTION						
METHANE PSIA			METHANE	ETHANE	PROPANE	METHANE	ETHANE	PROPANE	FRACTION PROPANE	
13.4466	25.8383	10.9451	0.0105	0.2584	0.7311	0.0119	0.1973	0.7908		
23.1889	18.6838	8.0173	0.0259	0.2389	0.7352	0.0258	0.1849	0.7893		
29.5371	14.1553	6.1677	0.0423	0.2195	0.7382	0.0397	0.1739	0.7864		
34.0500	11.0000	4.9500	0.0591	0.2021	0.7388	0.0535	0.1621	0.7845		
37.0058	8.8024	4.0968	0.0733	0.1866	0.7401	0.0665	0.1515	0.7820		
39.1336	7.2090	3.4774	0.0881	0.1725	0.7394	0.0790	0.1420	0.7791		
40.9668	6.0088	3.0144	0.1015	0.1596	0.7389	0.0914	0.1330	0.7756		
42.4121	5.0933	2.6746	0.1140	0.1483	0.7377	0.1030	0.1243	0.7727		
43.6947	4.4205	2.4048	0.1260	0.1377	0.7363	0.1142	0.1175	0.7683		
45.0498	3.8580	2.1820	0.1338	0.1284	0.7378	0.1259	0.1108	0.7633		
44.7750	3.3744	1.9906	0.1273	0.1223	0.7504	0.1337	0.1046	0.7617		
23.7665	22.8927	5.0149	0.0455	0.3573	0.5971	0.0329	0.2923	0.6748		
15.9536	28.7395	5.5069	0.0326	0.3971	0.5704	0.0200	0.3286	0.6514		
10.5053	33.6628	5.7619	0.0246	0.4271	0.5483	0.0124	0.3590	0.6286		
22.1617	24.5879	4.2203	0.0658	0.3933	0.5409	0.0328	0.3405	0.6267		
28.3827	18.8780	3.2693	0.0603	0.3799	0.5598	0.0506	0.3240	0.6253		
32.3941	14.9430	2.6229	0.0751	0.3590	0.5659	0.0678	0.3085	0.6237		
35.4939	12.2105	2.1956	0.0902	0.3391	0.5707	0.0847	0.2928	0.6226		

TABLE 4.13 TERNARY ADSORPTION OF METHANE-ETHANE & PROPANE ON LINDE 5A PELLETS

AT 300.00 DEGREE KELVIN AND 50.0 PSIA TOTAL PRESSURE.

HENRY CONSTANT (MOLECULES/CAVITY PSIA)			MOLECULAR VOLUME CUBIC ANGSTROM/MOLECULE		
HK1	HK2	HK3	BETA1	BETA2	BETA3
0.122	1.820	34.950	83.5344	105.1899	133.1647
			167.4126		
BETA4			BETA4		
			167.4126		
PARTIAL PRESSURES			ADSORB PHASE CONCENTRATION		
METHANE PSIA	ETHANE PSIA	PROPANE PSIA	EXPERIMENTAL CONCENTRATION		
			METHANE (MILLIMOLES/GM PELLETT)	ETHANE (MILLIMOLES/GM PELLETT)	PROPANE (MILLIMOLES/GM PELLETT)
13.4466	25.8383	10.9451	0.0220	0.5400	1.5280
23.1889	18.6838	8.0173	0.0530	0.4890	1.5050
29.5371	14.1553	6.1677	0.0850	0.4410	1.4830
34.0500	11.0000	4.9500	0.1170	0.4000	1.4620
37.0058	8.8024	4.0968	0.1430	0.3640	1.4440
39.1336	7.2090	3.4774	0.1700	0.3330	1.4270
40.9668	6.0088	3.0144	0.1940	0.3050	1.4120
42.4121	5.0933	2.6746	0.2160	0.2810	1.3980
43.6947	4.4205	2.4048	0.2370	0.2590	1.3850
45.0498	3.8580	2.1820	0.2490	0.2390	1.3730
44.7750	3.3744	1.9906	0.2310	0.2220	1.3620
23.7665	22.8927	5.0149	0.0980	0.7690	1.2850
15.9536	28.7395	5.5069	0.0710	0.8660	1.2440
10.5053	33.6628	5.7619	0.0540	0.9370	1.2030
22.1617	24.5879	4.2203	0.1450	0.8660	1.1910
28.3827	18.8780	3.2693	0.1270	0.8000	1.1790
32.3941	14.9430	2.6229	0.1550	0.7410	1.1680
35.4939	12.2105	2.1956	0.1830	0.6880	1.1580
			THEORETICAL CONCENTRATION		
			METHANE (MILLIMOLES/GM PELLETT)	ETHANE (MILLIMOLES/GM PELLETT)	PROPANE (MILLIMOLES/GM PELLETT)
			0.0240	0.3961	1.5882
			0.0508	0.3636	1.5519
			0.0765	0.3355	1.5175
			0.1015	0.3074	1.4882
			0.1242	0.2831	1.4609
			0.1455	0.2616	1.4355
			0.1663	0.2420	1.4115
			0.1854	0.2238	1.3911
			0.2037	0.2096	1.3701
			0.2226	0.1959	1.3495
			0.2341	0.1831	1.3333
			0.0642	0.5715	1.3194
			0.0397	0.6510	1.2903
			0.0248	0.7177	1.2569
			0.0641	0.6653	1.2244
			0.0969	0.6198	1.1962
			0.1272	0.5785	1.1696
			0.1561	0.5397	1.1477

TABLE 4.14 TERNARY ADSORPTION OF METHANE-ETHANE-& N-BUTANE ON LINDE 5A PELLETS
AT 300.00 DEGREE KELVIN AND 50.00 PSIA TOTAL PRESSURE.

			HENRY CONSTANT (MOLECULES/CAVITY/PSIA)			
			HK1	HK2	HK3	HK4
			0.122	1.8206	34.950	1385.000
			MOLECULAR VOLUME CUBIC ANGSTROM/MOLECULE			
			BETA1	BETA2	BETA3	BETA4
			83.5344	105.1899	133.1647	167.4126
PARTIAL PRESSURES			ADSORB PHASE MOLE FRACTIONS			
			EXPERIMENTAL MOLE FRACTION		THEORETICAL MOLE FRACTION	
			METHANE	ETHANE	N-BUTANE	ETHANE
			PSIA	PSIA	PSIA	N-BUTANE
METHANE	ETHANE	N-BUTANE				
PSIA	PSIA	PSIA				
16.3008	29.6701	4.1391	0.0145	0.1679	0.8176	0.0143
26.4350	20.8250	2.7350	0.0377	0.1463	0.8161	0.0281
32.9090	14.9800	2.0110	0.0392	0.1171	0.8437	0.0410
37.4349	11.0582	1.5669	0.0591	0.0999	0.8410	0.0530
40.7302	8.2992	1.3605	0.0573	0.0802	0.8625	0.0637
42.6476	6.3363	1.0661	0.0675	0.0662	0.8663	0.0731
44.2150	4.9050	0.8800	0.0773	0.0540	0.8687	0.0816
29.5189	18.3928	1.7583	0.0395	0.1509	0.8096	0.0342
19.4072	28.2887	2.2841	0.0203	0.2008	0.7790	0.0182
12.3999	35.1121	2.5481	0.0113	0.2320	0.7567	0.0104
7.8773	39.5869	2.6458	0.0063	0.2491	0.7447	0.0062
4.9439	42.4839	2.6121	0.0037	0.2677	0.7285	0.0038
3.0775	44.3595	2.5230	0.0025	0.2797	0.7178	0.0023
1.9554	45.6241	2.4305	0.0019	0.2923	0.7059	0.0014
17.0784	31.3513	1.5803	0.0196	0.2593	0.7211	0.0159
26.2823	22.5199	1.0978	0.0337	0.2275	0.7388	0.0296
33.1683	16.6322	0.7995	0.0526	0.1974	0.7500	0.0440
16.3095	27.6290	5.8615	0.0030	0.1246	0.8724	0.0146
27.1810	19.2583	4.1156	0.0263	0.0988	0.8749	0.0293
33.0672	13.6751	3.0577	0.0342	0.0799	0.8859	0.0418
37.7550	9.9250	2.3200	0.0451	0.0636	0.8914	0.0542
41.1321	7.2920	1.8658	0.0495	0.0508	0.8997	0.0654
42.9900	5.4850	1.5250	0.0610	0.0396	0.8994	0.0742
						0.0844
						0.8414
						0.7825
						0.7960
						0.8098
						0.8217
						0.8324
						0.8414

TABLE 4.15 TERNARY ADSORPTION OF METHANE-ETHANE & N-BUTANE ON LINDE 5A PELLETS
AT 300.00 DEGREE KELVIN AND 50.00 PSIA TOTAL PRESSURE.

HENRY CONSTANT (MOLECULES/CAVITY/PSIA)			
HK1	HK2	HK3	HK4
0.122	1.820	34.950	1385.000
MOLECULAR VOLUME CUBIC ANGSTROM/MOLECULE			
BETA1	BETA2	BETA3	BETA4
83.5344	105.1899	133.1647	167.4126
PARTIAL PRESSURES			
METHANE PSIA	ETHANE PSIA	N-BUTANE PSIA	
16.3008	29.6701	4.1391	
26.4350	20.8250	2.7350	
32.9090	14.9800	2.0110	
37.4349	11.0582	1.5669	
40.7302	8.2992	1.3605	
42.6476	6.3363	1.0661	
44.2150	4.9050	0.8800	
29.5189	18.3928	1.7583	
19.4072	28.2887	2.2841	
12.3999	35.1121	2.5481	
7.8773	39.5869	2.6458	
4.9439	42.4839	2.6121	
3.0775	44.3595	2.5230	
1.9554	45.6241	2.4305	
17.0784	31.3513	1.5803	
26.2823	22.5199	1.0978	
33.1683	16.6322	0.7995	
16.3095	27.6290	5.8615	
27.1810	19.2583	4.1156	
33.0672	13.6751	3.0577	
37.7550	9.9250	2.3200	
41.1321	7.2920	1.8658	
42.9900	5.4850	1.5250	
ADSORB PHASE CONCENTRATION			
EXPERIMENTAL CONCENTRATION METHANE (MILLIMOLES/GM PELLETT)	ETHANE (MILLIMOLES/GM PELLETT)	N-BUTANE (MILLIMOLES/GM PELLETT)	
0.0230	0.2670	1.3000	
0.0600	0.2330	1.3000	
0.0600	0.1790	1.2900	
0.0900	0.1520	1.2800	
0.0850	0.1190	1.2800	
0.0990	0.0970	1.2700	
0.1130	0.0790	1.2700	
0.0610	0.2330	1.2500	
0.0320	0.3170	1.2300	
0.0180	0.3710	1.2100	
0.0100	0.3980	1.1900	
0.0060	0.4300	1.1700	
0.0040	0.4520	1.1600	
0.0030	0.4720	1.1400	
0.0310	0.4100	1.1400	
0.0520	0.3510	1.1400	
0.0800	0.3000	1.1400	
0.0050	0.2100	1.4700	
0.0440	0.1650	1.4610	
0.0560	0.1310	1.4520	
0.0730	0.1030	1.4440	
0.0790	0.0810	1.4360	
0.0970	0.0630	1.4300	
THEORETICAL CONCENTRATION			
ETHANE (MILLIMOLES/GM PELLETT)	N-BUTANE (MILLIMOLES/GM PELLETT)		
0.3642	1.3239		
0.3140	1.3214		
0.2662	1.3203		
0.2237	1.3195		
0.1848	1.3208		
0.1547	1.3181		
0.1289	1.3159		
0.3060	1.3097		
0.3767	1.3043		
0.4146	1.2993		
0.4376	1.2949		
0.4538	1.2900		
0.4660	1.2850		
0.4754	1.2806		
0.4206	1.2776		
0.3713	1.2738		
0.3254	1.2693		
0.3457	1.3333		
0.2925	1.3326		
0.2442	1.3323		
0.2012	1.3313		
0.1634	1.3306		
0.1333	1.3296		

TABLE 4.16 QUATERNARY ADSORPTION OF METHANE-ETHANE-PROPANE- & N-BUTANE ON LINDE 5A PELLETS

AT 300.00 DEGREE KELVIN AND 50.00 PSIA TOTAL PRESSURE

[illegible]

TABLE 4.17 QUATERNARY ADSORPTION OF METHANE-ETHANE-PROPANE- & N-BUTANE ON LINDE 5A PELLETS

HENRY CONSTANT (MOLECULES/CAVITY/PSIA)									
HK1		HK2		HK3		HK4			
0.1220		1.820		34.950		1385.000			
MOLECULAR VOLUME (CUBIC ANGSTROM/MOLECULE)									
BETA1		BETA2		BETA3		BETA4			
83.5344		105.1899		133.1647		167.4126			
PARTIAL PRESSURES				ADSORB PHASE CONCENTRATION					
METHANE PSIA		PROPANE PSIA		ETHANE PSIA		EXPERIMENTAL CONCENTRATION ETHANE PROPANE N-BUTANE ML/IMOLE/GM PELLETT		THEORETICAL FROM RUTHVEN MODEL ETHANE PROPANE N-BUTANE ML/IMOLE/GM PELLETT	
15.9250	29.1300	2.8250	2.1000	0.0320	0.3770	0.1810	1.1360	0.0182	0.2682
25.8748	20.5909	2.0546	1.4497	0.0550	0.3280	0.1750	1.1330	0.0361	0.2406
32.3150	15.0400	1.5650	1.0500	0.0830	0.2840	0.1700	1.1300	0.0534	0.2147
36.6800	11.2650	1.2300	0.8000	0.0960	0.2480	0.1650	1.1270	0.0701	0.1901
39.6176	8.6160	1.0028	0.6536	0.1180	0.2180	0.1610	1.1240	0.0849	0.1660
42.0374	6.7579	0.8328	0.5017	0.1430	0.1920	0.1570	1.1220	0.1011	0.1487
43.4157	5.4476	0.7310	0.4707	0.1540	0.1690	0.1540	1.1200	0.1106	0.1278
29.6197	18.0652	1.2323	0.9479	0.0930	0.3360	0.1410	1.1080	0.0507	0.2670
19.3751	27.7549	1.4723	1.2977	0.0650	0.4320	0.1280	1.0960	0.0278	0.3317
12.4740	34.8566	1.5422	1.5120	0.0500	0.4960	0.1180	1.0840	0.0164	0.3736
7.9420	38.9310	1.5135	1.5634	0.0420	0.5310	0.1080	1.0730	0.0101	0.4017
5.0419	41.8778	1.4277	1.5475	0.0370	0.5670	0.0990	1.0630	0.0064	0.4269
3.2667	43.7811	1.3437	1.5484	0.0320	0.5850	0.0910	1.0530	0.0041	0.4433
17.6600	30.3900	0.9350	1.0000	0.0610	0.5200	0.0890	1.0510	0.0277	0.4021
26.6466	22.0170	0.6857	0.7007	0.0820	0.4590	0.0870	1.0500	0.0502	0.3627
32.6521	16.4791	0.5319	0.5018	0.1150	0.4060	0.0850	1.0480	0.0724	0.3286
37.0150	12.7158	0.4196	0.4045	0.1230	0.3590	0.0830	1.0470	0.0925	0.2917
39.1964	10.0199	0.3543	0.2994	0.1510	0.3200	0.0820	1.0450	0.1116	0.2681
41.4967	8.1407	0.3013	0.2511	0.1720	0.2850	0.0800	1.0440	0.1291	0.2414

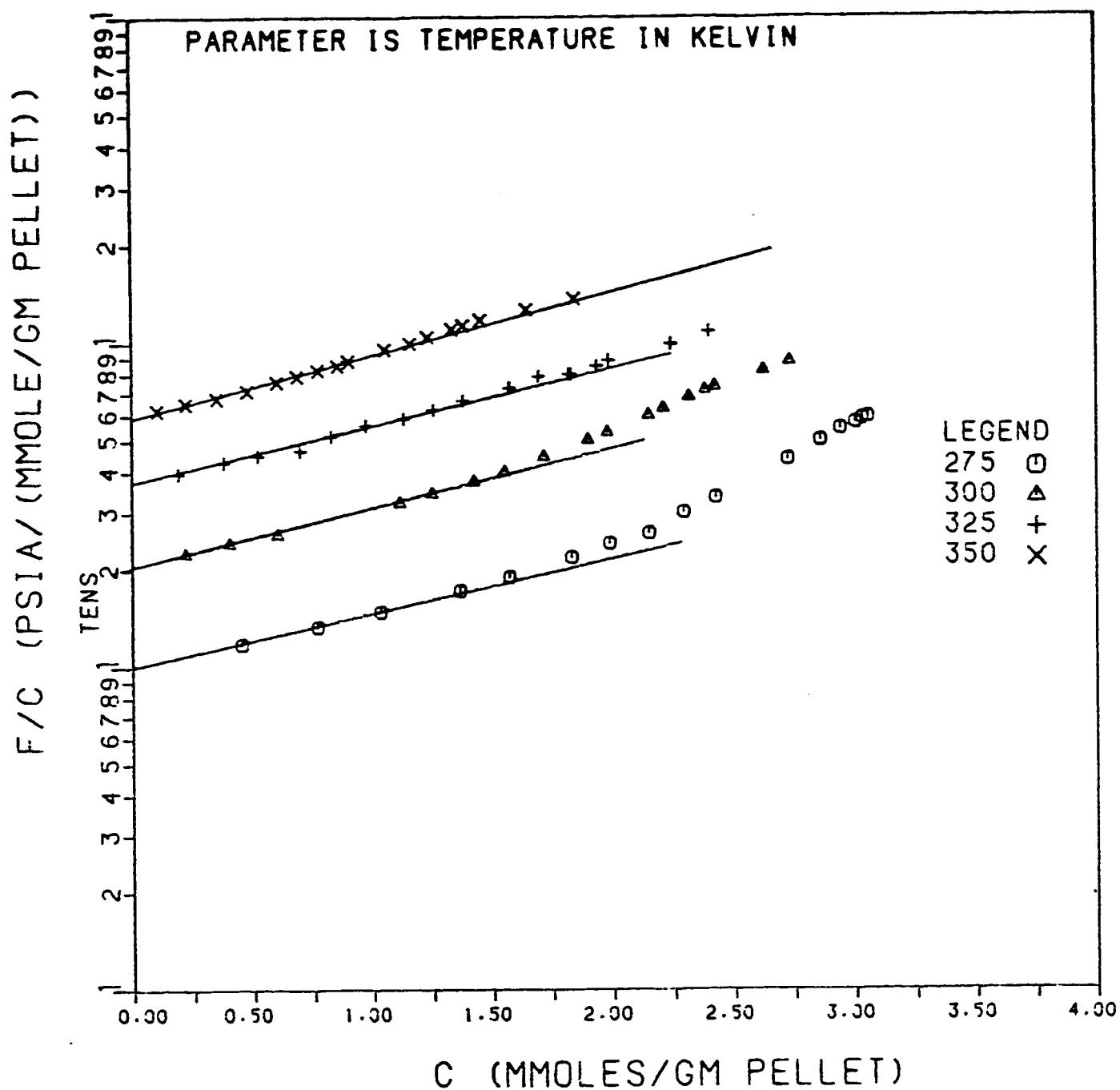


Fig. 4.1: Virial Isotherm of Methane on Linde 5A Pellets.

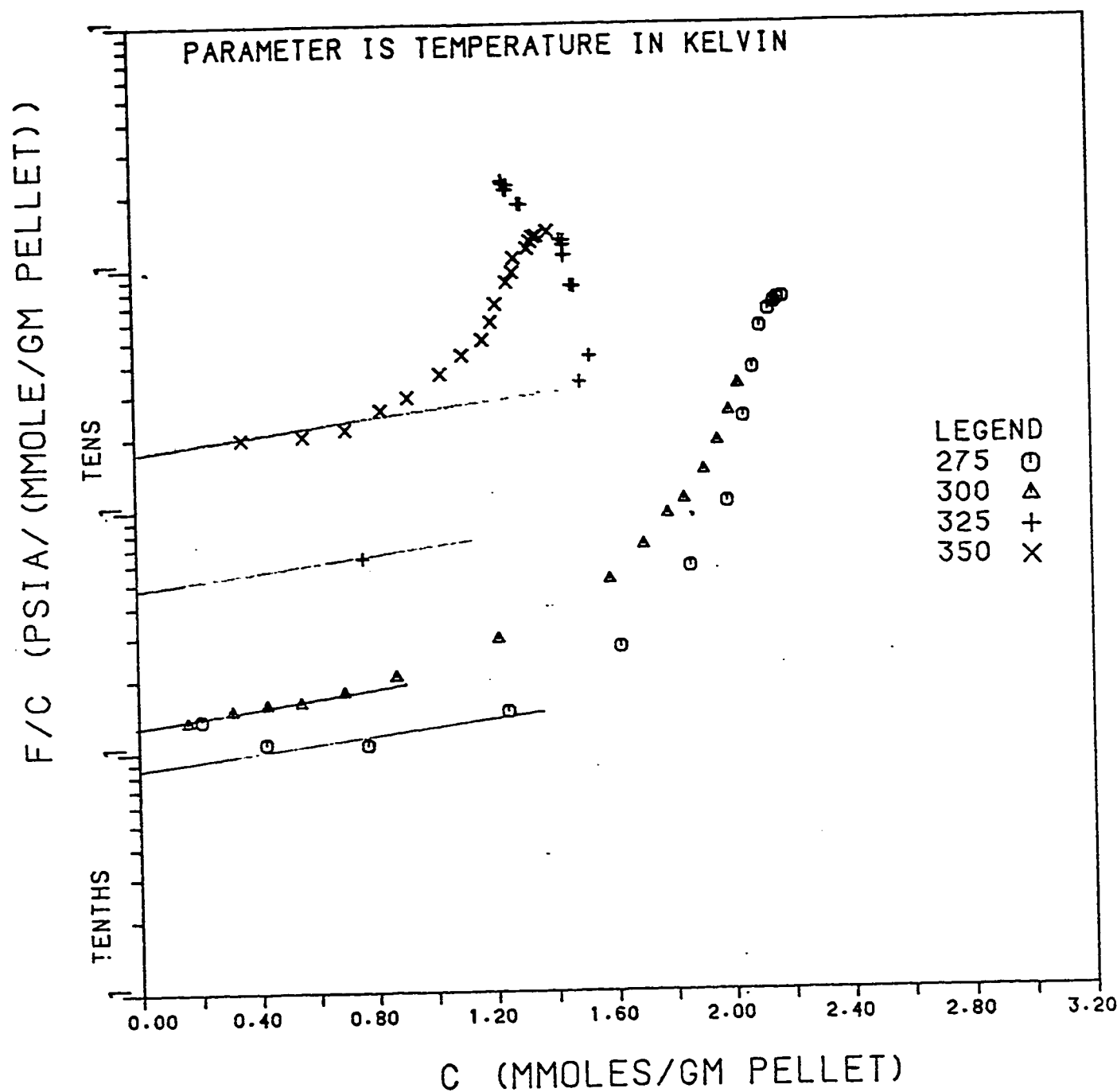


Fig. 4.2: Virial Isotherm of Ethane on Linde 5A Pellets.

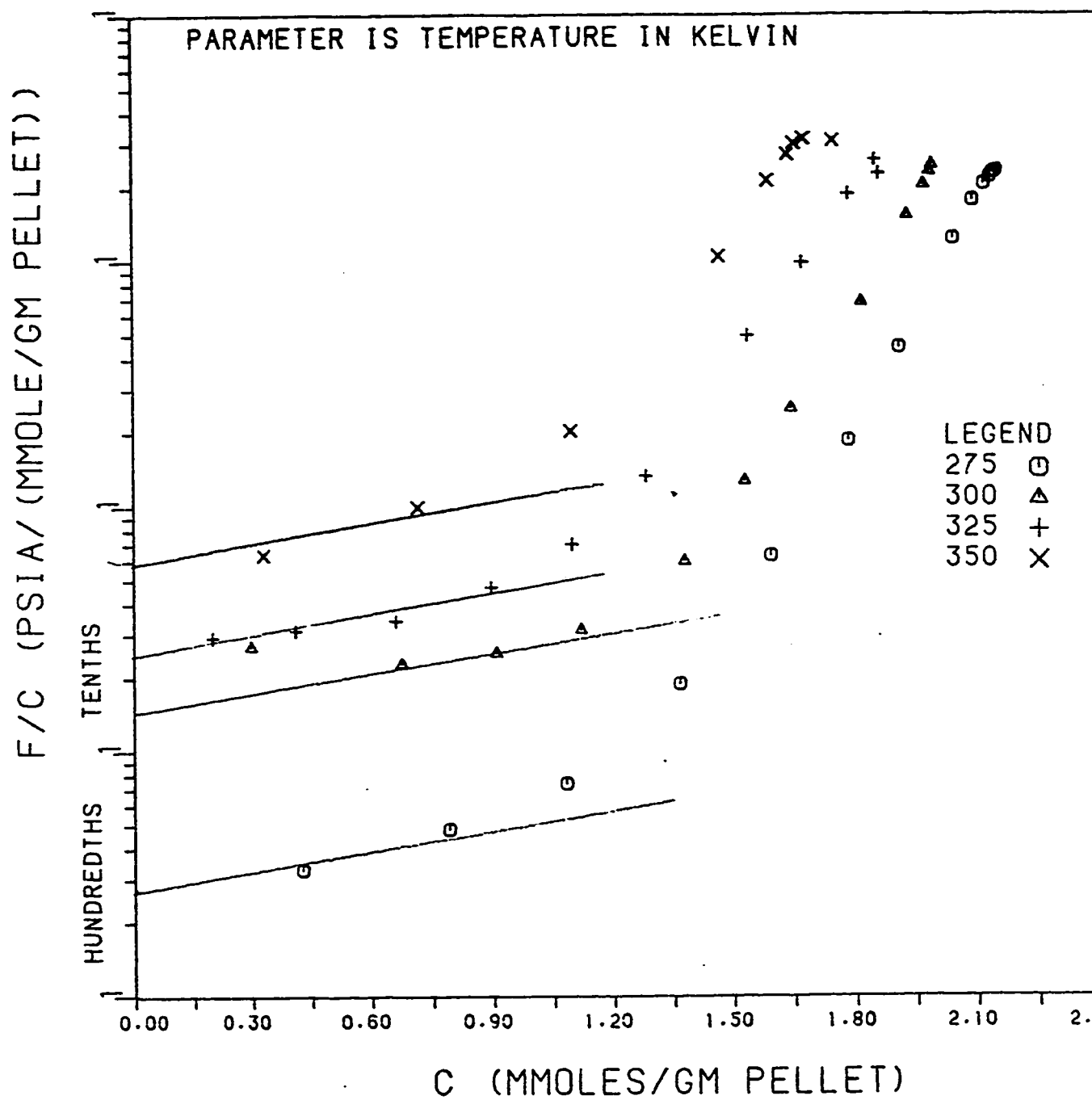


Fig. 4.3: Virial Isotherm of Propane on Linde 5A Pellets.

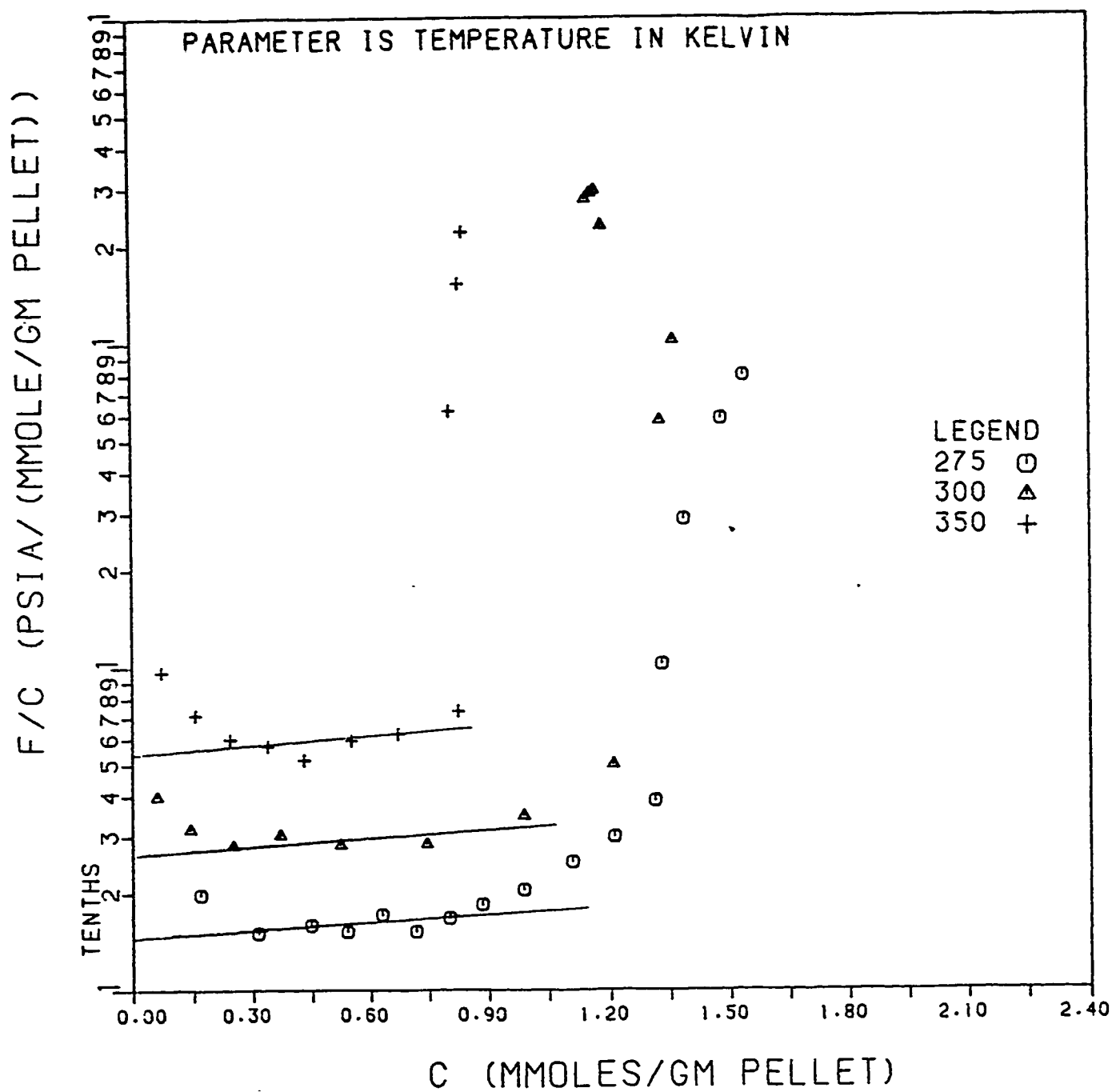


Fig. 4.4: Virial Isotherm of n-Butane on Linde 5A Pellets.

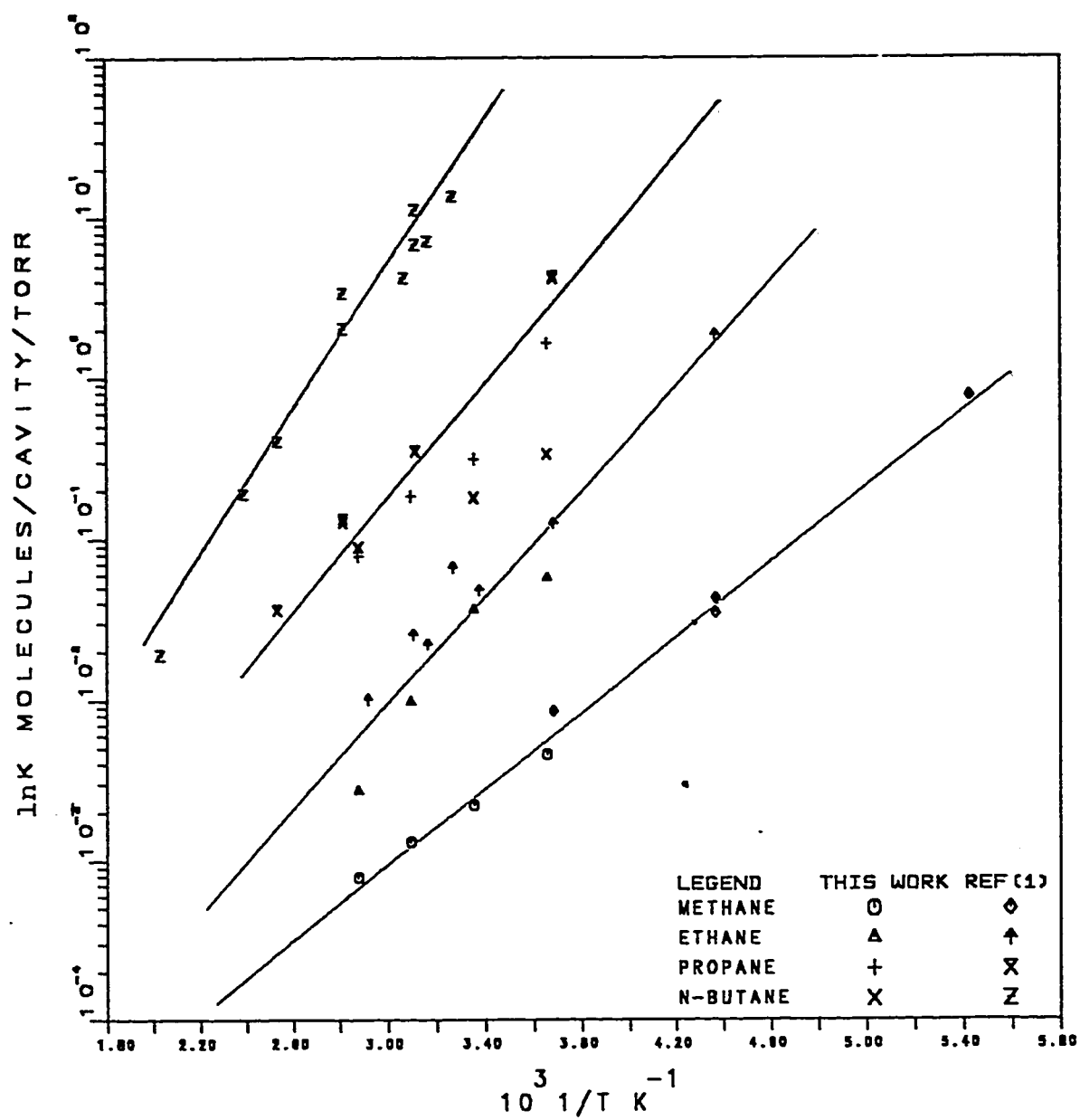


Fig. 4.5: Van't Hoff Plot For Light Alkanes on Linde 5A Pellets.

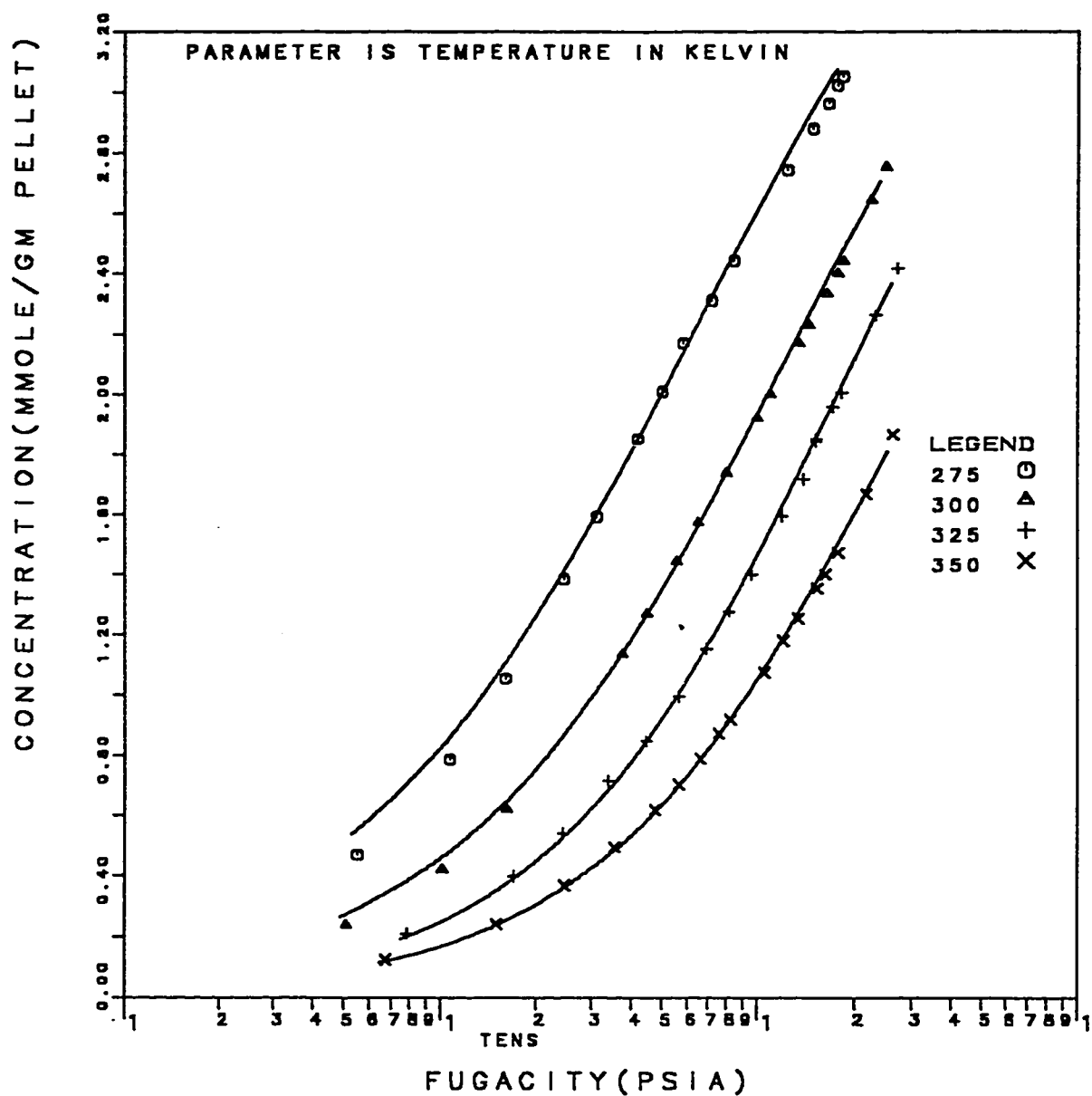


Fig. 4.6: Methane Isotherms on Linde 5A Pellets: Fit of LRC Model With Theoretical N_0 and Optimized K .

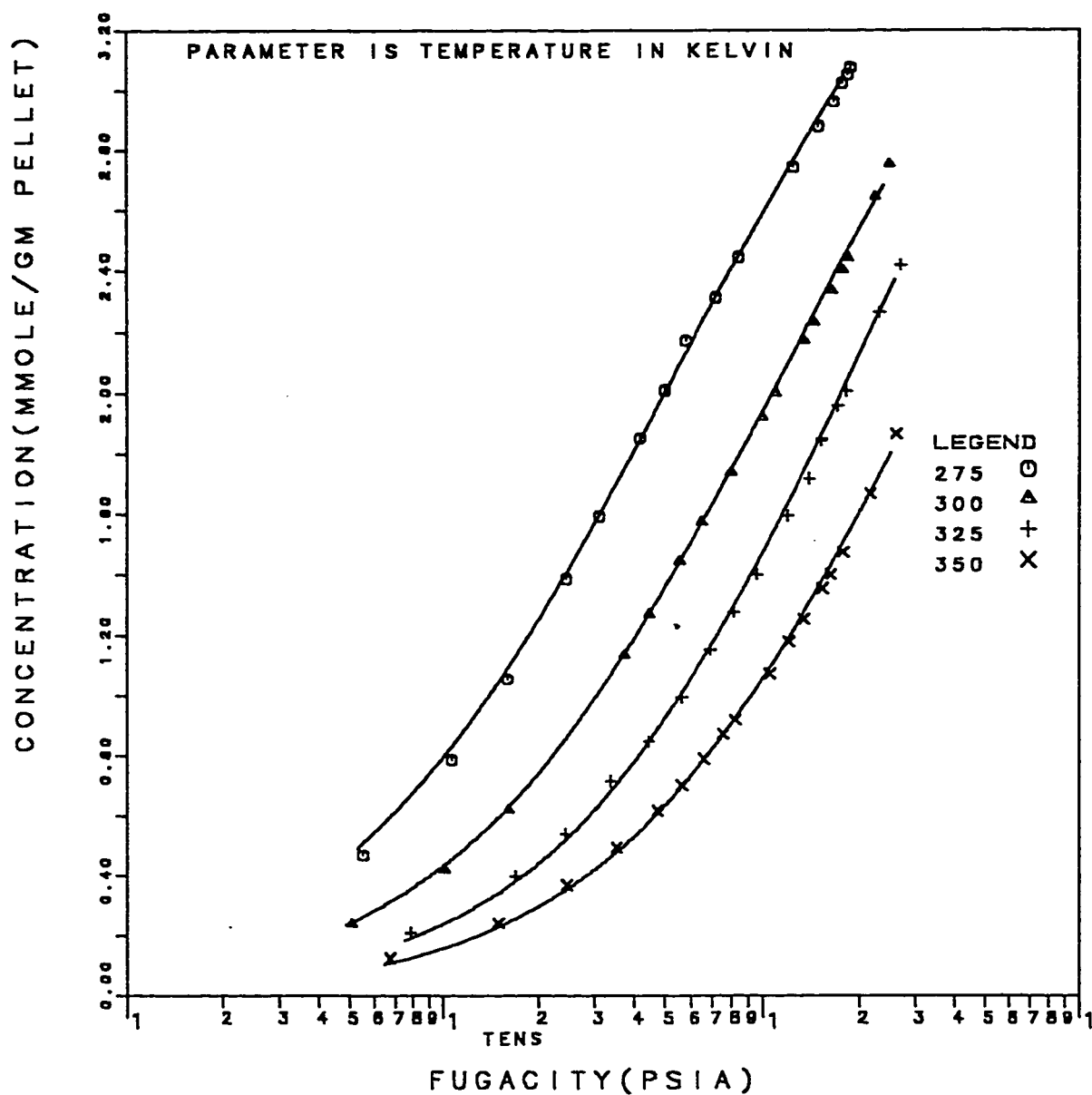


Fig. 4.7: Methane Isotherms on Linde 5A Pellets: Fit of Toth Model With Theoretical N_0 and Optimized K .

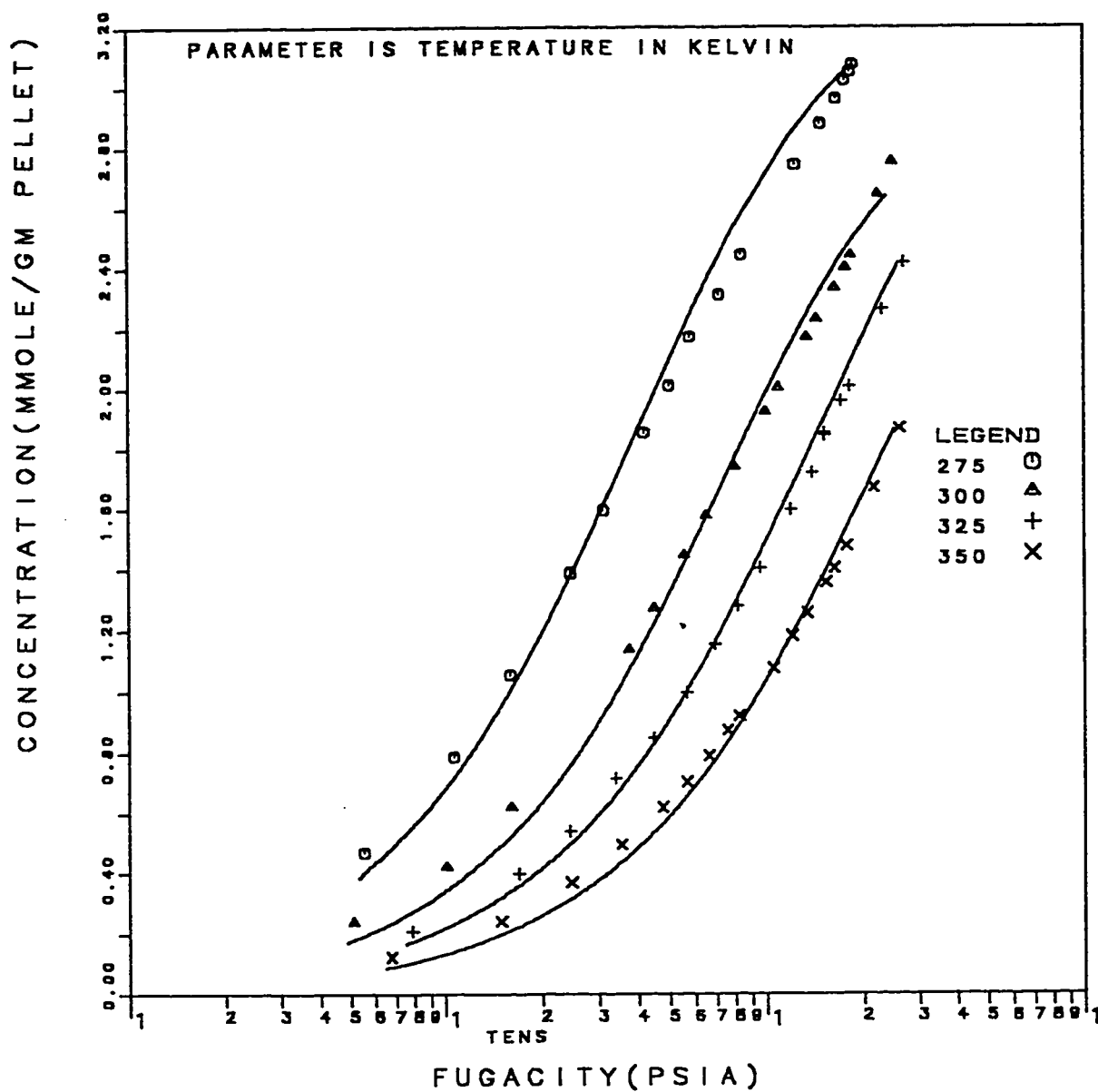


Fig. 4.8: Methane Isotherms on Linde 5A Pellets: Fit of Mathews and Weber Model With Theoretical N_0 and Optimized K.

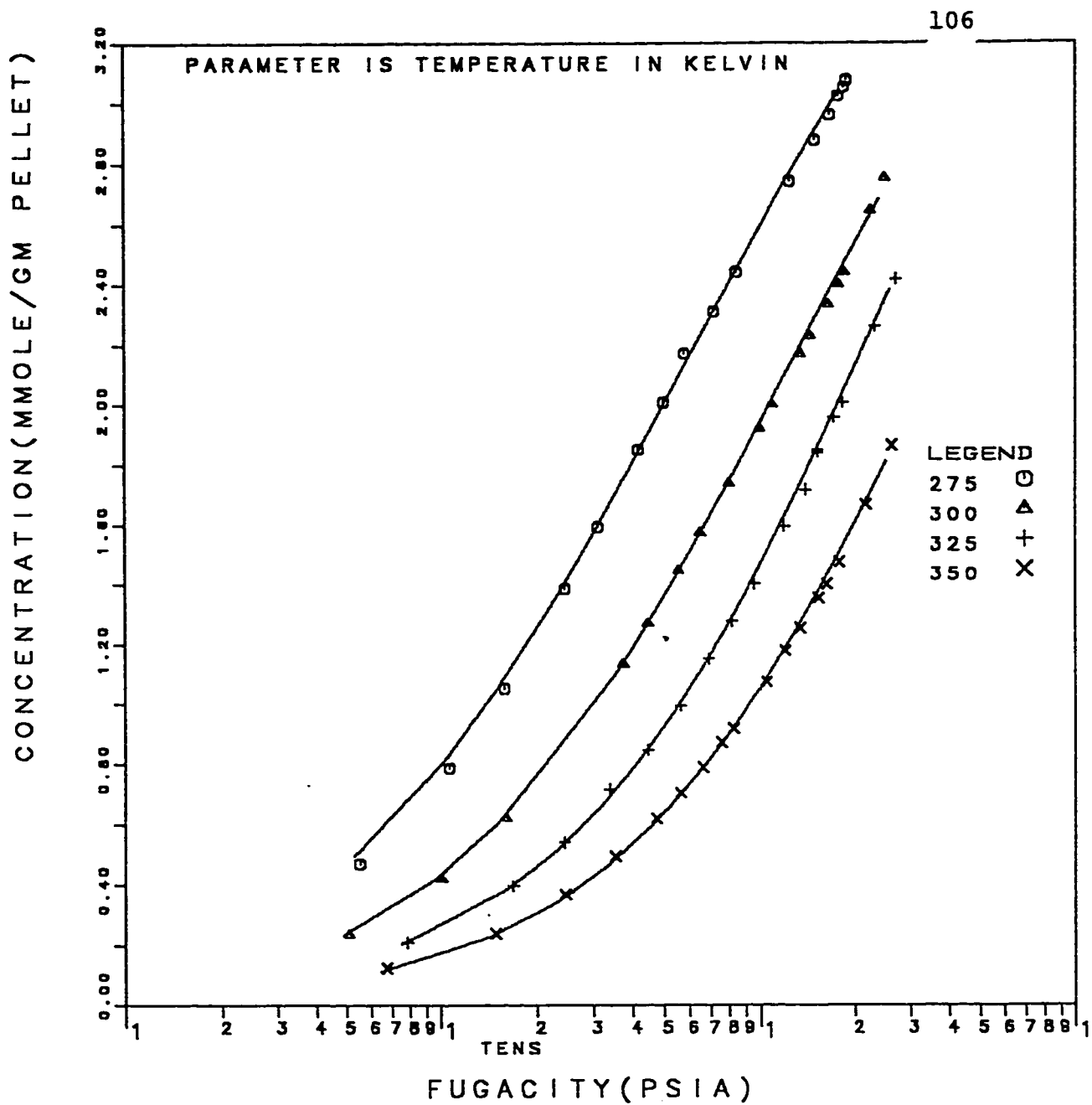


Fig. 4.9: Methane Isotherms on Linde 5A Pellets: Fit of Jaroniec Model With Theoretical N_0 and Optimized K .

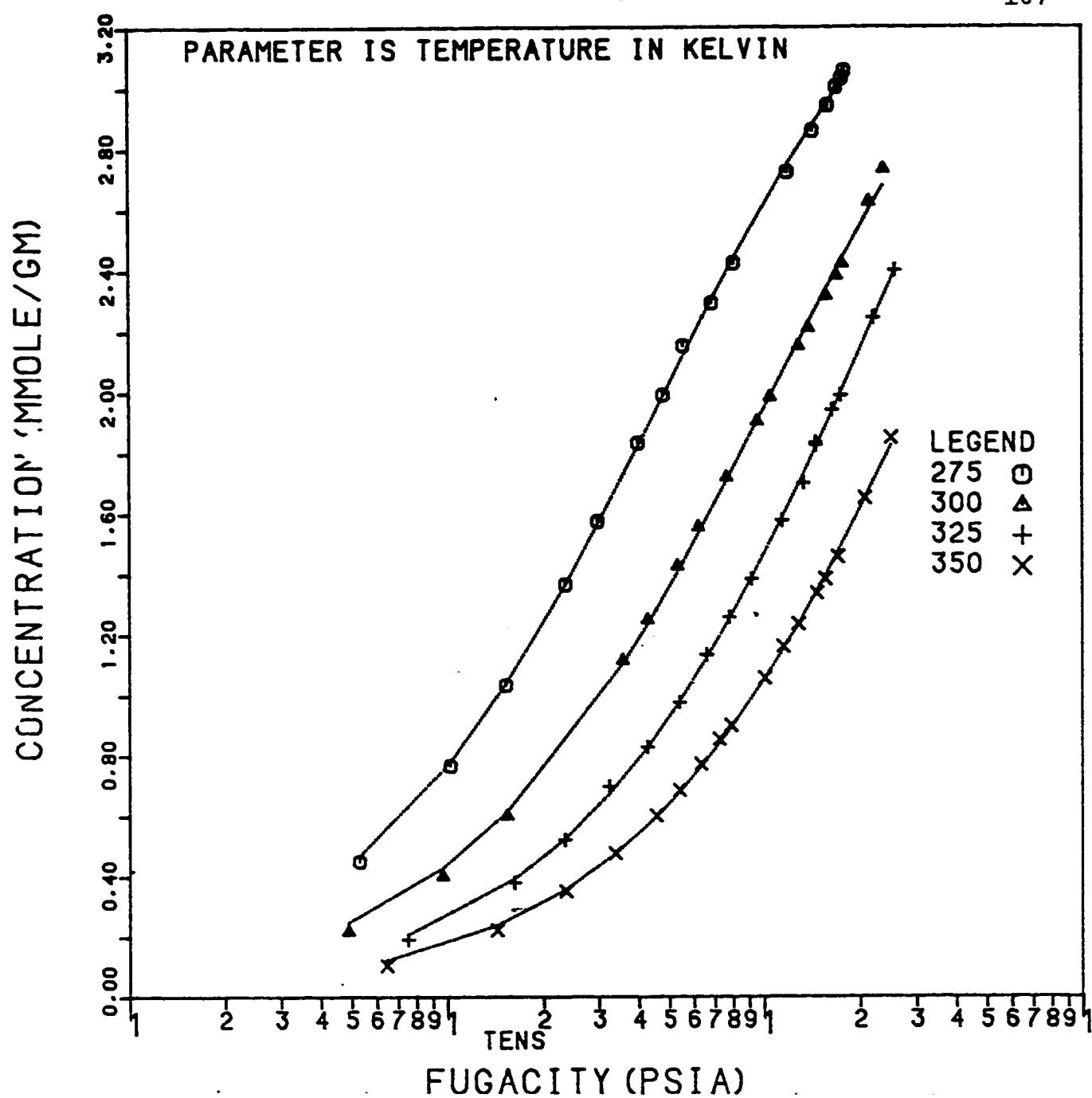


Fig. 4.10: Methane Isotherms on Linde 5A Pellets: Fit of LRC Model With Optimized N_0 and K .

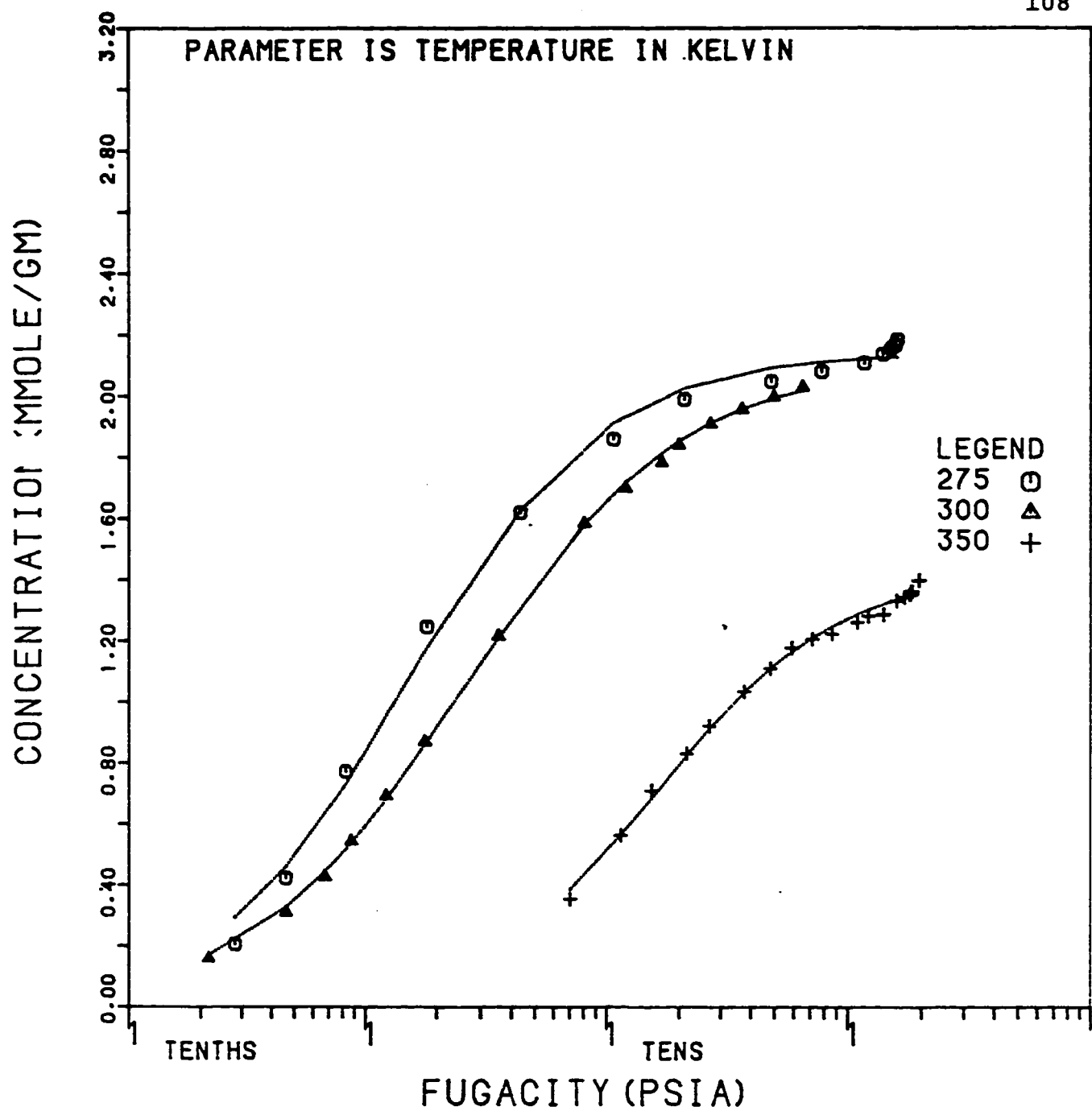


Fig. 4.11: Ethane Isotherms on Linde 5A Pellets: Fit of LRC Model With Optimized N_o and K .

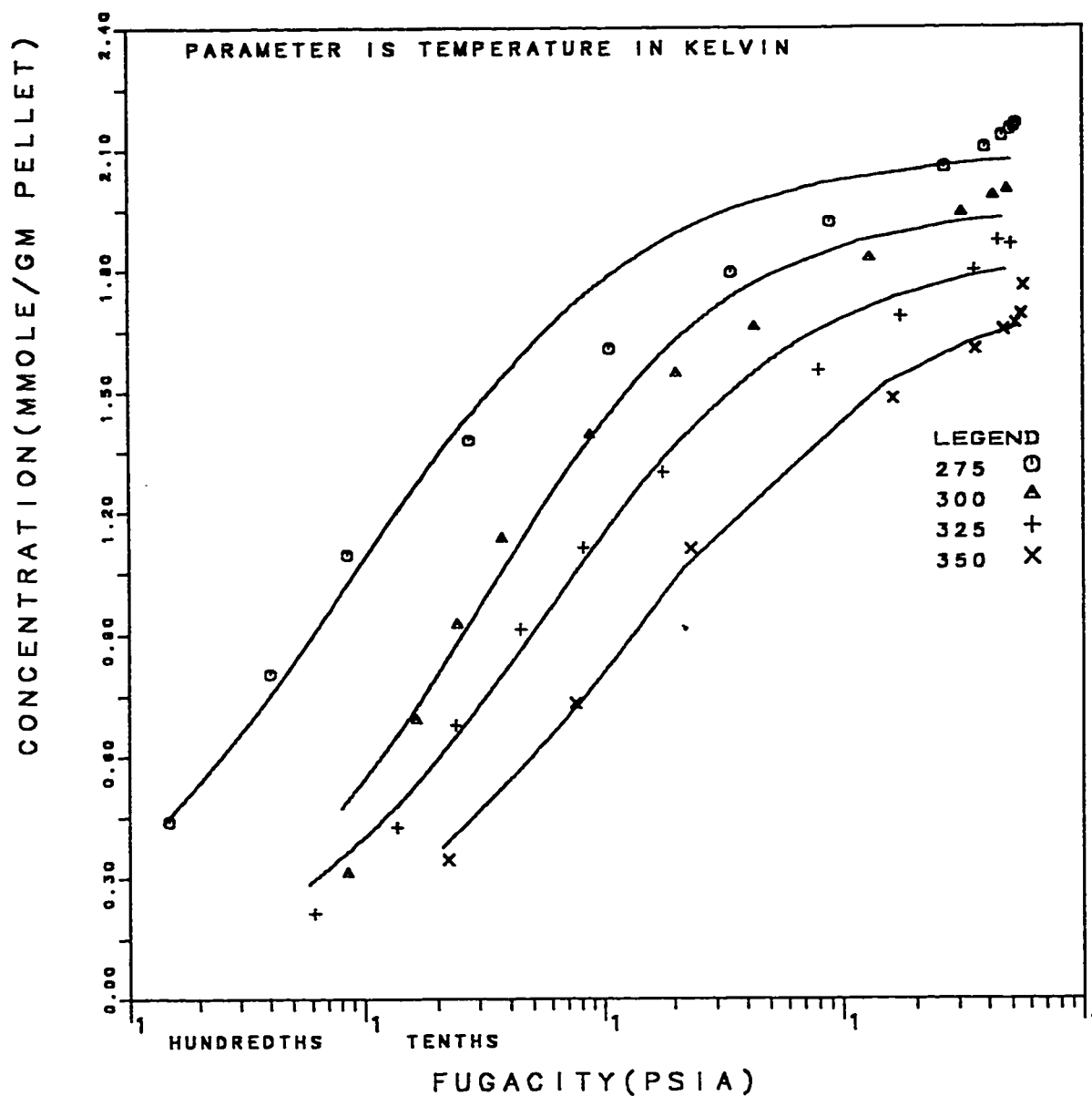


Fig. 4.12: Propane Isotherms on Linde 5A Pellets: Fit of LRC Model With Optimized N_0 and K .

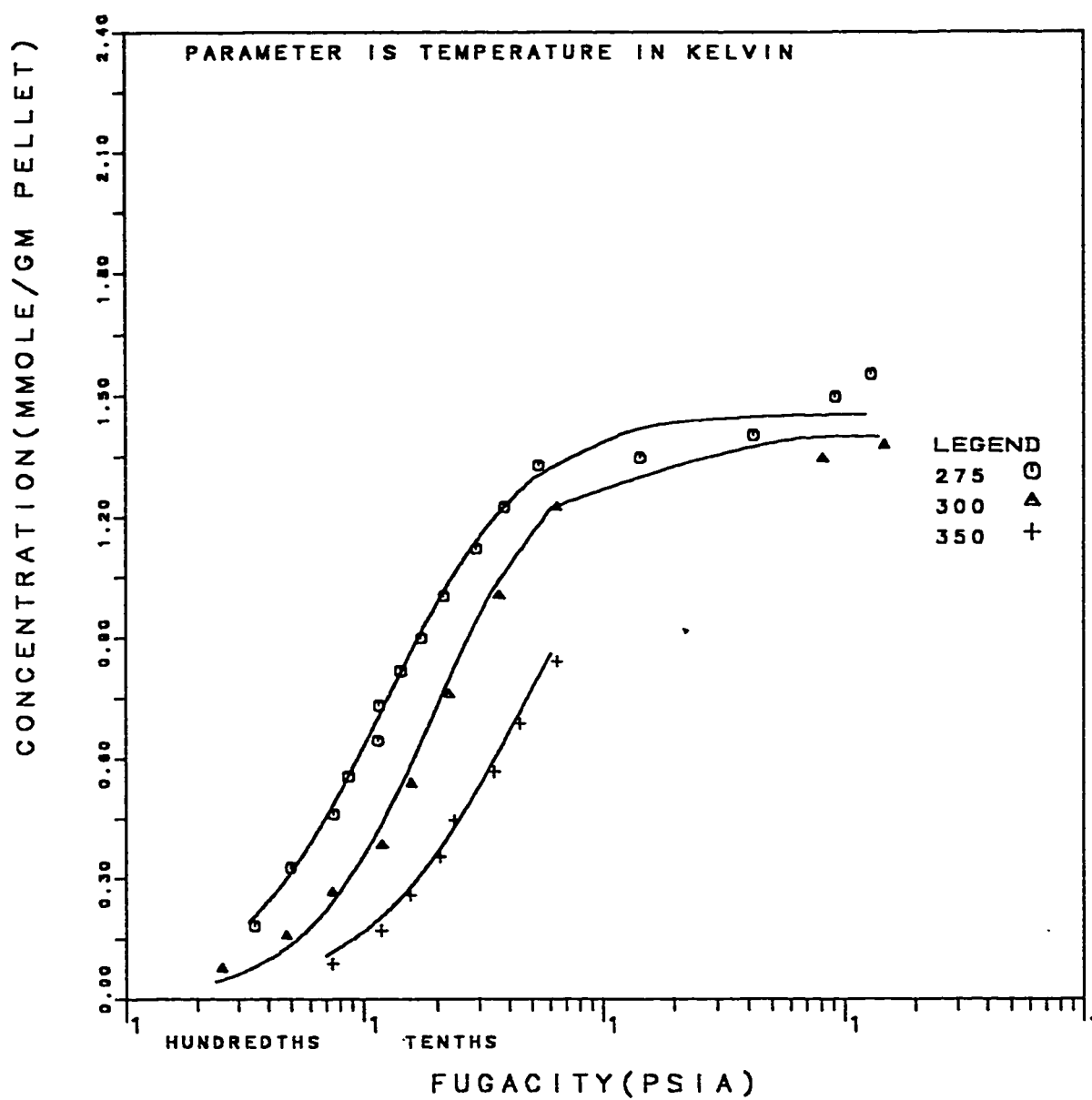


Fig. 4.13: n-Butane Isotherms on Linde 5A Pellets: Fit of LRC Model With Optimized N_0 and K .

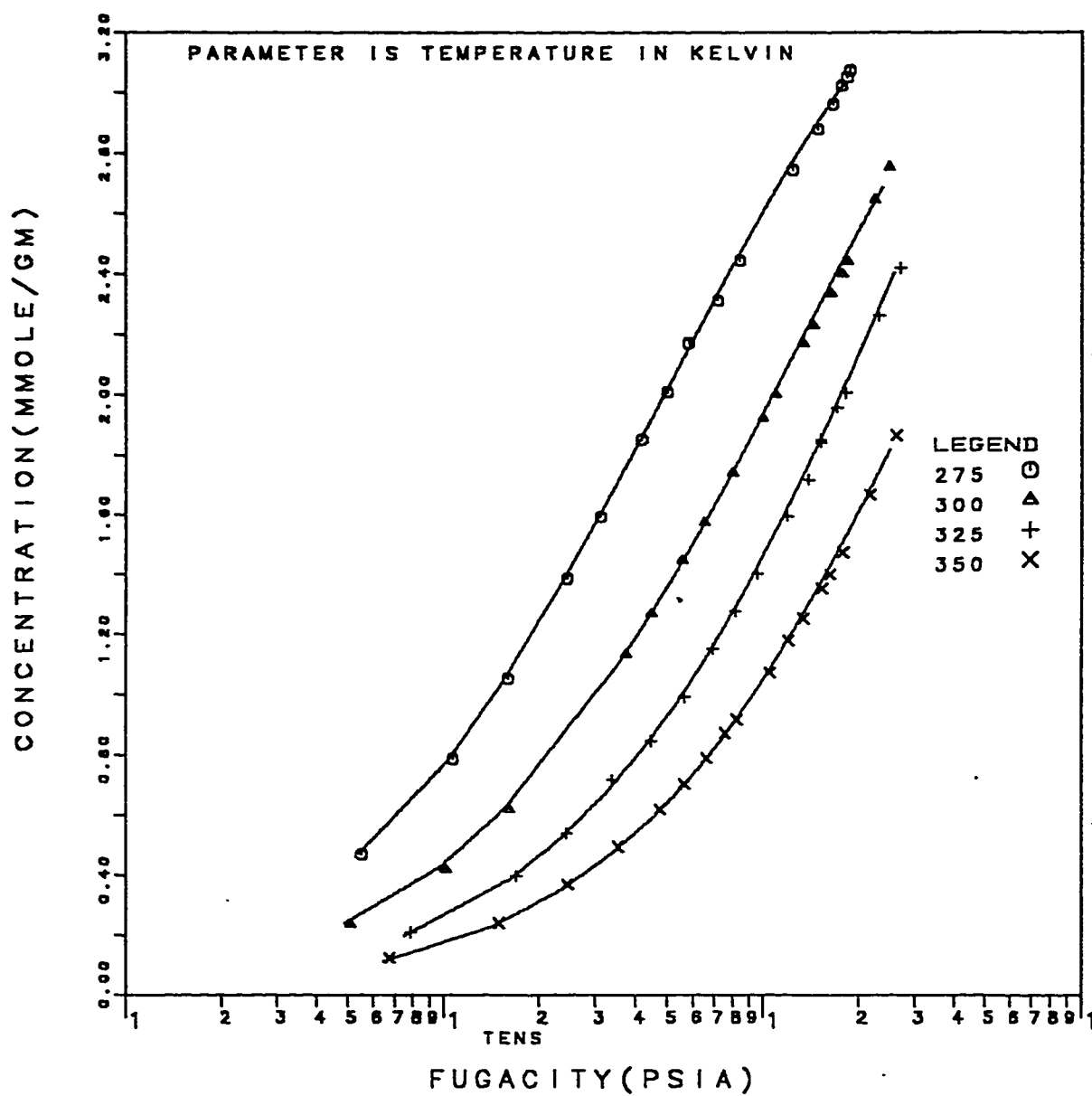


Fig. 4.14: Methane Isotherms on Linde 5A Pellets: Fit of Toth Model With Optimized N_0 and K .

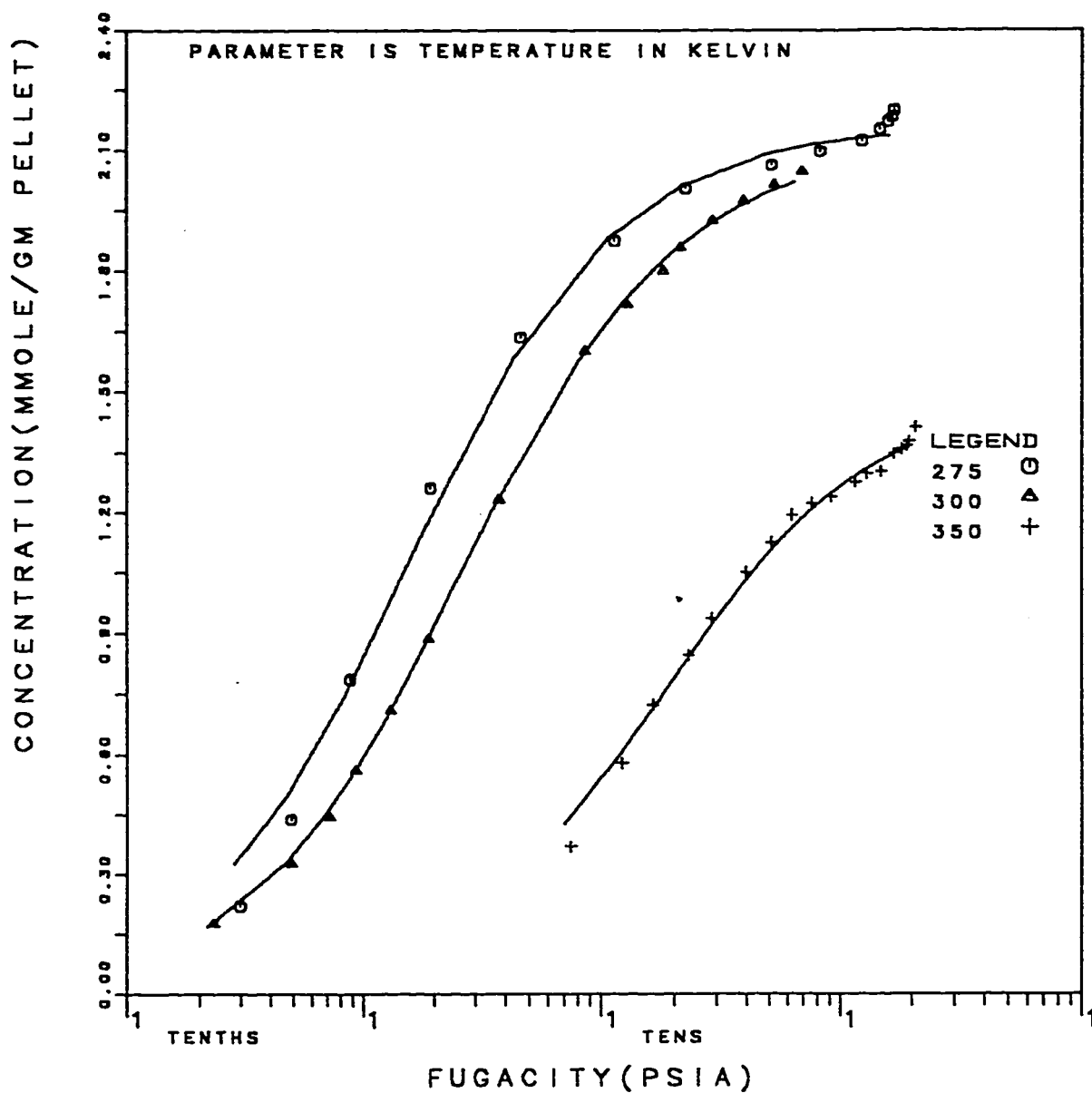


Fig. 4.15: Ethane Isotherms on Linde 5A Pellets: Fit of Toth Model With Optimized N_0 and K .

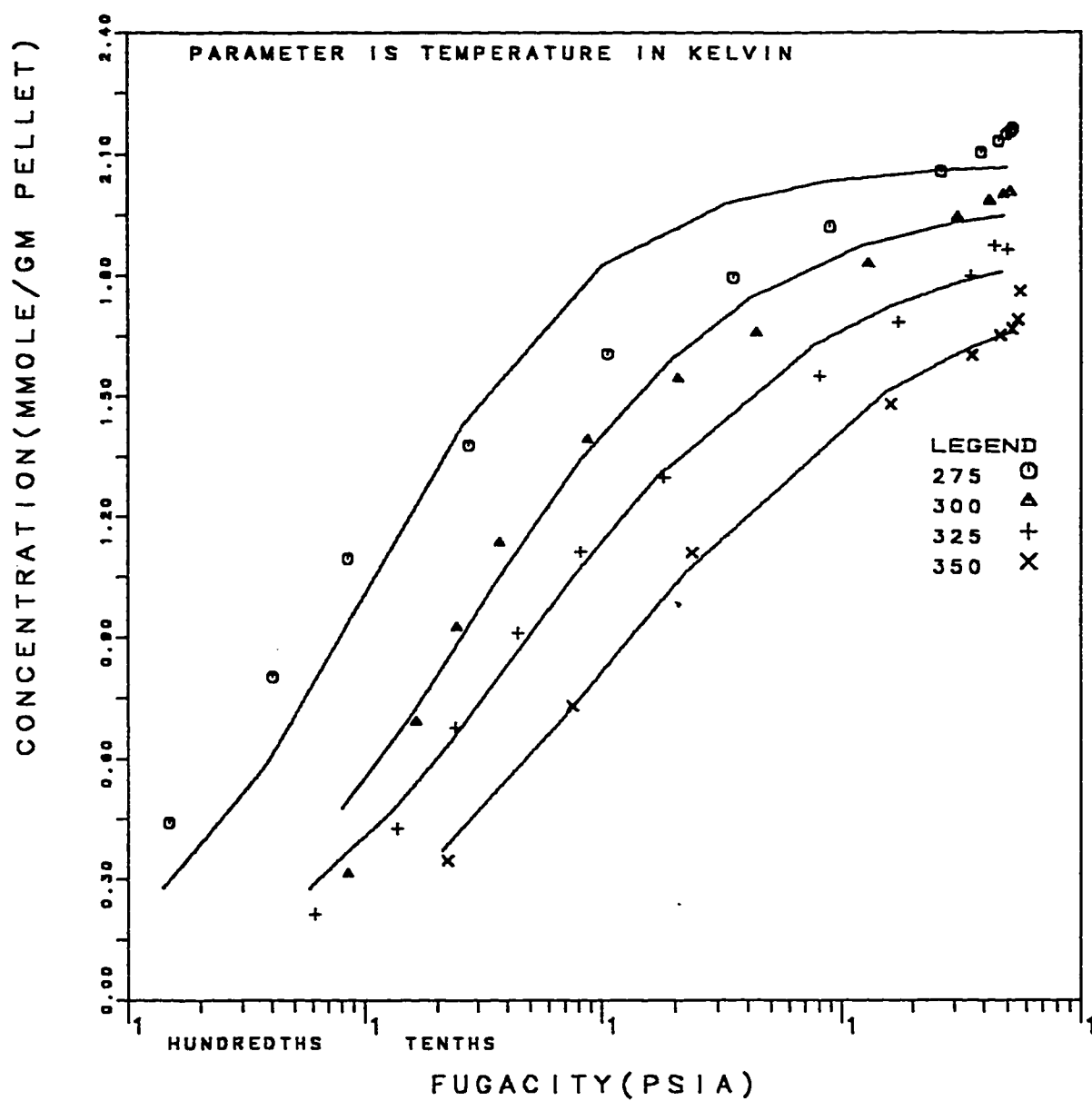


Fig. 4.16: Propane Isotherms on Linde 5A Pellets: Fit of Toth Model With Optimized N_0 and K .

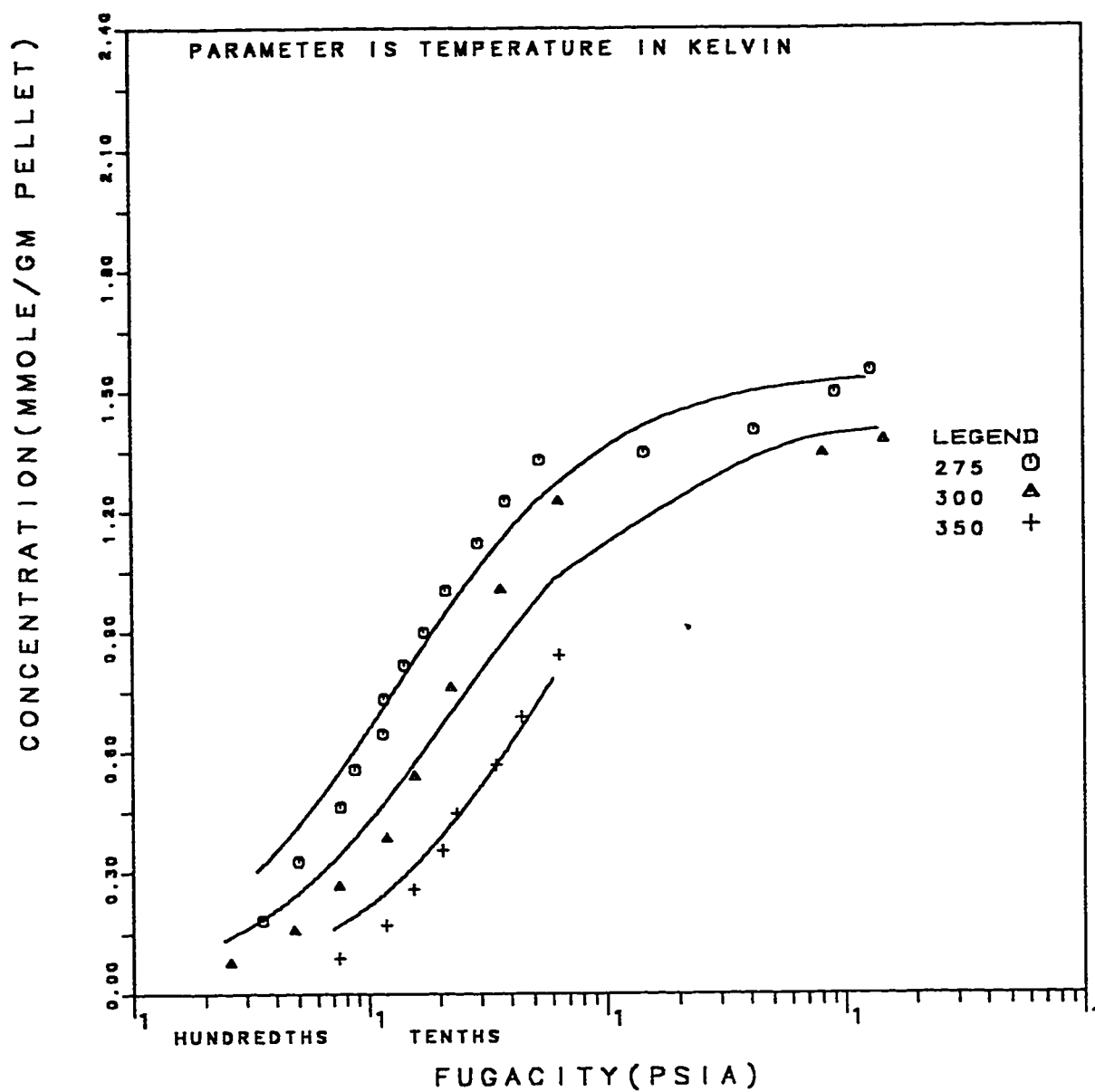


Fig. 4.17: n-Butane Isotherms on Linde 5A Pellets: Fit of Toth Model With Optimized N_0 and K .

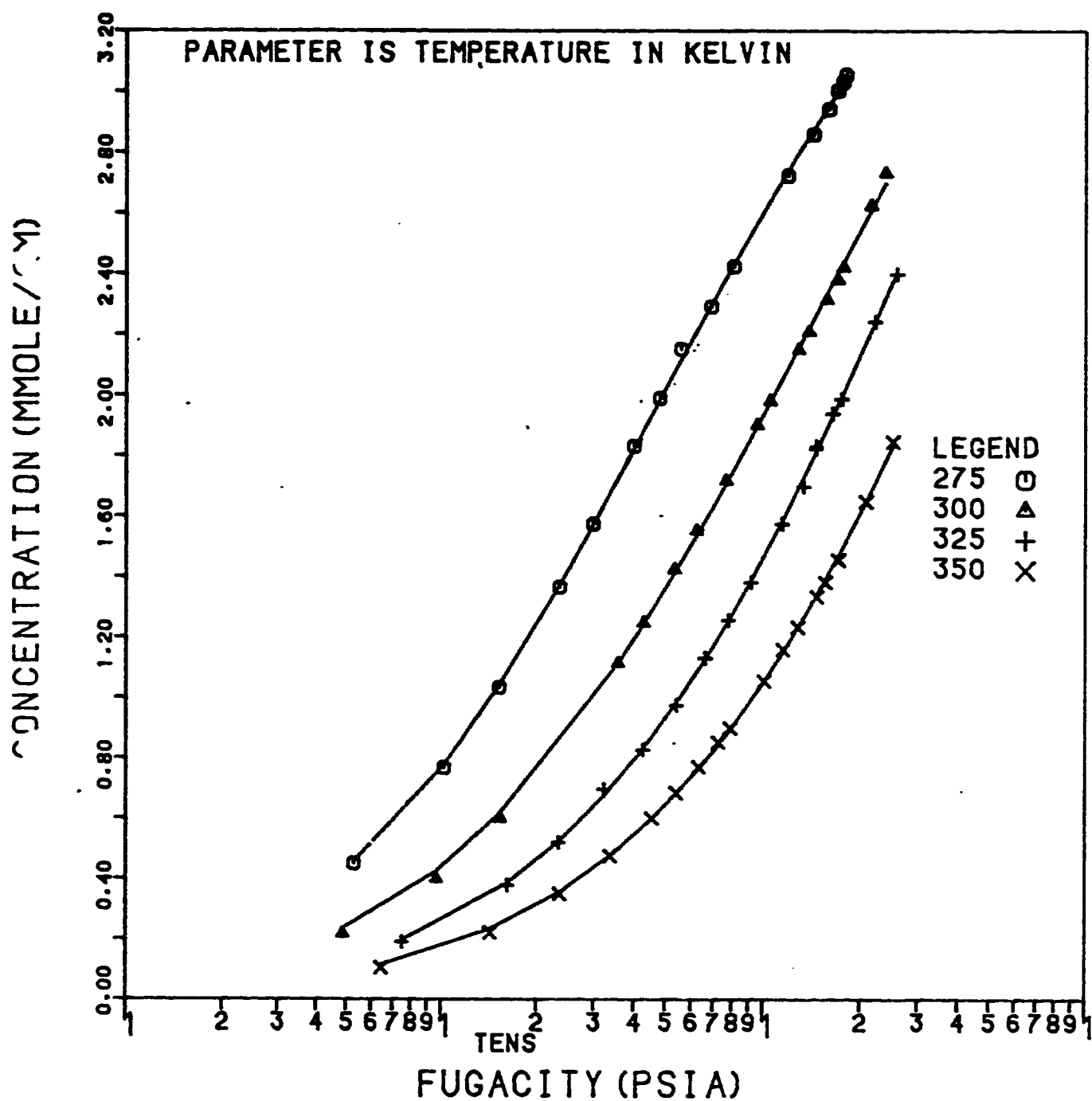


Fig. 4.18: Methane Isotherms on Linde 5A Pellets: Fit of Mathews and Weber Model With Optimized N_0 and K .

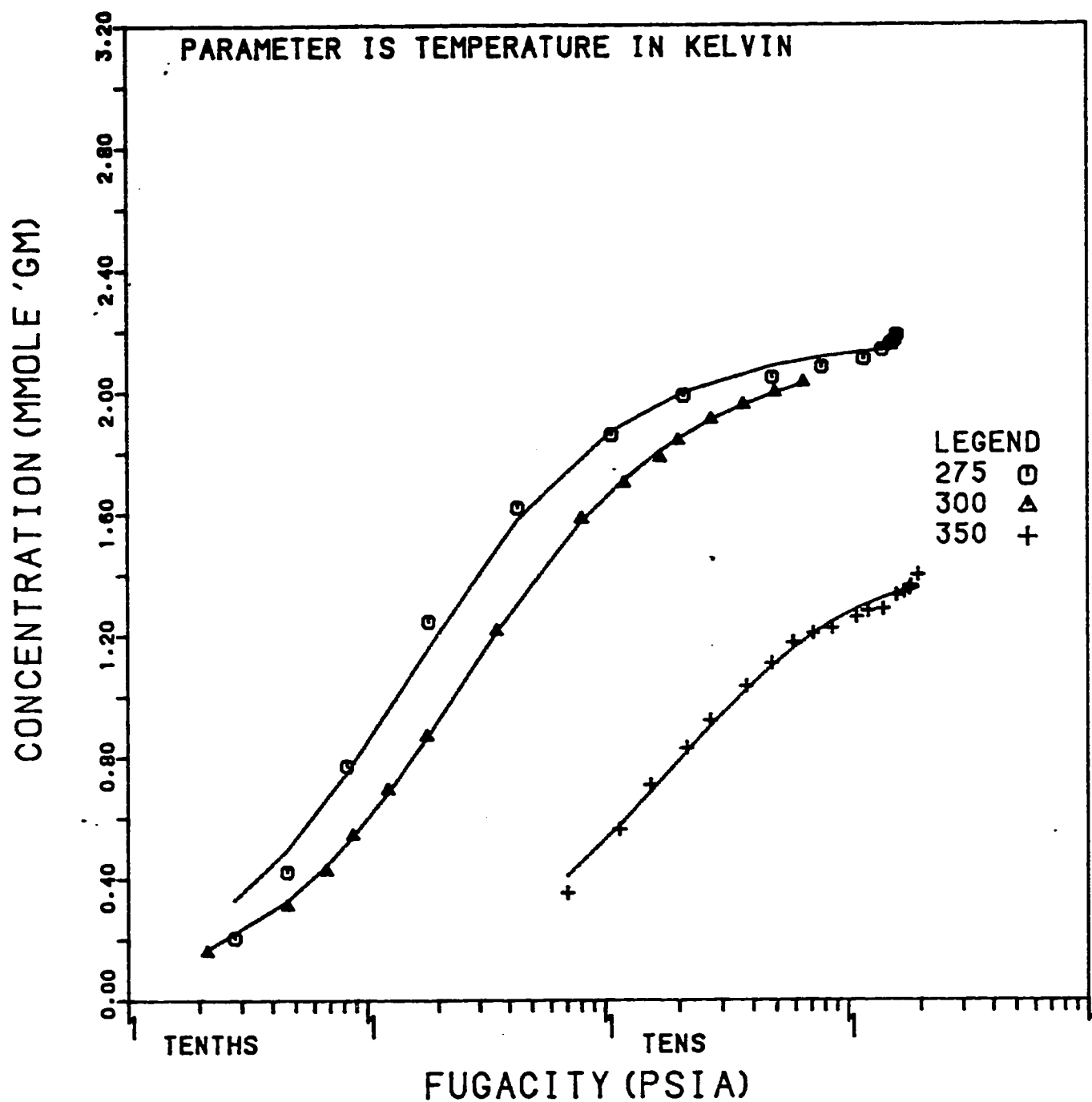


Fig. 4.19: Ethane Isotherms on Linde 5A Pellets: Fit of Mathews and Weber Model With Optimized N_0 and K .

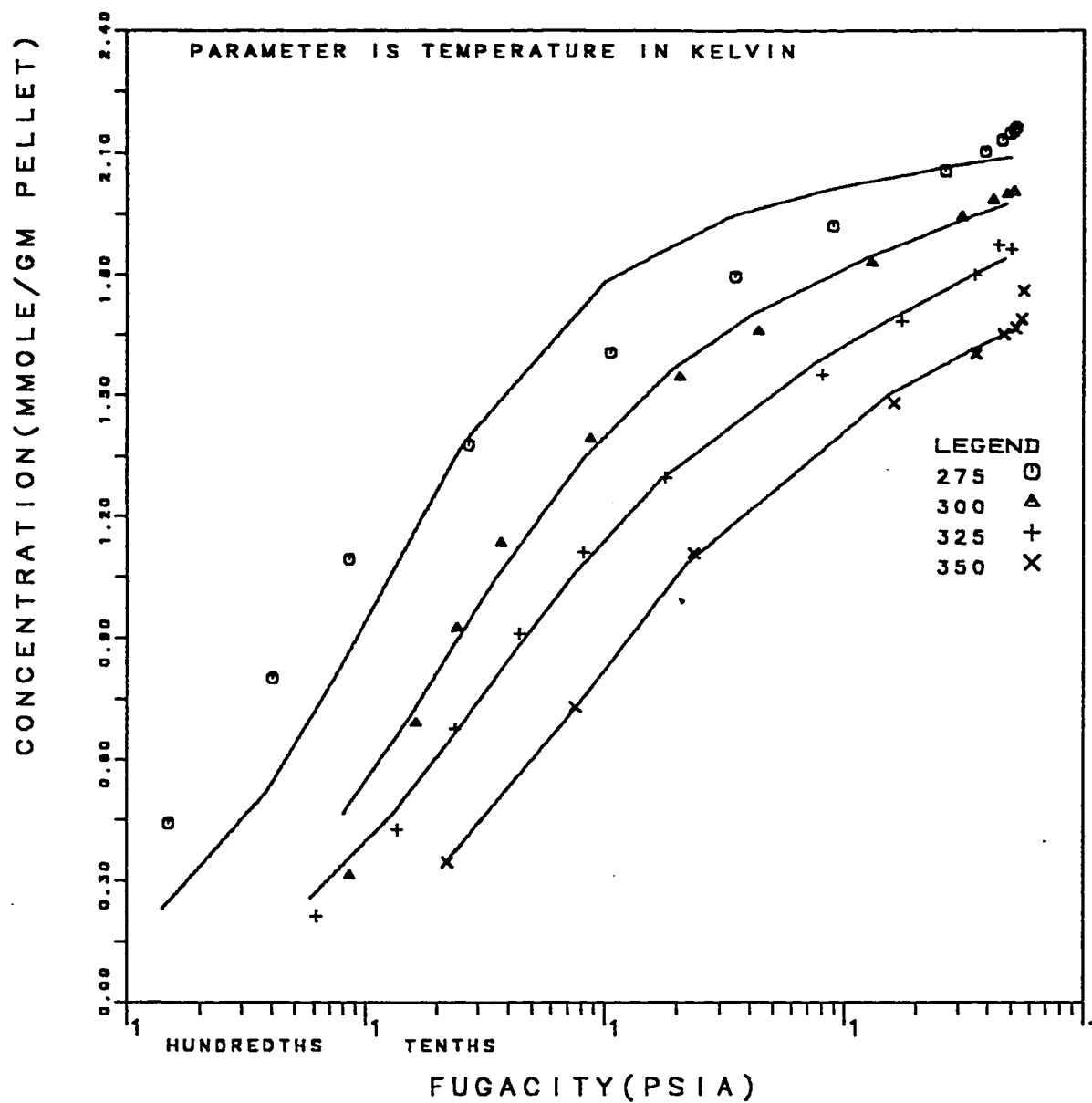


Fig. 4.20: Propane Isotherms on Linde 5A Pellets: Fit of Mathews and Weber Model With Optimized N_0 and K .

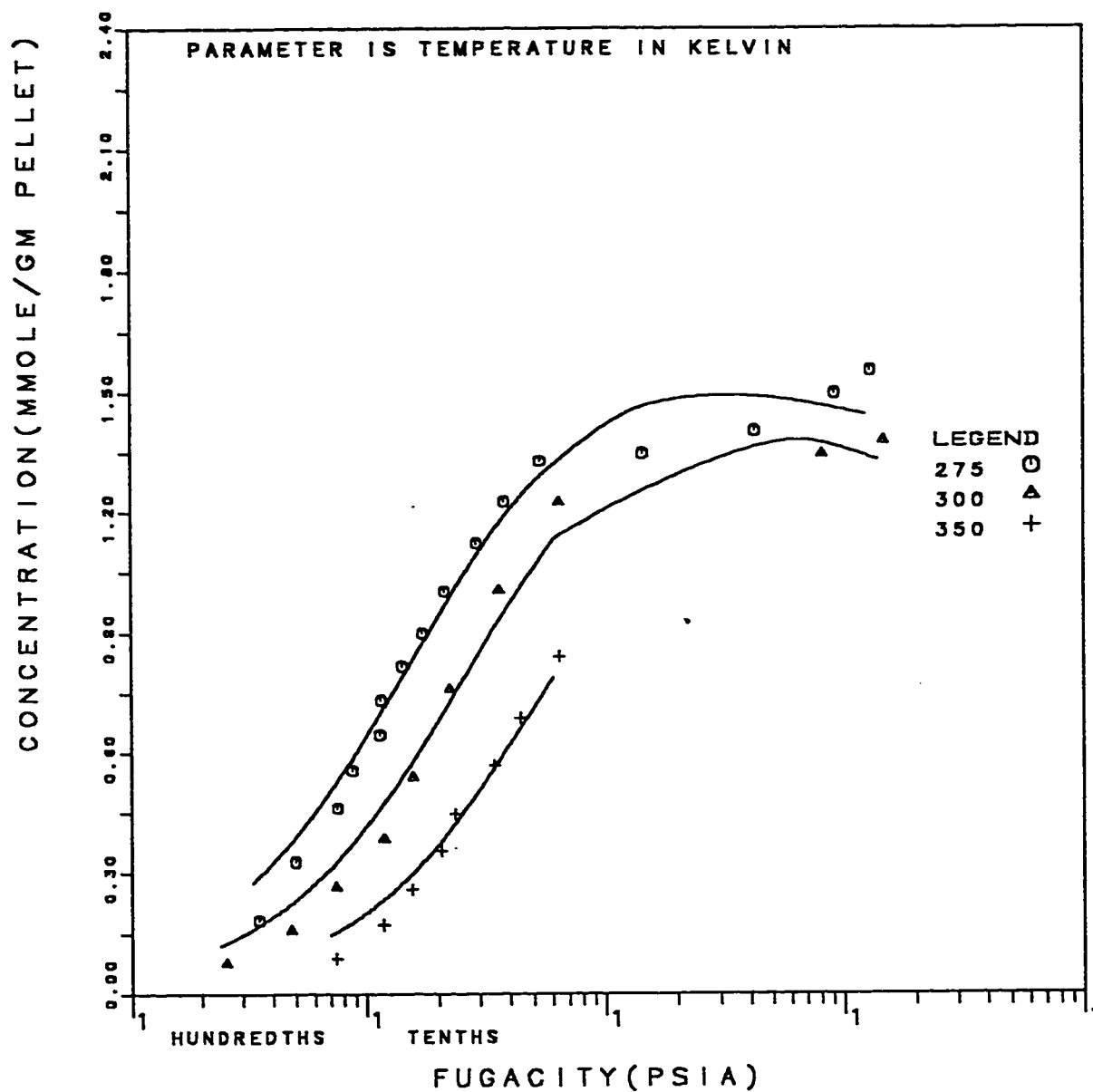


Fig. 4.21: n-Butane Isotherms on Linde 5A Pellets: Fit of Mathews and Weber Model With Optimized N_0 and K .

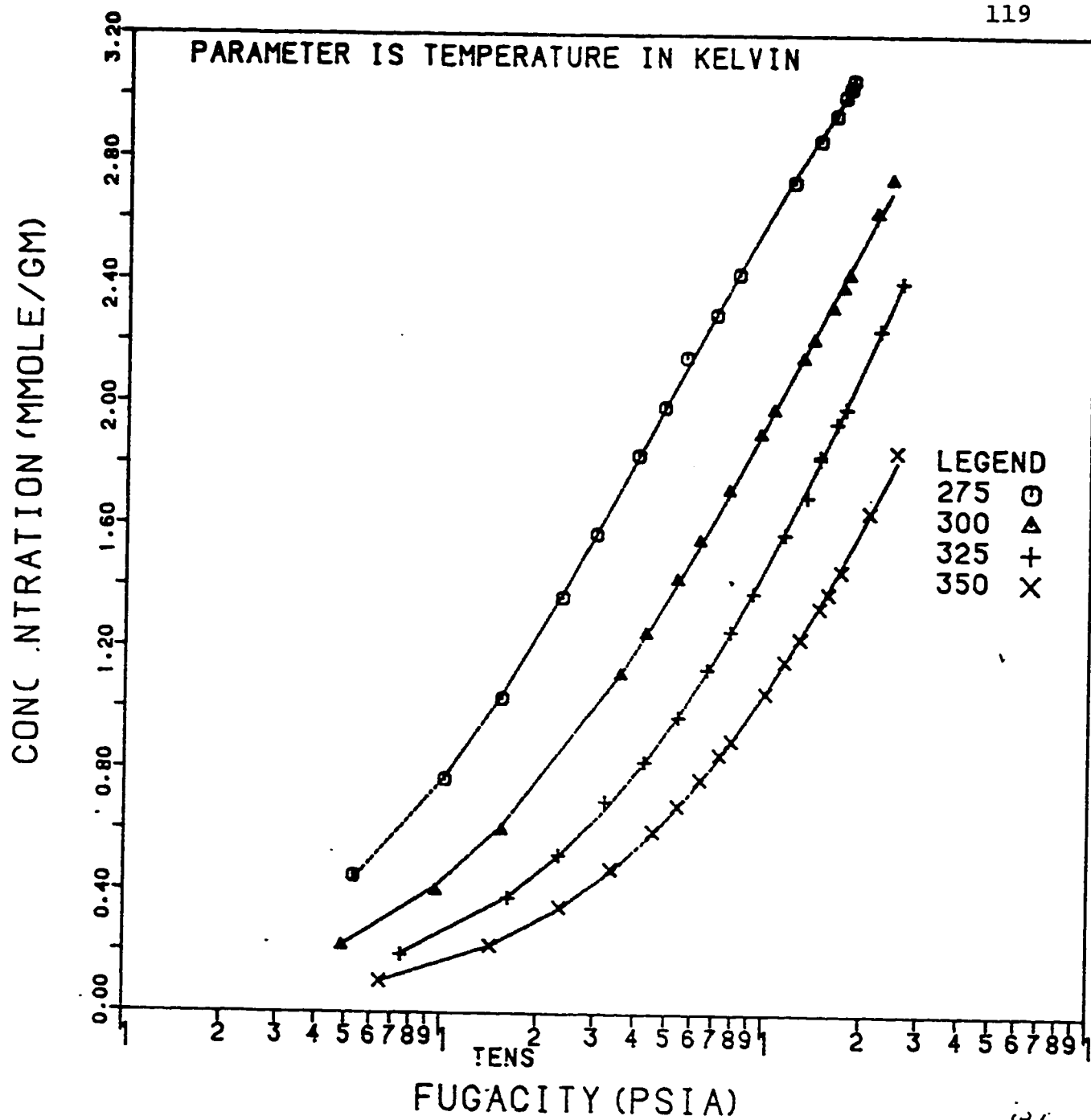


Fig. 4.22: Methane Isotherms on Linde 5A Pellets: Fit of Jaroniec Model. With Optimized N_0 and K .

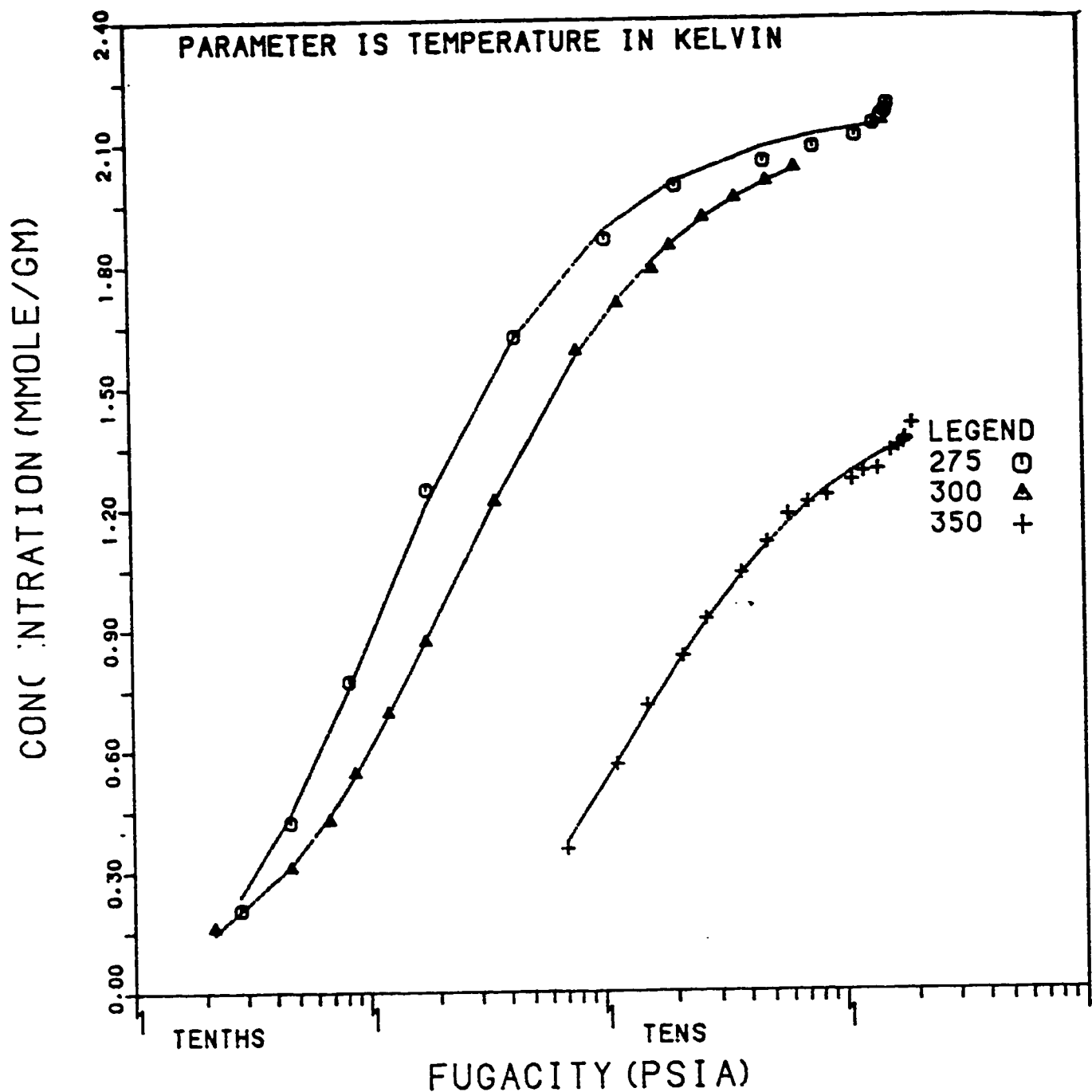


Fig. 4.23: Ethane Isotherms on Linde 5A Pellets: Fit of Jaroniec Model With Optimized N_0 and K .

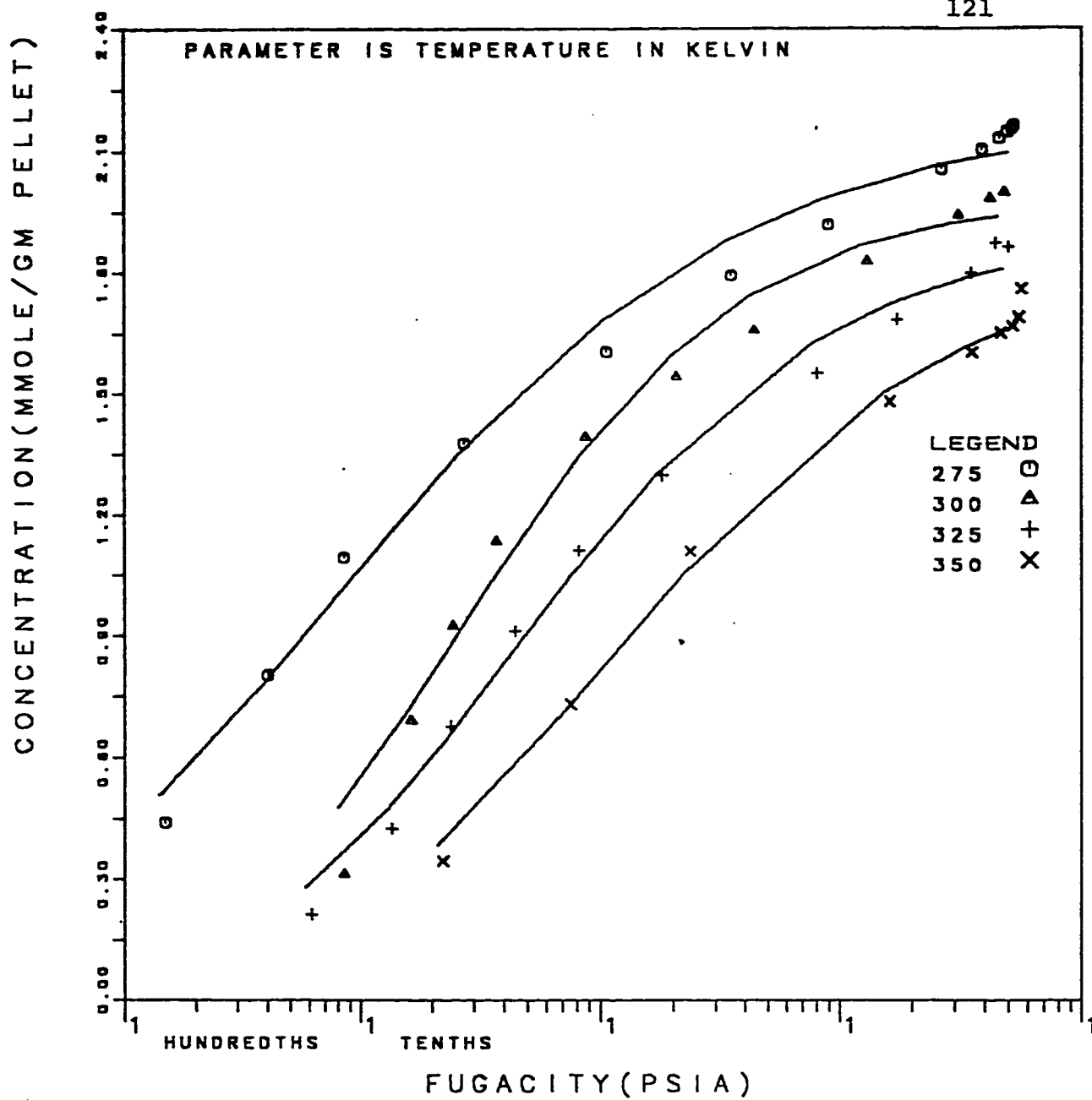


Fig. 4.24: Propane Isotherms on Linde 5A Pellets: Fit of Jaroniec Model With Optimized N_0 and K .

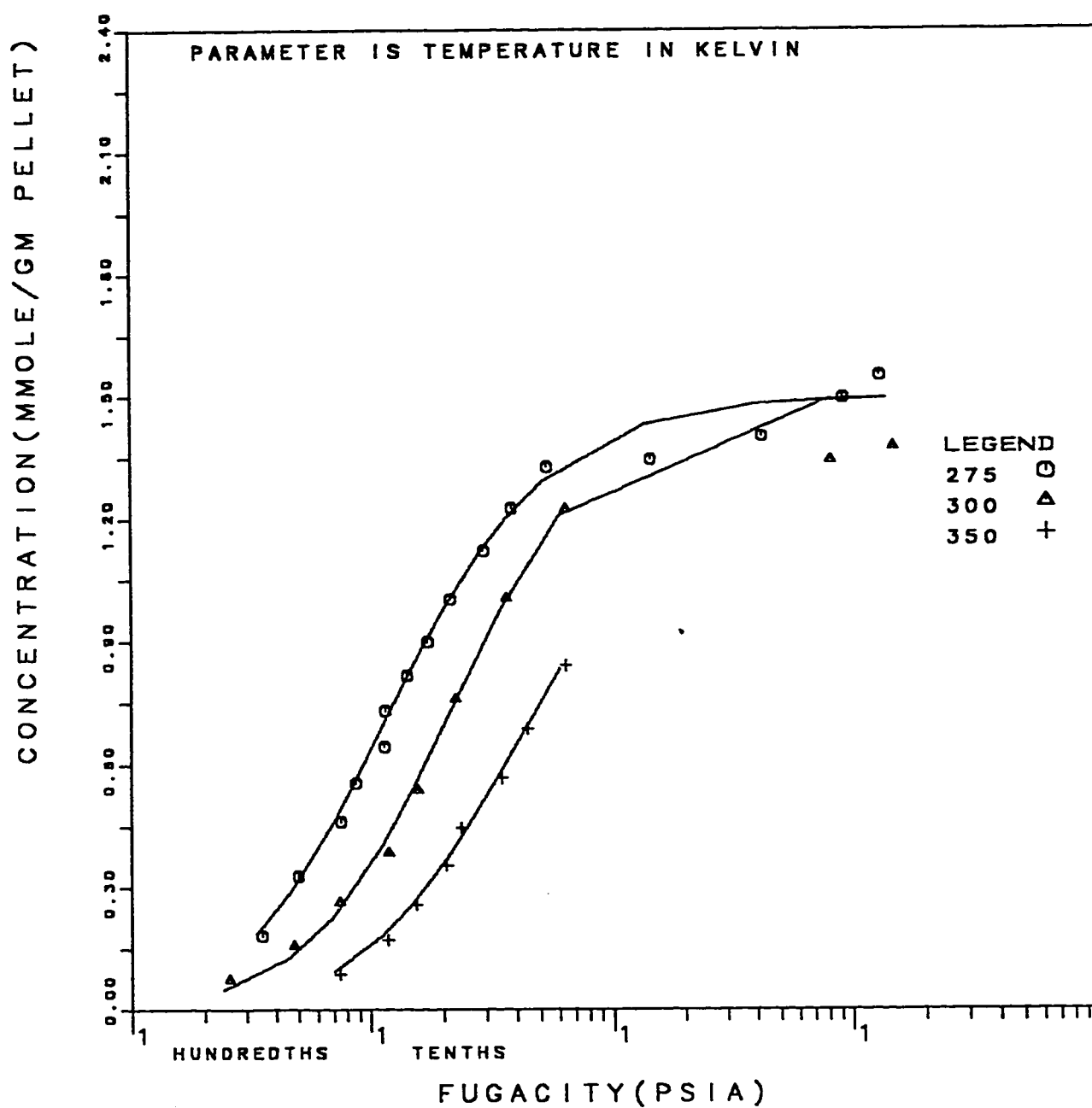


Fig. 4.25: n-Butane Isotherms on Linde 5A Pellets: Fit of Jaroniec Model With Optimized N_0 and K .

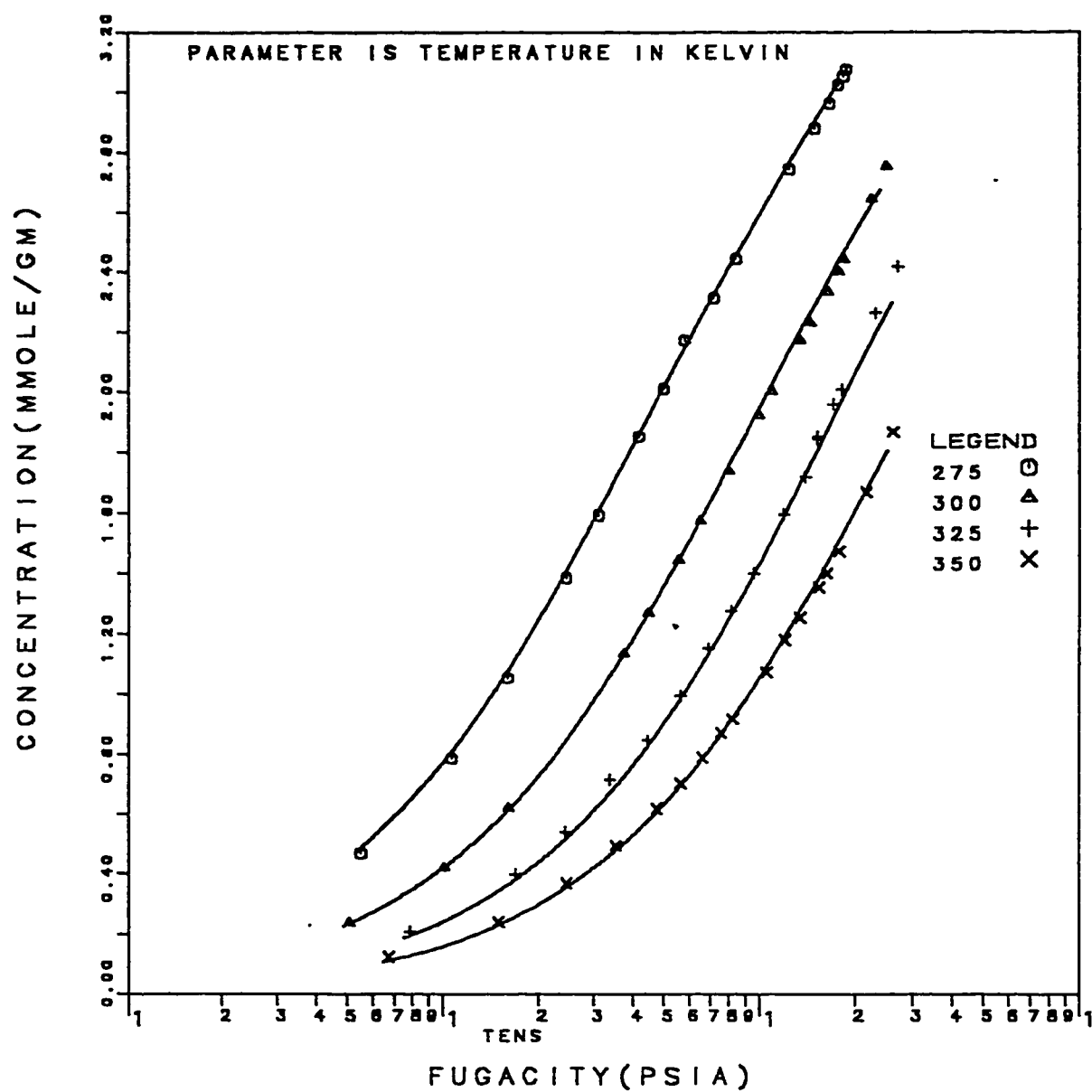


Fig. 4.26: Methane Isotherms on Linde 5A Pellets: Fit of Ruthven Model With Optimized β and K' .

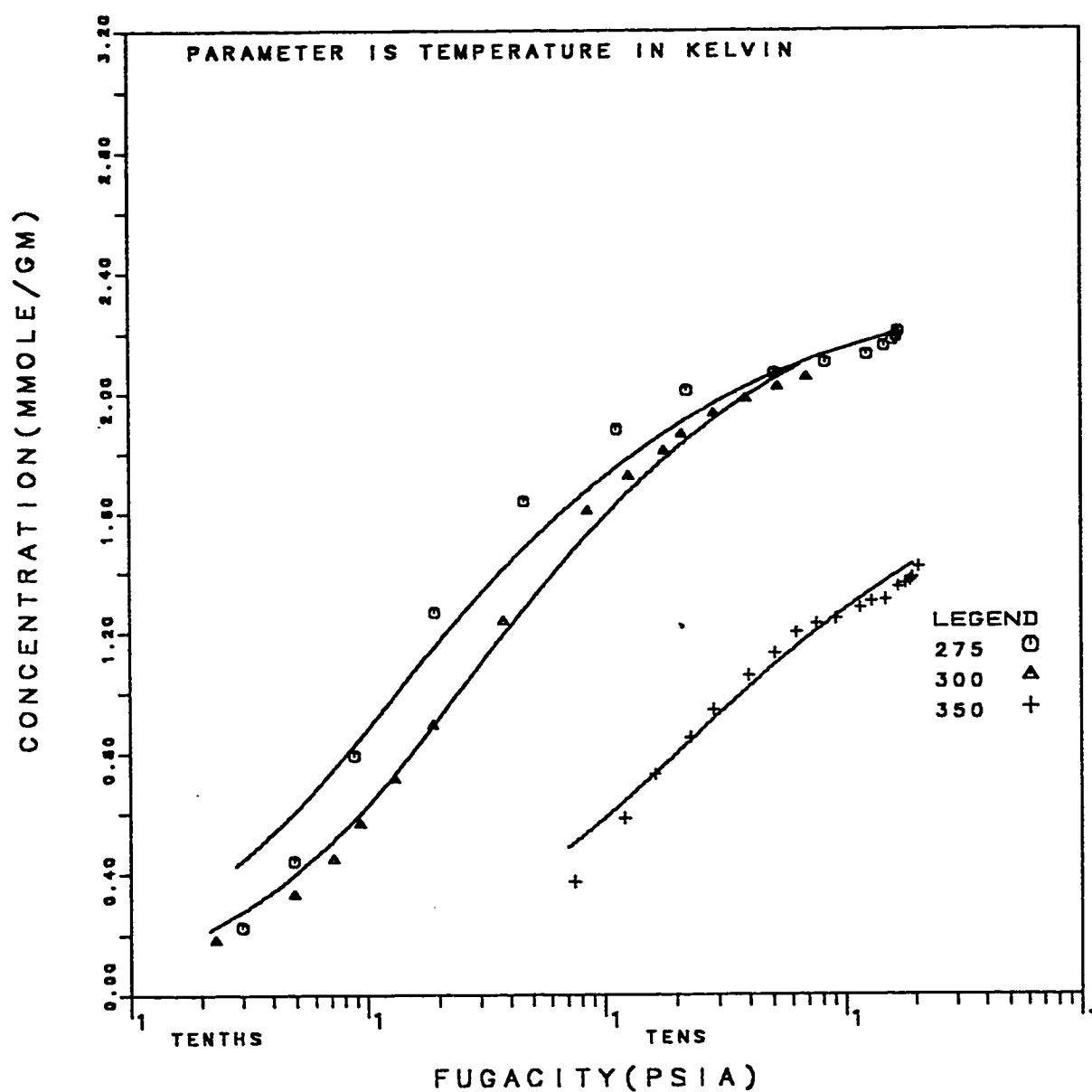


Fig. 4.27: Ethane Isotherms on Linde 5A Pellets: Fit of Ruthven Model With Optimized β and K' .

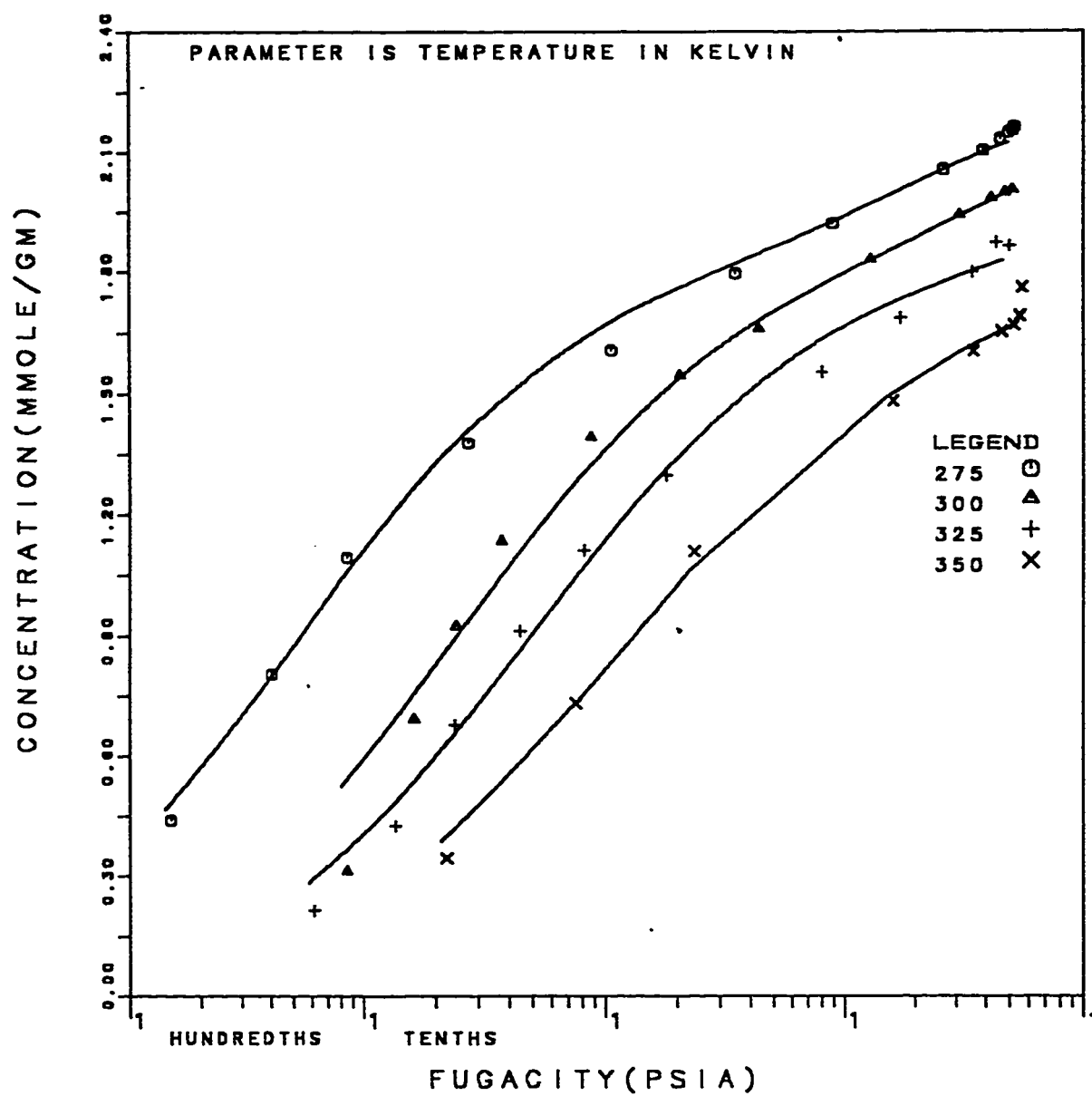


Fig. 4.28: Propane Isotherms on Linde 5A Pellets: Fit of Ruthven Model With Optimized β and K' .

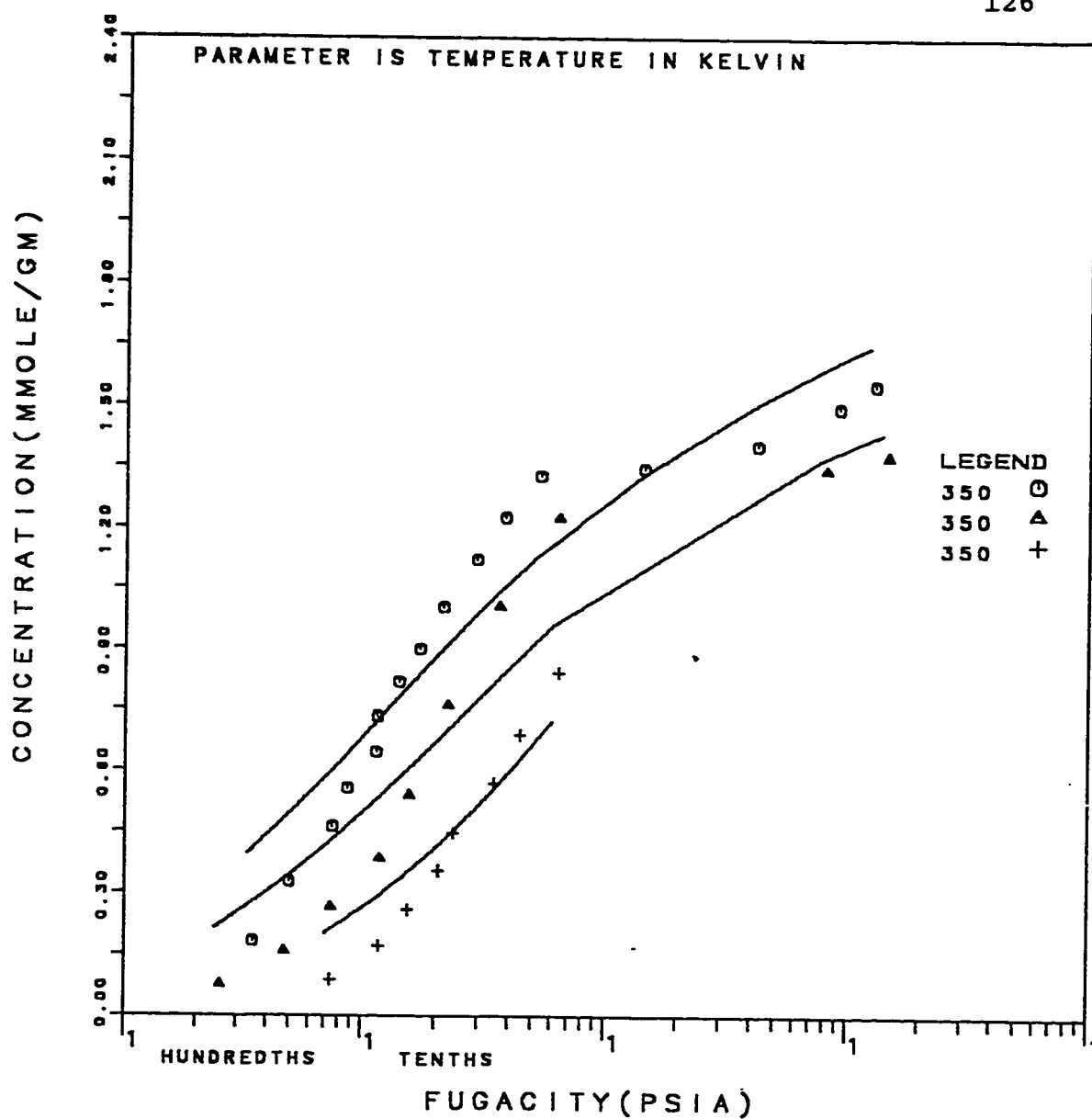


Fig. 4.29: n-Butane Isotherms on Linde 5A Pellets: Fit of Ruthven Model With Optimized β and K' .

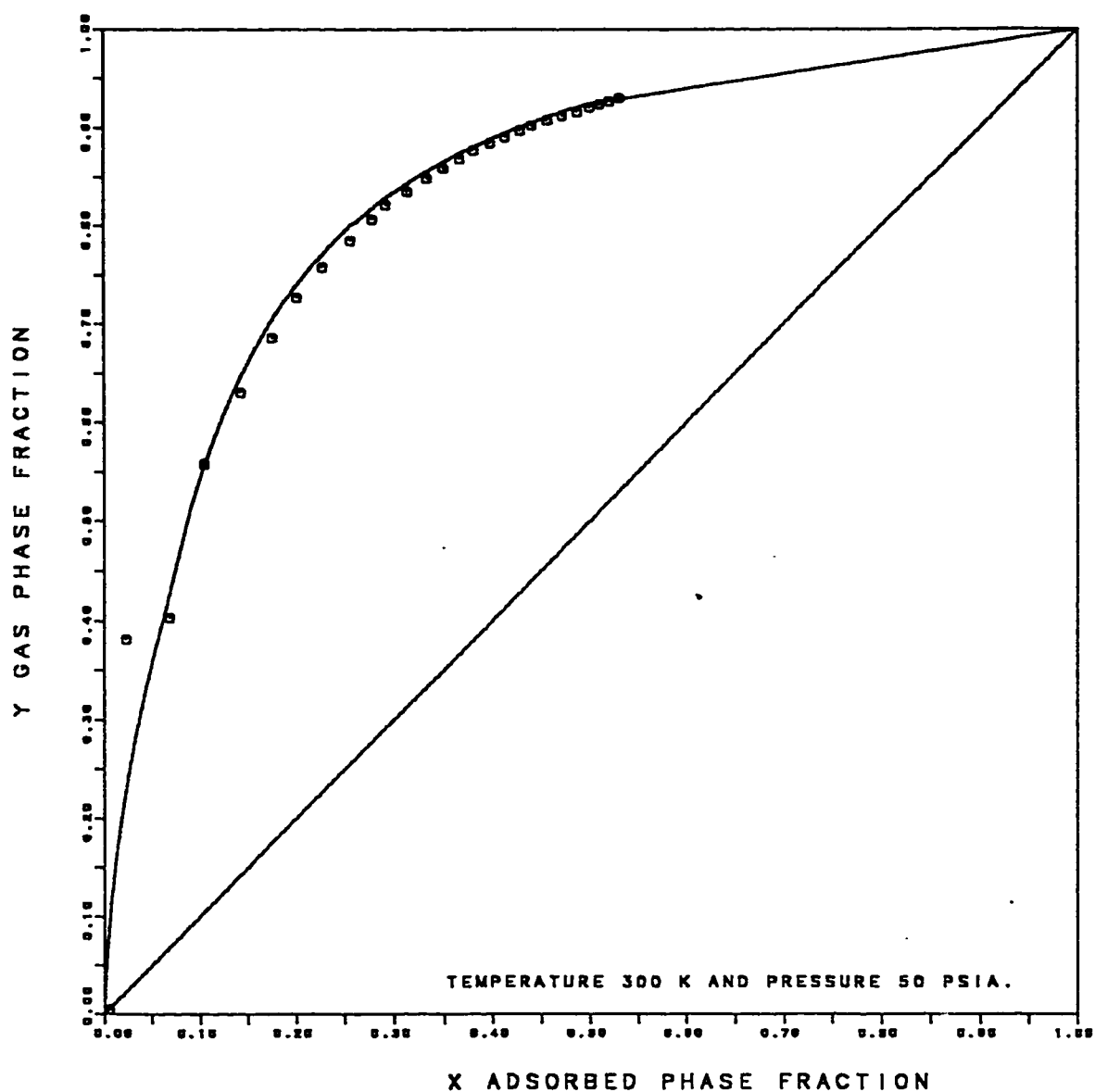


Fig. 4.30: X-Y Plot of Methane-Ethane Binary on Linde 5A Pellets: Fit of Ruthven Model With Theoretical β and Intrinsic K' .

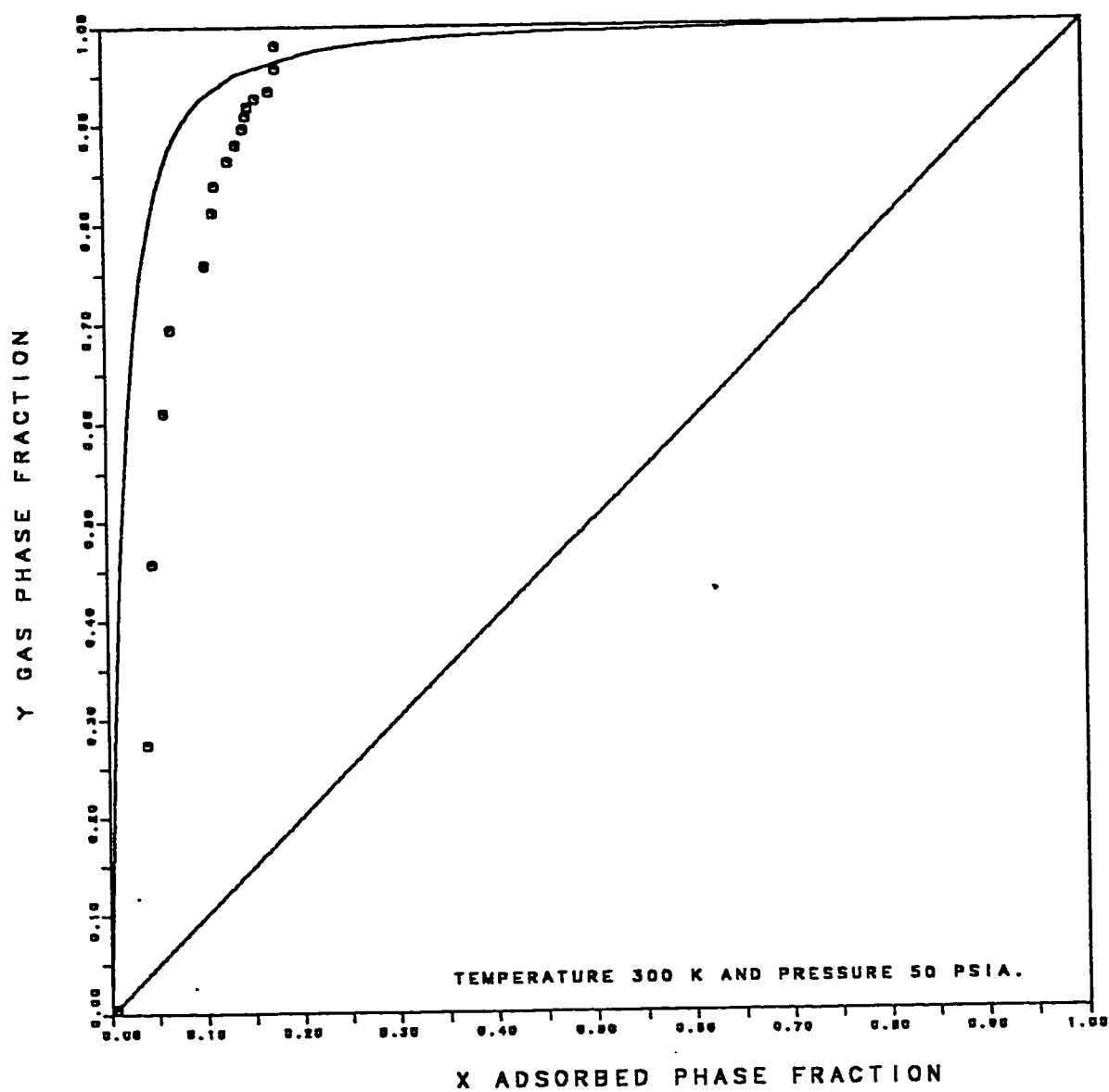


Fig. 4.31: X-Y Plot of Methane-Propane Binary on Linde 5A Pellets: Fit of Ruthven Model With Theoretical β and Intrinsic K' .

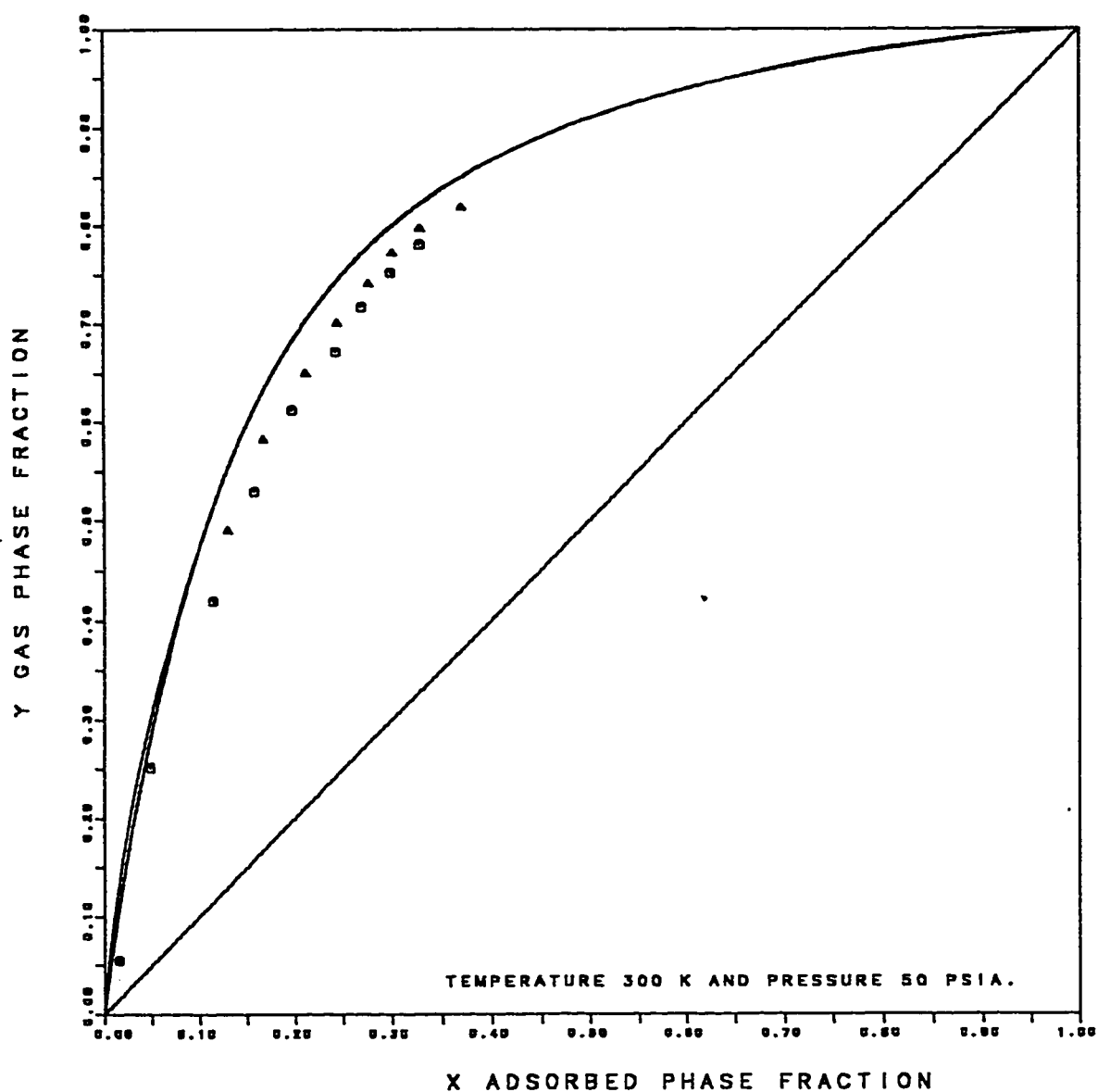


Fig. 4.32: X-Y Plot of Ethane-Propane Binary on Linde 5A Pellets: Fit of Ruthven Model With Theoretical β and Intrinsic K' .

LITERATURE CITED

1. Ruthven, D.M., and K.F. Loughlin, J. Chem. Soc., Faraday Trans. 1, 68, 696 (1972).
2. Holborow, K.A., Ph.D Thesis, University of New Brunswick, N.B., July, 1974.
3. Hasanain, M.A. and K.F. Loughlin, "Demethanization of Natural Gas by Pressure Swing Adsorption", KACST Project No AR-6-147 Report # 2, March 16th (1986). Report # 3, September 16th (1986)
4. Barrer, R.M., and J.A. Lee, Surface Sci., 12, 354 (1968).
5. Rolniak, P., and R. Kobayashi, "Adsorption of Methane and Several Mixtures of Methane and Carbon Dioxide at Elevated Pressures and Near Ambient Temperatures on 5A and 13X Molecular Sieves by Tracer Perturbation Chromatography ", AIChE J., 26, 4, 616 (1980).

CHAPTER 5

PURE AND MULTICOMPONENT EQUILIBRIUM RESULTS ON LINDE S-115 PELLETS.

Pure component equilibrium adsorption data was measured for methane (up to 250 psia), ethane (up to 65 psia), propane (up to 50 psia) and n-butane (up to 30 psia) at 275, 300, 325 and 350 °K. The data was analysed using the Soave-Redlich-Kwong equation of state and the intrinsic Henry constant was measured from the Barrer and Lee adsorption isotherm plotted in the form $\ln(f/C)$ versus C in Figures 5.1 to 5.4. The Henry constant for propane and n-butane at 275 °K was not evaluated because of error in measurement of low pressure. Since the apparatus was designed for high pressure adsorption, the vacuum 2.0×10^{-4} torr created by the pump is insufficient at very low pressures to get a true accurate reading. Also the pressure gauges employed are for high pressure measurement introducing further complications for low pressure measurement. The data is thermodynamically consistent, since all the isotherms $(d\ln C/d\ln f)$ approach 1 as the fugacity approaches zero.

The intrinsic Equilibrium constants are tabulated in Table 5.1 and plotted in Figure 5.5. The data have been regressed to obtain the

preexponential factor K'_0 and $(-\Delta U_0)$ the heat of adsorption; values are also tabulated in Table 5.1 together with the theoretical saturation concentration N_0 which is obtained from the equation

$$N_0 = 0.152 \times p_{\text{adsorbate}} \quad (5.1)$$

for silicalite. The figure 0.152 comes from multiplying the voidage of 0.190 cc/gm zeolite by 0.8 to convert to 0.152 cc/gm pellet.

5.1: Fit of LRC Model To Silicalite Pure Component Data:

An attempt was made to model the pure component data using the intrinsic Equilibrium constant and theoretical saturation concentration, but this was unsuccessful. The decision was made to relax one of the parameters and optimize the other two.

In Table 5.2 the results of regressing the data using the intrinsic Equilibrium constant and optimizing N_0 and n values are reported. The regressed fit is shown in Figures 5.6 to 5.9 inclusive. As may be observed by examining the fit of model to the data and from the calculation of sum of least squares, the model isotherm represents the data quite well with the possible exception of the very high concentration regions for ethane, propane and n-butane. This is probably due to the optimized N_0 being on average 77%, 80%, 85% and 89% of the theoretical

saturation concentration for the gases methane, ethane, propane and n-butane respectively. Interestingly the optimized N_0 for methane is farthest from the predicted values. This is contrary to that anticipated as configurational rearrangement of the n-butane molecule should be more difficult than that for methane in the restricted pore space.

The alternative procedure of optimizing K and n while using the predicted value of N_0 is presented in Table 5.3 and in Figures 5.10 to 5.13 inclusive. The model fit is again reasonable being more accurate at the higher concentrations but in this case a few per cent too high. However the sum of least squares are approximately two to three times greater than the previous case of intrinsic K , optimized N_0 and n suggesting that optimization using the first technique is more appropriate for this model.

Finally the model was regressed by optimizing the three parameters K , N_0 and n . The regression results are presented in Table 5.4 and the fit is shown in Figures 5.14 to 5.17 inclusive. The model fit is good with the sum of least squares being minimal for this case as would be expected. Interestingly the optimized K , and N_0 values are close to those for the regression case of intrinsic K and optimized N_0 suggesting that the use of intrinsic K in calculating the isotherm is probably the best procedure.

One final regression was performed using intrinsic K and theoretical N_0 values. The experimental data was subdivided into three regions: region 1 where $\theta < 0.33$, region 2 where θ lies between 0.33 and 0.67 and region 3 where θ was greater than 0.67. For each of these regions values of n were regressed and are reported as n_1 , n_2 and n_3 for regions 1, 2 and 3 respectively in Table 5.5. This regression indicated that the n_1 appears to be about 0.9, n_2 approximately 2 and n_3 approximately 2.5 to 3.0. This suggests that n is a function of θ the loading and that the LRC model should be modified accordingly. It also suggests that the LRC model is not a good model for this data.

5.2: Fit of Toth Model To Silicallite Pure Component Data:

A similar analysis was carried out for this isotherm as for the LRC. The results of the analysis are presented in Tables 5.6 to 5.10 and Figures 5.18 to 5.33 inclusive. The fit of this model was a significant improvement. The use of intrinsic K and theoretical N_0 values for regression gave reasonable fits, as may be observed in Figures 5.18 to 5.21. This case was not reasonable for the LRC model. Conclusions regarding reduction in N_0 values when this property is optimized were analogous to those for the LRC regarding species percent N_0 reduction. The use of intrinsic K and optimized N_0 values is probably comparable

to that for optimizing both values.

A significant difference was observed from the LRC model when the isotherm was subdivided into the three regions as before. The values of n_1 , n_2 and n_3 optimized did not vary significantly suggesting that the Toth model gives a satisfactory representation of the data.

For the Toth model the value of heterogeneous parameter n is less than one for all components, as indicated, this shows that the widening of quasi-Gaussian energy distribution was on the left-hand side.

5.3: Fit of Mathews & Weber Model To Silicalite Pure Component Data:

A similar analysis was carried out for this isotherm as for the LRC and Toth models. For this isotherm it was observed that any calculations using theoretical N_0 values rose to a maximum and then decreased. As this was not the pattern of the experimental data, this calculation procedure was deemed unsatisfactory and was deleted.

The use of intrinsic K , optimized N_0 and n gave very good fits as may be observed in Figures 5.34 to 5.37. The optimized N_0 values were comparable to those determined in the LRC and Toth optimization procedures. The use of optimized K , N_0 and n in this isotherm model gave excellent model fits (see Figures 5.38 to 5.41) but the optimized

N_0 values appeared to be somewhat lower than for any of the other isotherm models (see Table 5.12). However the sum of least squares indicated that for this model, the fit with all parameters optimized was excellent.

When the data was subdivided into three regions as for the other isotherm models and using intrinsic K and theoretical N_0 values, the values n_1 , n_2 and n_3 were found to be approximately 2.0, 0.8 and 0.9 respectively. This suggests that n is a function of concentration, and that this model is inappropriate for this data.

5.4: Fit of Jaroniec Model To Silicalite Pure Component Data:

As in the previous models the data was regressed using intrinsic K and theoretical N_0 , it may be observed from the Figures 5.42 to 5.45 and Table 5.14 that the fit of the model for this case is better than any other model. The value of parameter n is always less than m , and this again shows that the widening of quasi-Gaussian energy distributions is towards left-hand side.

The use of intrinsic K , optimized N_0 , n and m gave a good fit for the data, as may be observed from Figures 5.46 to 5.49 and Table 5.15. The value of optimized N_0 is again comparable to the other three

models. With theoretical N_0 and optimized K , m and n it is interesting to observe that the value of parameter m is equal to one for all components and the value of optimized K and n are almost equal to that of Toth model. (see Table 5.16 and Figures 5.50 to 5.53)

Again for optimized K , N_0 , m and n the fit was good as shown in Figures 5.54 to 5.57. The value of parameter m equals to one for most of the isotherms as may be observed from Table 5.17. This shows that the Jaroniec isotherm model reduces to the Toth isotherm model for this system.

When the data was subdivided into three θ regions as previously and using intrinsic K and theoretical N_0 , the fit of the model was excellent with the values of m 's and n 's being given in Table 5.18. It may be observed that the value of sum of least squares is minimal for this case in comparison to any other case but that the value of parameters m and n are varying with the concentration indicating that this model isotherm does not characterize the data properly.

5.5: Fit of Ruthven Model To Silicalite Pure Component Data:

In the fit of the Ruthven model (Equation 2.30) the volume of each cavity (v) and the number of cells per gram of the adsorbent must be known. But for silicalite, which is a new type of adsorbent, these two

quantities are undefined. From prior knowledge of the pore volume the number of cells can be related to v . Using theoretical β and intrinsic K' the data was regressed to optimize v . Unfortunately the model did not fit the data. The reason for this may be the relation between the cavity volume (v) and the number of cells per gram. So both these quantities were regressed using theoretical β and intrinsic K' , but again the fit of the model was unsatisfactory.

Since for silicalite the fit of other models shows that the intrinsic Equilibrium constant and theoretical saturation concentration gave a good estimate of the data. Hence the data was not regressed by optimizing all the four variables, i.e. the volume of cavity, the number of cells, β and K' .

5.6: Derivation of Multicomponent Toth Model:

The Toth model given by Equation (2.26) can be extended to the multicomponent equilibrium adsorption using the method of Markham and Benton to give the equation

$$\frac{N_1}{N_{01}} = \left[\frac{(K_1 P_1)^{n_1}}{1 + \sum_{j=1}^r \{K_j P_j\}^{n_j}} \right]^{n_1} \quad (5.2)$$

where K_1 and K_j are the equilibrium constants of pure component 1 and j respectively,

n_1 and n_j are the heterogeneity parameters of pure component 1 and j respectively

N_1 is the concentration of component 1 in the mixed adsorbed phase,

N_{O1} is the saturation concentration of pure component 1 and

P_1 and P_j are the partial pressures of component 1 and j respectively.

With similar expressions for other components Equation 5.2 gives a simple equation for multicomponent adsorption equilibria in terms of pure component equilibrium constant, saturation concentration and heterogeneity parameter.

5.7: Fit of Multicomponent Toth Model To Silicalite:

From the analysis of pure component data it was decided that the Toth model would be used to fit the multicomponent data using Equation 5.2. Two sets of parameters were used to model the multicomponent data; intrinsic K and optimized N_O from Table 5.7 and optimized K and

N_0 from Table 5.9. The binary data are given in Tables 5.19 to 5.28 and plotted in Figures 5.58 to 5.64 inclusive. It can be observed that the fit of the model was reasonable with intrinsic K and optimised N_0 and with the optimized K and N_0 only the methane-ethane binary fits the model better.

The ternary and quaternary data are analysed using intrinsic K and optimized N_0 and are presented in Tables 5.29 to 5.36 inclusive. It can be observed from these tables that with the exception of methane the calculated concentrations for the other components are good. The reasons for the low methane concentration may be the optimized saturation concentration or that methane is the least adsorbed species.

Table 5.1 : Intrinsic Henry Constant (K'), Theoretical Saturation Concentration (N_o), Pre-exponential Factor (K'_o) And Heat Of Adsorption ($-\Delta U_o$) For Linde S-115 Pellets.

Component	T Degrees Kelvin	N_o mmoles/gm pellet	K' (mmole/gm pellet/psia)	K'_o	$-\Delta U_o$ Kcal/mole
Methane	275.00	3.129	0.1449	1.878×10^{-5}	4.87
	300.00	3.022	0.0645		
	325.00	2.922	0.0339		
	350.00	2.828	0.0217		
Ethane	275.00	2.481	5.5555	3.250×10^{-6}	7.83
	300.00	2.399	1.7240		
	325.00	2.323	0.5130		
	350.00	2.251	0.2780		
Propane	275.00	1.932	16.6667	2.005×10^{-6}	9.52
	300.00	1.895			
	325.00	1.860			
	350.00	1.826			
N-Butane	275.00	1.576	90.9000	3.787×10^{-7}	11.53
	300.00	1.508			
	325.00	1.445			
	350.00	1.388			

Table 5.2 : Optimised Parameters Of LRC Model (Intrinsic K) For Linde S-115 Pellets.

Component	T Temperature Degrees Kelvin	N ₀ Saturation Conc mmoles/gm pellet	K Equilibrium Constant (1/(psia))	n Parameter	Sum of Least Squares
Methane	275.00	2.353	0.0463	1.1130	0.0059
	275.00	2.462	0.0463	1.1928	0.0238
	300.00	2.343	0.0214	1.1588	0.0540
	325.00	2.208	0.0116	1.1126	0.0574
	350.00	2.208	0.0076	1.1169	0.0078
Ethane	275.00	2.036	2.2392	1.2766	0.0352
	300.00	1.911	0.7186	1.1538	0.0059
	325.00	1.826	0.2251	1.0522	0.0036
	350.00	1.838	0.1235	1.0863	0.0007
Propane	275.00				
	300.00	1.584	8.7951	0.9792	0.0647
	325.00	1.581	2.9870	1.2499	0.0348
	350.00	1.555	0.9283	1.1415	0.0098
N-Butane	275.00				
	300.00	1.341	60.2851	1.0895	0.0221
	325.00	1.243	19.7720	1.0637	0.0077
	350.00	1.292	4.0026	1.1598	0.0197

Table 5.3 : Optimised Parameters Of LRC Model (Theoretical N_0) For Linde S-115 Pellets.

Component	T Temperature Degrees Kelvin	N_0 Saturation Conc mmoles/gm pellet	K Equilibrium Constant (1/(psia))	n Parameter	Sum of Least Squares
Methane	275.00	3.129	0.0189	1.5271	0.0864
	275.00	3.129	0.0215	1.6540	0.1306
	300.00	3.022	0.0107	1.4956	0.0875
	325.00	2.922	0.0060	1.3696	0.0766
	350.00	2.828	0.0044	1.2764	0.0162
Ethane	275.00	2.481	0.8459	2.0886	0.0986
	300.00	2.399	0.2952	1.7830	0.0702
	325.00	2.323	0.1136	1.3826	0.0514
	350.00	2.251	0.0686	1.3826	0.0268
Propane	275.00	1.932	3.2685 1.4106 0.4737	1.8705	0.1501
	300.00	1.895		2.0184	0.0502
	325.00	1.860		1.6675	0.0413
	350.00	1.826			
N-Butane	275.00	1.576	36.9660 11.6610 3.5008	1.9956	0.1216
	300.00	1.508		1.3066	0.0059
	325.00	1.445		1.3979	0.0465
	350.00	1.388			

Table 5.4 : Optimised Parameters (N_o , K & n) Of LRC Model For Linde S-115 Pellets.

Component	T Temperature Degrees Kelvin	N_o Saturation Conc mmoles/gm pellet	K Equilibrium Constant (1/(psia))	n Parameter	Sum of Least Squares
Methane	275.00	2.301	0.0502	1.0770	0.0045
	275.00	2.349	0.0552	1.0980	0.0137
	300.00	2.161	0.0289	1.0305	0.0205
	325.00	1.845	0.0191	0.8973	0.0189
	350.00	2.001	0.0096	1.0379	0.0667
Ethane	275.00	2.084	1.8440	1.3610	0.0203
	300.00	1.929	0.6810	1.1817	0.0052
	325.00	1.805	0.2427	1.0342	0.0007
	350.00	1.800	0.1314	1.0522	0.0002
Propane	275.00	1.728	10.4967	0.9159	0.0390
	300.00	1.637	6.5232	1.0635	0.0126
	325.00	1.628	2.2665	1.2923	0.0042
	350.00	1.588	0.7991	1.1979	0.0028
N-Butane	275.00	1.627	3084.6000	4.9380	0.0023
	300.00	1.349	55.2700	1.0099	0.0190
	325.00	1.242	17.6200	1.0610	0.0005
	350.00	1.256	4.9300	1.0630	0.0058

Table 5.5 : Intrinsic Equilibrium Constant K, Theoretical Saturation Concentration N_0 And Optimised n's For LRC Model At Different Range Of Concentrations For Linde S-115 Pellets.

Component	T Temperature Degrees Kelvin	n_1 Parameter	SS Sum of Least Squares	n_2 Parameter	SS Sum of Least Squares	n_3 Parameter	SS Sum of Least Squares
Methane	275.00	0.9484	0.02250	1.8833	0.67310	2.6452	0.17520
	275.00	0.9770	0.00571	1.4910	0.58670	3.1010	0.03160
	300.00	0.9531	0.00376	1.1489	0.57460	3.4531	0.03290
	325.00	0.8706	0.00686	1.4218	0.80825	10.0000	0.01953
	350.00	0.9185	0.04181	0.9149	0.68690	10.0000	0.08008
Ethane	275.00	0.9381	0.03527	3.3926	0.09638	3.0191	0.00099
	300.00	0.9036	0.00667	2.9167	0.17950	2.8351	0.00035
	325.00	0.9147	0.00979	2.1641	0.21056	2.5856	0.00051
	350.00	0.9457	0.02130	2.3477	0.19187	2.3566	0.00005
Propane	300.00	0.6956	0.03246	2.5674	0.11570	2.7915	0.00515
	325.00	0.7522	0.08526	2.2332	0.08596	2.6169	0.00251
	350.00	0.8696	0.02645	2.3955	0.03860	2.2899	0.00018
N-Butane	300.00	0.7649	0.00269	1.7730	0.00629	2.6440	0.01685
	325.00	0.7961	0.02090	2.2654	0.04589	2.0233	0.00068
	350.00	1.0389	0.00126	1.2862	0.00113	1.7115	0.00763

Table 5.6 : Optimised Parameters Of Toth Model (Intrinsic K & Theoretical N_0) For Linde S-115 Pellets.

Component	T Temperature Degrees Kelvin	N_0 Saturation Conc mmoles/gm pellet	K Equilibrium Constant (1/(psia))	n Parameter	Sum of Least Squares
Methane	275.00	3.129	0.0463	0.6482	0.1301
	275.00	3.129	0.0463	0.6532	0.3083
	300.00	3.022	0.0214	0.6941	0.1838
	325.00	2.922	0.0116	0.7104	0.0925
	350.00	2.828	0.0076	0.7337	0.0214
Ethane	275.00	2.481	2.2392	0.5865	0.4204
	300.00	2.399	0.7186	0.6174	0.2073
	325.00	2.323	0.2251	0.6933	0.0566
	350.00	2.251	0.1235	0.7186	0.0456
Propane	275.00	1.932	8.7951 2.9870 0.9283	0.6298	0.2079
	300.00	1.895		0.6304	0.2081
	325.00	1.860		0.6684	0.1110
	350.00	1.826			
N-Butane	275.00	1.576	60.2851 19.7720 4.0026	0.7401	0.1951
	300.00	1.508		0.7413	0.0059
	325.00	1.445		0.8749	0.1012
	350.00	1.388			

Table 5.7 : Optimised Parameters Of Toth Model (Intrinsic K) For Linde S-115 Pellets.

Component	T Temperature Degrees Kelvin	N ₀ Saturation Conc mmoles/gm pellet	K Equilibrium Constant (1/(psia))	n Parameter	Sum of Least Squares
Methane	275.00	2.298	0.0463	1.0000	0.0244
	275.00	2.372	0.0463	1.0000	0.0746
	300.00	2.322	0.0214	1.0000	0.1076
	325.00	2.234	0.0116	1.0000	0.0749
	350.00	2.828	0.0076	0.7301	0.0219
Ethane	275.00	2.015	2.2392	0.9046	0.0552
	300.00	1.872	0.7186	0.9911	0.0198
	325.00	1.829	0.2251	1.0000	0.0088
	350.00	1.807	0.1235	1.0000	0.0091
Propane	275.00				
	300.00	1.652	8.7951	0.8262	0.0125
	325.00	1.608	2.9870	0.8344	0.0088
	350.00	1.561	0.9283	0.9127	0.0096
N-Butane	275.00				
	300.00	1.355	60.2851	0.8253	0.0438
	325.00	1.248	19.7720	0.9203	0.0005
	350.00	1.278	4.0026	1.0000	0.0359

Table 5.8 : Optimised Parameters Of Toth Model (Theoretical N_0) For Linde S-115 Pellets.

Component	T Temperature Degrees Kelvin	N_0 Saturation mmoles/gm pellet	K Equilibrium Constant (1/(psia))	n Parameter	Sum of Least Squares
Methane	275.00	3.129	0.0886	0.5320	0.0408
	275.00	3.129	0.1295	0.5000	0.0767
	300.00	3.022	0.0439	0.5516	0.0519
	325.00	2.922	0.0179	0.5993	0.0528
	350.00	2.828	0.0100	0.6482	0.0097
Ethane	275.00	2.481	5.2731	0.5000	0.1550
	300.00	2.399	1.8015	0.5000	0.0451
	325.00	2.323	0.3346	0.6068	0.0247
	350.00	2.251	0.1888	0.6225	0.0124
Propane	275.00	1.932	27.6840	0.4658	0.1055
	300.00	1.895	14.9606	0.4408	0.0339
	325.00	1.860	2.3836	0.5259	0.0220
	350.00	1.826			
N-Butane	275.00	1.576	300.0000	0.4645	0.0962
	300.00	1.508	24.5850	0.6821	0.0033
	325.00	1.445	9.0772	0.6366	0.0314
	350.00	1.388			

Table 5.9 : Optimised Parameters (N_0 , K & n) Of Toth Model For Linde S-115 Pellets.

Component	T Temperature Degrees Kelvin	N_0 Saturation Conc mmoles/gm pellet	K Equilibrium Constant (1/(psia))	n Parameter	Sum of Least Squares
Methane	275.00	2.344	0.0614	0.8608	0.0043
	275.00	2.369	0.0688	0.8633	0.0150
	300.00	2.192	0.0314	0.9267	0.0201
	325.00	2.000	0.0160	0.9975	0.0232
	350.00	2.027	0.0105	0.9269	0.0068
Ethane	275.00	2.124	4.5115	0.6357	0.0138
	300.00	1.967	1.0750	0.7550	0.0031
	325.00	1.824	0.2653	0.9278	0.0005
	350.00	1.817	0.1483	0.9112	0.0003
Propane	275.00	1.737	10.2979	1.0000	0.0431
	300.00	1.644	7.7990	0.8858	0.0112
	325.00	1.642	4.2706	0.7077	0.0028
	350.00	1.611	1.2900	0.7530	0.0017
N-Butane	275.00	1.388	1718.7000	0.8000	0.0607
	300.00	1.353	70.7200	0.8563	0.0176
	325.00	1.254	20.2400	0.9025	0.0005
	350.00	1.263	5.8240	0.8911	0.0049

Table 5.10: Intrinsic Equilibrium Constant K , Theoretical Saturation Concentration N_0 And Optimised n 's For Toth Model At Different Range Of Concentrations For Linde S-115 Pellets.

Component	T Temperature Degrees Kelvin	n_1 Parameter	SS Sum of Least Squares	n_2 Parameter	SS Sum of Least Squares	n_3 Parameter	SS Sum of Least Squares
Methane	275.00	0.7376	0.00059	0.6920	0.01028	0.6239	0.04259
	275.00	0.8933	0.00327	0.7289	0.02024	0.6362	0.14903
	300.00	0.8282	0.00012	0.7561	0.03892	0.6724	0.34387
	325.00	0.7897	0.00132	0.7392	0.01338	0.6782	0.02471
	350.00	0.7778	0.00233	0.7266	0.00895	0.7162	0.00273
Ethane	275.00	0.7862	0.00036	0.6886	0.03684	0.5420	0.08910
	300.00	0.7904	0.00011	0.6844	0.04484	0.5728	0.01899
	325.00	0.7869	0.00062	0.7292	0.00496	0.6559	0.00992
	350.00	0.7934	0.00023	0.7339	0.01536	0.6816	0.00076
Propane	300.00	0.6671	0.03618	0.7104	0.00567	0.5526	0.09000
	325.00	0.7362	0.00003	0.6968	0.01488	0.5638	0.04961
	350.00	0.7989	0.00042	0.7350	0.00623	0.6217	0.02244
N-Butane	300.00	0.8373	0.00426	0.8156	0.00302	0.6164	0.12317
	325.00	0.7485	0.00007	0.7641	0.00083	0.7170	0.00184
	350.00	1.0000	0.00261	0.9636	0.00949	0.7588	0.03064

Table 5.11: Optimised Parameters Of Mathews and Weber Model (Intrinsic K) For Linde S-115 Pellets.

Component	T Temperature Degrees Kelvin	N ₀ Saturation Conc mmoles/gm pellet	K Equilibrium Constant (1/(psia))	n Parameter	Sum of Least Squares
Methane	275.00	2.365	0.0463	0.9759	0.0157
	275.00	2.495	0.0463	0.9637	0.0365
	300.00	2.473	0.0214	0.9219	0.0396
	325.00	2.337	0.0116	0.8751	0.0204
	350.00	2.243	0.0076	0.8550	0.0111
Ethane	275.00	1.825	2.2392	1.0224	0.0536
	300.00	1.837	0.7186	1.0051	0.0212
	325.00	1.808	0.2251	0.9939	0.0120
	350.00	1.815	0.1235	0.9852	0.0078
Propane	275.00				
	300.00	1.461	8.7951	1.0228	0.0071
	325.00	1.371	2.9870	1.0328	0.0106
	350.00	1.449	0.9283	1.0176	0.0104
N-Butane	275.00				
	300.00	1.215	60.2851	1.0175	0.0220
	325.00	1.166	19.7720	1.0178	0.0008
	350.00	1.314	4.0026	0.9879	0.0255

Table 5.12: Optimised Parameters (N_o , K & n) Of Mathews & Weber Model For Linde S-115 Pellets.

Component	T Temperature Degrees Kelvin	N_o Saturation mmoles/gm pellet	K Equilibrium Constant (1/(psia))	n Parameter	Sum of Least Squares
Methane	275.00	1.994	0.0683	1.0475	0.0047
	275.00	2.106	0.0702	1.0301	0.0174
	300.00	1.999	0.0338	1.0311	0.0198
	325.00	2.259	0.0127	0.9019	0.0188
	350.00	1.850	0.0113	1.0336	0.0068
Ethane	275.00	1.527	3.9340	1.0611	0.0016
	300.00	1.541	1.1322	1.0558	0.0006
	325.00	1.682	0.2811	1.0247	0.0005
	350.00	1.654	0.1569	1.0287	0.0004
Propane	275.00	1.666	11.3059	1.0079	0.0398
	300.00	1.472	8.2519	1.0212	0.0052
	325.00	1.335	3.5526	1.0383	0.0003
	350.00	1.281	1.3109	1.0501	0.0003
N-Butane	275.00	1.164	1500.0000	1.0225	0.0189
	300.00	1.199	72.8680	1.0195	0.0086
	325.00	1.131	21.4730	1.0299	0.0005
	350.00	1.141	6.1051	1.0222	0.0026

Table 5.13: Intrinsic Equilibrium Constant K , Theoretical Saturation Concentration N_o And Optimised n 's For Mathews And Weber Model At Different Range Of Concentrations For Linde S-115 Pellets.

Component	T Temperature Degrees Kelvin	n_1 Parameter	SS Sum of Least Squares	n_2 Parameter	SS Sum of Least Squares	n_3 Parameter	SS Sum of Least Squares
Methane	275.00	2.0760	0.00447	0.6482	0.28880	0.8253	0.21230
	275.00	1.2370	0.00370	0.6557	0.25070	0.8533	0.24840
	300.00	1.4800	0.00050	0.7323	0.36000	0.7858	0.14870
	325.00	1.9640	0.00135	0.6027	0.52280	0.6699	0.04480
	350.00	1.8870	0.00979	0.7724	0.67980	0.5328	0.02370
Ethane	275.00	2.4920	0.01430	0.8267	0.16010	0.9434	0.35390
	300.00	1.9390	0.00114	0.8473	0.17910	0.9210	0.07090
	325.00	1.9493	0.00129	0.7690	0.14340	0.8722	0.02820
	350.00	1.9737	0.00423	0.8209	0.17046	0.8692	0.00164
Propane	300.00	5.5000	0.02450	0.8386	0.14580	0.9700	0.12717
	325.00	1.3790	0.09517	0.8587	0.16795	0.9601	0.13270
	350.00	2.0294	0.02011	0.8481	0.06098	0.9505	0.07620
N-Butane	300.00	4.0200	0.00120	0.8617	0.00734	0.9828	0.08700
	325.00	4.6430	0.01090	0.8000	0.04360	0.9356	0.02590
	350.00	0.4899	0.60240	0.8150	0.26080	0.9719	0.13470

Table 5.14: Optimised Parameters Of Jaroniec Model (Intrinsic K & Theoretical N_0) For Linde S-115 Pellets.

Component	T Temperature Degrees Kelvin	N_0 Saturation conc mmoles/gm pellet	K Equilibrium Constant (1/(psia))	n Parameters	m Parameters	Sum of least squares
Methane	275.00	3.129	0.0463	0.5731	0.8437	0.0539
	275.00	3.129	0.0463	0.5489	0.7532	0.0996
	300.00	3.022	0.0214	0.6018	0.8176	0.0659
	325.00	2.922	0.0116	0.6422	0.8879	0.0598
	350.00	2.828	0.0076	0.6805	0.9275	0.0107
Ethane	275.00	2.481	2.2392	0.4490	0.6201	0.0796
	300.00	2.399	0.7186	0.5114	0.7208	0.0509
	325.00	2.323	0.2251	0.6410	0.8935	0.0313
	350.00	2.251	0.1235	0.6585	0.8774	0.0167
Propane	275.00	1.932	8.7951 2.9870 0.9283	0.5018 0.4753 0.5653	0.7250 0.6210 0.7470	0.1248 0.0434 0.0311
	300.00	1.895				
	325.00	3.237				
	350.00	3.178				
n-Butane	275.00	1.576	60.2851 19.7720 4.0026	0.4915 0.7043 0.7020	0.5335 0.9304 0.7564	0.1137 0.0038 0.0434
	300.00	1.508				
	325.00	1.445				
	350.00	1.388				

Table 5.15: Optimised Parameters Of Jaroniec Model (Intrinsic K) For Linde S-115 Pellets.

Component	T Temperature Degrees Kelvin	N _O Saturation conc mmoles/gm pellet	K Equilibrium Constant (1/(psia))	n Parameters	m	Sum of least squares
Methane	275.00	2.292	0.0463	0.9518	0.8994	0.0047
	275.00	2.319	0.0463	0.9725	0.8485	0.0129
	300.00	2.192	0.0214	1.0000	0.8409	0.0240
	325.00	2.084	0.0116	1.0000	0.8652	0.0321
	350.00	2.039	0.0076	1.0000	0.8811	0.0071
Ethane	275.00	2.100	2.2392	0.7020	0.7854	0.0184
	300.00	1.941	0.7186	0.8243	0.8616	0.0048
	325.00	1.802	0.2251	0.9867	0.9375	0.0009
	350.00	1.787	0.1235	0.9767	0.9263	0.0001
Propane	275.00					
	300.00	1.652	8.7951	0.8272	1.0000	0.0125
	325.00	1.634	2.9870	0.7433	0.8684	0.0035
	350.00	1.597	0.9283	0.8034	0.8840	0.0024
n-Butane	275.00					
	300.00	1.351	60.2851	0.8928	0.9494	0.0184
	325.00	1.253	19.7720	0.9074	0.9892	0.0005
	350.00	1.255	4.0026	0.9775	0.8565	0.0074

Table 5.16: Optimised Parameters Of Jaroniec Model (Theoretical N_O) For Linde S-115 Pellets.

Component	T Temperature Degrees Kelvin	N_O Saturation conc mmoles/gm pellet	K Equilibrium Constant (1/(psia))	n Parameters	m	Sum of least squares
Methane	275.00	3.129	0.0884	0.5323	1.0000	0.0408
	275.00	3.129	0.1000	0.5117	0.9356	0.0812
	300.00	3.022	0.0433	0.5534	1.0000	0.0520
	325.00	2.922	0.0176	0.6027	1.0000	0.0529
	350.00	2.828	0.0099	0.6499	1.0000	0.0097
Ethane	275.00	2.481	14.6350	0.4057	1.0000	0.0576
	300.00	2.399	2.3589	0.4697	1.0000	0.0365
	325.00	2.323	0.3343	0.6071	1.0000	0.0247
	350.00	2.251	0.1880	0.6233	1.0000	0.0124
Propane	275.00	1.932				
	300.00	1.895	27.7030	0.4657	1.0000	0.1055
	325.00	1.860	15.0750	0.4406	1.0000	0.0339
	350.00	1.826	2.3903	0.5256	1.0000	0.0220
n-Butane	275.00	1.576				
	300.00	1.508	330.7860	0.4552	1.0000	0.0953
	325.00	1.445	24.5380	0.6826	1.0000	0.0033
	350.00	1.388	9.0694	0.6368	1.0000	0.0314

Table 5.17: Optimised Parameters (N_o , K & n) Of Jaroniec Model For Linde S-115 Pellets.

Component	T Temperature Degrees Kelvin	N_o Saturation conc mmoles/gm pellet	K Equilibrium Constant ($1/(\text{psia})$)	n Parameters	m	Sum of least squares
Methane	275.00	2.346	0.0615	0.8589	1.0000	0.0043
	275.00	2.312	0.0417	1.0000	0.8097	0.0126
	300.00	2.200	0.0316	0.9184	1.0000	0.0201
	325.00	1.974	0.0165	1.0000	1.0000	0.0227
	350.00	1.971	0.0091	1.0000	0.9376	0.0066
Ethane	275.00	2.121	4.4624	0.6395	1.0000	0.0138
	300.00	1.969	1.0844	0.7512	1.0000	0.0031
	325.00	1.825	0.2658	0.9260	1.0000	0.0005
	350.00	1.777	0.1174	1.0000	0.9068	0.0001
Propane	275.00	1.737	10.3328	1.0000	1.0000	0.0431
	300.00	1.644	7.8541	0.8824	1.0000	0.0112
	325.00	1.642	4.3063	0.7052	1.0000	0.0028
	350.00	1.612	1.2973	0.7507	1.0000	0.0017
n-Butane	275.00					
	300.00	1.353	71.6128	0.8509	1.0000	0.0176
	325.00	1.241	17.3046	0.9487	0.9355	0.0005
	350.00	1.264	5.8673	0.8871	1.0000	0.0049

Table 5.18: Intrinsic Equilibrium Constant K, Theoretical Saturation Concentration N_0 And Optimised n's And m's For Jaroniec Model At Different Range Of Concentrations For Linde S-115 Pellets.

Component	T Temperature Degrees Kelvin	n_1 Parameters	m_1 Parameters	SS Sum of Least Squares	n_2 Parameters	m_2 Parameters	SS Sum of Least Squares	n_3 Parameters	m_3 Parameters	SS Sum of Least Squares
Methane	275.00	0.7054	0.9750	0.00029	0.6232	0.8795	0.00327	0.4453	0.5621	0.00497
	275.00	0.7418	0.9246	0.00167	0.6234	0.8316	0.00042	0.3974	0.4442	0.02022
	300.00	0.8086	0.9906	0.00008	0.6364	0.8305	0.01196	0.4706	0.5729	0.00864
	325.00	0.7961	1.0000	0.00149	0.6490	0.8666	0.00544	0.3500	0.4189	0.01037
	350.00	0.7494	0.9770	0.00202	0.6465	0.8766	0.00371	0.4099	0.5189	0.00049
Ethane	275.00	0.7248	0.9470	0.00028	0.4952	0.6302	0.00137	0.3450	0.3622	0.00027
	300.00	0.7468	0.9725	0.00015	0.5225	0.6896	0.00247	0.3729	0.3922	0.00019
	325.00	0.7821	1.0000	0.00058	0.6613	0.8791	0.00091	0.4339	0.4693	0.00001
	350.00	0.7642	0.9755	0.00002	0.6477	0.8334	0.00249	0.4332	0.4386	0.00005
Propane	300.00	0.6679	1.0000	0.00362	0.6479	0.8812	0.00337	0.3175	0.2707	0.00157
	325.00	0.7272	0.9899	0.00004	0.5611	0.7284	0.00159	0.3414	0.2966	0.00060
	350.00	0.7508	0.9536	0.00002	0.6183	0.7797	0.00045	0.4306	0.4228	0.00015
N-Butane	300.00	0.8584	1.0000	0.00511	0.6811	0.7733	0.00012	0.3030	0.2217	0.00115
	325.00	0.7417	0.9856	0.00000	0.7328	0.9485	0.00067	0.5760	0.6560	0.00008
	350.00	1.0000	0.9648	0.00057	0.7762	0.7717	0.00109	0.4700	0.3583	0.00048

TABLE 5.19: BINARY ADSORPTION OF METHANE & ETHANE ON LINDE S-115 PELLETS

AT 300.00 DEGREE KELVIN AND 50.00 PSIA TOTAL PRESSURE.

FIT OF THE MULTICOMPONENT TOTH MODEL, EQUILIBRIUM CONSTANT AND

SATURATION CONCENTRATION FROM TABLE 5.9.

PARTIAL PRESSURES		ADSORB PHASE CONCENTRATION AND MOLE FRACTION				THEORETICAL	
METHANE PSIA	ETHANE PSIA	EXPERIMENTAL METHANE MMOLE/GM PELLETS	THEORETICAL METHANE MMOLE/GM PELLETS	ETHANE MMOLE/GM PELLETS	EXPERIMENTAL METHANE MMOLE/GM PELLETS	METHANE MOLE FRACTION	ETHANE MOLE FRACTION
15.1040	34.8760	0.0380	0.0491	1.7394	0.0207	0.0275	0.9725
24.2741	25.7859	0.1520	0.0964	1.6446	0.0811	0.0554	0.9446
30.1481	19.9318	0.1680	0.1413	1.5572	0.0925	0.0832	0.9168
30.2288	19.9852	0.1680	0.1414	1.5575	0.0925	0.0832	0.9168
38.1241	16.5419	0.2570	0.1980	1.4663	0.1406	0.1190	0.8810
36.7267	13.2893	0.3110	0.2205	1.4074	0.1694	0.1354	0.8646
38.4556	11.3444	0.3570	0.2533	1.3461	0.1968	0.1584	0.8416
40.1581	9.9019	0.4600	0.2853	1.2894	0.2530	0.1812	0.8188
41.2945	8.7655	0.4600	0.3136	1.2388	0.2530	0.2020	0.7980
42.1131	7.8668	0.4770	0.3389	1.1938	0.2665	0.2211	0.7789

TABLE 5.20: BINARY ADSORPTION OF METHANE & ETHANE ON LINDE S-115 PELLETS

AT 300.00 DEGREE KELVIN AND 50.00 PSIA TOTAL PRESSURE.

FIT OF THE MULTICOMPONENT TOTH MODEL, EQUILIBRIUM CONSTANT AND

SATURATION CONCENTRATION FROM TABLE 5.7.

PARTIAL PRESSURES		ADSORB PHASE CONCENTRATION AND MOLE FRACTION				THEORETICAL	
METHANE PSIA	ETHANE PSIA	EXPERIMENTAL METHANE MMOLE/GM PELLETS	THEORETICAL METHANE MMOLE/GM PELLETS	ETHANE MMOLE/GM PELLETS	EXPERIMENTAL METHANE MMOLE/GM PELLETS	METHANE MOLE FRACTION	ETHANE MOLE FRACTION
15.1040	34.8760	0.0380	0.0380	2.2743	0.0207	0.0165	0.9835
24.2741	25.7859	0.1520	0.0802	2.2112	0.0811	0.0350	0.9650
30.1481	19.9318	0.1680	0.1247	2.1444	0.0925	0.0350	0.9450
30.2288	19.9852	0.1680	0.1247	2.1448	0.0925	0.0550	0.9450
38.1241	16.5419	0.2570	0.1834	2.0723	0.1406	0.0813	0.9187
36.7267	13.2893	0.3110	0.2131	2.0114	0.1694	0.0958	0.9042
38.4556	11.3444	0.3570	0.2531	1.9503	0.1968	0.0958	0.8851
40.1581	9.9019	0.4600	0.2934	1.8911	0.2530	0.1343	0.8657
41.2945	8.7655	0.4600	0.3305	1.8354	0.2530	0.1526	0.8474
42.1131	7.8668	0.4770	0.3647	1.7835	0.2665	0.1698	0.8302

TABLE 5.21: BINARY ADSORPTION OF METHANE & ETHANE ON LINDE S-115 PELLETS

AT 300.00 DEGREE KELVIN AND 95.00 PSIA TOTAL PRESSURE

FIT OF THE MULTICOMPONENT TOTH MODEL, EQUILIBRIUM CONSTANT AND

SATURATION CONCENTRATION FROM TABLE 5.9.

PARTIAL PRESSURES		ADSORB PHASE CONCENTRATION AND MOLE FRACTION				THEORETICAL	
METHANE PSIA	ETHANE PSIA	EXPERIMENTAL METHANE MMOLE/GM PELLETS	ETHANE MMOLE/GM PELLETS	THEORETICAL METHANE/GM PELLETS	EXPERIMENTAL METHANE MMOLE FRACTION	THEORETICAL METHANE MMOLE FRACTION	ETHANE MMOLE FRACTION
91.4565	3.5435	0.9230	0.6850	0.8488	0.5740	0.5699	0.4301
82.3480	12.8520	0.4470	1.2840	0.4404	0.2582	0.2716	0.7284
63.9635	31.0365	0.1890	1.5550	0.2065	0.1084	0.1186	0.8814
44.3851	50.9848	0.0790	1.6820	0.1041	0.0449	0.0576	0.9424
28.7357	66.1642	0.0390	1.7620	0.0566	0.0217	0.0307	0.9693
18.1450	76.8549	0.0220	1.8150	0.0323	0.0120	0.0173	0.9827
11.5599	83.7401	0.0110	1.8830	0.0194	0.0058	0.0104	0.9896

TABLE 5.22: BINARY ADSORPTION OF METHANE & ETHANE ON LINDE S-115 PELLETS

AT 300.00 DEGREE KELVIN AND 95.00 PSIA TOTAL PRESSURE.

FIT OF THE MULTICOMPONENT TOTH MODEL, EQUILIBRIUM CONSTANT AND

SATURATION CONCENTRATION FROM TABLE 5.7.

PARTIAL PRESSURES		ADSORB PHASE CONCENTRATION AND MOLE FRACTION				THEORETICAL	
METHANE PSIA	ETHANE PSIA	EXPERIMENTAL METHANE MMOLE/GM PELLETS	ETHANE MMOLE/GM PELLETS	THEORETICAL METHANE/GM PELLETS	EXPERIMENTAL METHANE MMOLE FRACTION	THEORETICAL METHANE MMOLE FRACTION	ETHANE MMOLE FRACTION
91.4565	3.5435	0.9230	0.6850	1.0788	0.5740	0.4957	0.5043
82.3480	12.8520	0.4470	1.2840	0.4507	0.2582	0.1973	0.8027
63.9635	31.0365	0.1890	1.5550	0.1719	0.1084	0.0737	0.9263
44.3851	50.9848	0.0790	1.6820	0.0767	0.0449	0.0326	0.9674
28.7357	66.1642	0.0390	1.7620	0.0391	0.0217	0.0166	0.9834
18.1450	76.8549	0.0220	1.8150	0.0215	0.0120	0.0091	0.9909
11.5599	83.7401	0.0110	1.8830	0.0126	0.0058	0.0053	0.9947

SATURATION CONCENTRATION FROM TABLE 5.9:

SATURATION CONCENTRATION FROM TABLE 5.7:

PARTIAL PRESSURES		ADSORB EXPERIMENTAL		PHASE CONCENTRATION AND MOLE FRACTION		THEORETICAL EXPERIMENTAL		THEORETICAL	
METHANE PSIA	PROPANE PSIA	METHANE MMOLE/GM PELLET	PROPANE MMOLE/GM PELLET	METHANE MMOLES/GM PELLET	PROPANE MMOLE/GM PELLET	METHANE MOLE FRACTION	PROPANE MOLE FRACTION	METHANE MOLE FRACTION	PROPANE MOLE FRACTION
18.9706	31.4294	0.0250	1.7460	0.0070	1.7684	0.0141	0.9859	0.0040	0.9960
29.0517	20.7883	0.0870	1.7190	0.0152	1.7156	0.0482	0.9518	0.0088	0.9912
36.4397	14.4418	0.0960	1.6860	0.0258	1.6596	0.0539	0.9461	0.0153	0.9847
39.2820	10.6319	0.1260	1.6520	0.0357	1.6098	0.0709	0.9291	0.0217	0.9783
41.7993	8.2807	0.1590	1.6200	0.0463	1.5622	0.0894	0.9106	0.0288	0.9712
43.3255	6.5944	0.2090	1.5920	0.0575	1.5156	0.1160	0.8840	0.0365	0.9635
45.1249	5.4551	0.2230	1.5660	0.0692	1.4716	0.1247	0.8753	0.0449	0.9551
45.5847	4.6353	0.2840	1.5430	0.0792	1.4340	0.1554	0.8446	0.0523	0.9477
45.9516	4.0284	0.2990	1.5220	0.0887	1.3997	0.1642	0.8358	0.0596	0.9404
46.3978	3.5621	0.3110	1.5030	0.0980	1.3678	0.1714	0.8266	0.0669	0.9331
46.9410	3.1989	0.3560	1.4850	0.1072	1.3383	0.1934	0.8066	0.0742	0.9258

TABLE 5.27: BINARY ADSORPTION OF ETHANE & PROPANE ON LINDE S-115 PELLETS

AT 300.00 DEGREE KELVIN AND 50.00 PSIA TOTAL PRESSURE.

FIT OF THE MULTICOMPONENT TOTH MODEL, EQUILIBRIUM CONSTANT AND

SATURATION CONCENTRATION FROM TABLE 5.9.

PARTIAL PRESSURES		ADSORB PHASE CONCENTRATION AND MOLE FRACTION				THEORETICAL	
ETHANE PSIA	PROPANE PSIA	EXPERIMENTAL ETHANE PROPANE MMOLE/GM PELLETT	THEORETICAL ETHANE PROPANE MMOLE/GM PELLETT	EXPERIMENTAL ETHANE PROPANE MMOLE/GM PELLETT	THEORETICAL ETHANE PROPANE MMOLE/GM PELLETT	ETHANE MOLE FRACTION	PROPANE MOLE FRACTION
14.4116	35.4384	0.0900	1.4800	0.0385	1.5372	0.0573	0.9427
22.6074	27.2326	0.2400	1.3800	0.0779	1.4684	0.1481	0.8519
28.2037	21.7763	0.3400	1.2900	0.1199	1.4045	0.2086	0.7914
32.0500	17.9500	0.4300	1.2000	0.1625	1.3453	0.2638	0.7362
34.8102	15.1398	0.5100	1.1200	0.2052	1.2900	0.3129	0.6871
36.9230	13.0270	0.5600	1.0500	0.2475	1.2382	0.3478	0.6522

TABLE 5.28: BINARY ADSORPTION OF ETHANE & PROPANE ON LINDE S-115 PELLETS

AT 300.00 DEGREE KELVIN AND 50.00 PSIA TOTAL PRESSURE.

FIT OF THE MULTICOMPONENT TOTH MODEL, EQUILIBRIUM CONSTANT AND

SATURATION CONCENTRATION FROM TABLE 5.7.

PARTIAL PRESSURES		ADSORB PHASE CONCENTRATION AND MOLE FRACTION				THEORETICAL	
ETHANE PSIA	PROPANE PSIA	EXPERIMENTAL ETHANE PROPANE MMOLE/GM PELLETT	THEORETICAL ETHANE PROPANE MMOLE/GM PELLETT	EXPERIMENTAL ETHANE PROPANE MMOLE/GM PELLETT	THEORETICAL ETHANE PROPANE MMOLE/GM PELLETT	ETHANE MOLE FRACTION	PROPANE MOLE FRACTION
14.4116	35.4384	0.0900	1.4800	0.1887	1.6942	0.0573	0.9427
22.6074	27.2326	0.2400	1.3800	0.3419	1.5474	0.1481	0.8519
28.2037	21.7763	0.3400	1.2900	0.4782	1.4192	0.2086	0.7914
32.0500	17.9500	0.4300	1.2000	0.5970	1.3094	0.2638	0.7362
34.8102	15.1398	0.5100	1.1200	0.7016	1.2140	0.3129	0.6871
36.9230	13.0270	0.5600	1.0500	0.7947	1.1302	0.3478	0.6522

TABLE 5.29 TERNARY ADSORPTION OF METHANE-ETHANE-& PROPANE ON LINDE S-115 PELLETS

AT 300.00 DEGREE KELVIN AND 50.00 PSIA TOTAL PRESSURE.

FIT OF THE MULTICOMPONENT TOTH MODEL, EQUILIBRIUM CONSTANT

AND SATURATION CONCENTRATION FROM TABLE 5.7.

METHANE PSIA	PARTIAL PRESSURES		ADSORB PHASE MOLE FRACTIONS			
	ETHANE PSIA	PROPANE PSIA	EXPERIMENTAL METHANE	ETHANE	PROPANE	THEORETICAL MOLE FRACTION METHANE ETHANE PROPANE
17.5374	24.0060	8.4066	0.0063	0.3373	0.6564	0.0103 0.3667 0.6230
27.6407	16.4686	5.8107	0.0141	0.3231	0.6628	0.0222 0.3464 0.6314
34.1086	11.9433	4.2780	0.0503	0.2998	0.6499	0.0356 0.3271 0.6373
37.7654	9.0453	3.3293	0.0549	0.2863	0.6588	0.0489 0.3080 0.6431
40.3096	7.1506	2.7198	0.0852	0.2668	0.6480	0.0621 0.2902 0.6477

AT 300.00 DEGREE KELVIN AND 95.0 PSIA TOTAL PRESSURE.

55.8877	23.9000	15.8122	0.0630	0.1946	0.7424	0.0221 0.2462 0.7317
34.1756	44.3421	17.2122	0.0537	0.2846	0.6617	0.0110 0.3701 0.6190

TABLE 5.30 TERNARY ADSORPTION OF METHANE-ETHANE-& PROPANE ON LINDE S-115 PELLETS

AT 300.00 DEGREE KELVIN AND 50.00 PSIA TOTAL PRESSURE.

FIT OF THE MULTICOMPONENT TOTH MODEL, EQUILIBRIUM CONSTANT

AND SATURATION CONCENTRATION FROM TABLE 5.7.

METHANE PSIA	PARTIAL PRESSURES		ADSORB PHASE CONCENTRATION			
	ETHANE PSIA	PROPANE PSIA	EXPERIMENTAL METHANE (MILLIMOLES/GM PELLETS)	ETHANE	PROPANE (MILLIMOLES/GM PELLETS)	THEORETICAL CONCENTRATION METHANE ETHANE PROPANE (MILLIMOLES/GM PELLETS)
17.5374	24.0060	8.4066	0.0100	0.5380	1.0470	0.0164 0.5858 0.9953
27.6407	16.4686	5.8107	0.0220	0.5040	1.0340	0.0353 0.5502 1.0028
34.1086	11.9433	4.2780	0.0790	0.4710	1.0210	0.0562 0.5163 1.0058
37.7654	9.0453	3.3293	0.0840	0.4380	1.0080	0.0767 0.4829 1.0083
40.3096	7.1506	2.7198	0.1310	0.4100	0.9960	0.0967 0.4521 1.0090

AT 300.00 DEGREE KELVIN AND 95.0 PSIA TOTAL PRESSURE.

55.8877	23.9000	15.8122	0.1030	0.3180	1.2130	0.0356 0.3968 1.1793
34.1756	44.3421	17.2122	0.0870	0.4610	1.0720	0.0177 0.5970 0.9986

TABLE 5.31 TERNARY ADSORPTION OF METHANE-ETHANE-& N-BUTANE ON LINDE S-115 PELLETS

AT 300.00 DEGREE KELVIN AND 50.00 PSIA TOTAL PRESSURE.

FIT OF THE MULTICOMPONENT TOTH MODEL, EQUILIBRIUM CONSTANT

AND SATURATION CONCENTRATION FROM TABLE 5.7.

METHANE PSIA	PARTIAL PRESSURES			ADSORB PHASE MOLE FRACTIONS			FRACTION N-BUTANE
	ETHANE PSIA	N-BUTANE PSIA	EXPERIMENTAL METHANE	ETHANE	N-BUTANE	THEORETICAL METHANE	ETHANE
17.5844	25.6646	6.7210	0.0316	0.1596	0.8088	0.0040	0.1492
28.1974	17.2462	4.5164	0.0169	0.1444	0.8387	0.0088	0.1402
35.0420	11.9143	3.1037	0.0487	0.1241	0.8271	0.0150	0.1327
39.3436	8.4351	2.2513	0.0622	0.1090	0.8289	0.0220	0.1231
42.1573	6.1899	1.7378	0.0771	0.0956	0.8273	0.0293	0.1125
26.8635	19.8391	3.2574	0.0519	0.1917	0.7564	0.0104	0.1990
16.5500	33.1251	0.2948	0.0143	0.6918	0.2939	0.0149	0.7803
26.0502	23.7647	0.1950	0.0359	0.6648	0.2993	0.0321	0.7696
31.9872	17.8678	0.1249	0.0707	0.6299	0.2994	0.0522	0.7690

TABLE 5.32 TERNARY ADSORPTION OF METHANE-ETHANE-& N-BUTANE ON LINDE S-115 PELLETS

AT 300.00 DEGREE KELVIN AND 50.00 PSIA TOTAL PRESSURE.

FIT OF THE MULTICOMPONENT TOTH MODEL, EQUILIBRIUM CONSTANT

AND SATURATION CONCENTRATION FROM TABLE 5.7.

METHANE PSIA	PARTIAL PRESSURES			ADSORB PHASE CONCENTRATION			FRACTION N-BUTANE PELLET)
	ETHANE PSIA	N-BUTANE PSIA	EXPERIMENTAL METHANE (MILLIMOLES/GM PELLET)	ETHANE	N-BUTANE	THEORETICAL METHANE (MILLIMOLES/GM PELLET)	ETHANE
17.5844	25.6646	6.7210	0.0430	0.2170	1.1000	0.0054	0.2045
28.1974	17.2462	4.5164	0.0220	0.1880	1.0920	0.0121	0.1917
35.0420	11.9143	3.1037	0.0640	0.1630	1.0860	0.0204	0.1808
39.3436	8.4351	2.2513	0.0810	0.1420	1.0800	0.0299	0.1672
42.1573	6.1899	1.7378	0.1000	0.1240	1.0730	0.0397	0.1523
26.8635	19.8391	3.2574	0.0710	0.2620	1.0340	0.0143	0.2738
16.5500	33.1251	0.2948	0.0240	1.1580	0.4920	0.0233	1.2245
26.0502	23.7647	0.1950	0.0590	1.0930	0.4920	0.0501	1.2010
31.9872	17.8678	0.1249	0.1160	1.0330	0.4910	0.0814	1.1984

TABLE 5.33 TERNARY ADSORPTION OF METHANE-PROPANE-& N-BUTANE ON LINDE S-115 PELLETS

AT 300.00 DEGREE KELVIN AND 50.00 PSIA TOTAL PRESSURE.

FIT OF THE MULTICOMPONENT TOTH MODEL, EQUILIBRIUM CONSTANT

AND SATURATION CONCENTRATION FROM TABLE 5.7.

METHANE PSIA	PARTIAL PRESSURES			ADSORB PHASE MOLE FRACTIONS			
	PROPANE PSIA	N-BUTANE PSIA		EXPERIMENTAL METHANE	PROPANE	N-BUTANE	THEORETICAL MOLE FRACTIONS METHANE PROPANE N-BUTANE
17.0732	18.9679	15.8689		0.0000	0.2222	0.7778	0.0019 0.1761 0.8220
28.7216	13.0863	10.6421		0.0000	0.2222	0.7778	0.0043 0.1798 0.8159
34.1887	8.9282	7.0132		0.0021	0.2218	0.7762	0.0072 0.1843 0.8084
39.1246	6.3064	4.8190		0.0049	0.2144	0.7807	0.0112 0.1877 0.8011
42.0588	4.5664	3.4448		0.0098	0.2077	0.7825	0.0158 0.1887 0.7955

TABLE 5.34 TERNARY ADSORPTION OF METHANE-PROPANE-& N-BUTANE ON LINDE S-115 PELLETS

AT 300.00 DEGREE KELVIN AND 50.00 PSIA TOTAL PRESSURE.

FIT OF THE MULTICOMPONENT TOTH MODEL, EQUILIBRIUM CONSTANT

AND SATURATION CONCENTRATION FROM TABLE 5.7.

METHANE PSIA	PARTIAL PRESSURES			ADSORB PHASE CONCENTRATION			
	PROPANE PSIA	N-BUTANE PSIA		EXPERIMENTAL METHANE (MILLIMOLES/GM PELLETS)	PROPANE	N-BUTANE (MILLIMOLES/GM PELLETS)	THEORETICAL CONCENTRATION METHANE PROPANE N-BUTANE (MILLIMOLES/GM PELLETS)
17.0732	18.9679	15.8689		0.0000	0.3240	1.1340	0.0024 0.2232 1.0416
28.7216	13.0863	10.6421		0.0000	0.3240	1.1340	0.0055 0.2276 1.0330
34.1887	8.9282	7.0132		0.0030	0.3240	1.1340	0.0092 0.2330 1.0221
39.1246	6.3064	4.8190		0.0070	0.3090	1.1250	0.0142 0.2370 1.0115
42.0588	4.5664	3.4448		0.0140	0.2960	1.1150	0.0199 0.2379 1.0030

TABLE 5.35: QUATERNARY ADSORPTION OF METHANE-ETHANE-PROPANE & N-BUTANE ON LINDE S-115 PELLETS

AT 300.00 DEGREE KELVIN AND 50.00 PSIA TOTAL PRESSURE.

FIT OF THE MULTICOMPONENT TOTH MODEL, EQUILIBRIUM CONSTANT

AND SATURATION CONCENTRATION FROM TABLE 5.7.

PARTIAL PRESSURES			EXPERIMENTAL MOLE FRACTION			ADSORBED PHASE MOLE FRACTIONS			THEORETICAL MOLE FRACTION		
METHANE	ETHANE	PROPANE	N-BUTANE	METHANE	ETHANE	PROPANE	N-BUTANE	METHANE	ETHANE	PROPANE	N-BUTANE
PSIA	PSIA	PSIA	PSIA								
17.8900	15.8700	9.0450	7.1950	0.0048	0.0901	0.1838	0.7213	0.0035	0.0796	0.1685	0.7484
29.3243	10.3815	6.0857	4.6286	0.0288	0.0821	0.1763	0.7128	0.0081	0.0747	0.1748	0.7424
35.6575	7.0383	4.2961	3.1381	0.0257	0.0754	0.1740	0.7249	0.0136	0.0695	0.1804	0.7365
39.7497	4.9099	3.1531	2.2372	0.0470	0.0683	0.1671	0.7177	0.0199	0.0640	0.1845	0.7317
42.3715	3.5393	2.4095	1.6697	0.0512	0.0629	0.1634	0.7226	0.0269	0.0586	0.1876	0.7270
26.6073	17.0576	3.3746	2.8804	0.0369	0.1333	0.1399	0.6899	0.0101	0.1423	0.6789	0.6789
16.3802	26.8389	3.4729	3.2830	0.0322	0.1972	0.1205	0.6501	0.0054	0.2274	0.1221	0.6451
9.9980	33.3833	3.2693	3.3933	0.0306	0.2329	0.1075	0.6289	0.0031	0.2692	0.1085	0.6192

TABLE 5.36: QUATERNARY ADSORPTION OF METHANE-ETHANE-PROPANE & N-BUTANE ON LINDE S-115 PELLETS

AT 300.00 DEGREE KELVIN AND 50.00 PSIA TOTAL PRESSURE.

FIT OF THE MULTICOMPONENT TOTH MODEL, EQUILIBRIUM CONSTANT

AND SATURATION CONCENTRATION FROM TABLE 5.7.

[illegible]

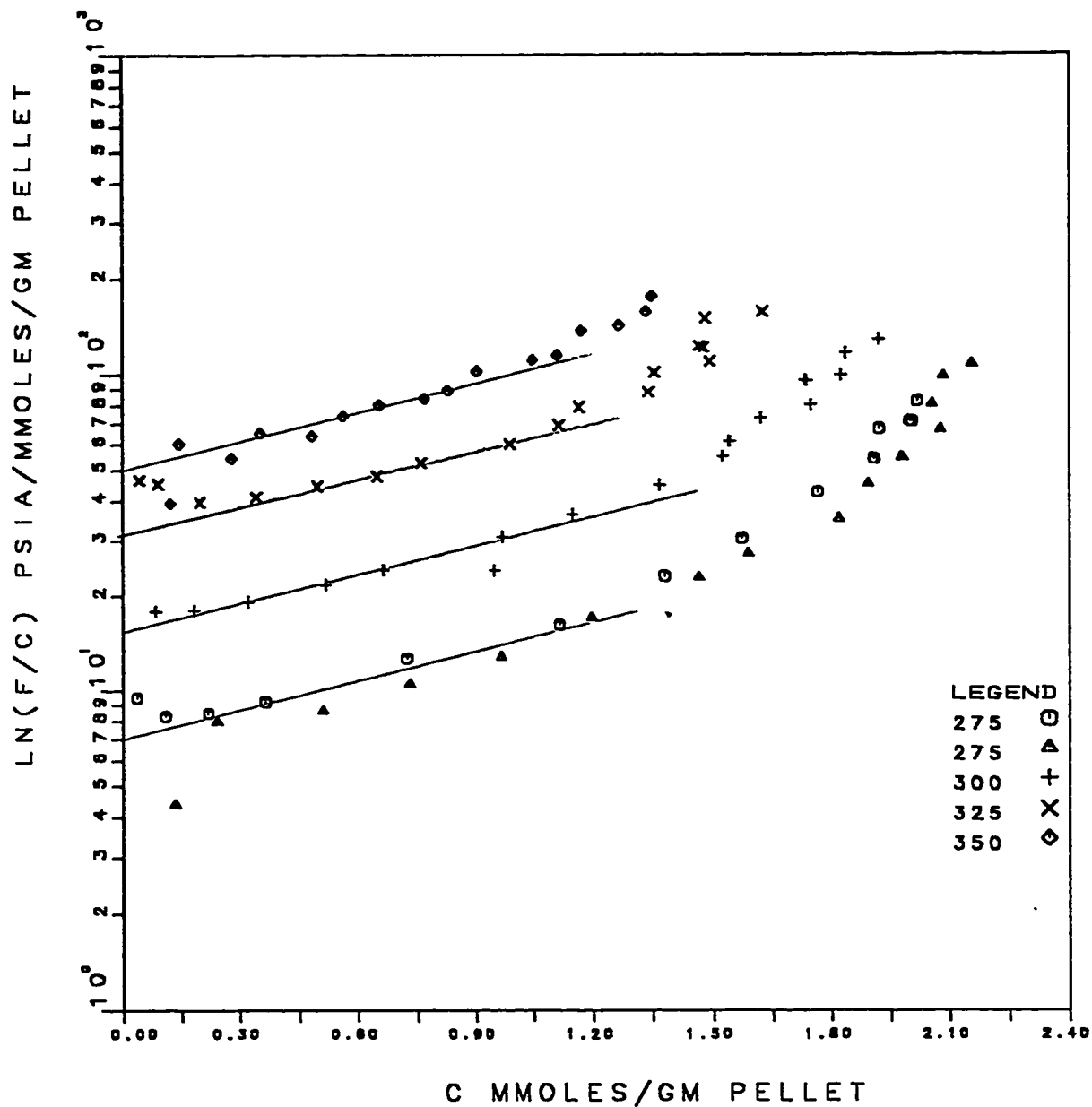


FIG. 5.1: VIRIAL ISOTHERMS FOR METHANE ON LINDE S-115 PELLETS.

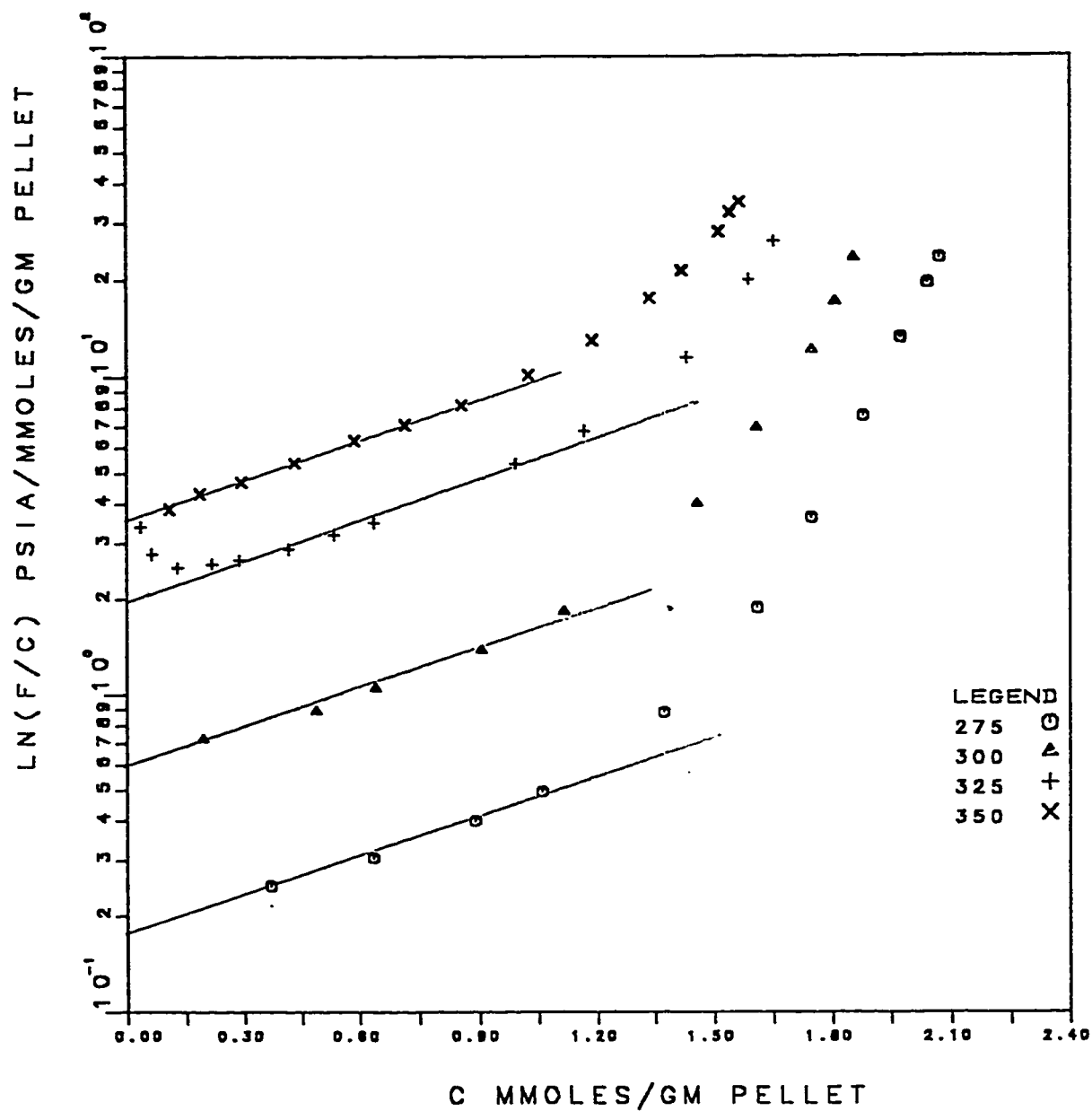


FIG. 5.2: VIRIAL ISOTHERMS FOR ETHANE ON LINDE S-115 PELLETS.

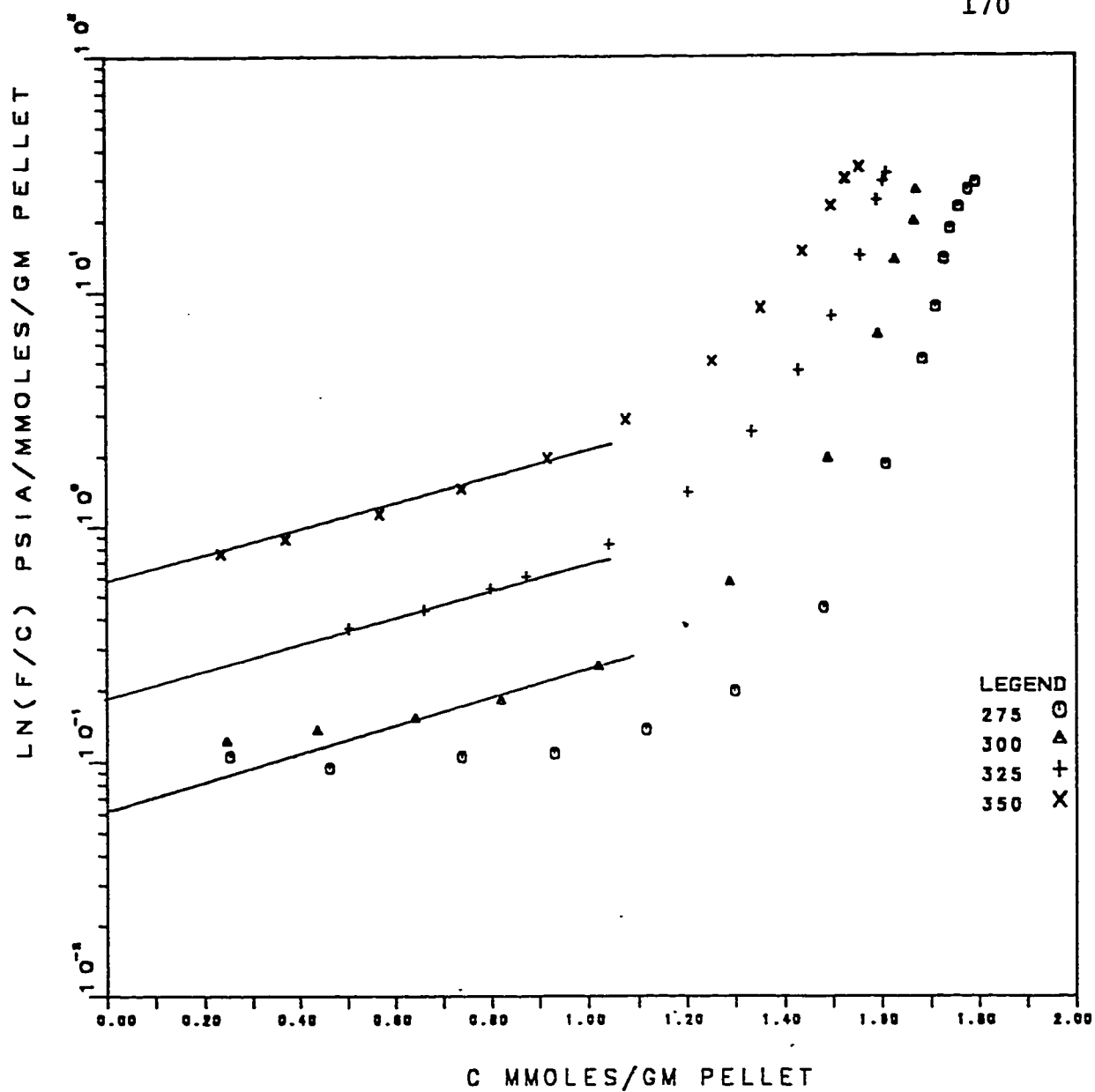


FIG. 5.3: VIRIAL ISOTHERMS FOR PROPANE ON LINDE S-115 PELLETS.

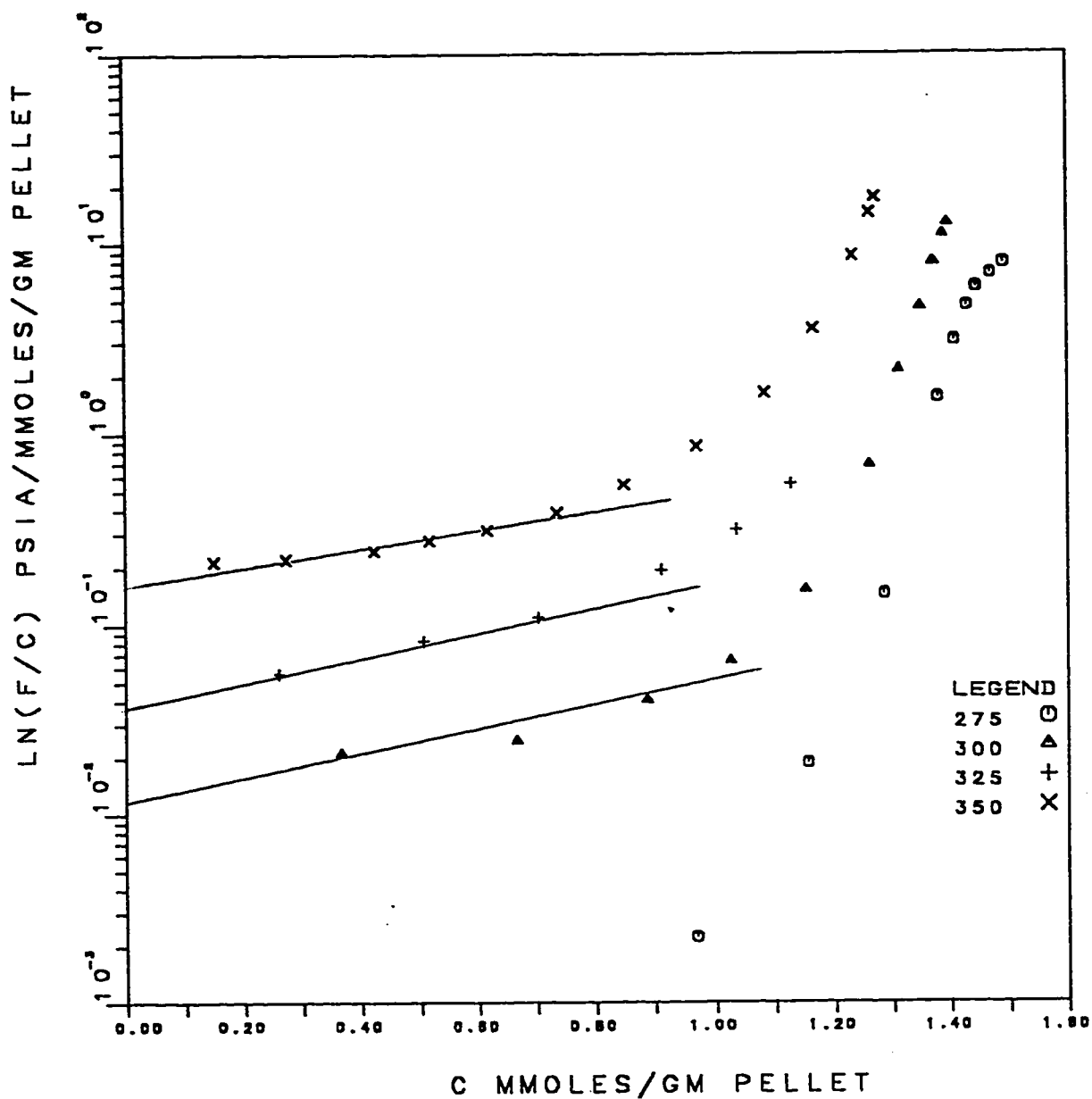


FIG. 5.4: VIRIAL ISOTHERMS FOR N-BUTANE ON LINDE S-115 PELLETS.

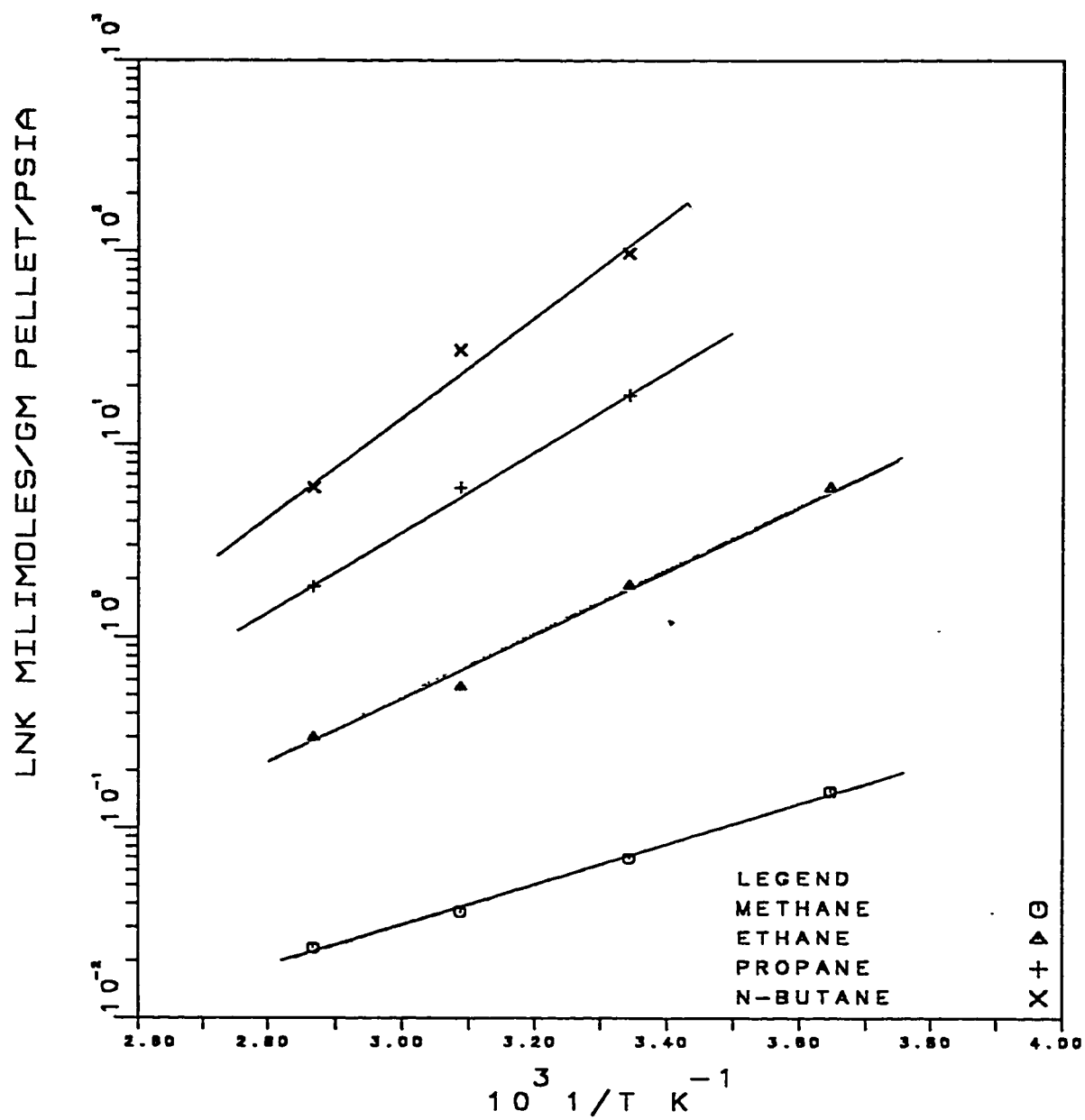


Fig. 5.5: Van't Hoff Plot For Light Alkanes on Linde S-115 Pellets.

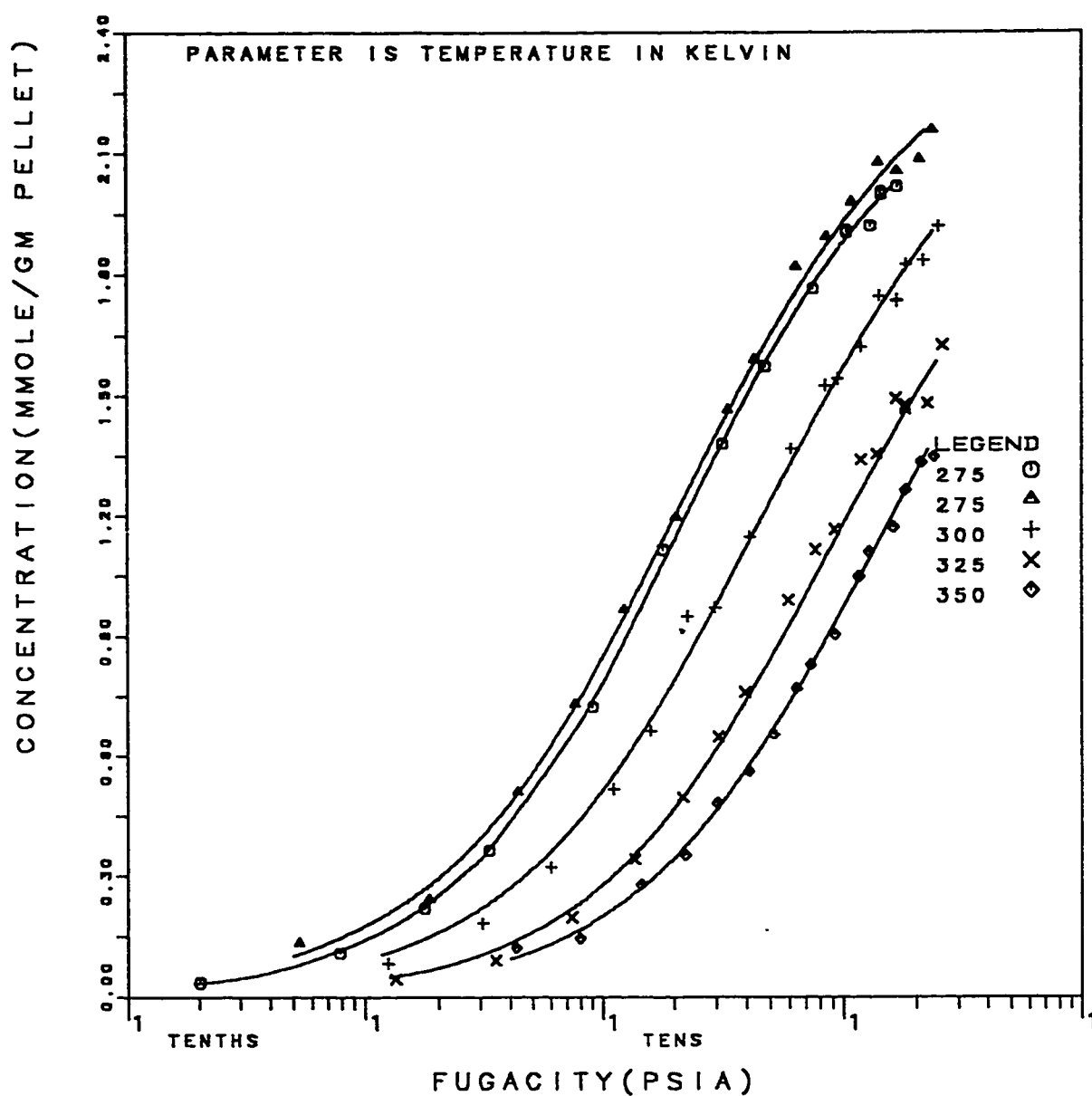


Fig. 5.6: Methane Isotherms on Linde S-115 Pellets: Fit of LRC Model With Optimized N_0 and Intrinsic K .

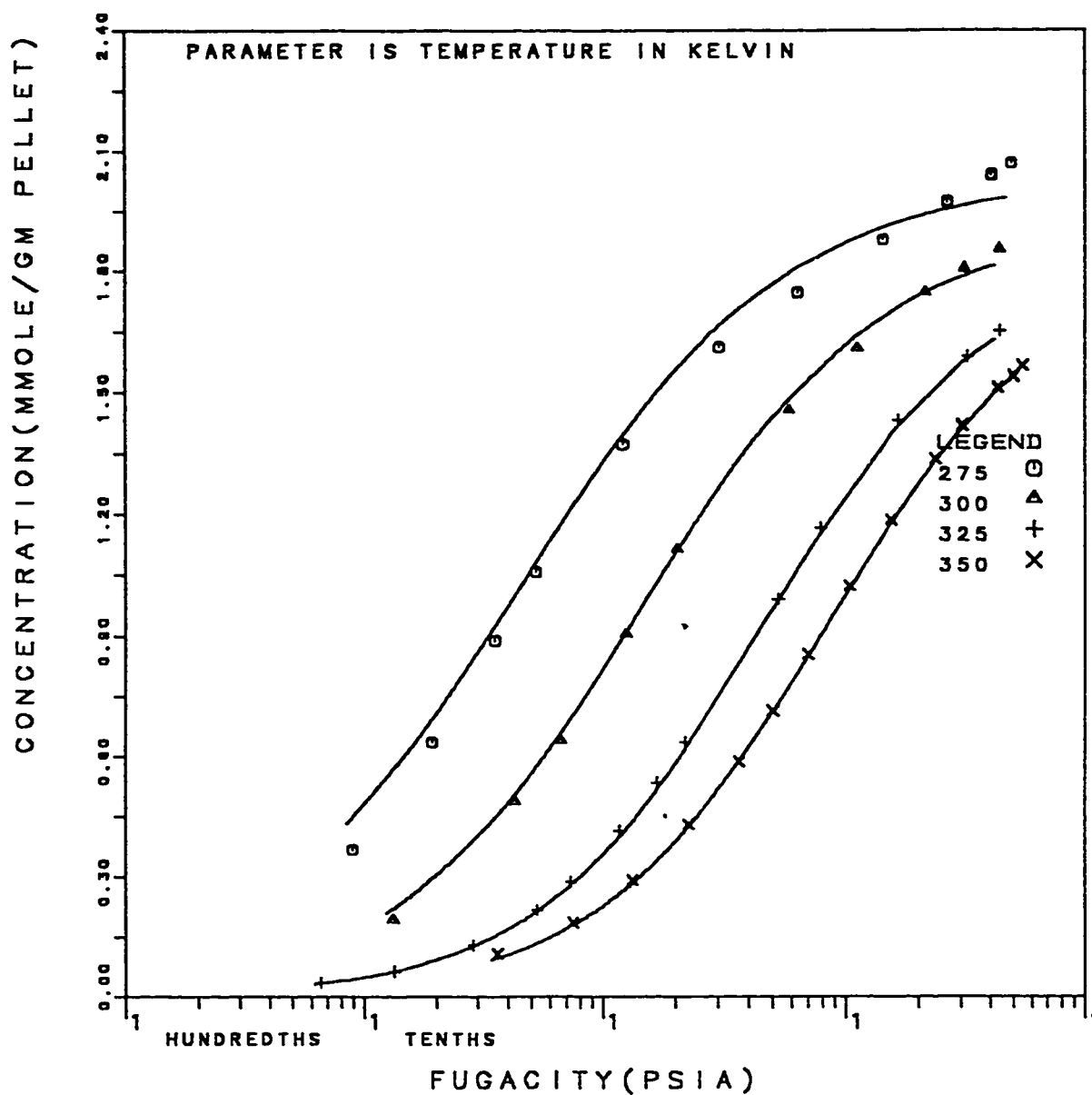


Fig. 5.7: Ethane Isotherms on Linde S-115 Pellets: Fit of LRC Model With Optimized N_0 and Intrinsic K .

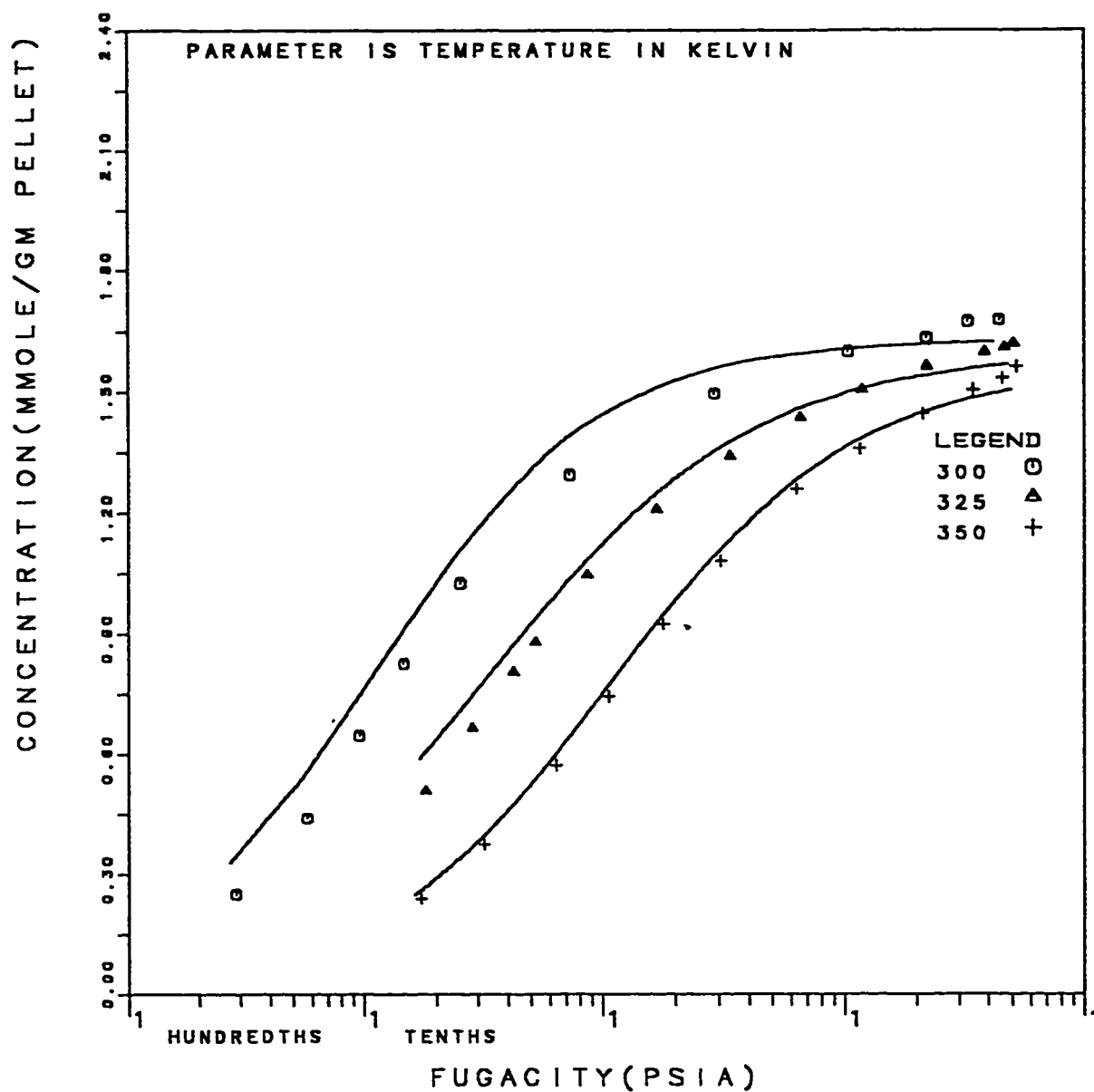


Fig. 5.8: Propane Isotherms on Linde S-115 Pellets: Fit of LRC Model Optimized N_0 and Intrinsic K.

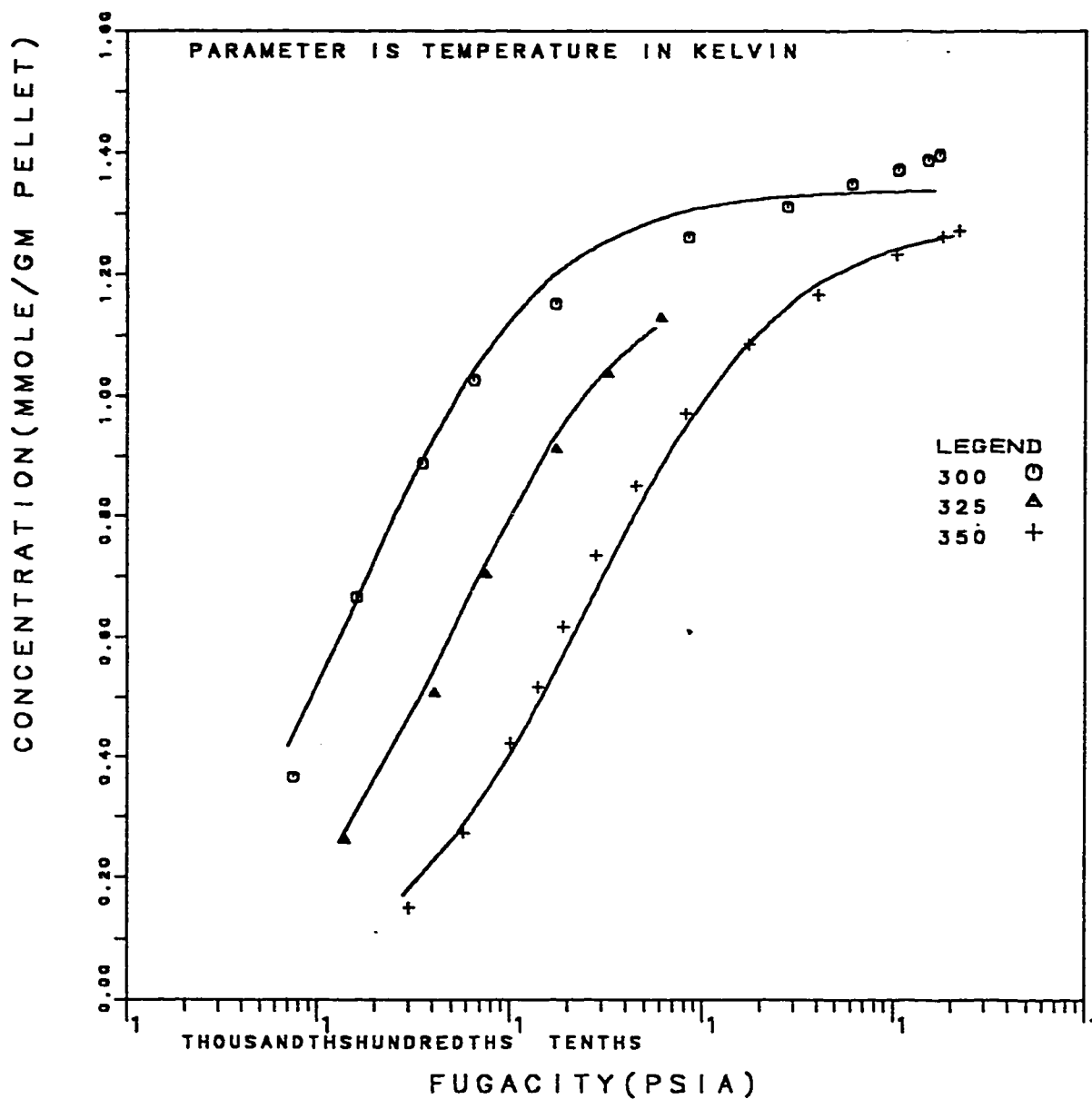


Fig. 5.9: n-Butane Isotherms on Linde S-115 Pellets: Fit of LRC Model With Optimized N_0 and Intrinsic K.

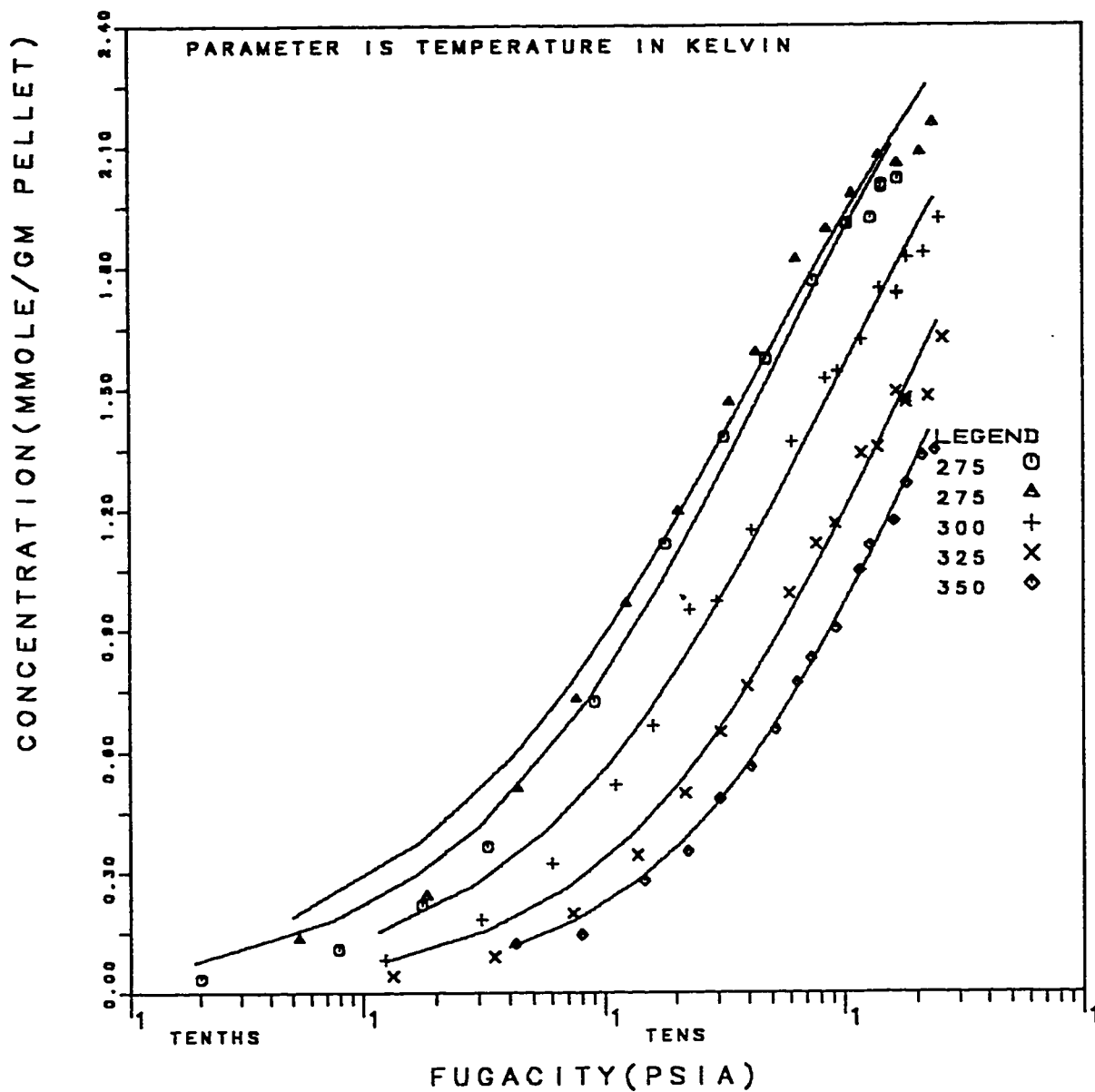


Fig. 5.10: Methane Isotherms on Linde S-115 Pellets: Fit of LRC Model With Theoretical N_o and Optimized K .

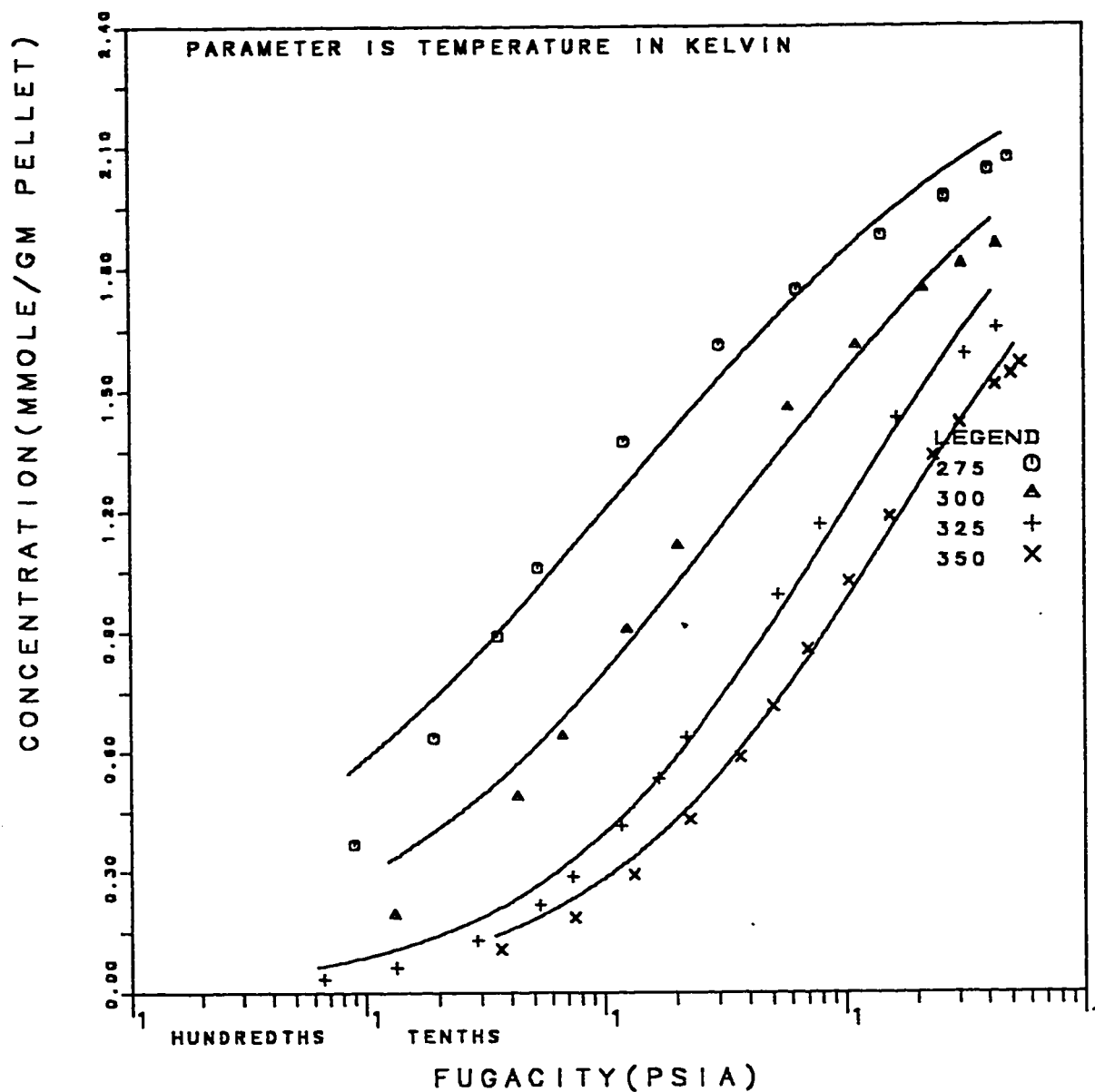


Fig. 5.11: Ethane Isotherms on Linde S-115 Pellets: Fit of LRC Model With Theoretical N_0 and optimized K .

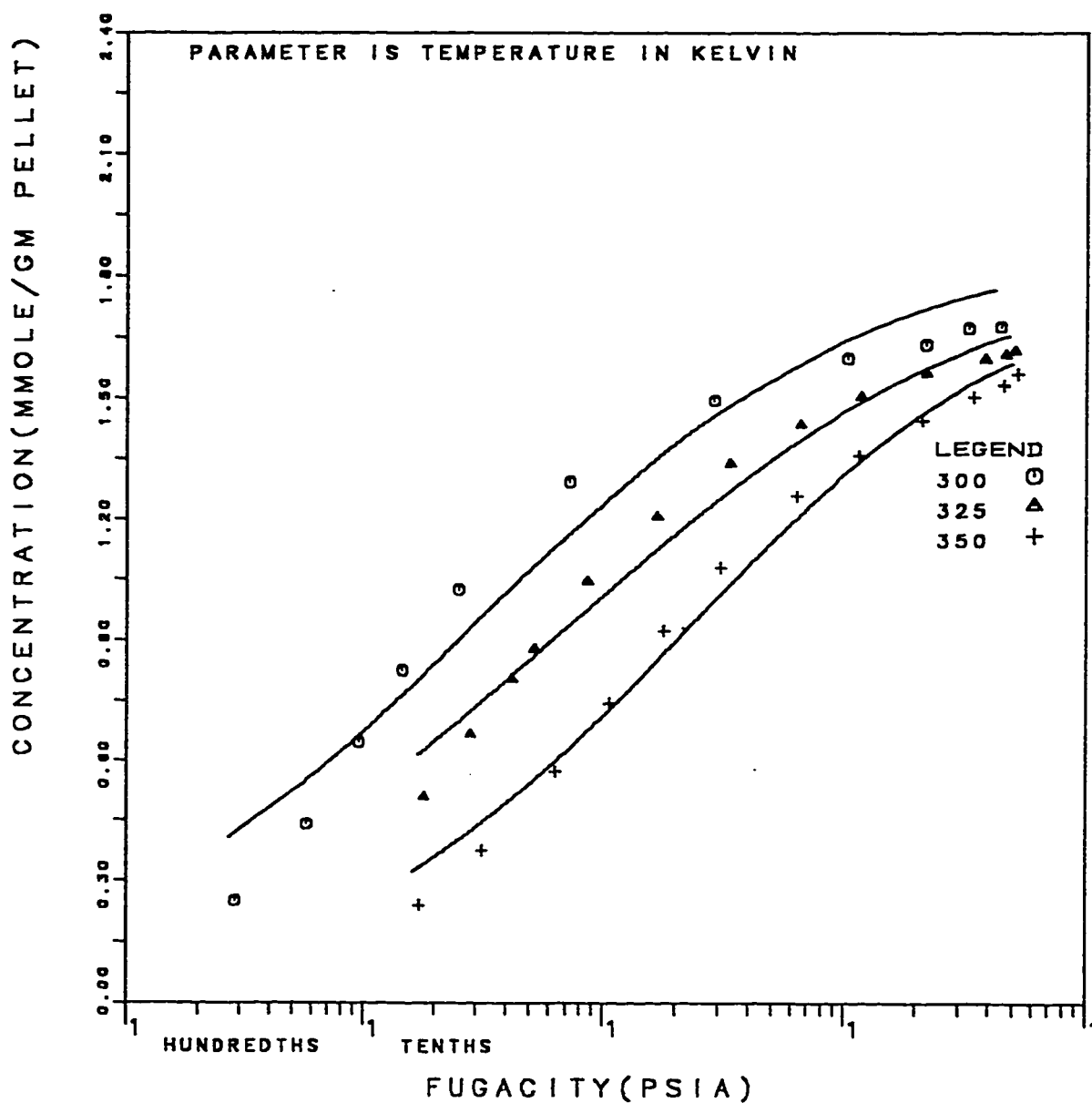


Fig. 5.12: Propane Isotherms on Linde S-115 Pellets: Fit of LRC Model With Theoretical N_0 and optimized K .

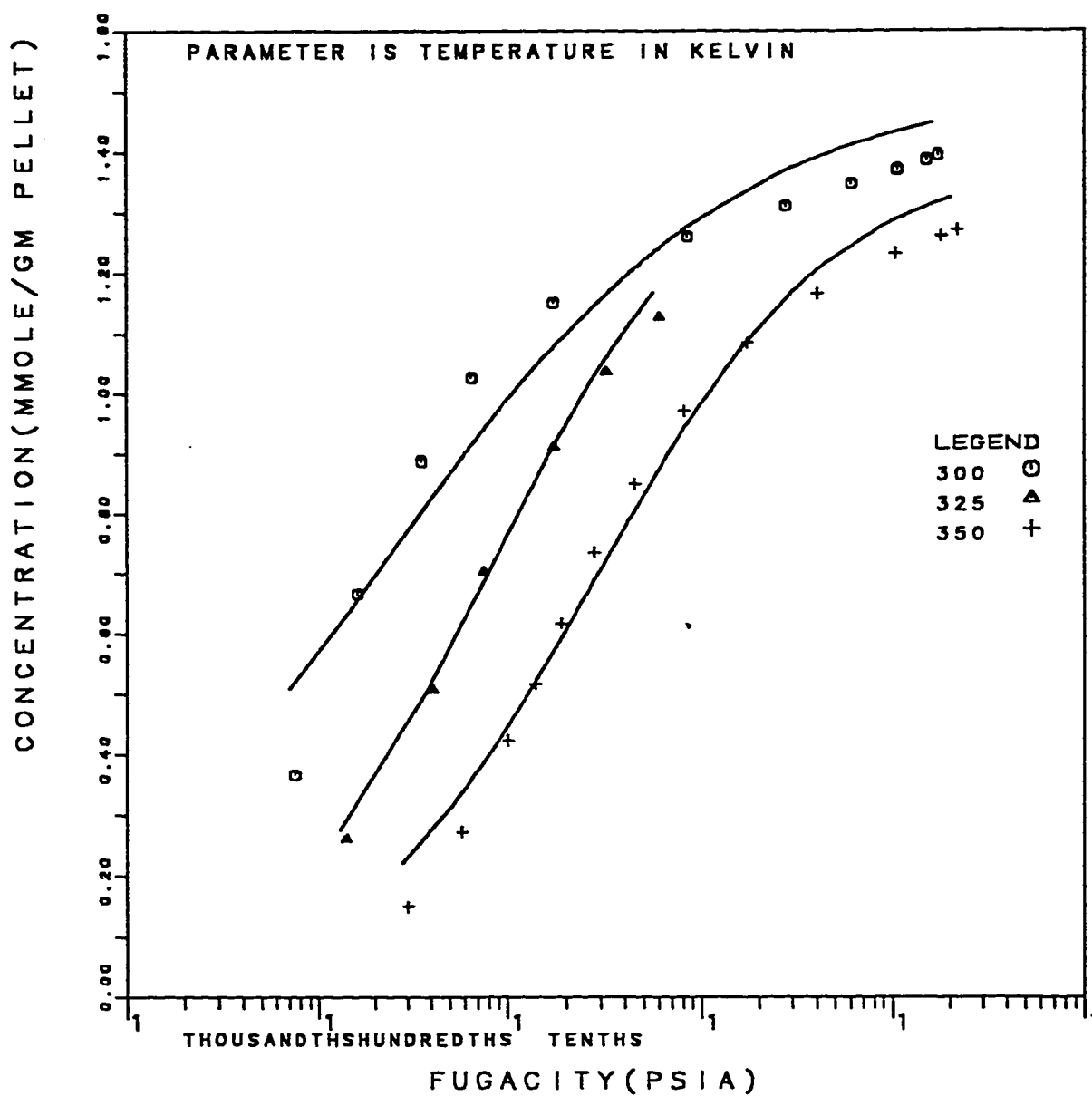


Fig. 5.13: n-Butane Isotherms on Linde S-115 Pellets: Fit of LRC Model With Theoretical N_0 and optimized K.

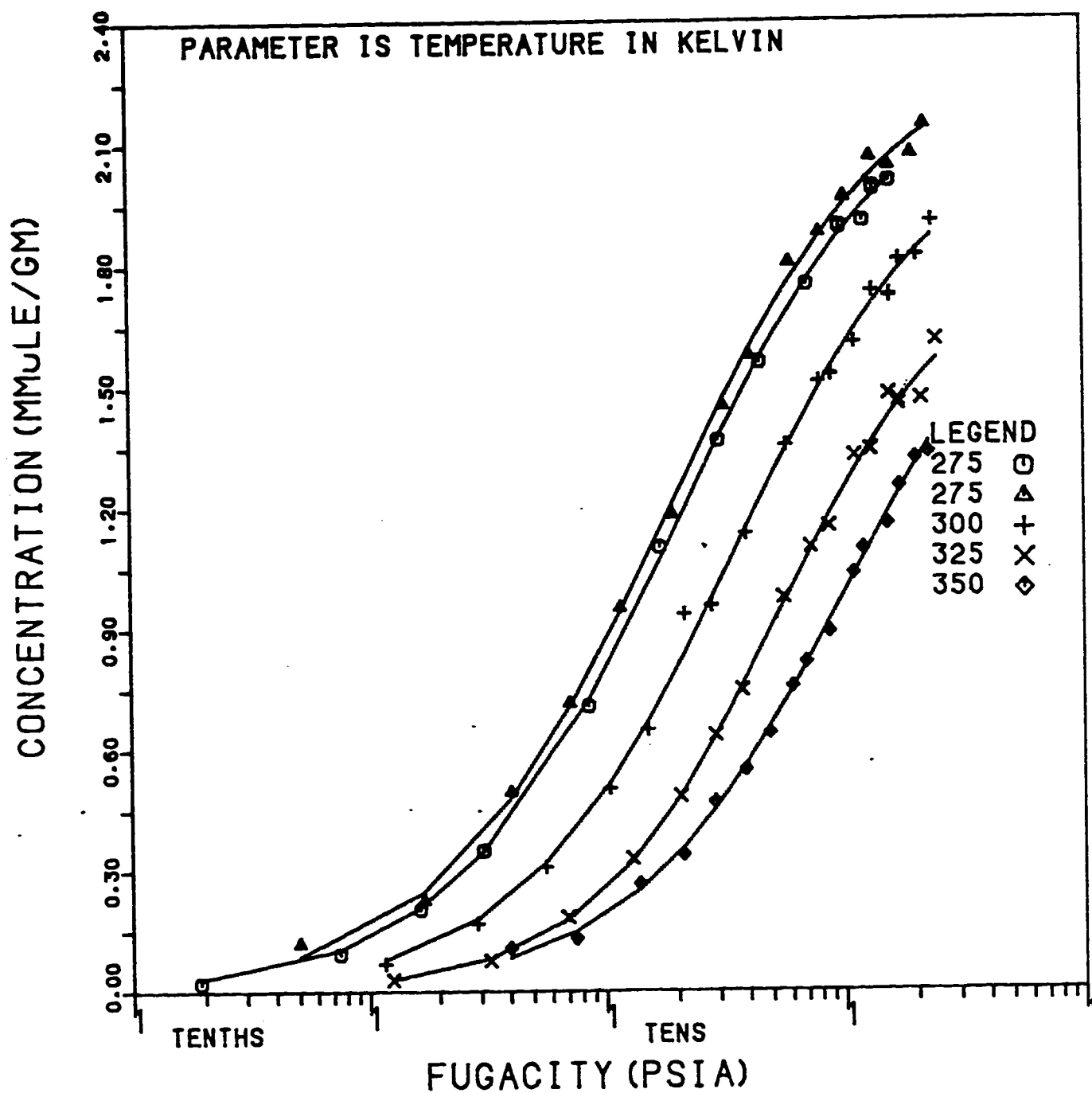


Fig. 5.14: Methane Isotherms on Linde S-115 Pellets: Fit of LRC Model With Optimized N_0 and K .

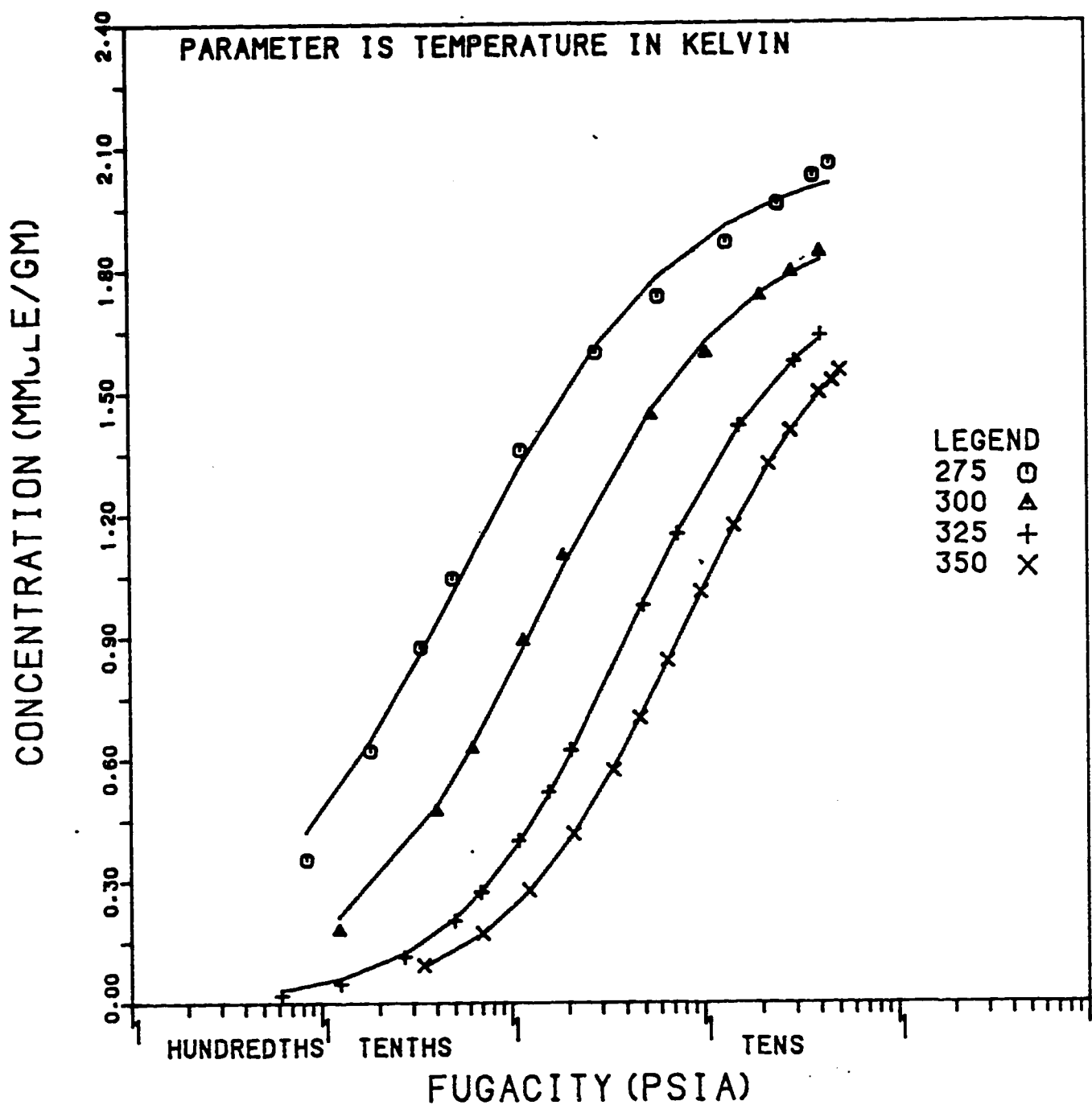


Fig. 5.15: Ethane Isotherms on Linde S-115 Pellets: Fit of LRC Model With Optimized N_0 and K .

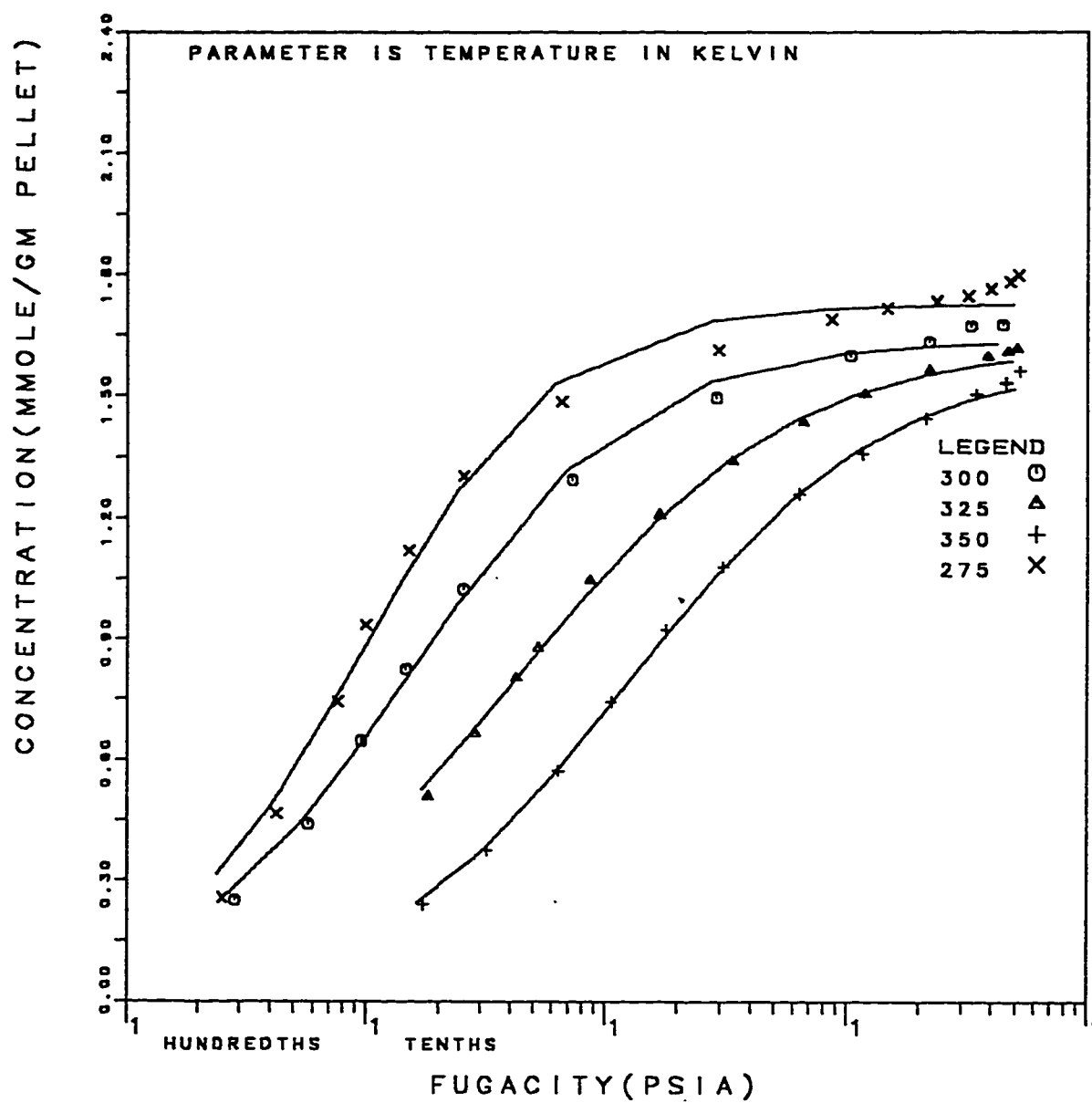


Fig. 5.16: Propane Isotherms on Linde S-115 Pellets: Fit of LRC Model With Optimized N_0 and K .

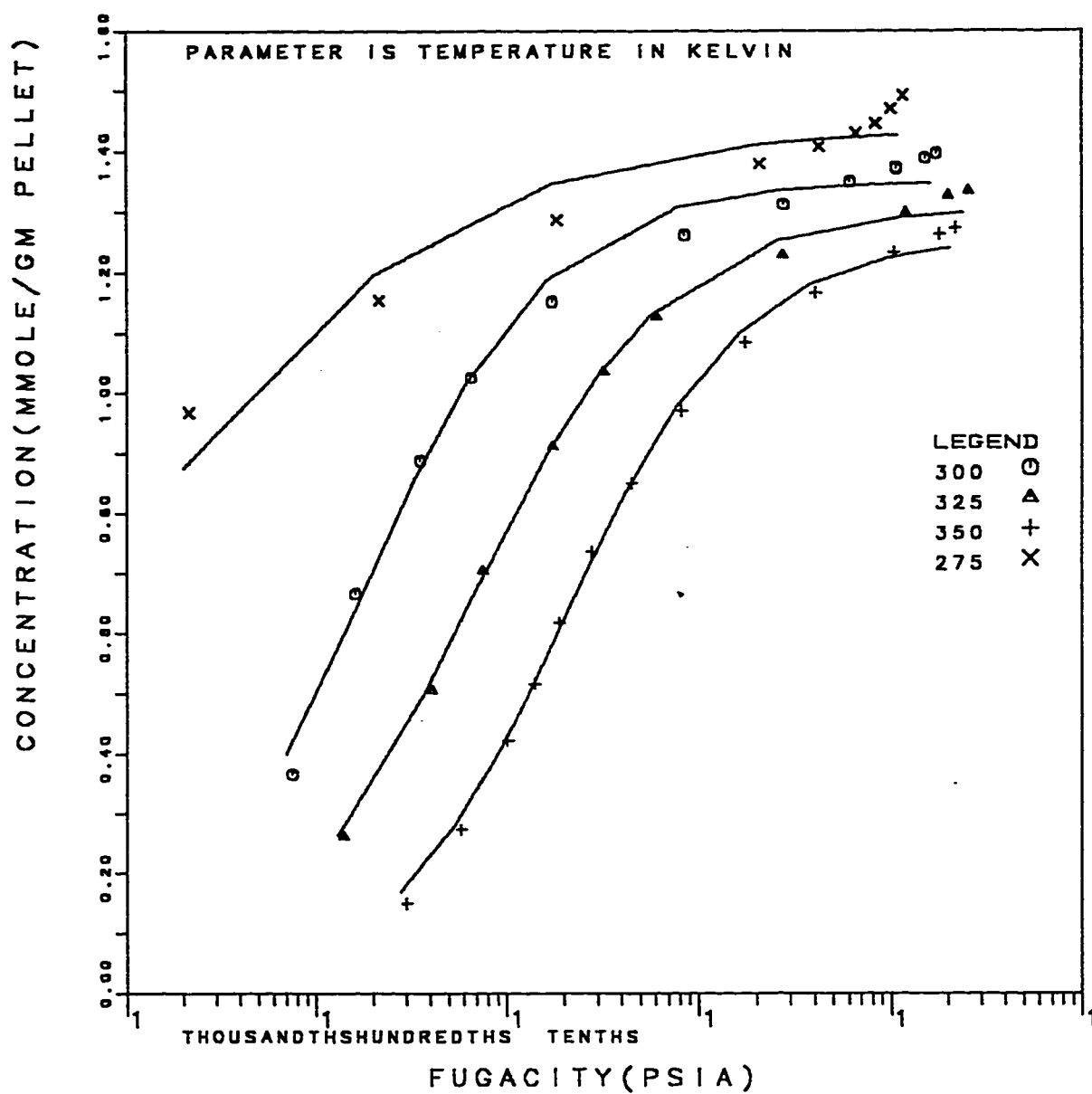


Fig. 5.17: n-Butane Isotherms on Linde S-115 Pellets: Fit of LRC Model With Optimized N_0 and K .

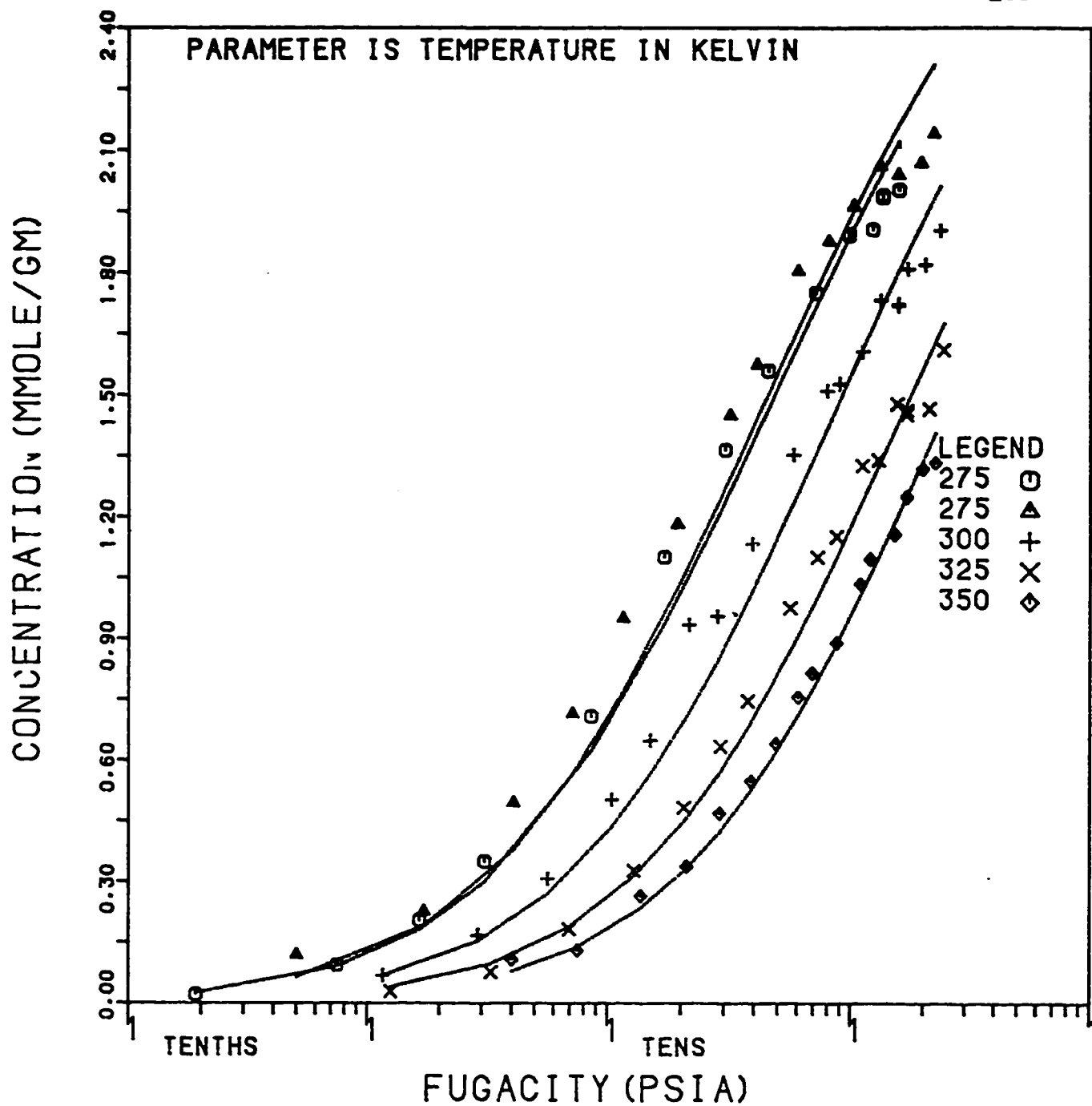


Fig. 5.18: Methane Isotherms on Linde S-115 Pellets: Fit of Toth Model With Theoretical N_0 and Intrinsic K .

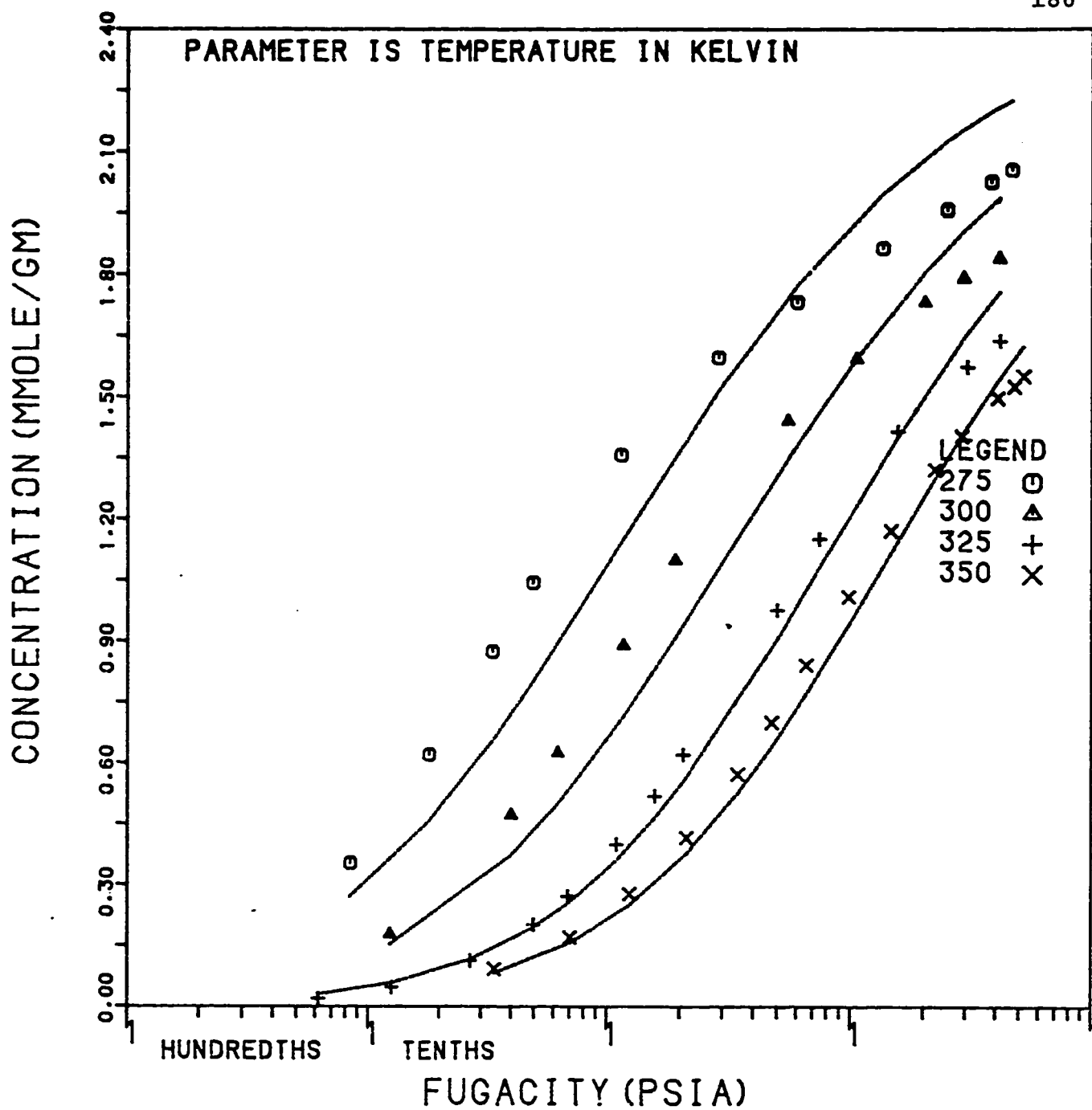


Fig. 5.19: Ethane Isotherms on Linde S-115 Pellets: Fit of Toth Model With Theoretical N_0 and Intrinsic K .

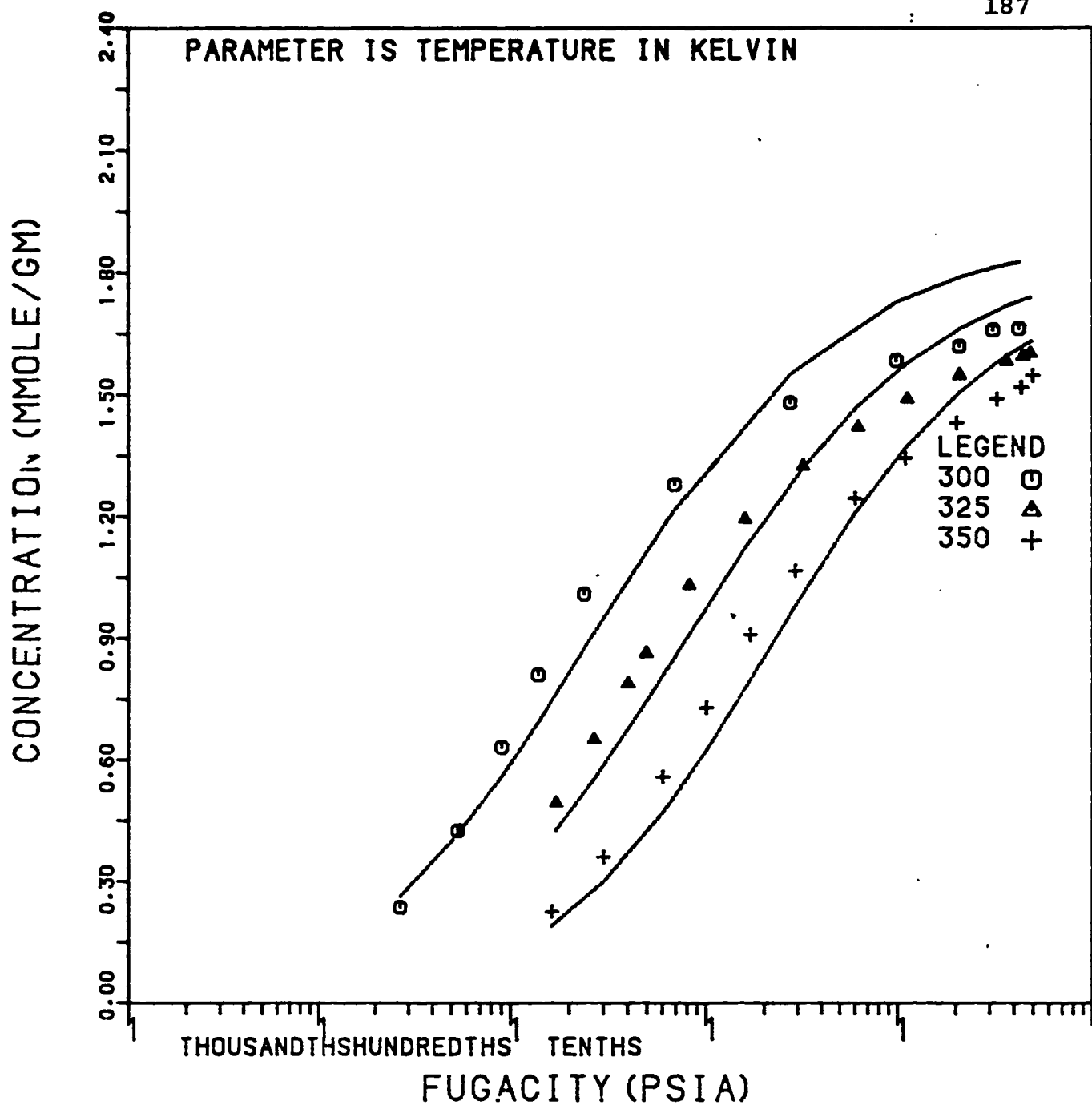


Fig. 5.20: Propane Isotherms on Linde S-115 Pellets: Fit of Toth Model With Theoretical N_0 and Intrinsic K .

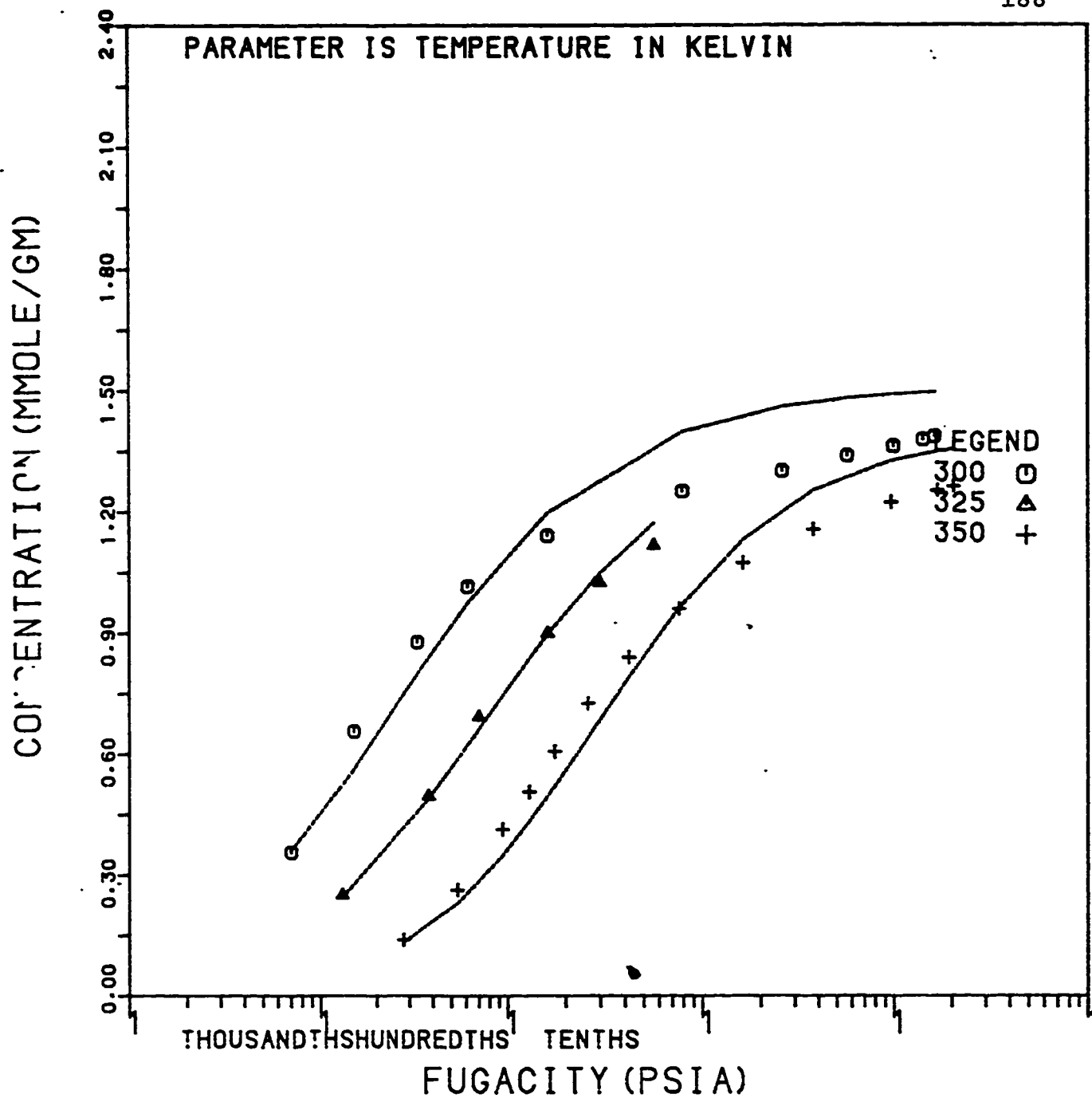


Fig. 5.21: n-Butane Isotherms on Linde S-115 Pellets: Fit of Toth Model With Theoretical N_0 and Intrinsic K .

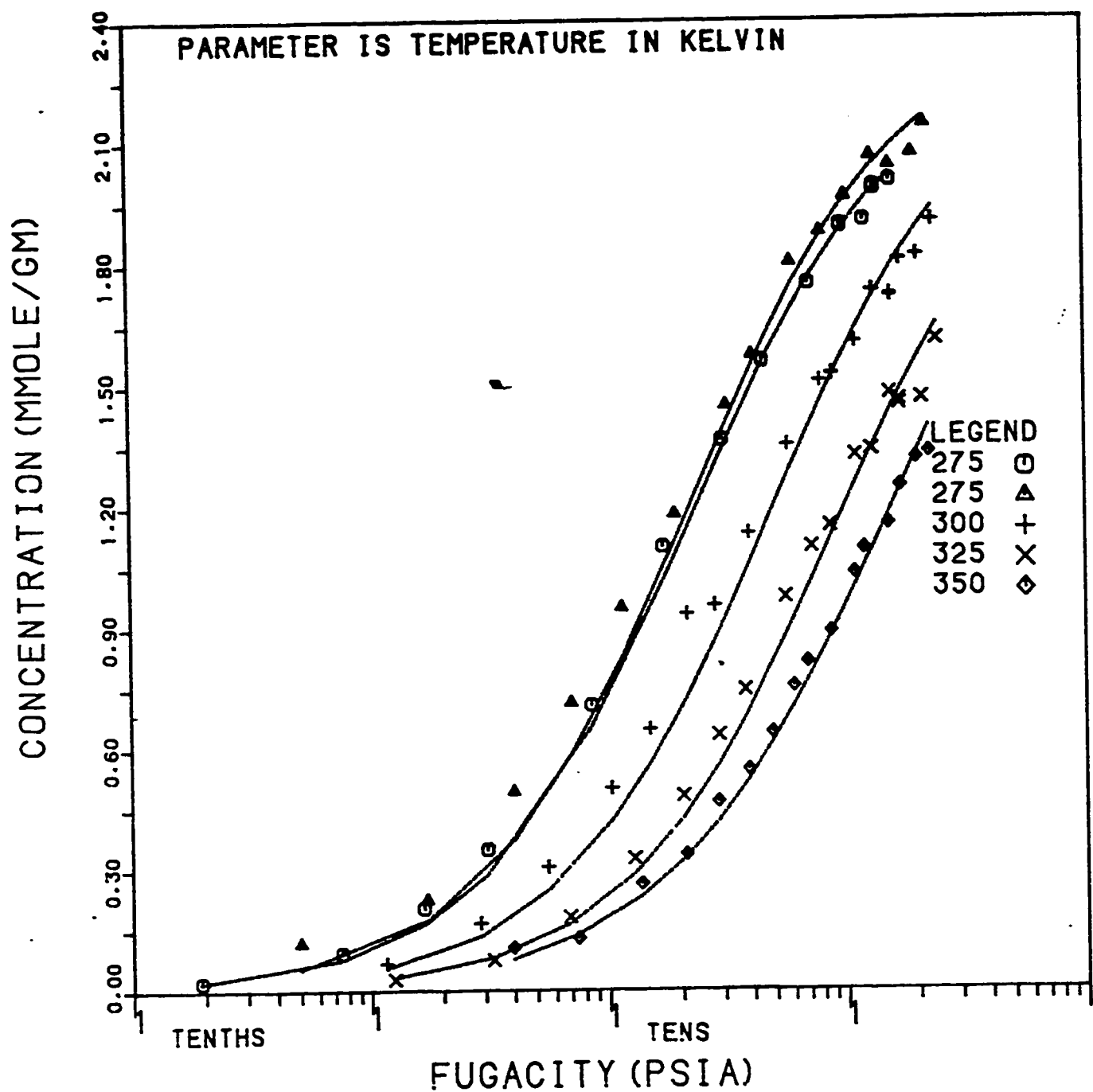


Fig. 5.22: Methane Isotherms on Linde S-115 Pellets: Fit of Toth Model With Optimized N_0 and Intrinsic K .

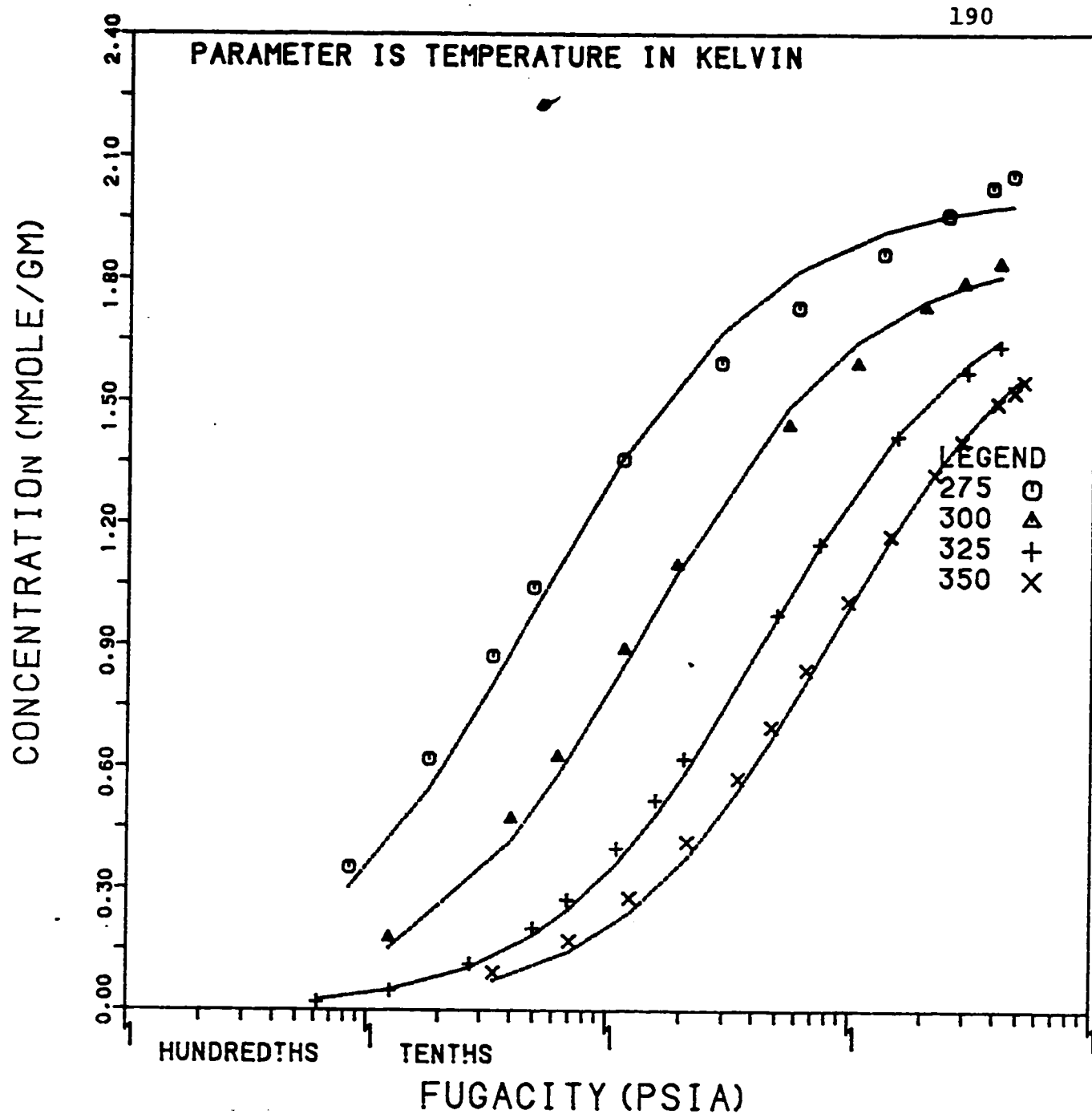


Fig. 5.23: Ethane Isotherms on Linde S-115 Pellets: Fit of Toth Model With Optimized N_0 and Intrinsic K .

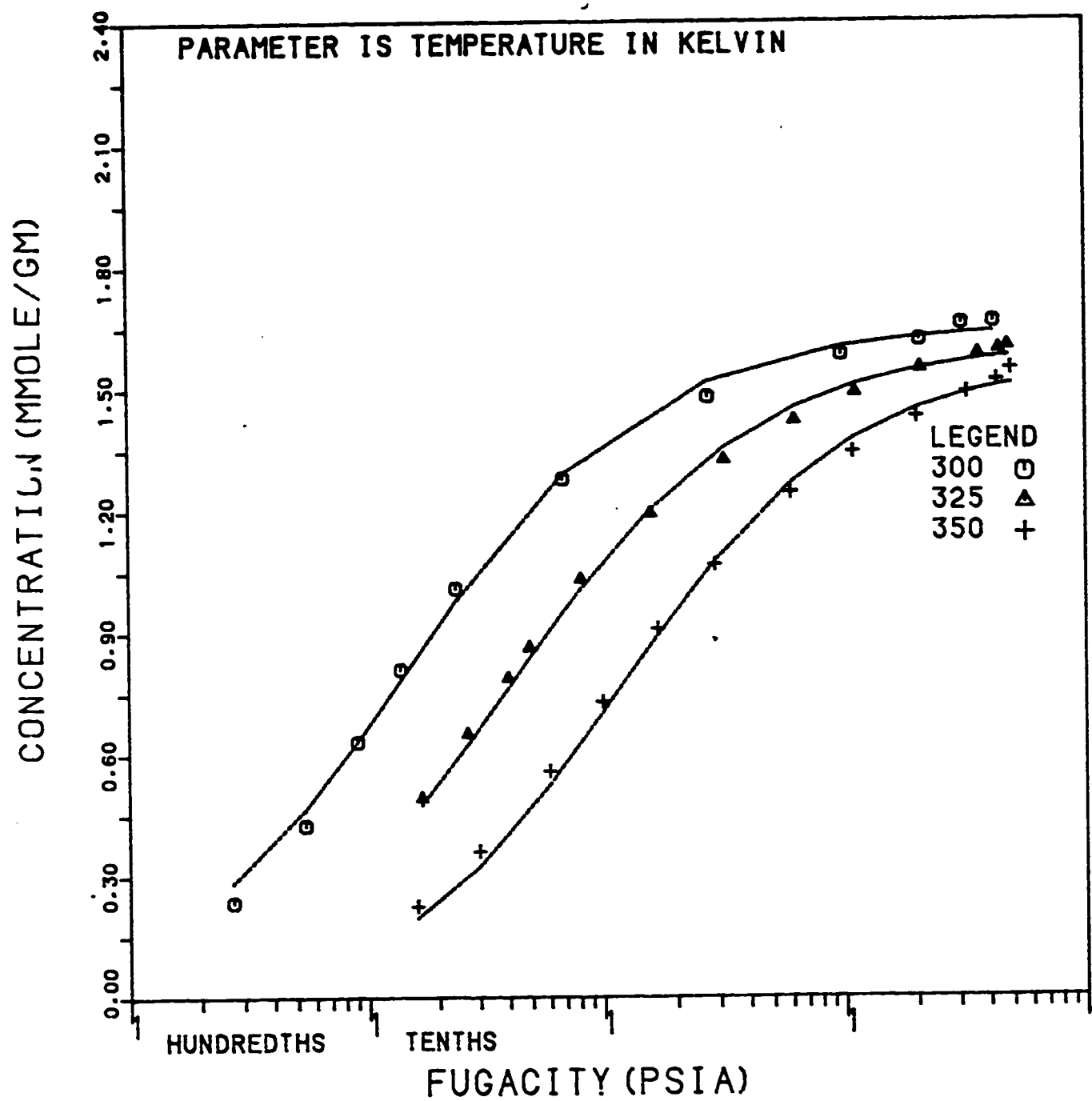


Fig. 5.24: Propane Isotherms on Linde S-115 Pellets: Fit of Toth Model With Optimized N_0 and Intrinsic K .

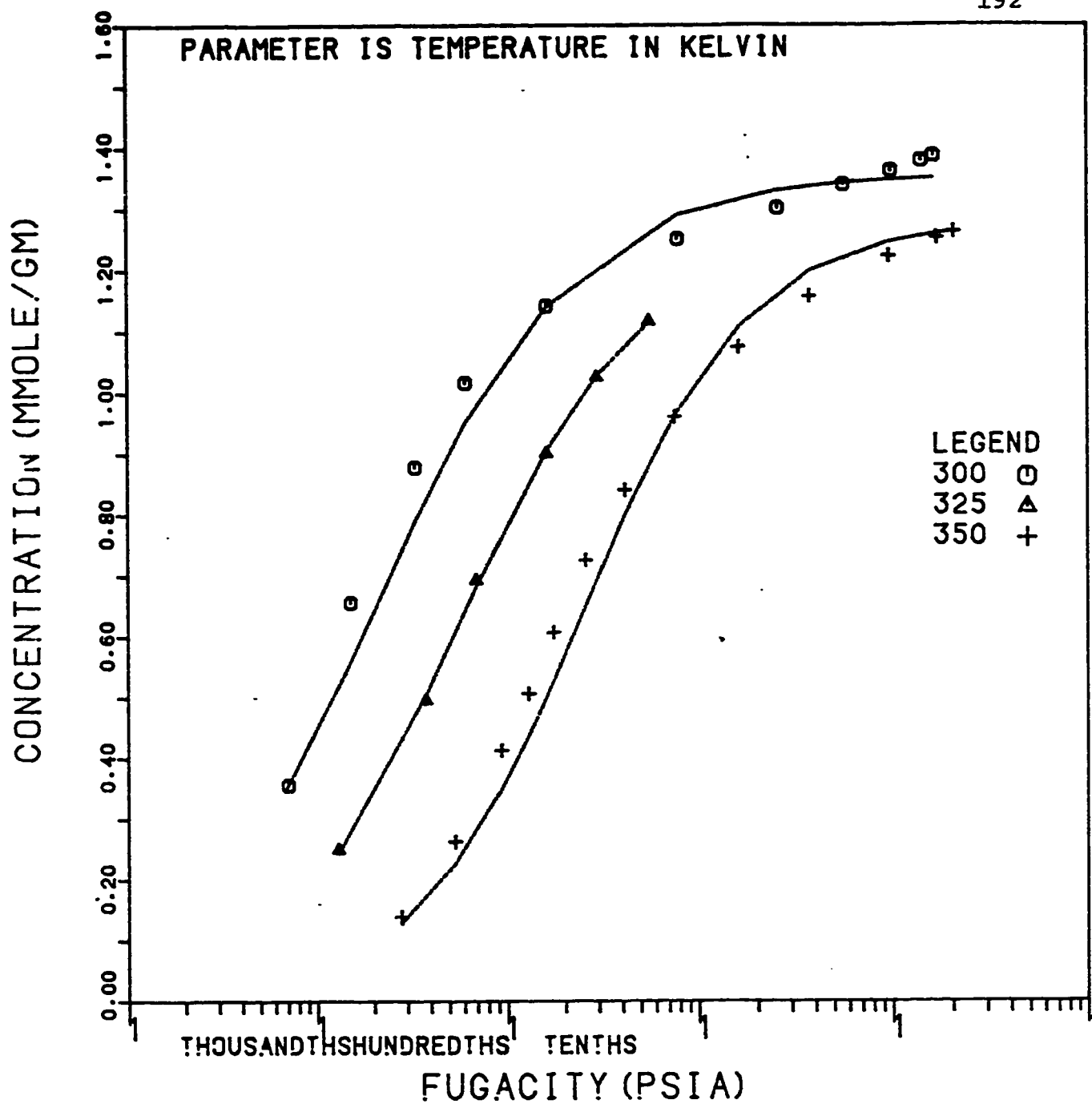


Fig. 5.25: n-Butane Isotherms on Linde S-115 Pellets: Fit of Toth Model With Optimized N_0 and Intrinsic K .

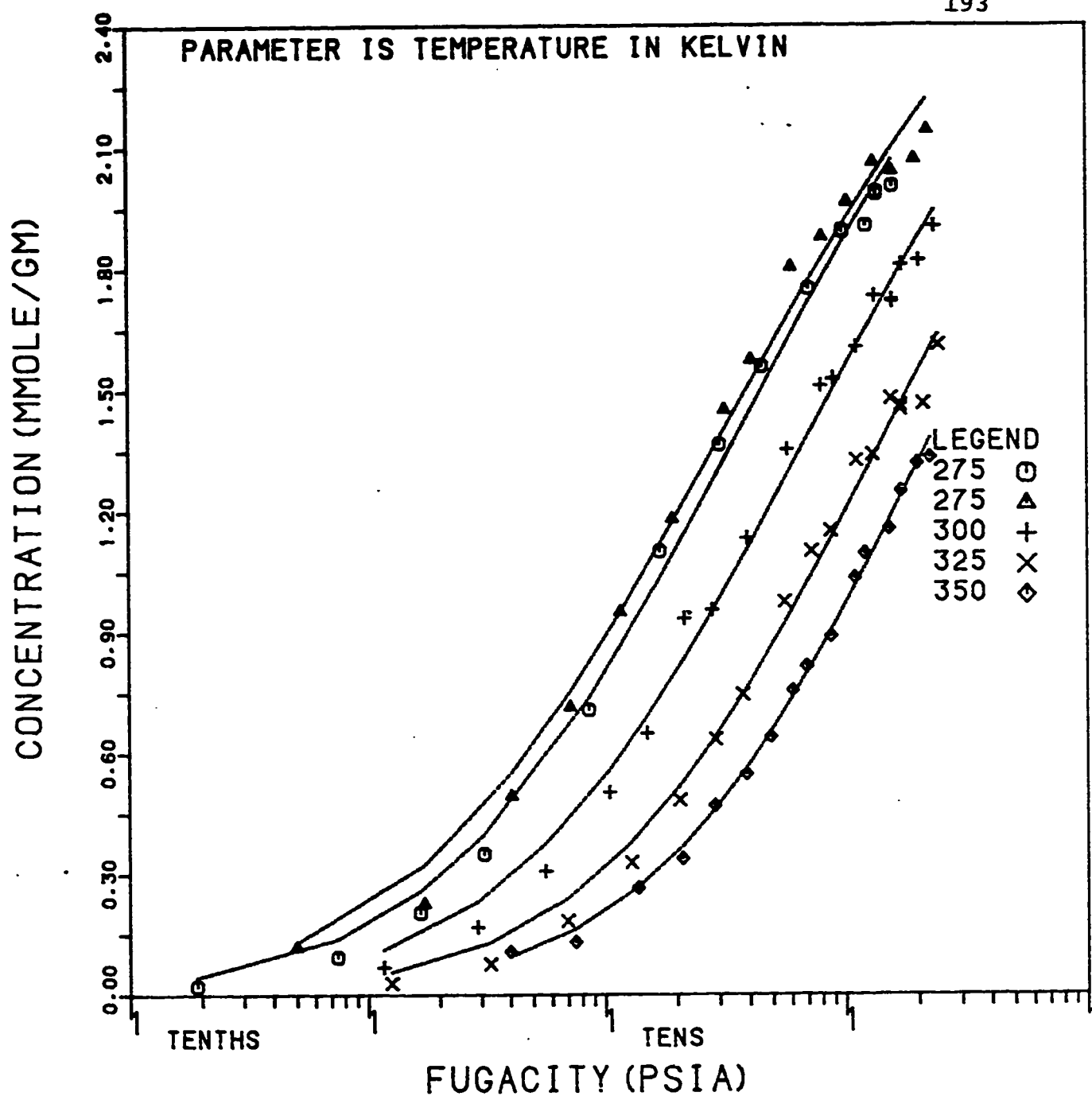


Fig. 5.26: Methane Isotherms on Linde S-115 Pellets: Fit of Toth Model With Theoretical N_0 and Optimized K.

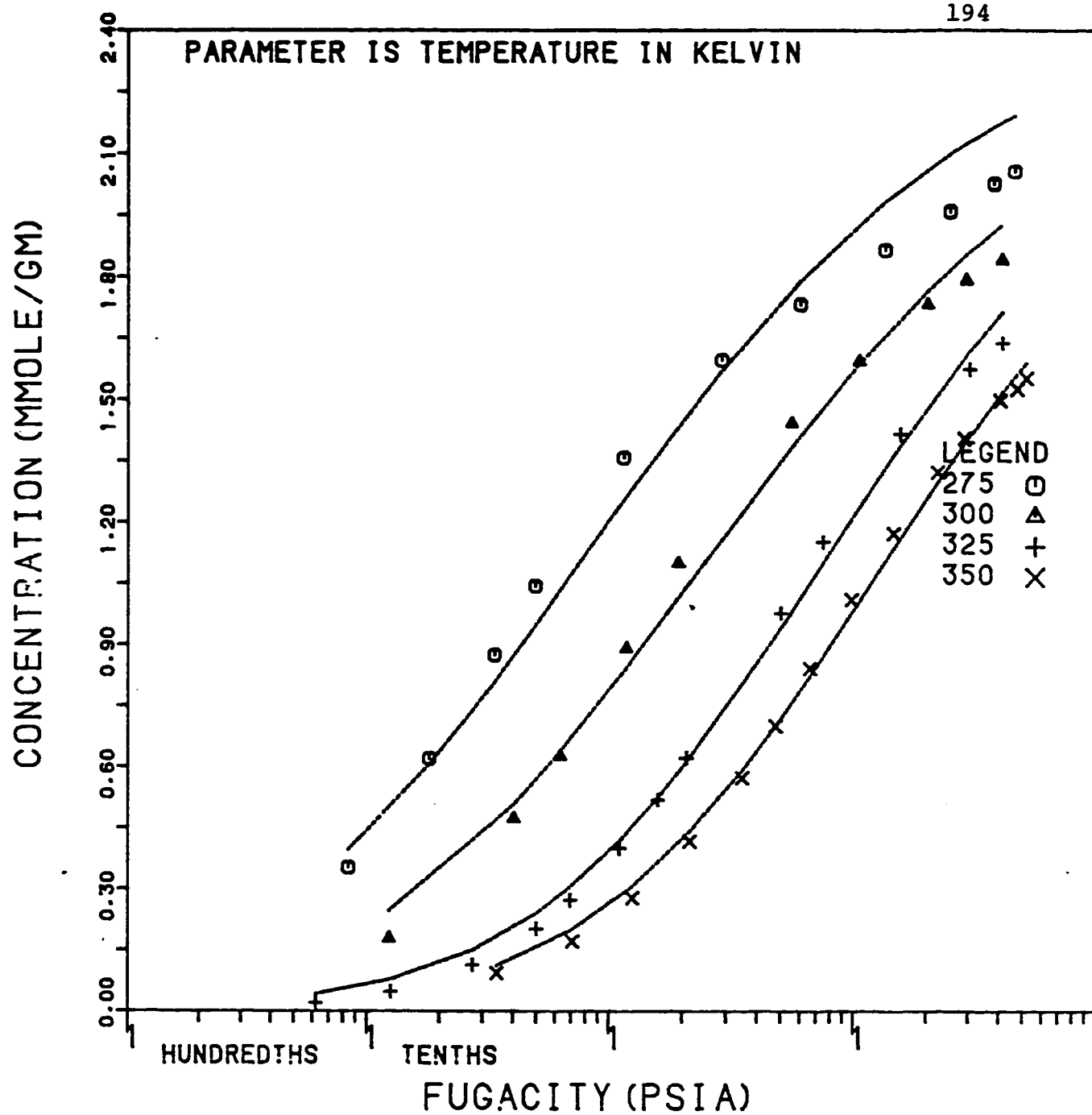


Fig. 5.27: Ethane Isotherms on Linde S-115 Pellets: Fit of Toth Model With Theoretical N_0 and optimized K .

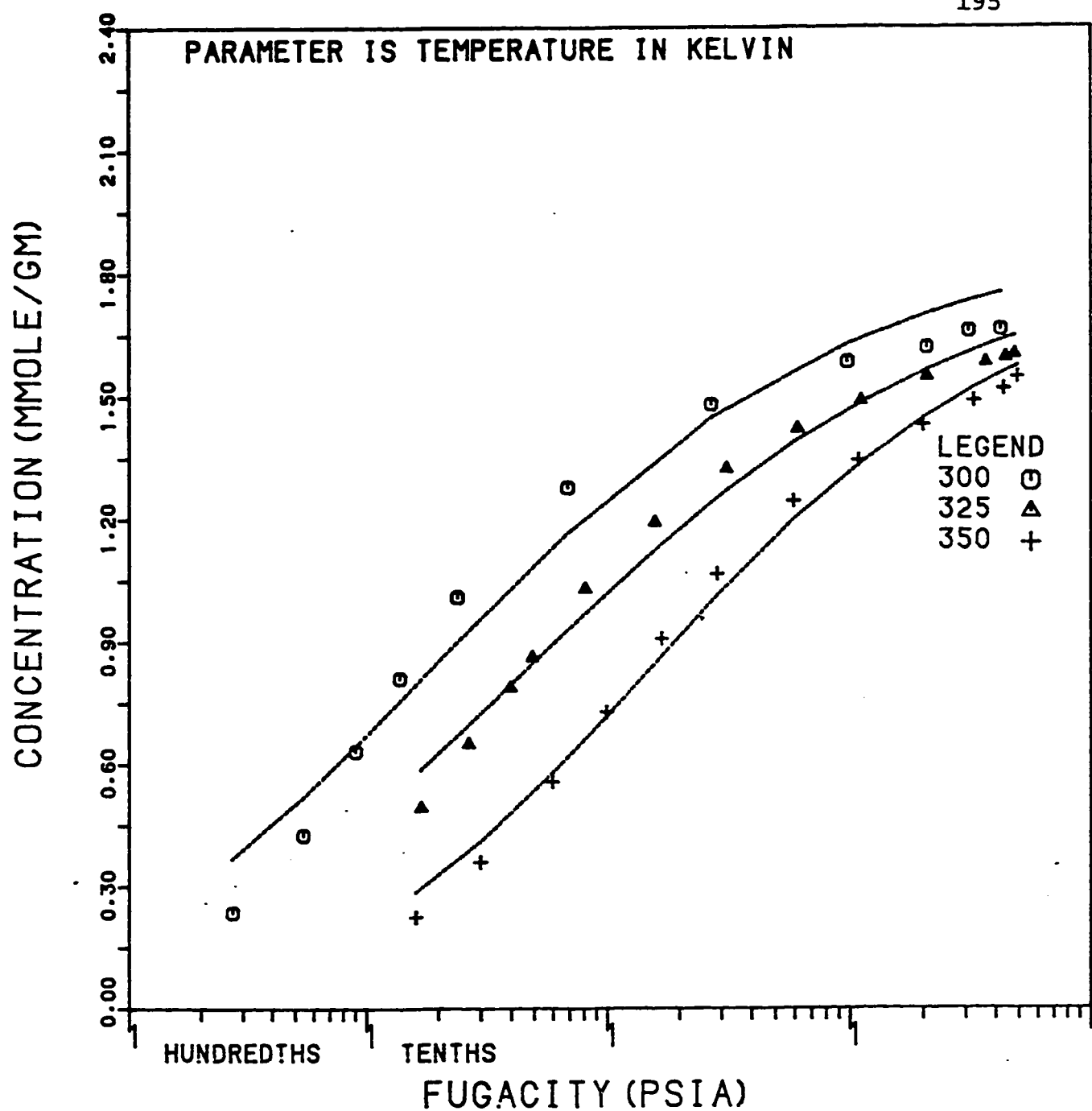


Fig. 5.28: Propane Isotherms on Linde S-115 Pellets: Fit of Toth Model With Theoretical N_0 and optimized K .

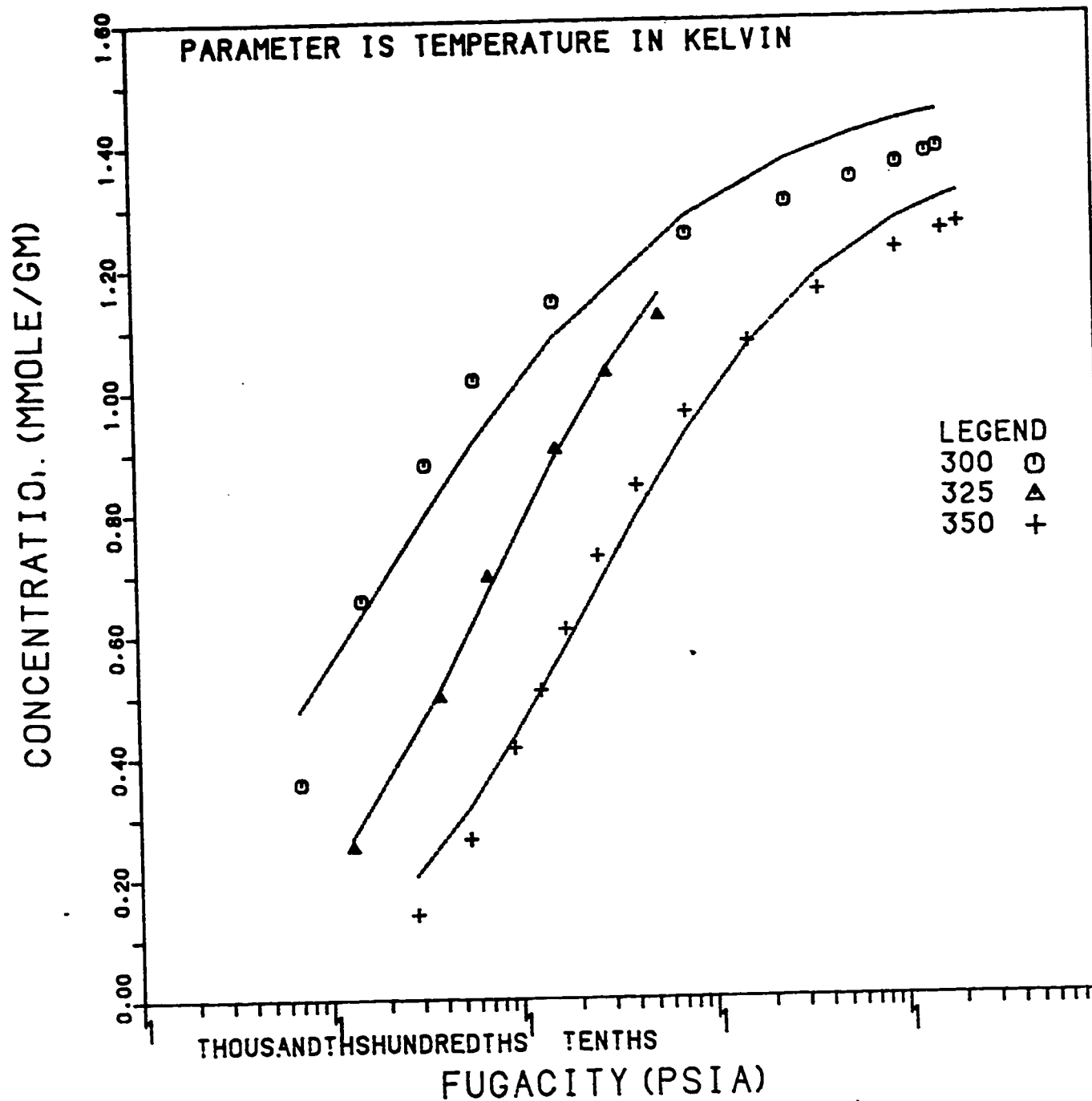


Fig. 5.29: n-Butane Isotherms on Linde S-115 Pellets: Fit of Toth Model With Theoretical N_0 and optimized K .

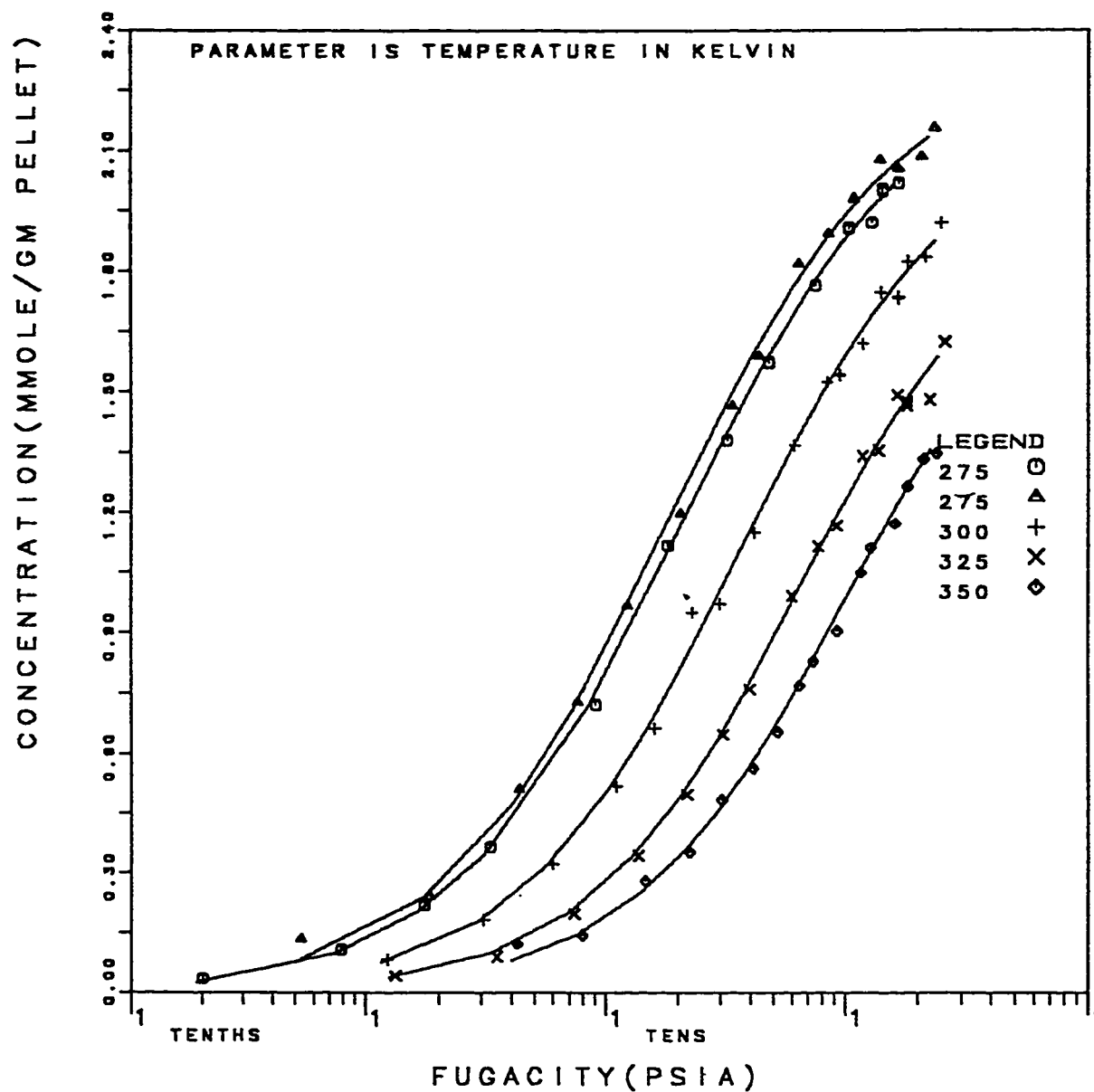


Fig. 5.30: Methane Isotherms on Linde S-115 Pellets: Fit of Toth Model With Optimized N_0 and K .

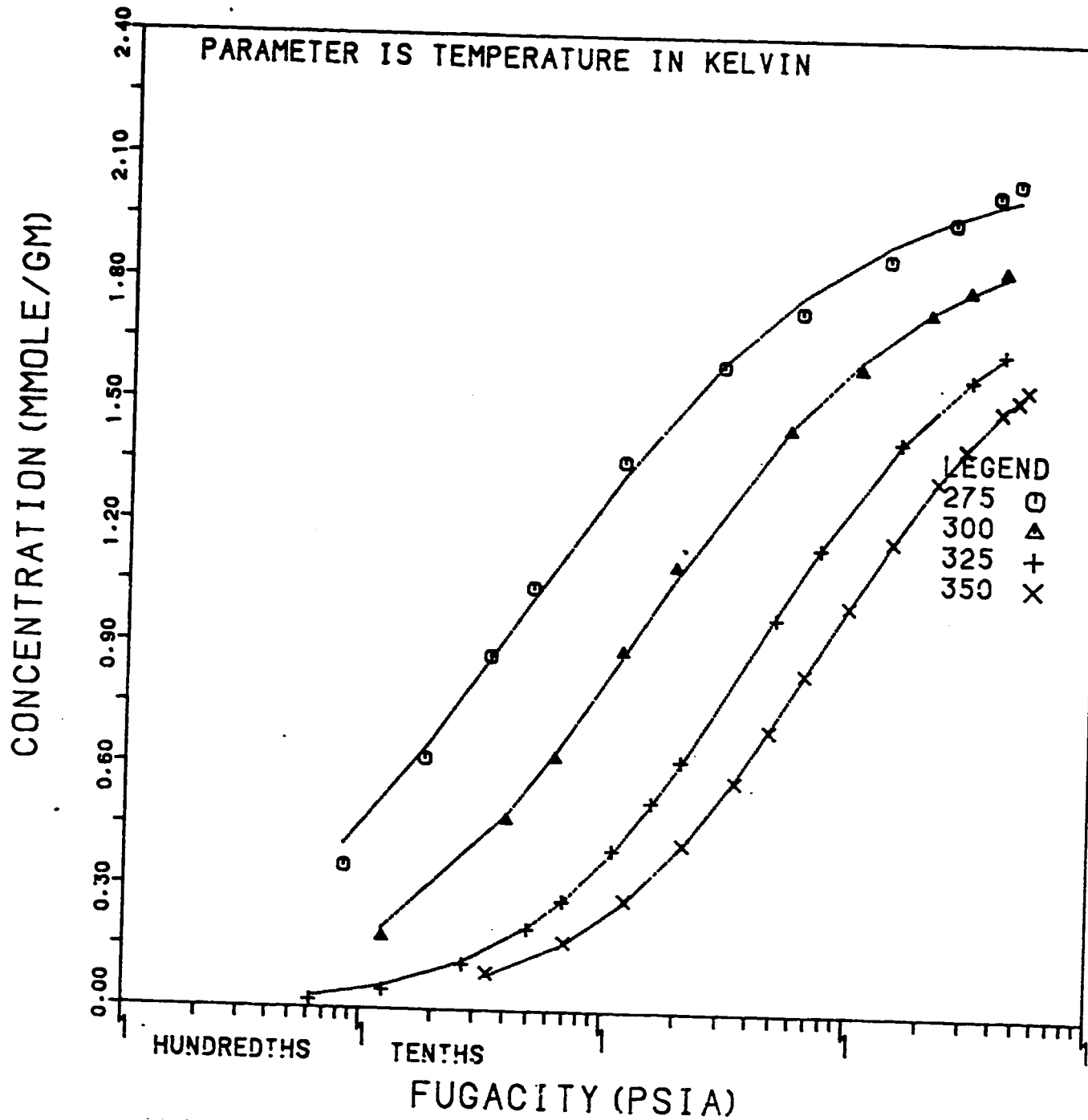


Fig. 5.31: Ethane Isotherms on Linde S-115 Pellets: Fit of Toth Model With Optimized N_0 and K .

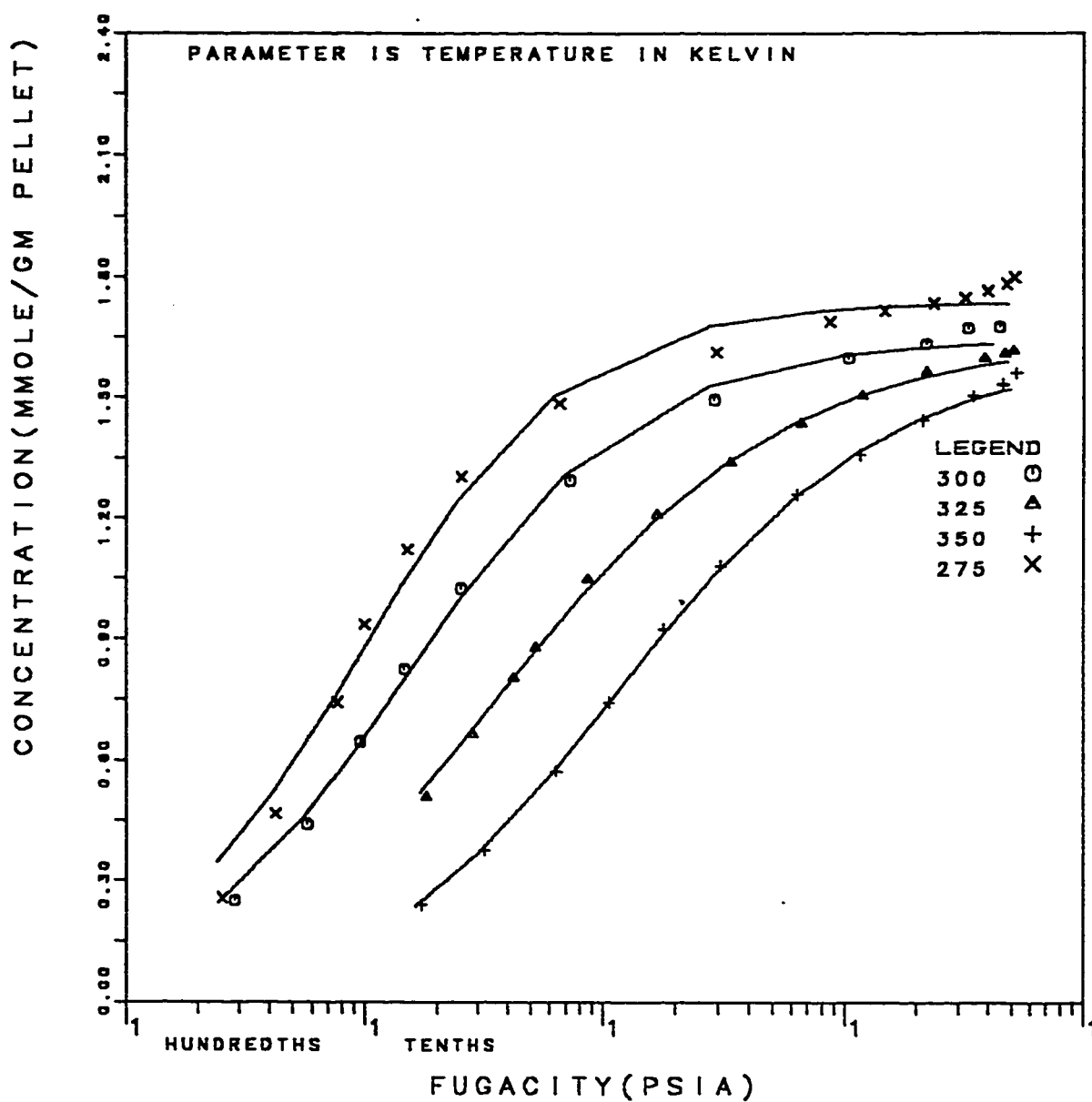


Fig. 5.32: Propane Isotherms on Linde S-115 Pellets: Fit of Toth Model With Optimized N_0 and K .

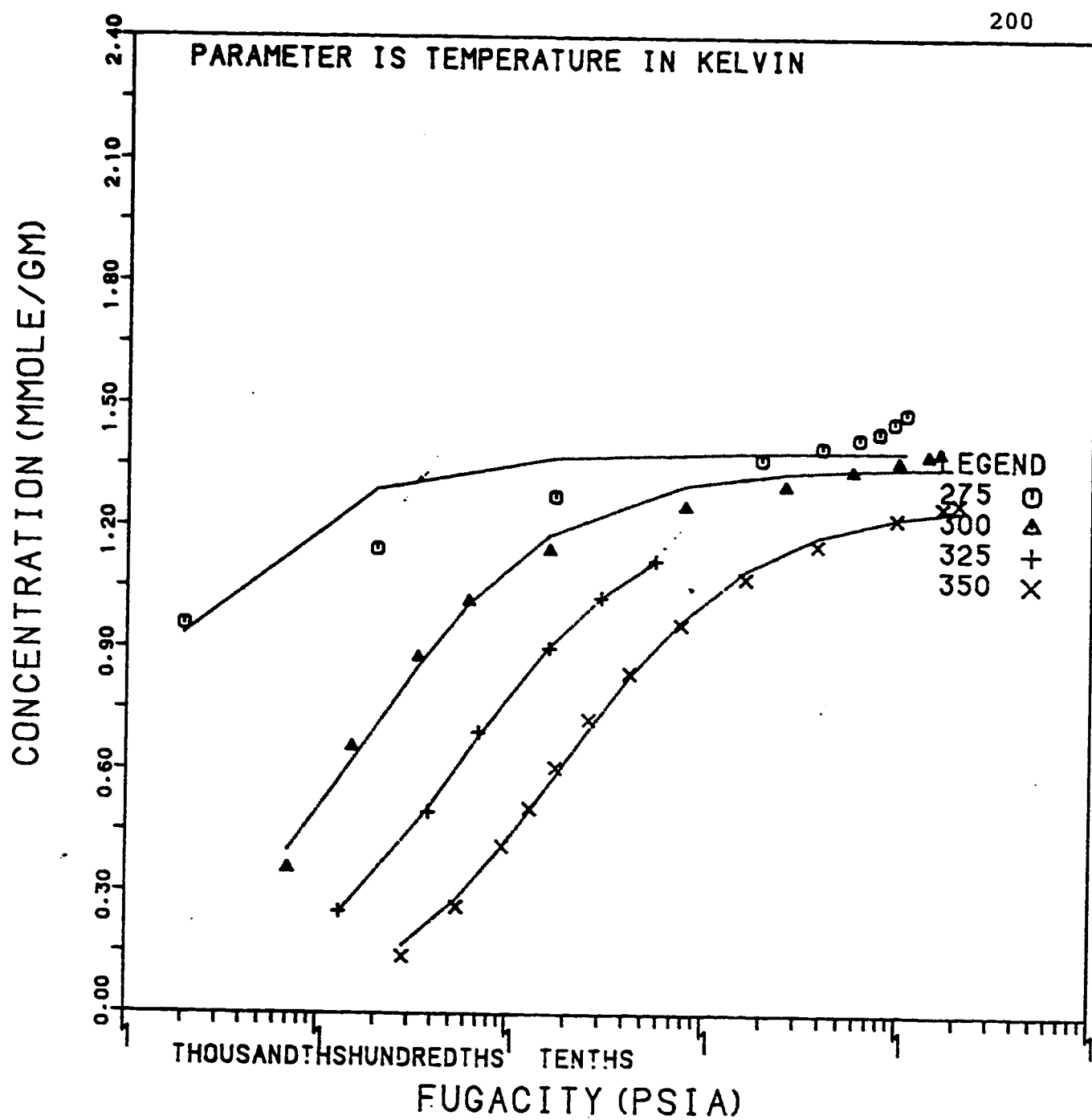


Fig. 5.33: n-Butane Isotherms on Linde S-115 Pellets: Fit of Toth Model With Optimized N_0 and K .

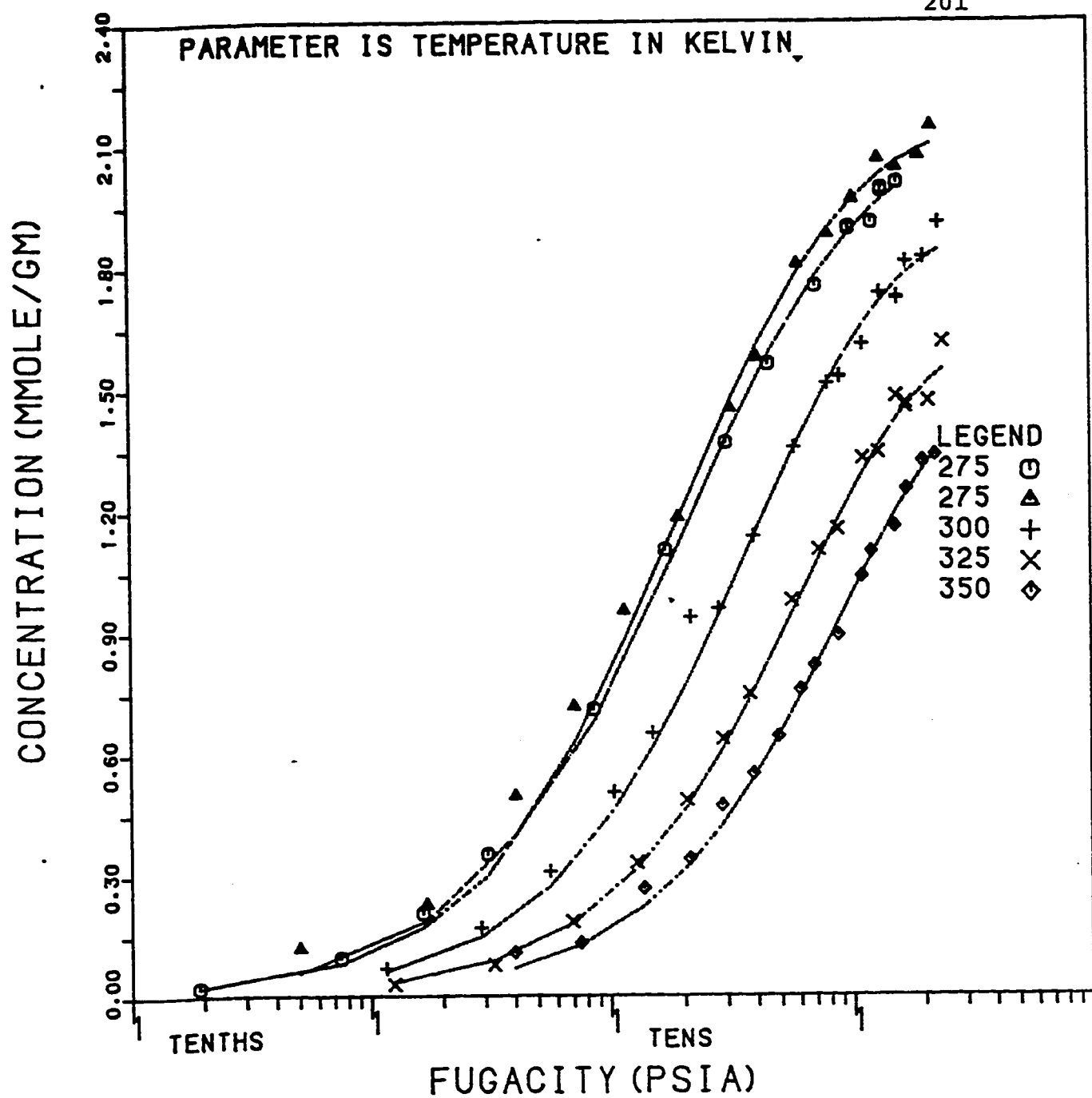


Fig. 5.34: Methane Isotherms on Linde S-115 Pellets: Fit of Mathews and Weber Model With Optimized N_0 and Intrinsic K .

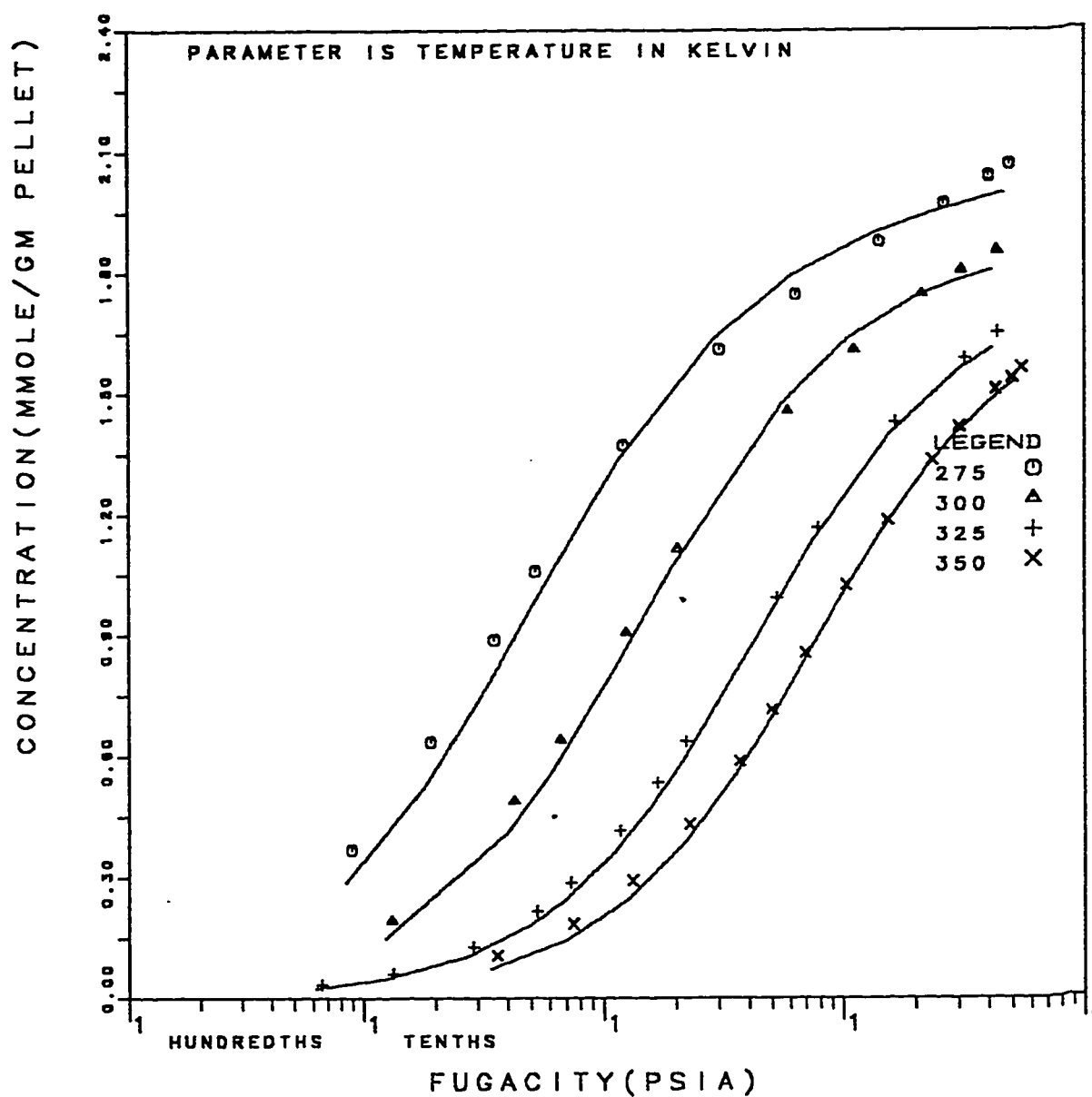


Fig. 5.35: Ethane Isotherms on Linde S-115 Pellets: Fit of Mathews and Weber Model With Optimized N_0 and Intrinsic K.

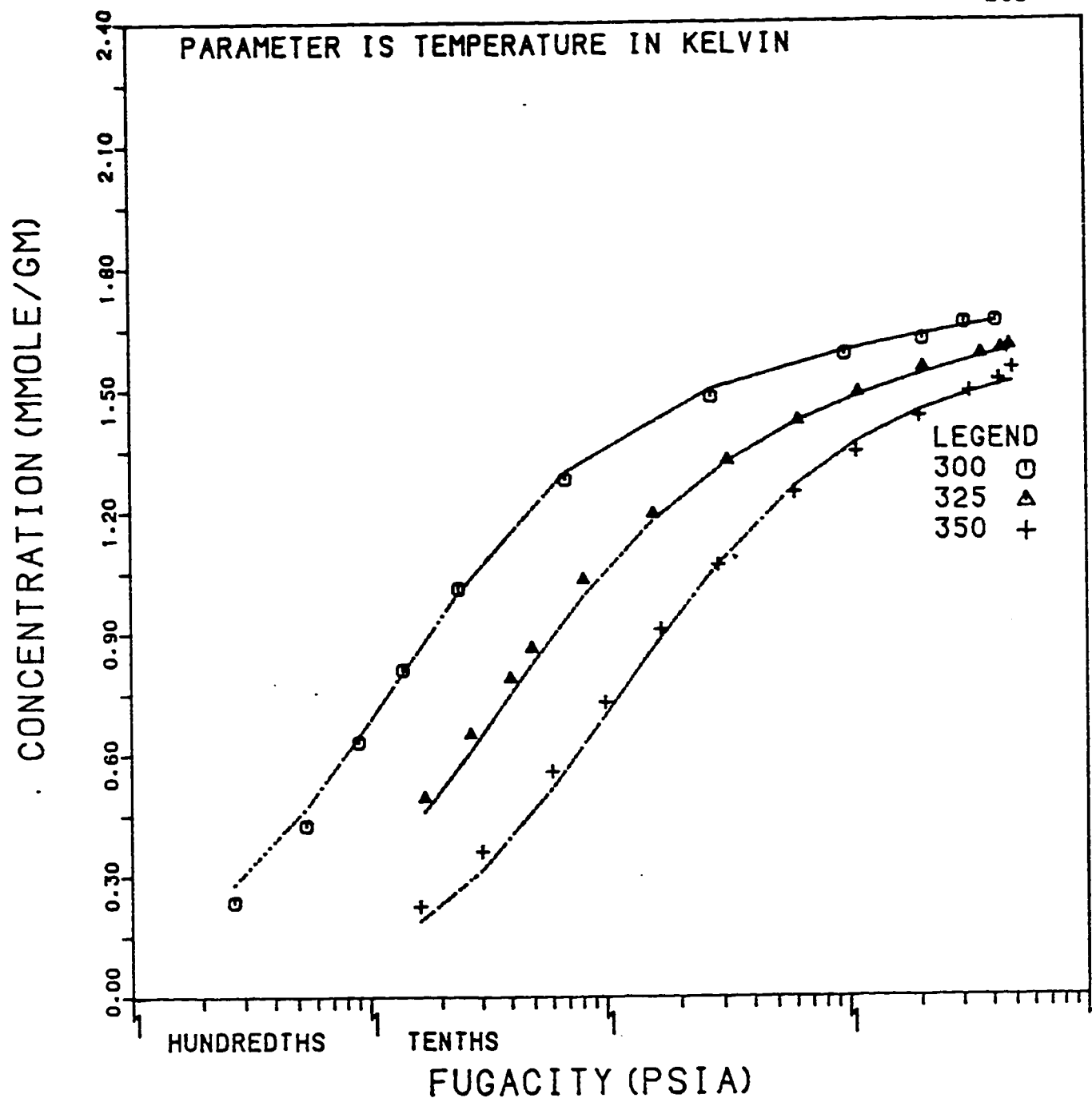


Fig. 5.36: Propane Isotherms on Linde S-115 Pellets: Fit of Mathews and Weber Model With Optimized N_0 and Intrinsic K .

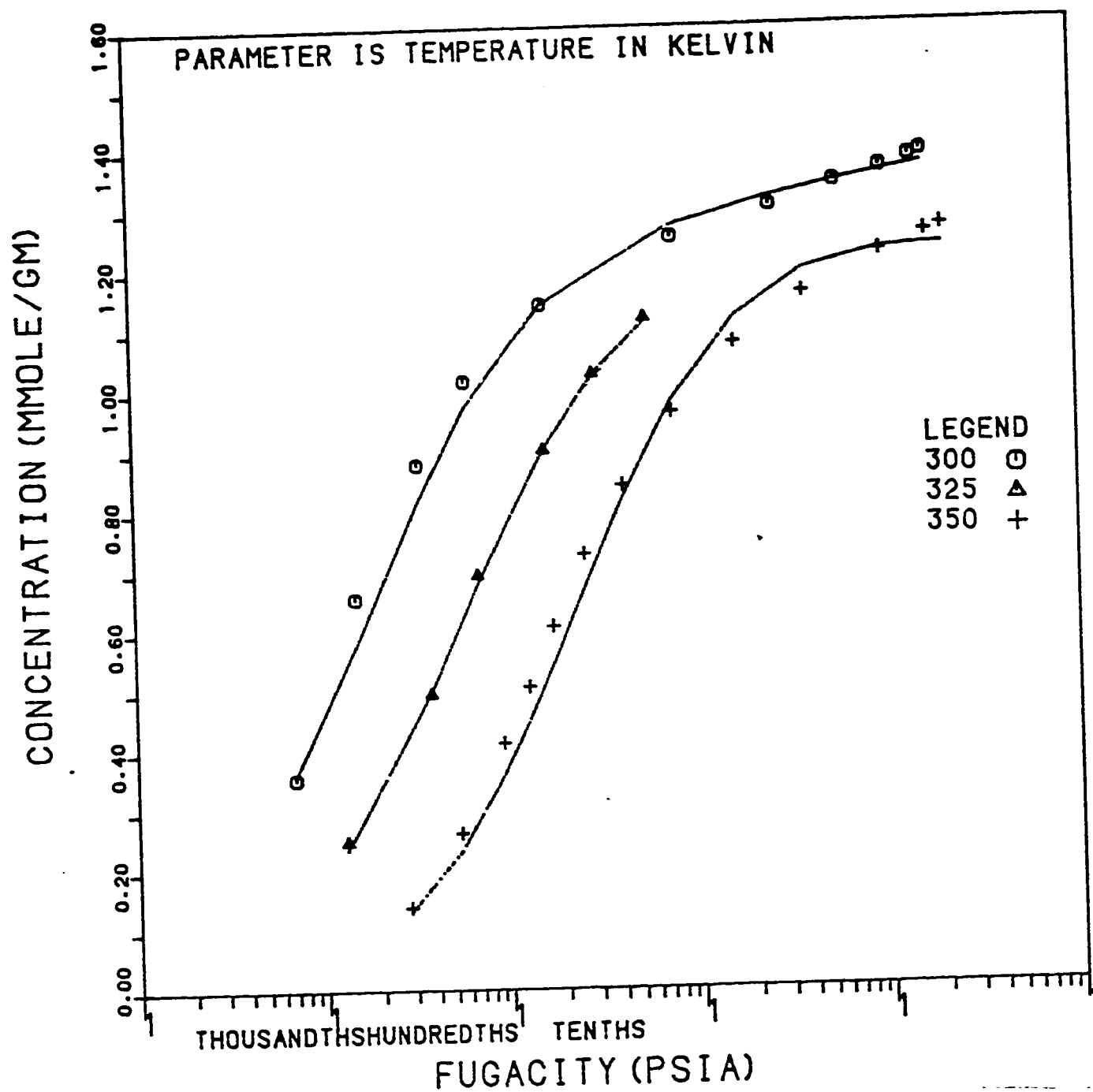


Fig. 5.37: n-Butane Isotherms on Linde S-115 Pellets: Fit of Mathews and Weber Model With Optimized N_0 and Intrinsic K .

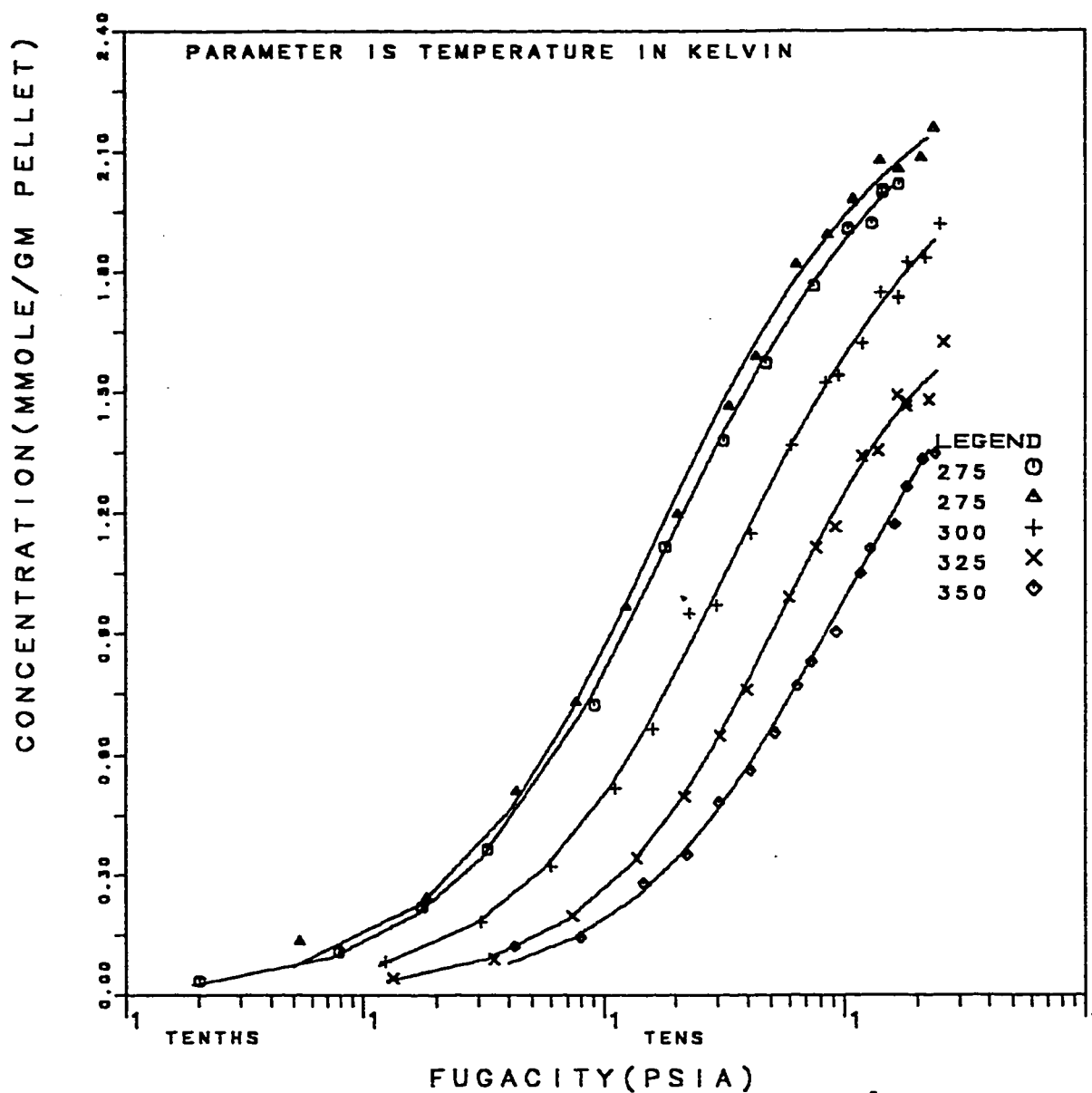


Fig. 5.38: Methane Isotherms on Linde S-115 Pellets: Fit of Mathews and Weber Model With Optimized N_0 and K .

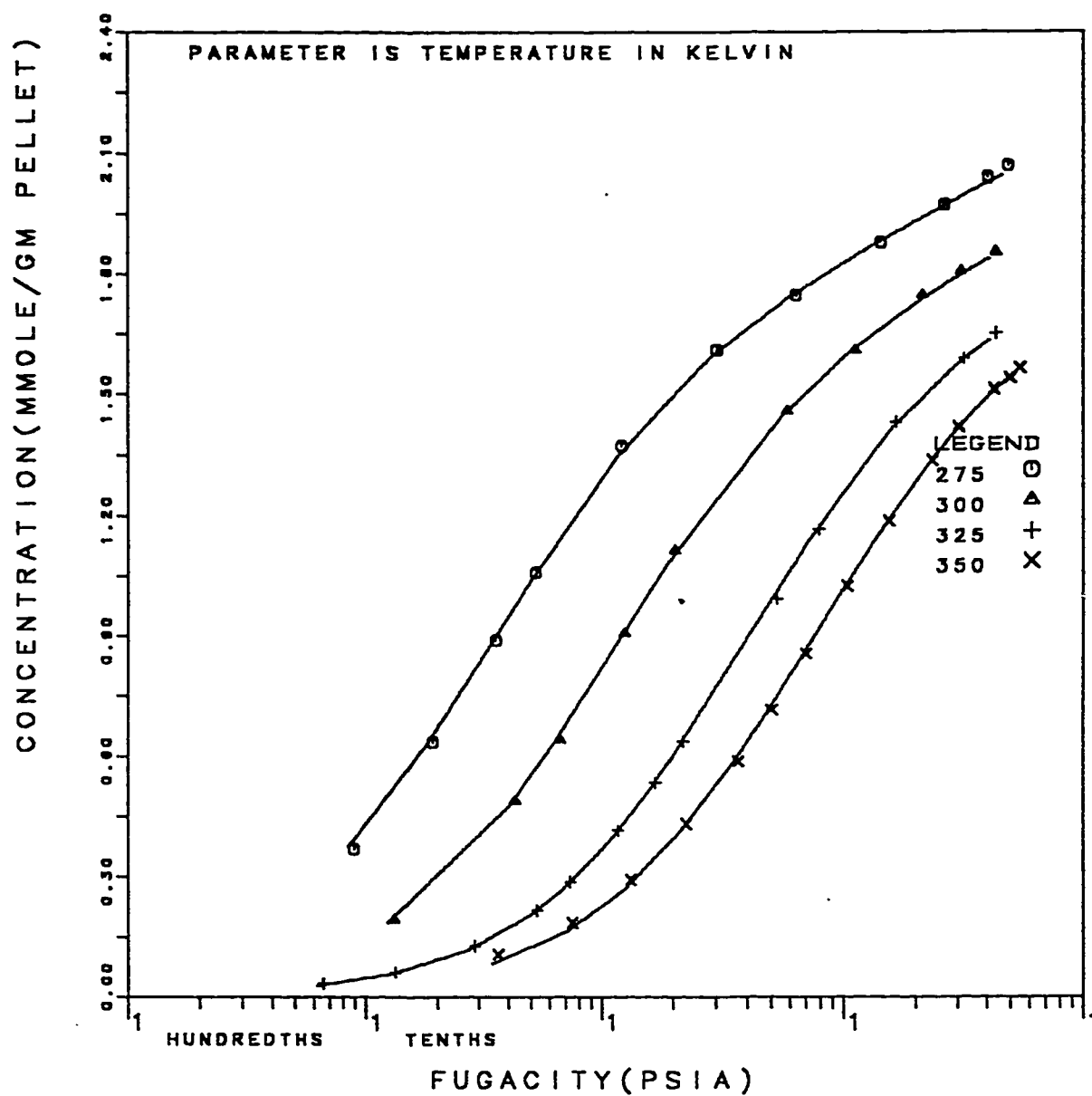


Fig. 5.39: Ethane Isotherms on Linde S-115 Pellets: Fit of Mathews and Weber Model With Optimized N_0 and K .

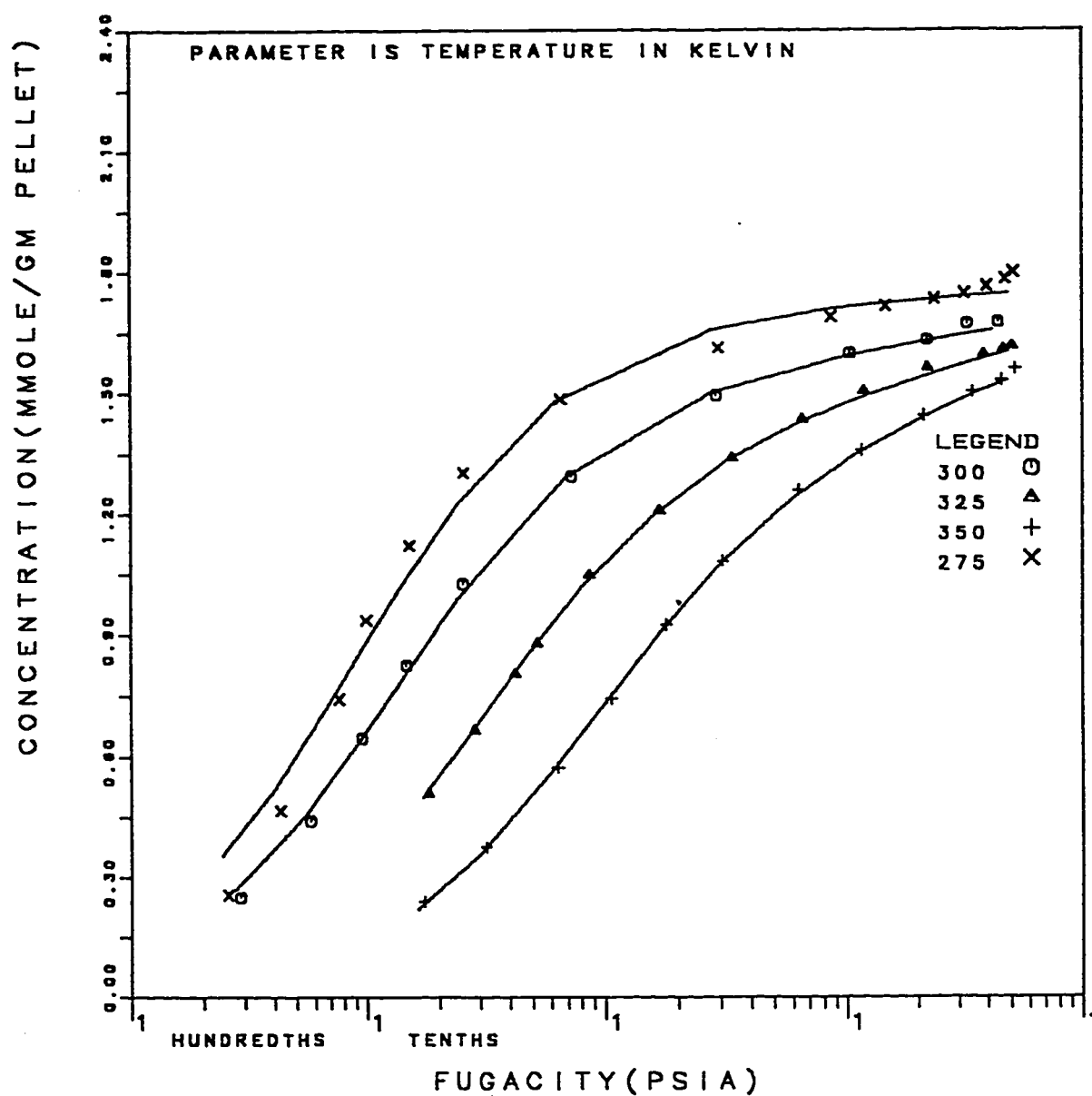


Fig. 5.40: Propane Isotherms on Linde S-115 Pellets: Fit of Mathews and Weber Model With Optimized N_0 and K .

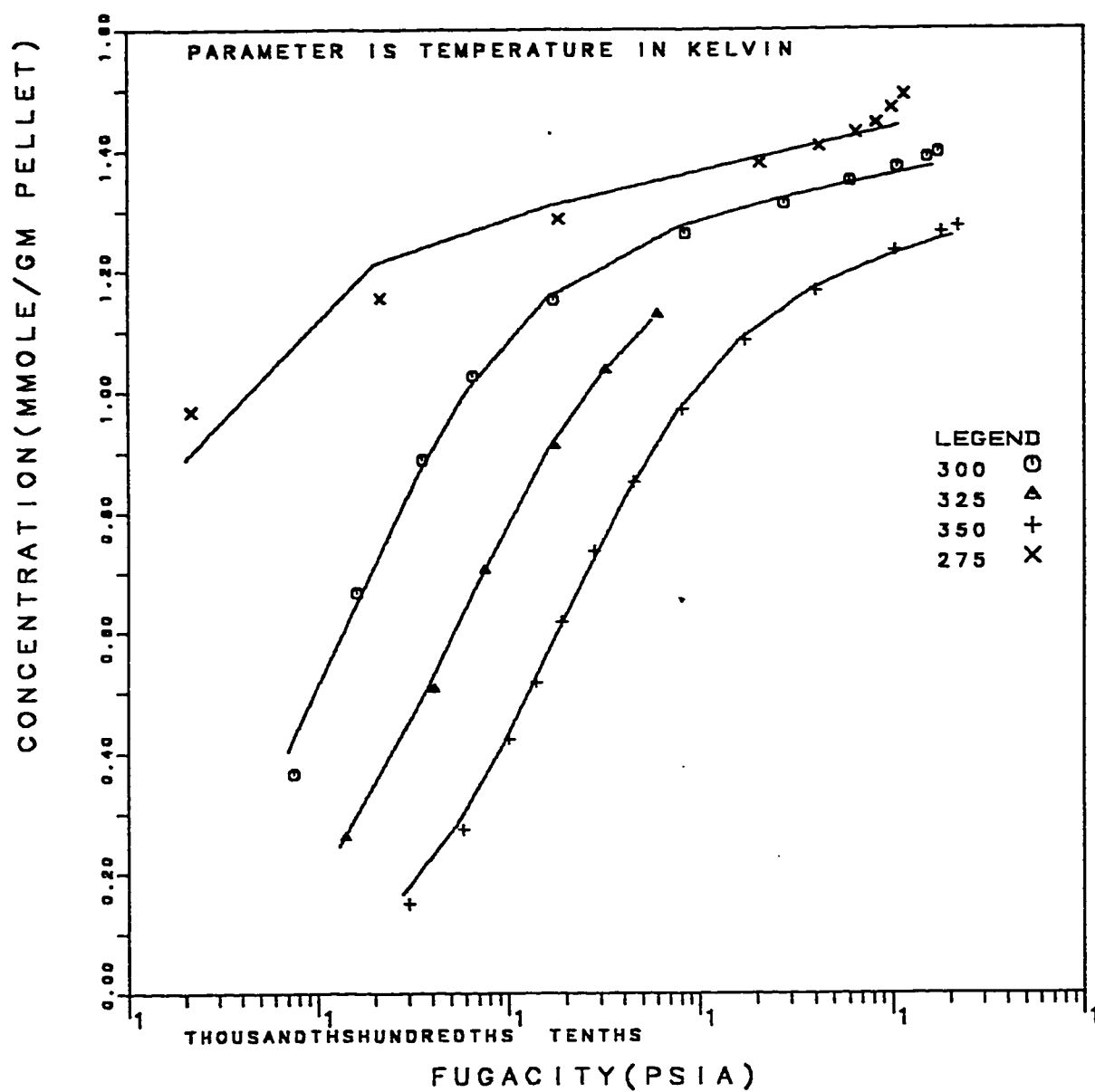


Fig. 5.41: n-Butane Isotherms on Linde S-115 Pellets: Fit of Mathews and Weber Model With Optimized N_0 and K .

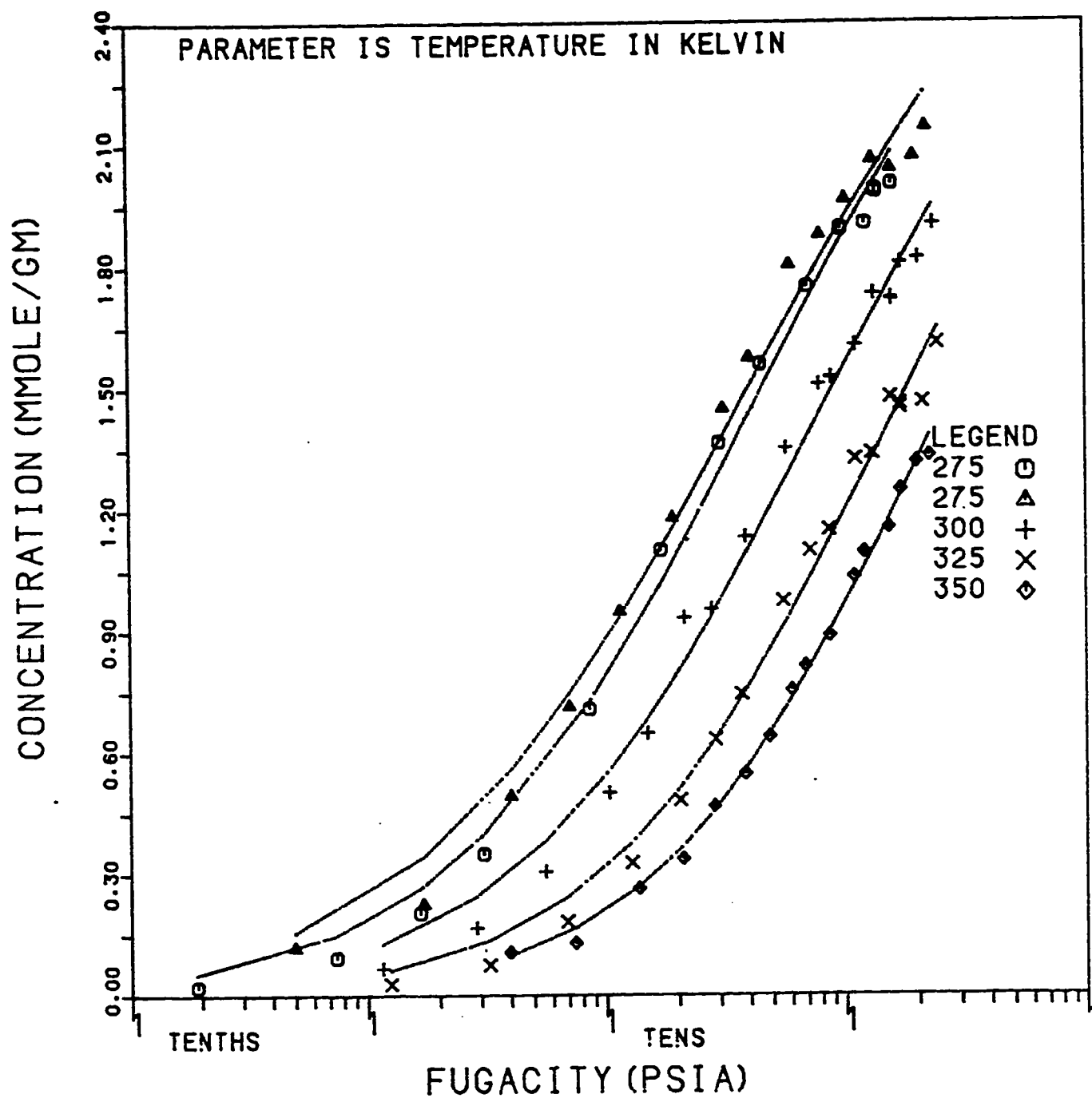


Fig. 5.42: Methane Isotherms on Linde S-115 Pellets: Fit of Jaroniec Model With Theoretical N_0 and Intrinsic K .

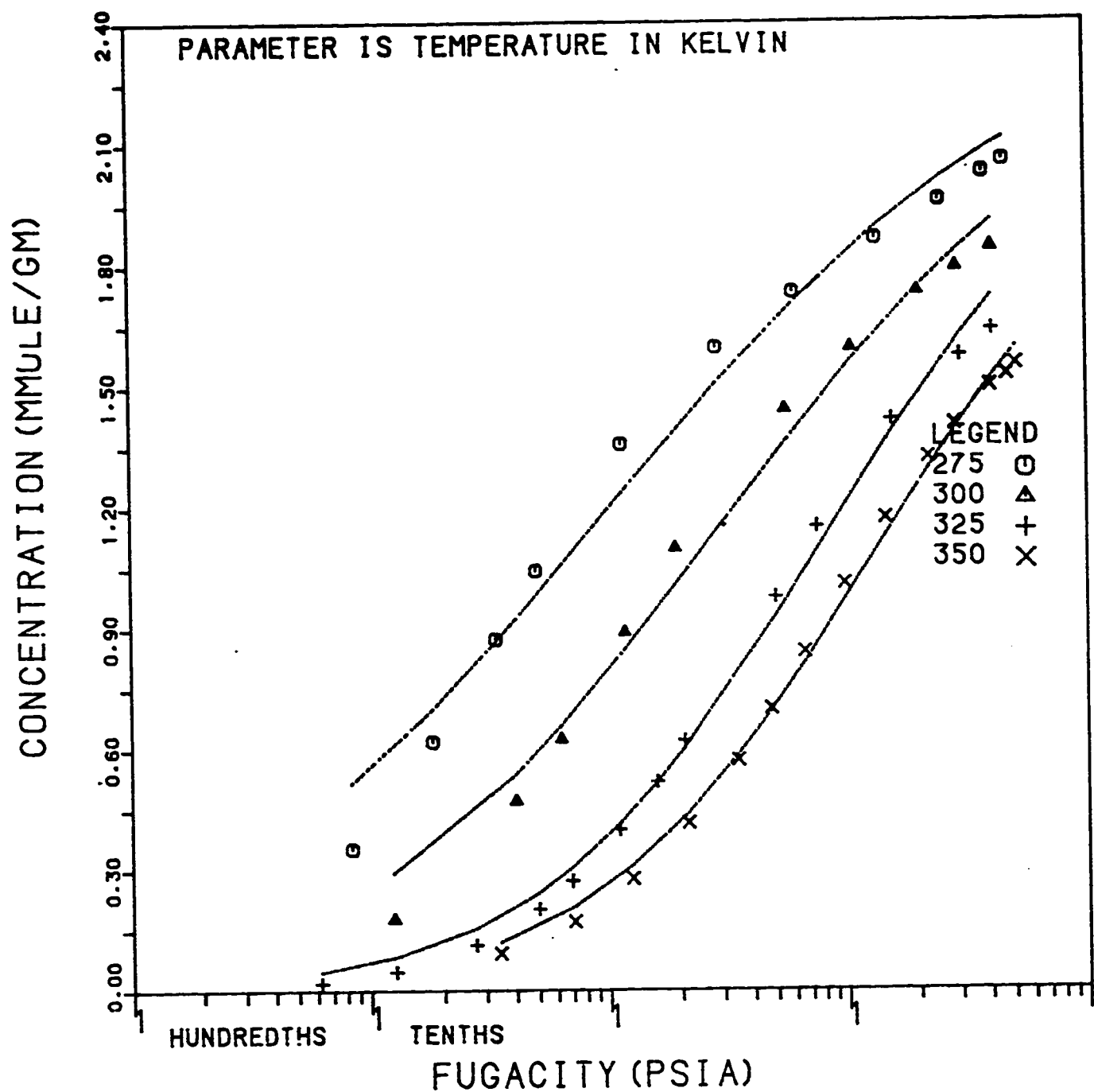


Fig. 5.43: Ethane Isotherms on Linde S-115 Pellets: Fit of Jaroniec Model With Theoretical N_0 and Intrinsic K .

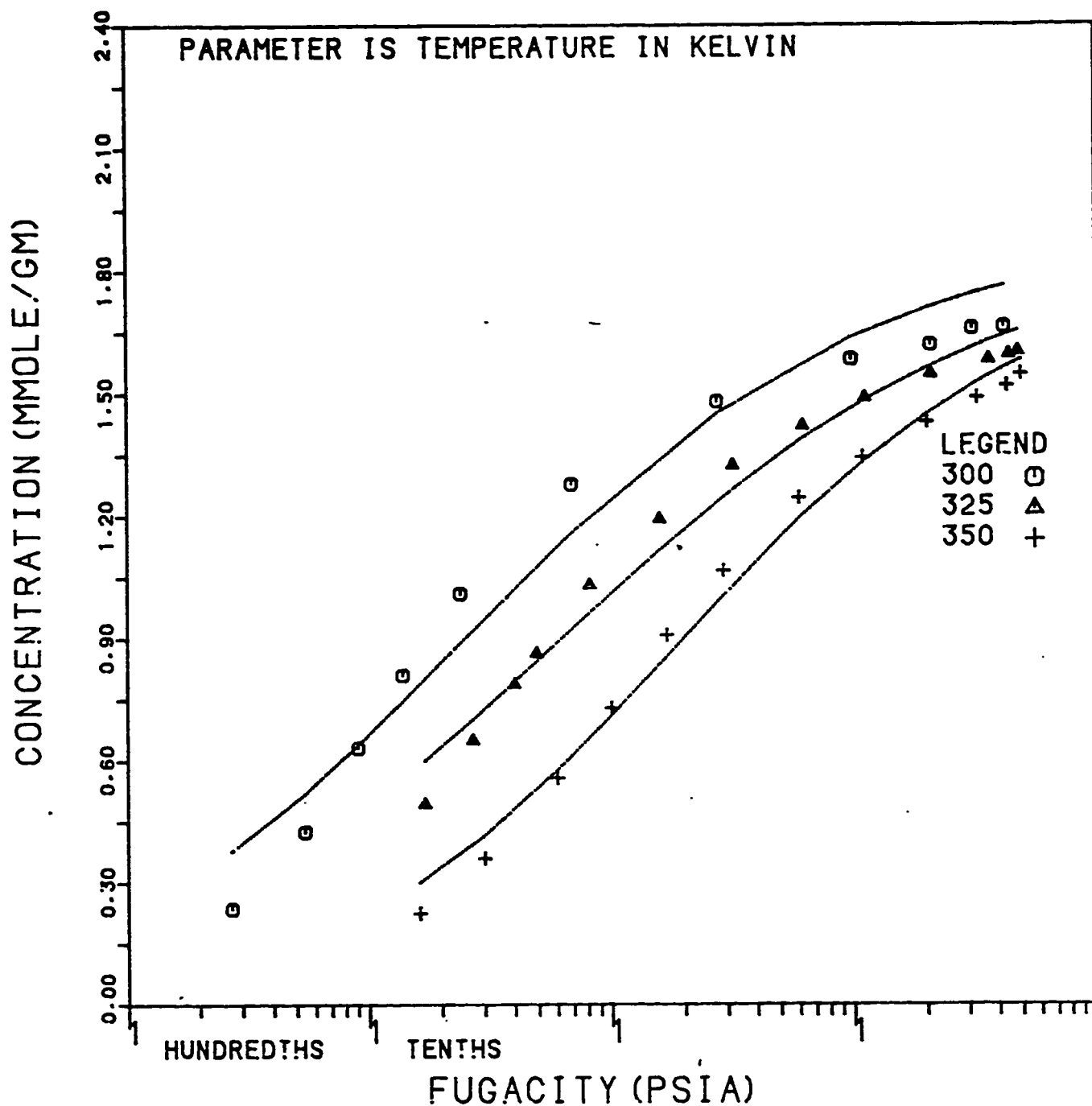


Fig. 5.44: Propane Isotherms on Linde S-115 Pellets: Fit of Jaroniec Model With Theoretical N_0 and Intrinsic K .

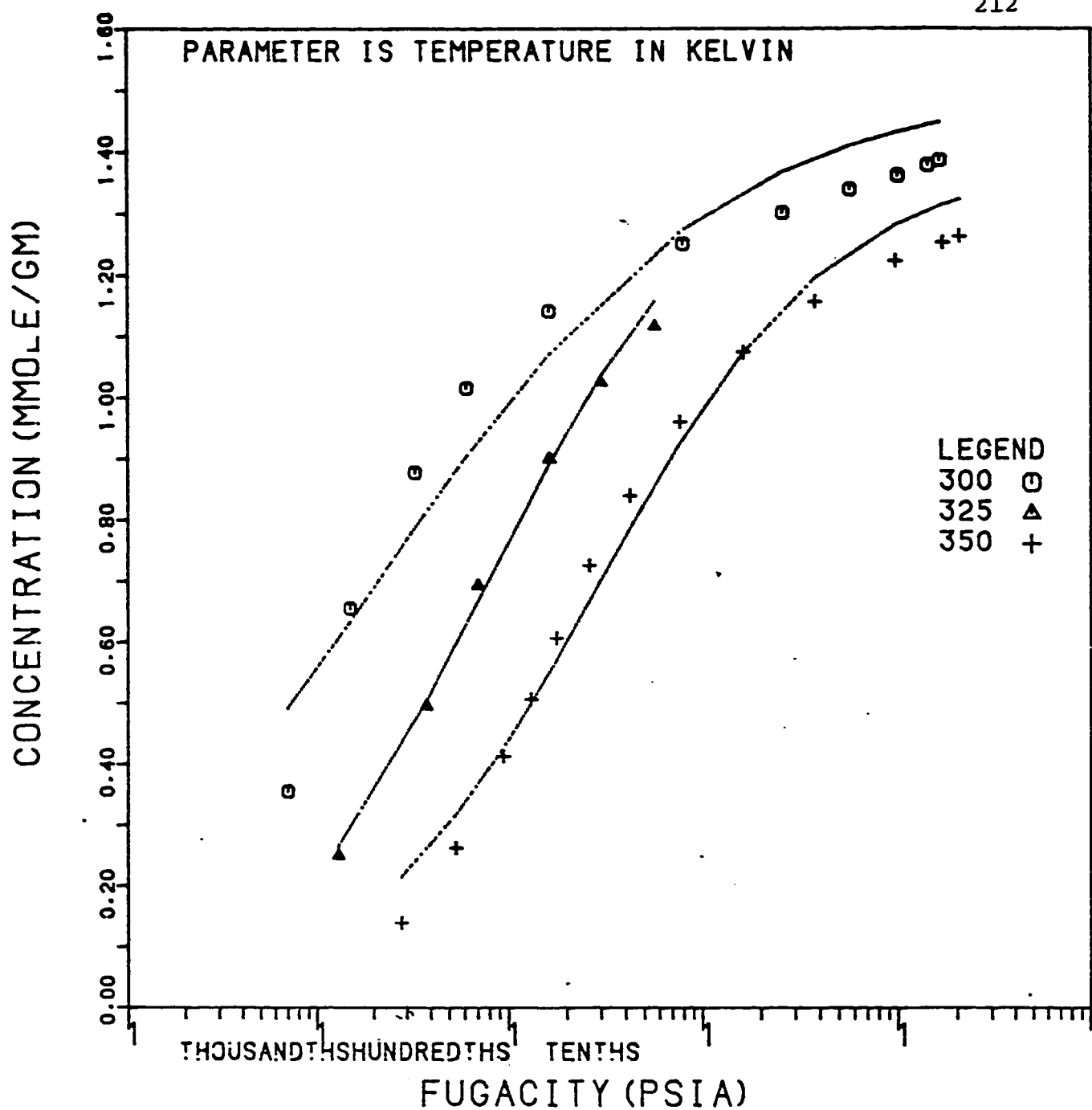


Fig. 5.45: n-Butane Isotherms on Linde S-115 Pellets: Fit of Jaroniec Model With Theoretical N_0 and Intrinsic K .

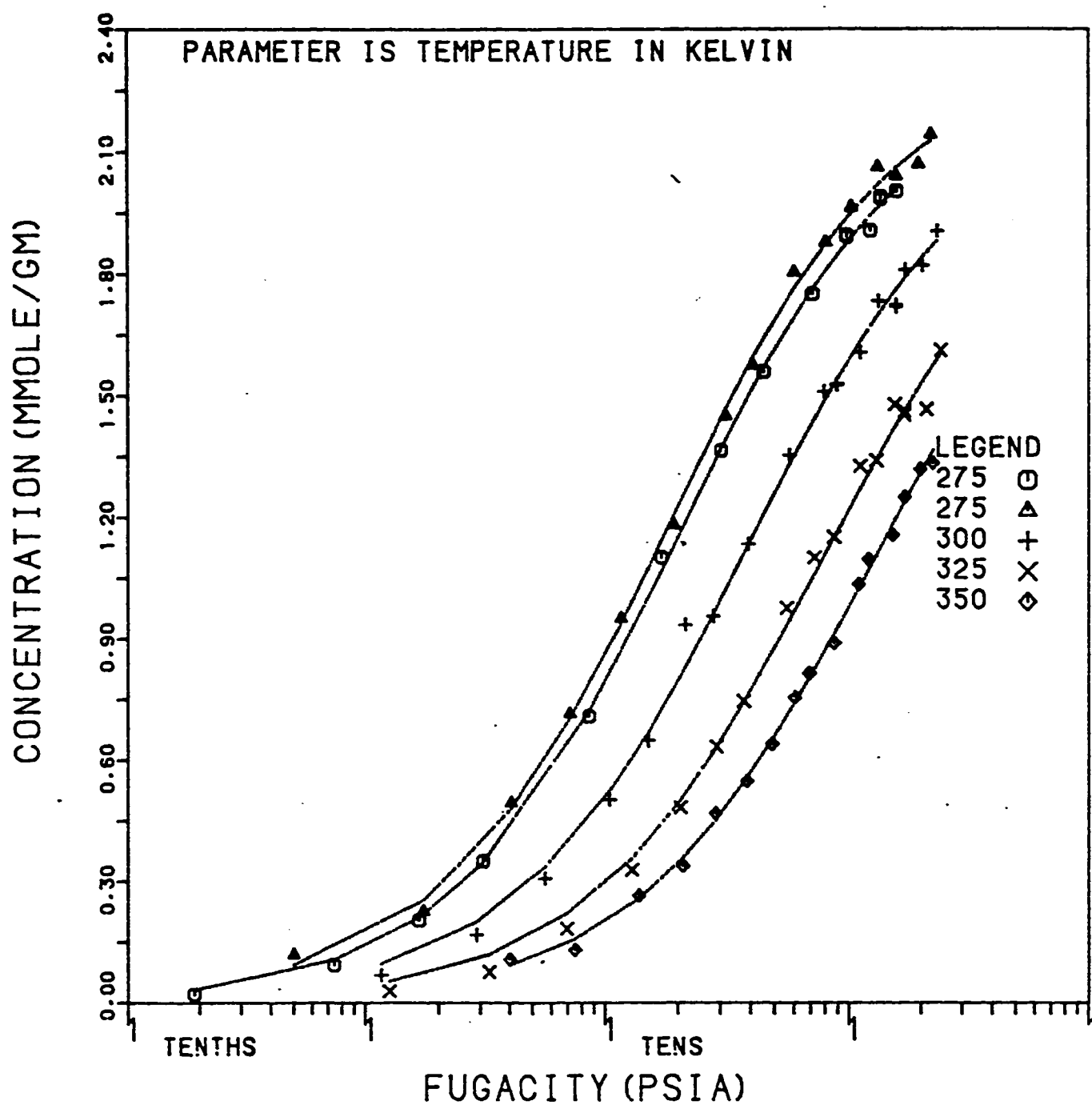


Fig. 5.46: Methane Isotherms on Linde S-115 Pellets: Fit of Jaroniec Model With Optimized N_0 and Intrinsic K .

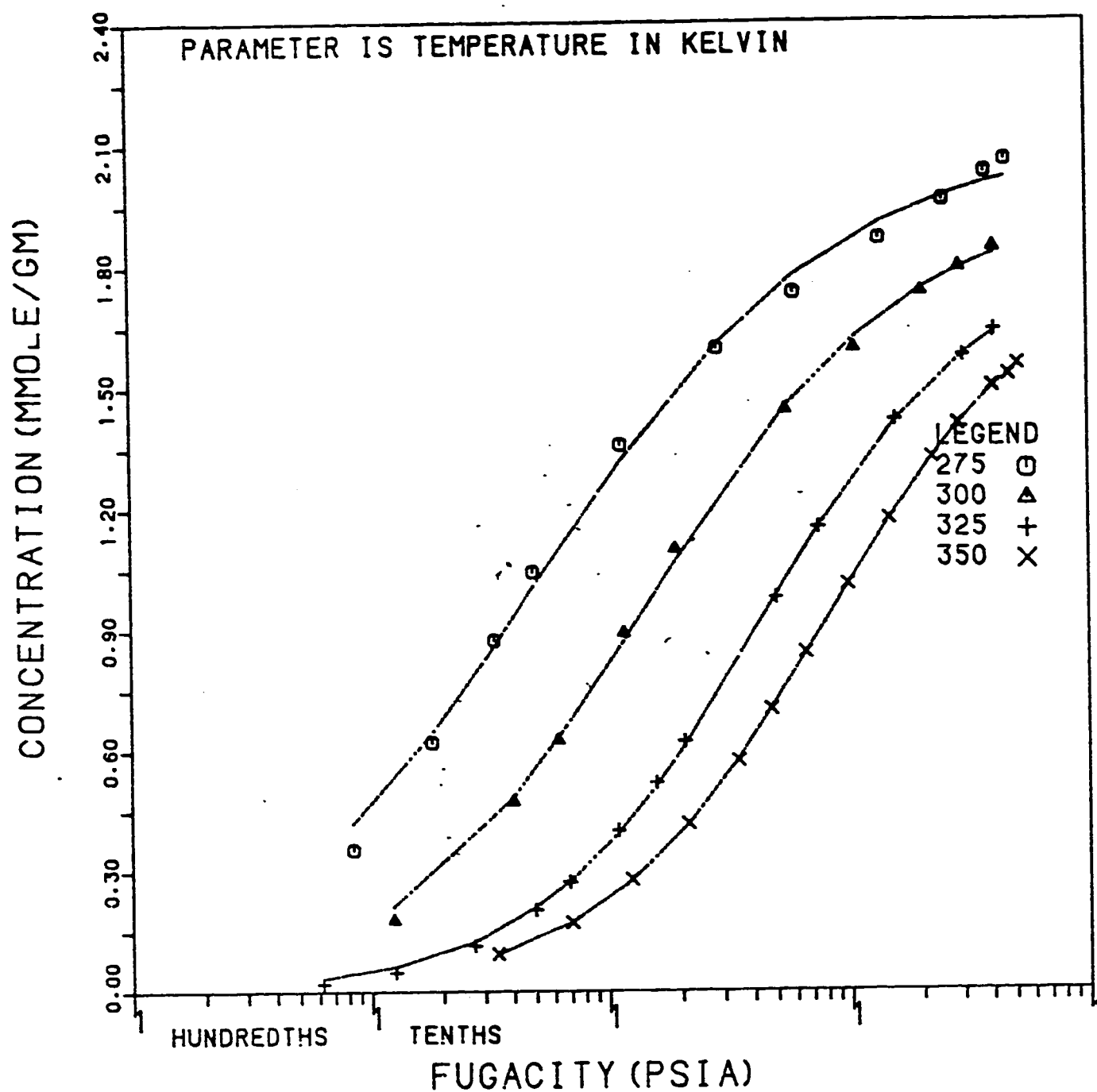


Fig. 5.47: Ethane Isotherms on Linde S-115 Pellets: Fit of Jaroniec Model With Optimized N_0 and Intrinsic K .

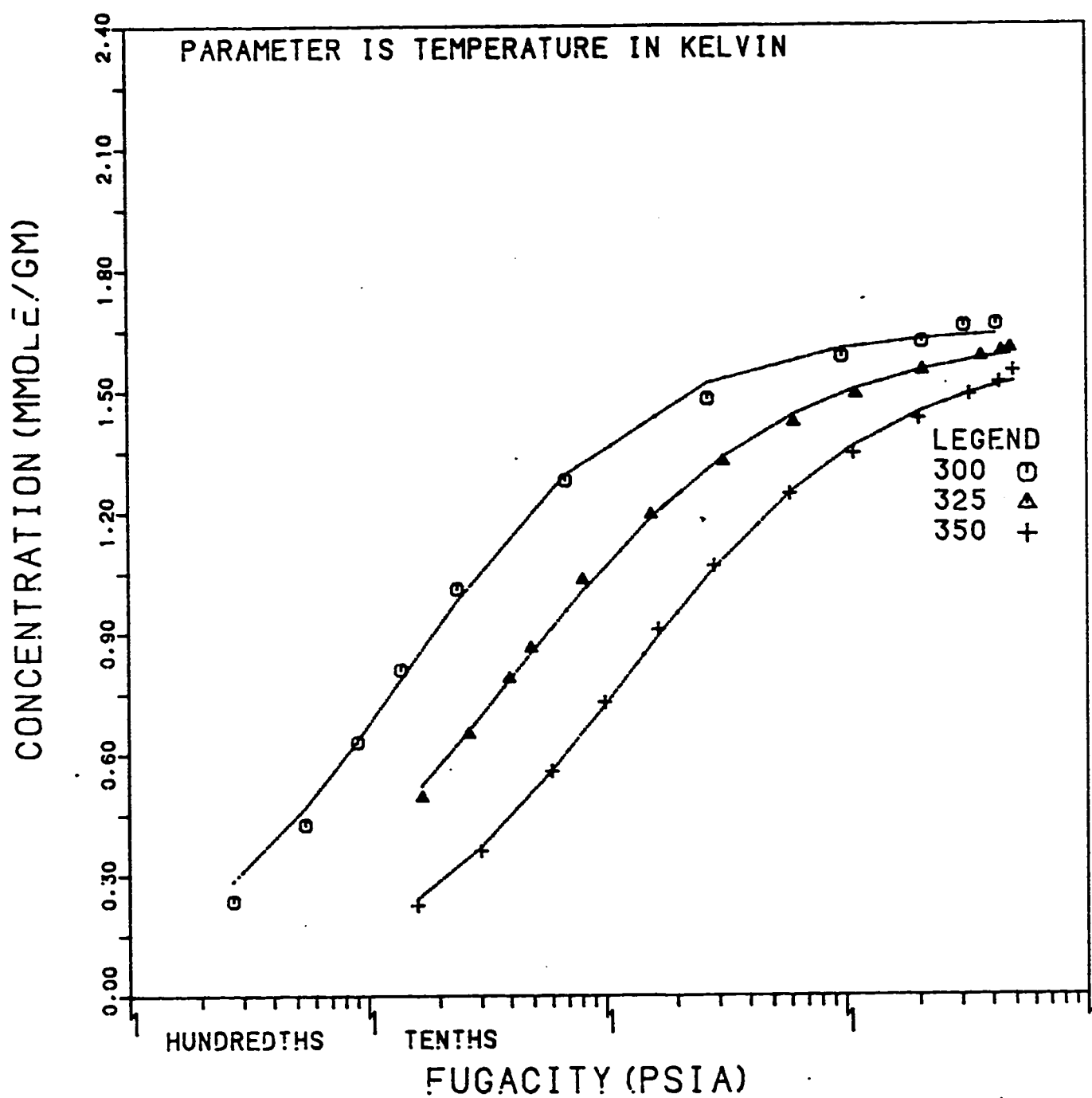


Fig. 5.48: Propane Isotherms on Linde S-115 Pellets: Fit of Jaroniec Model With Optimized N_0 and Intrinsic K .

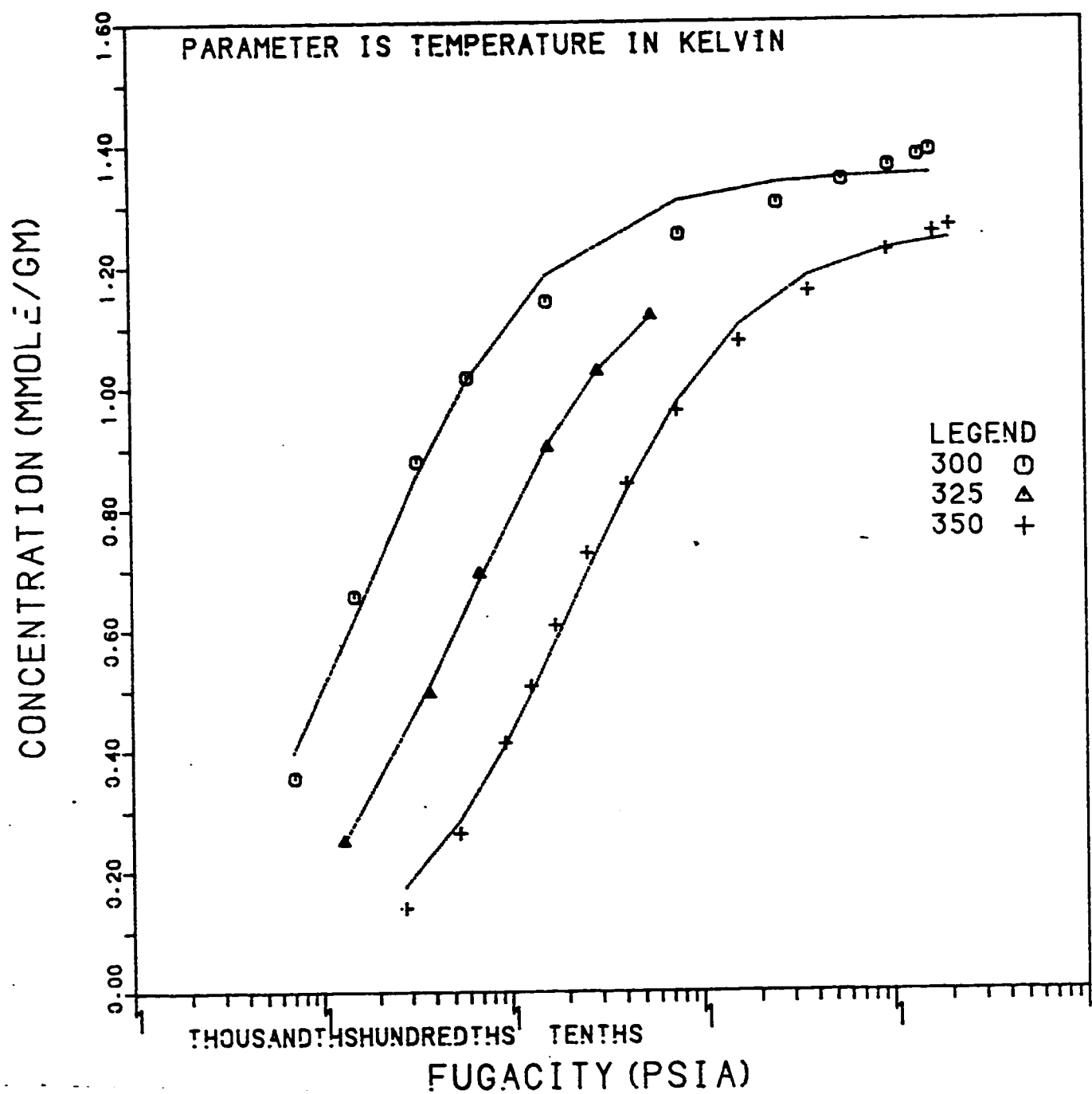


Fig. 5.49: n-Butane Isotherms on Linde S-115 Pellets: Fit of Jaroniec Model With Optimized N_0 and Intrinsic K .

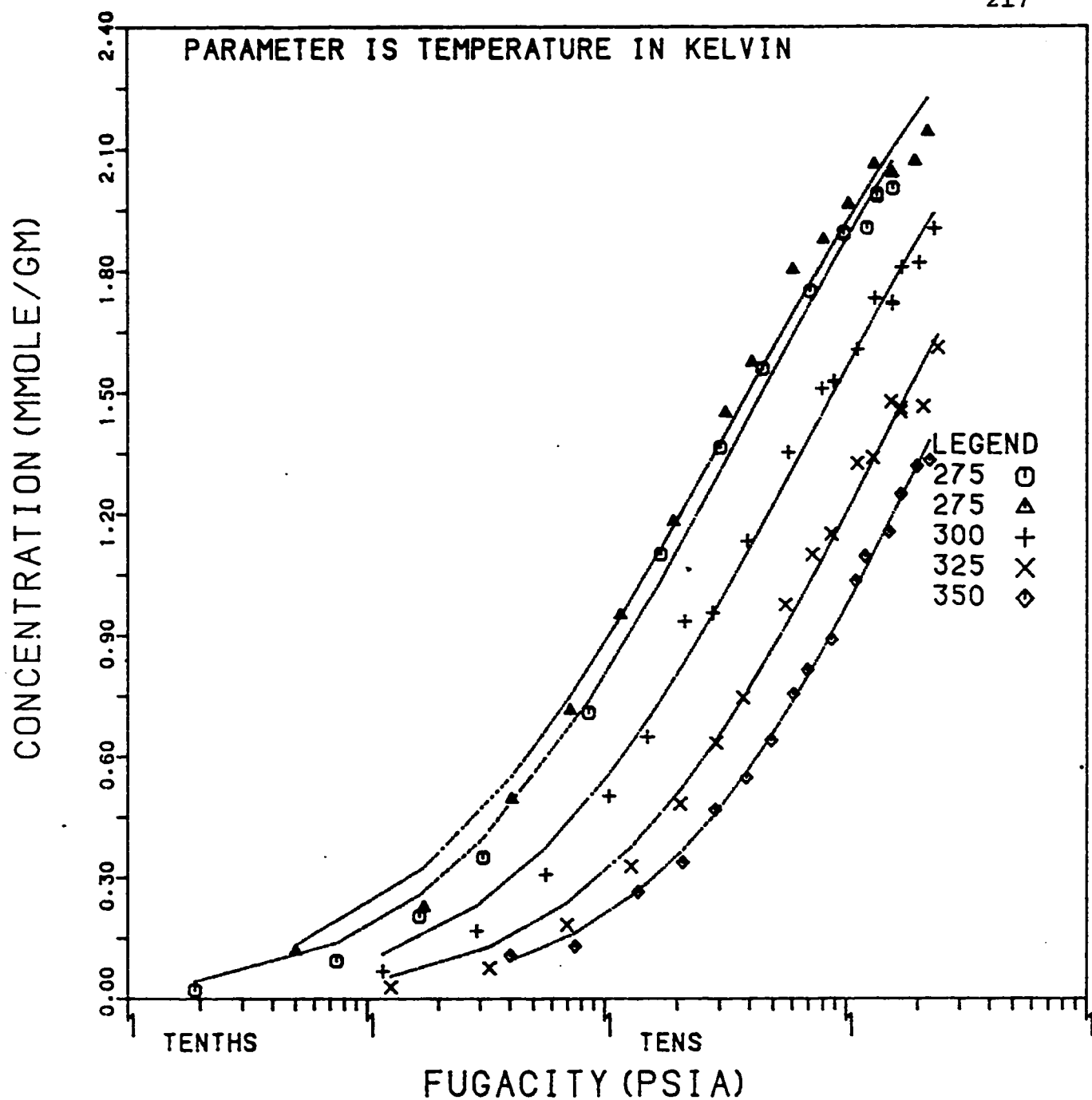


Fig. 5.50: Methane Isotherms on Linde S-115 Pellets: Fit of Jaroniec Model With Theoretical N_0 and Optimized K .

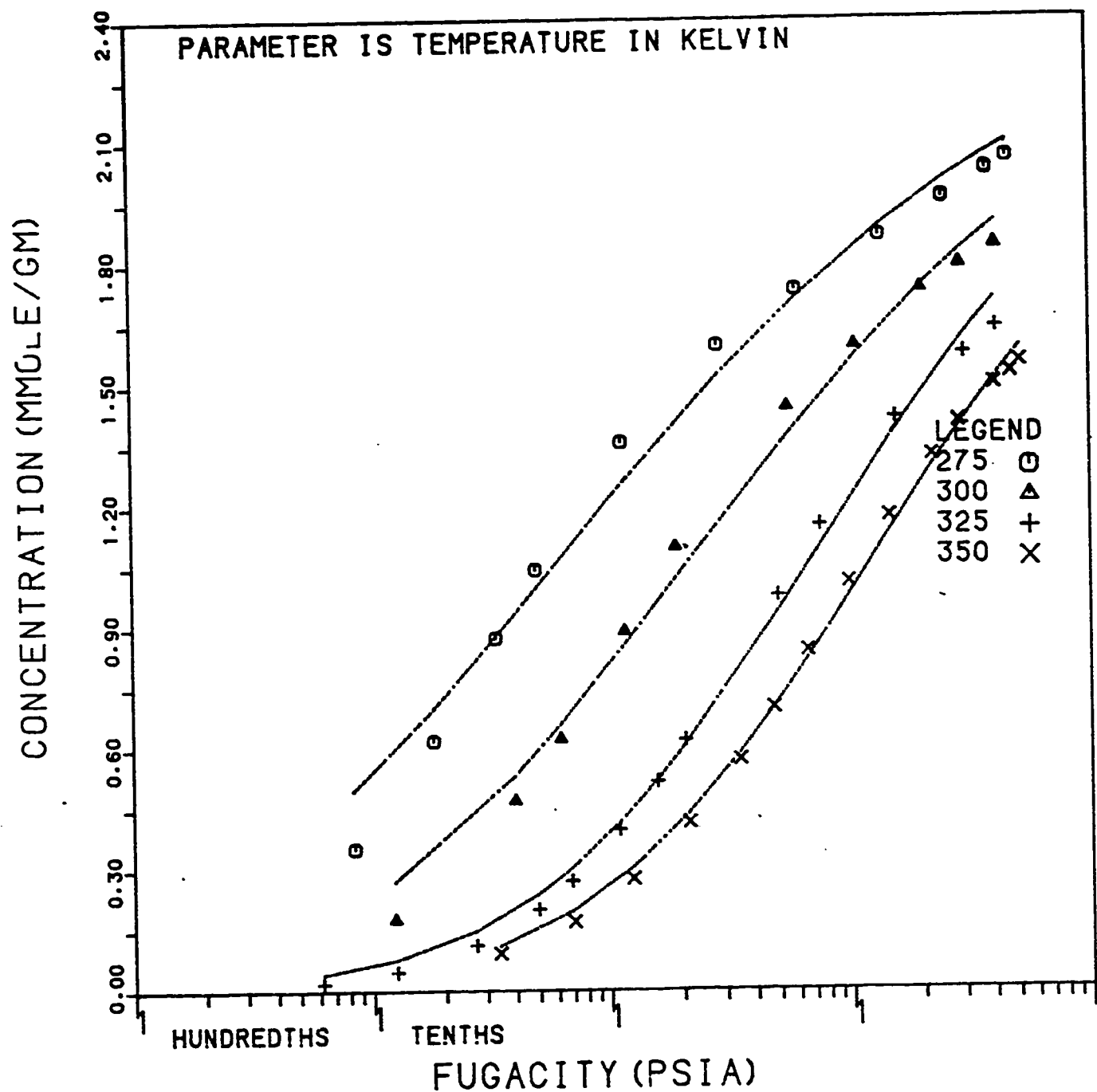


Fig. 5.51: Ethane Isotherms on Linde S-115 Pellets: Fit of Jaroniec Model With Theoretical N_0 and optimized K .

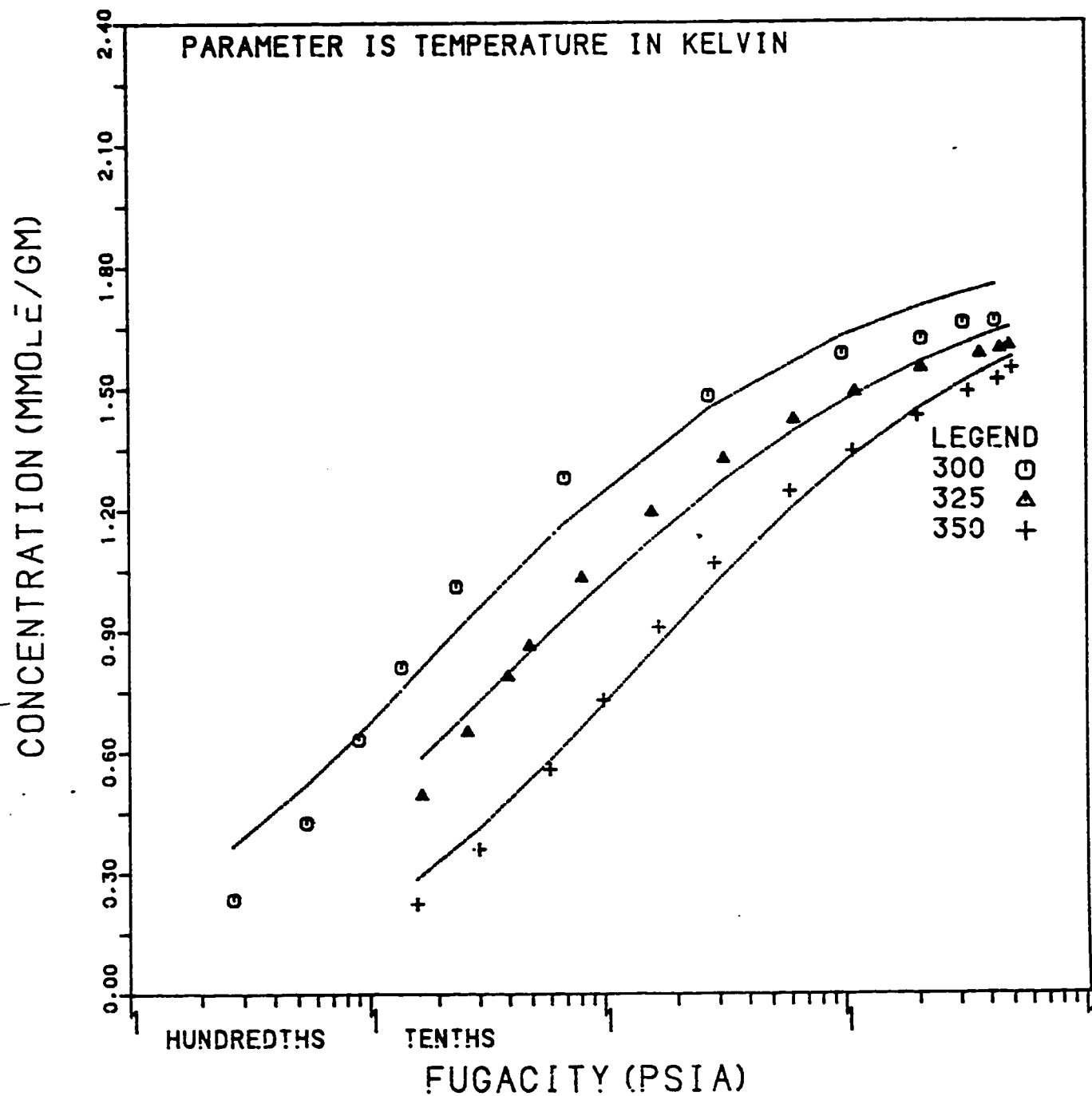


Fig. 5.52: Propane Isotherms on Linde S-115 Pellets: Fit of Jaroniec Model With Theoretical N_0 and optimized K .

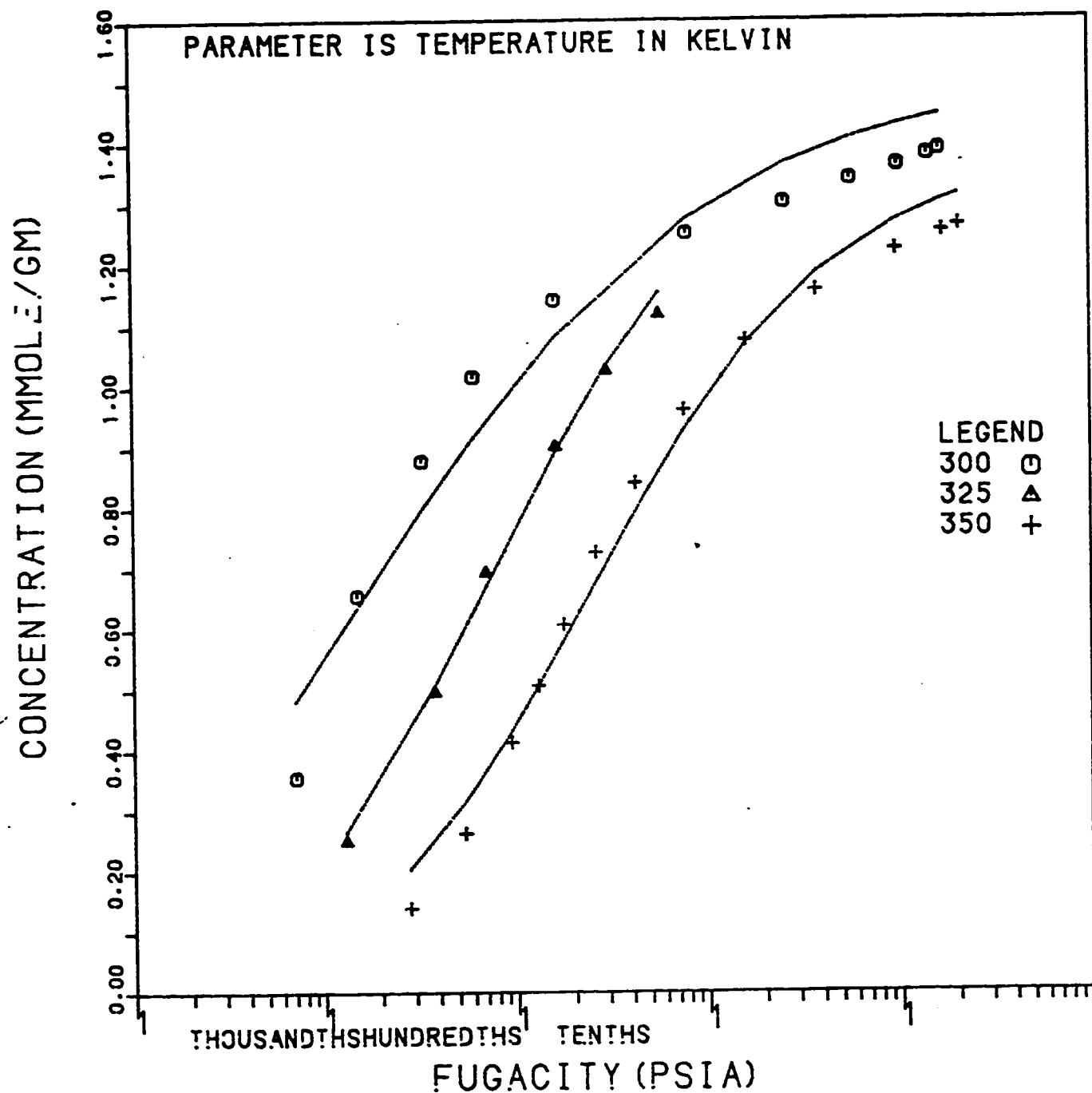


Fig. 5.53: n-Butane Isotherms on Linde S-115 Pellets: Fit of Jaroniec Model With Theoretical N_0 and optimized K .

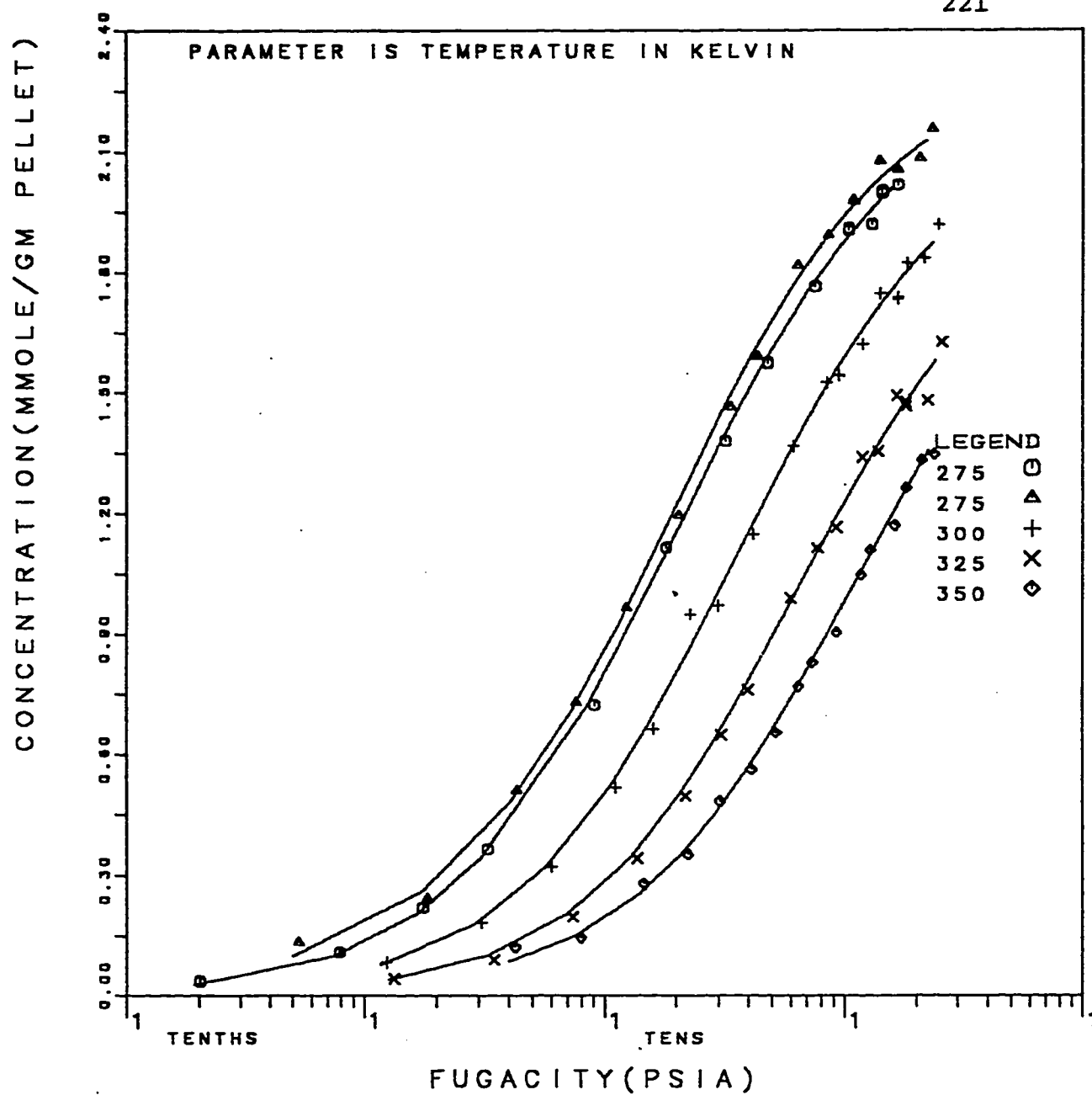


Fig. 5.54: Methane Isotherms on Linde S-115 Pellets: Fit of Jaroniec Model With Optimized N_0 and K .

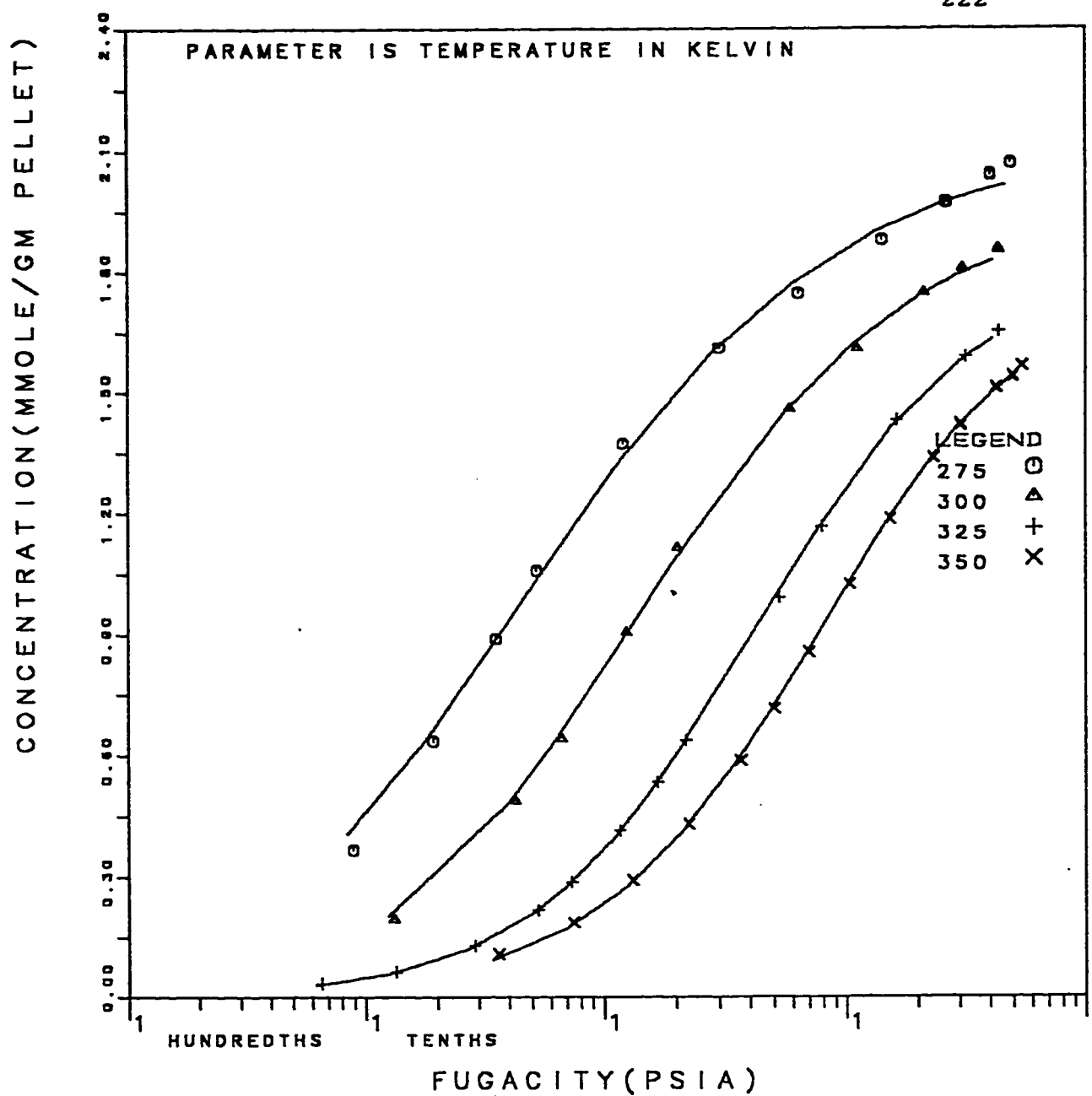


Fig. 5.55: Ethane Isotherms on Linde S-115 Pellets: Fit of Jaroniec Model With Optimized N_0 and K .

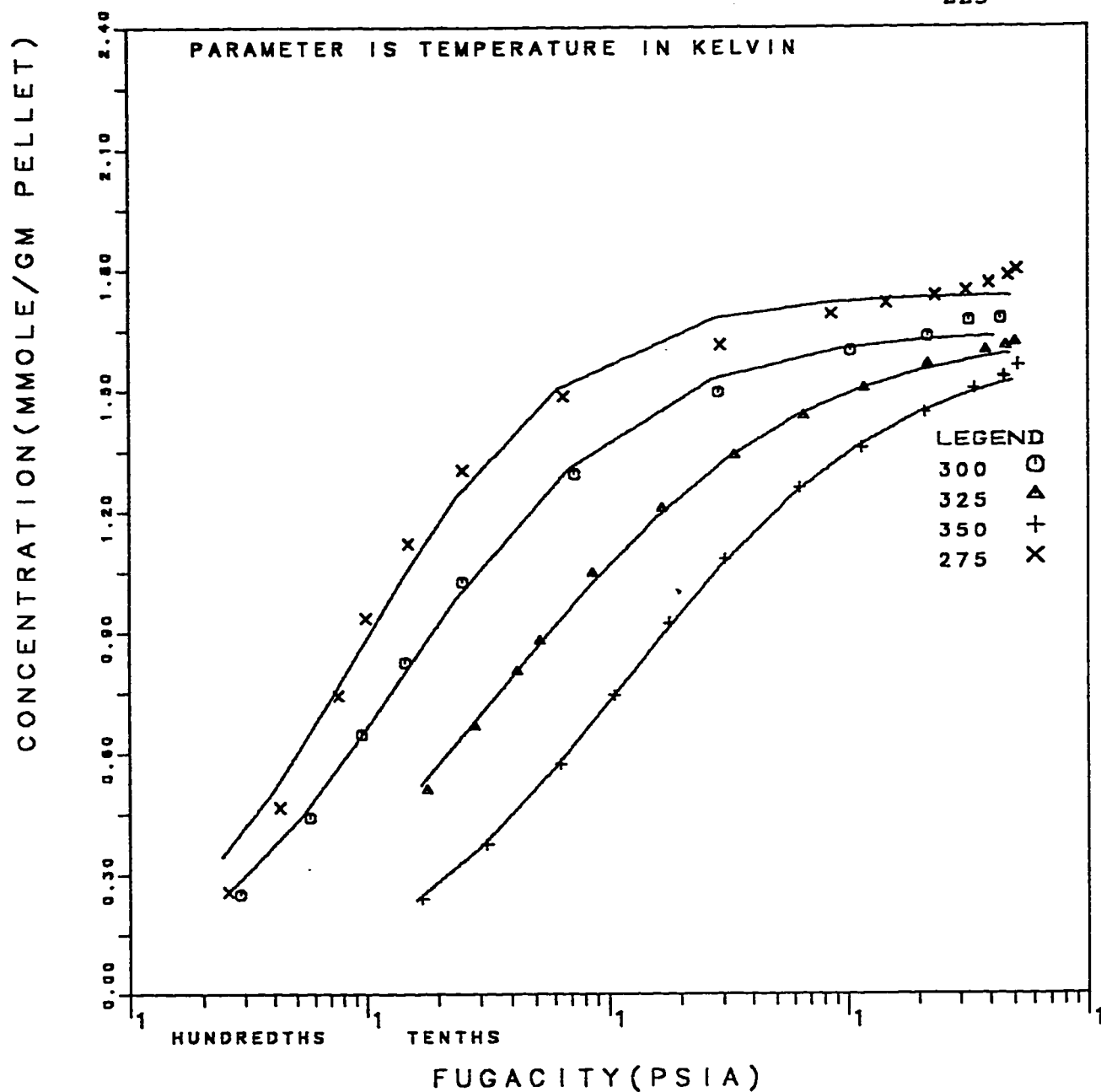


Fig. 5.56: Propane Isotherms on Linde S-115 Pellets: Fit of Jaroniec Model With Optimized N_0 and K .

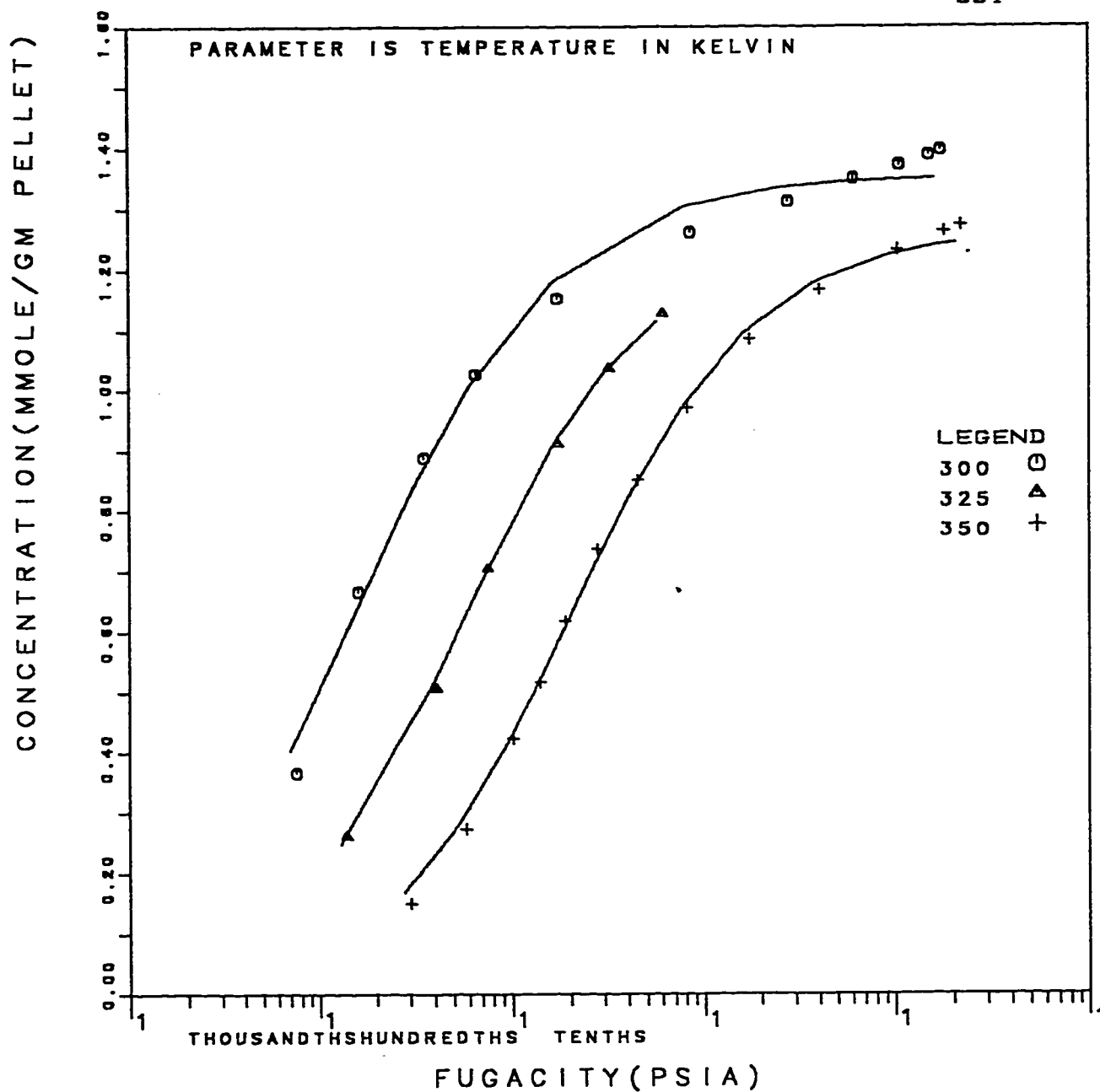


Fig. 5.57: n-Butane Isotherms on Linde S-115 Pellets: Fit of Jaroniec Model With Optimized N_0 and K .

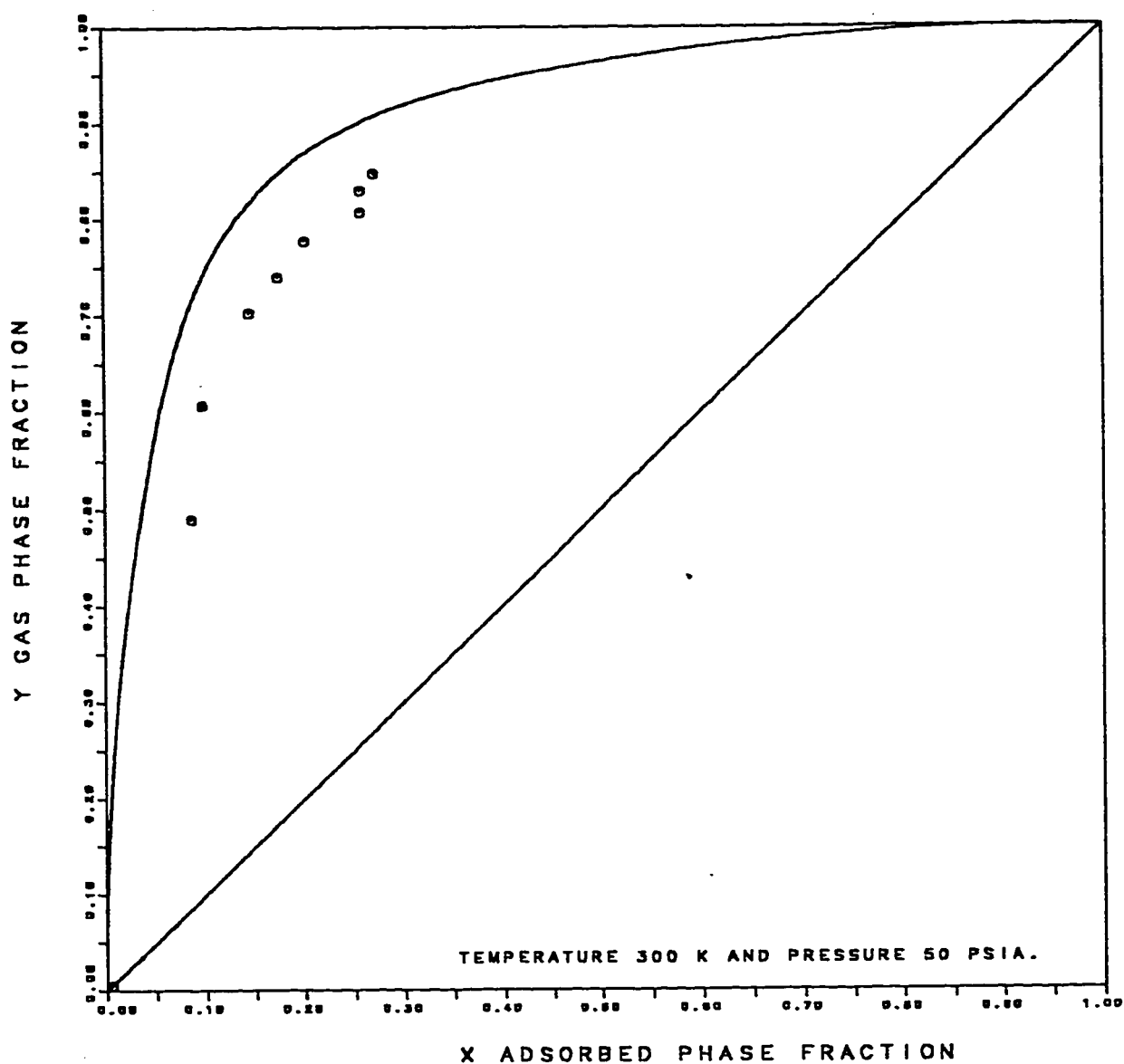


Fig. 5.58: X-Y Plot of Methane-Ethane Binary on Linde S-115 Pellets: Fit of Toth Model With Optimized N_0 and Intrinsic K at 50.00 Psia.

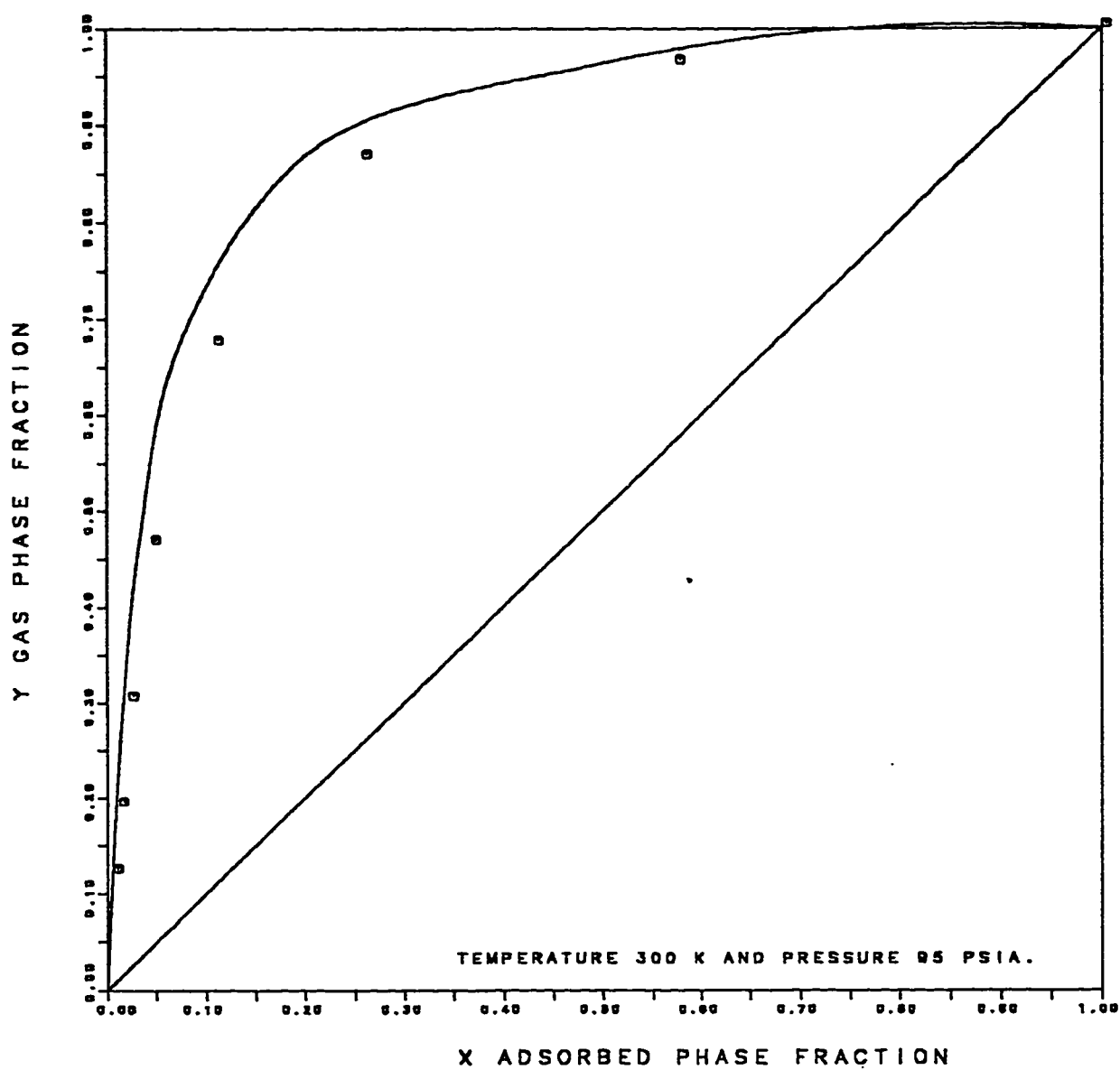


Fig. 5.59: X-Y Plot of Methane-Ethane Binary on Linde S-115 Pellets: Fit of Toth Model With Optimized N_0 and Intrinsic K at 95.00 psia.

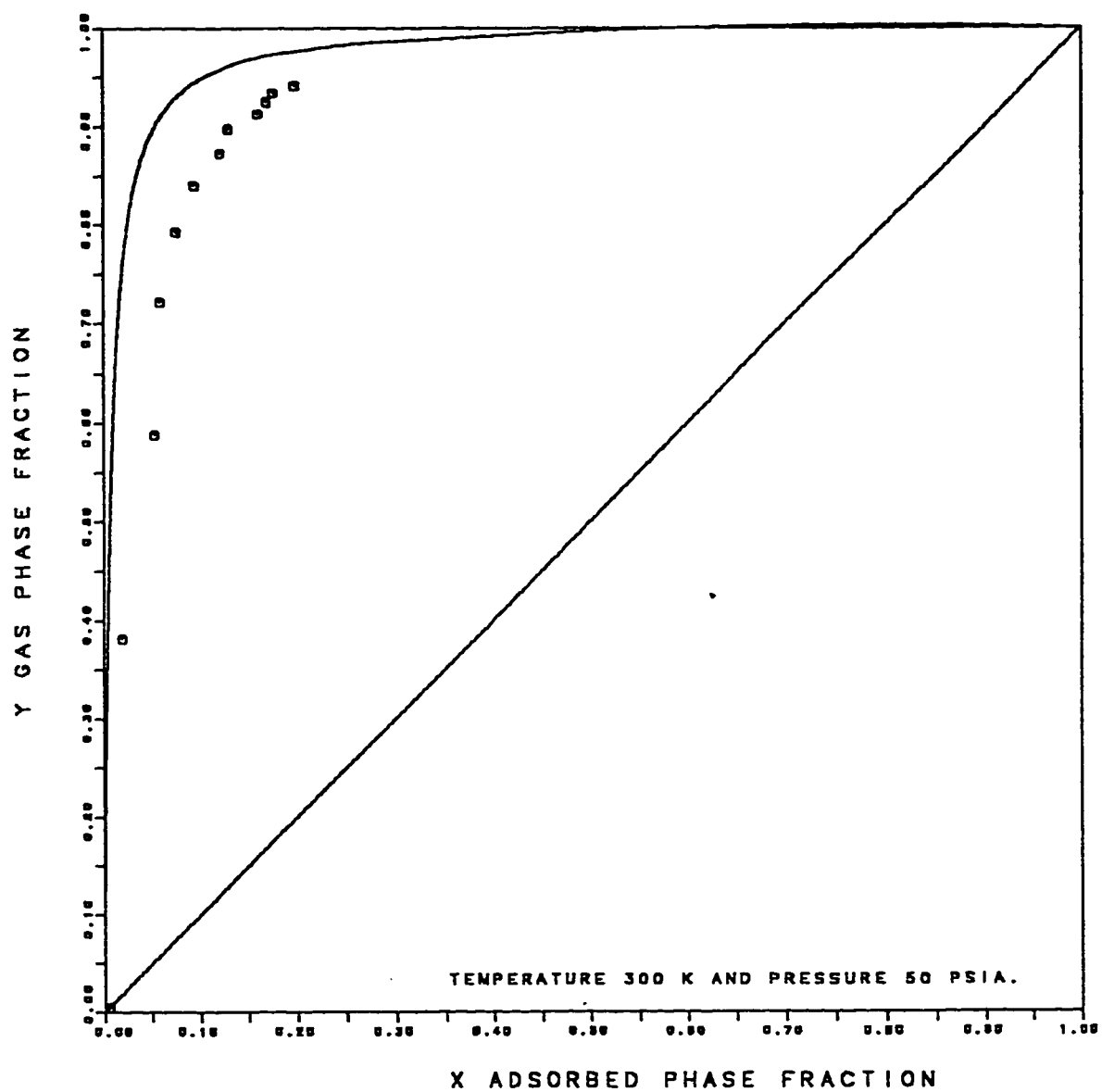


Fig. 5.60: X-Y Plot of Methane-Propane Binary on Linde S-115 Pellets: Fit of Toth Model With Optimized N_0 and Intrinsic K .

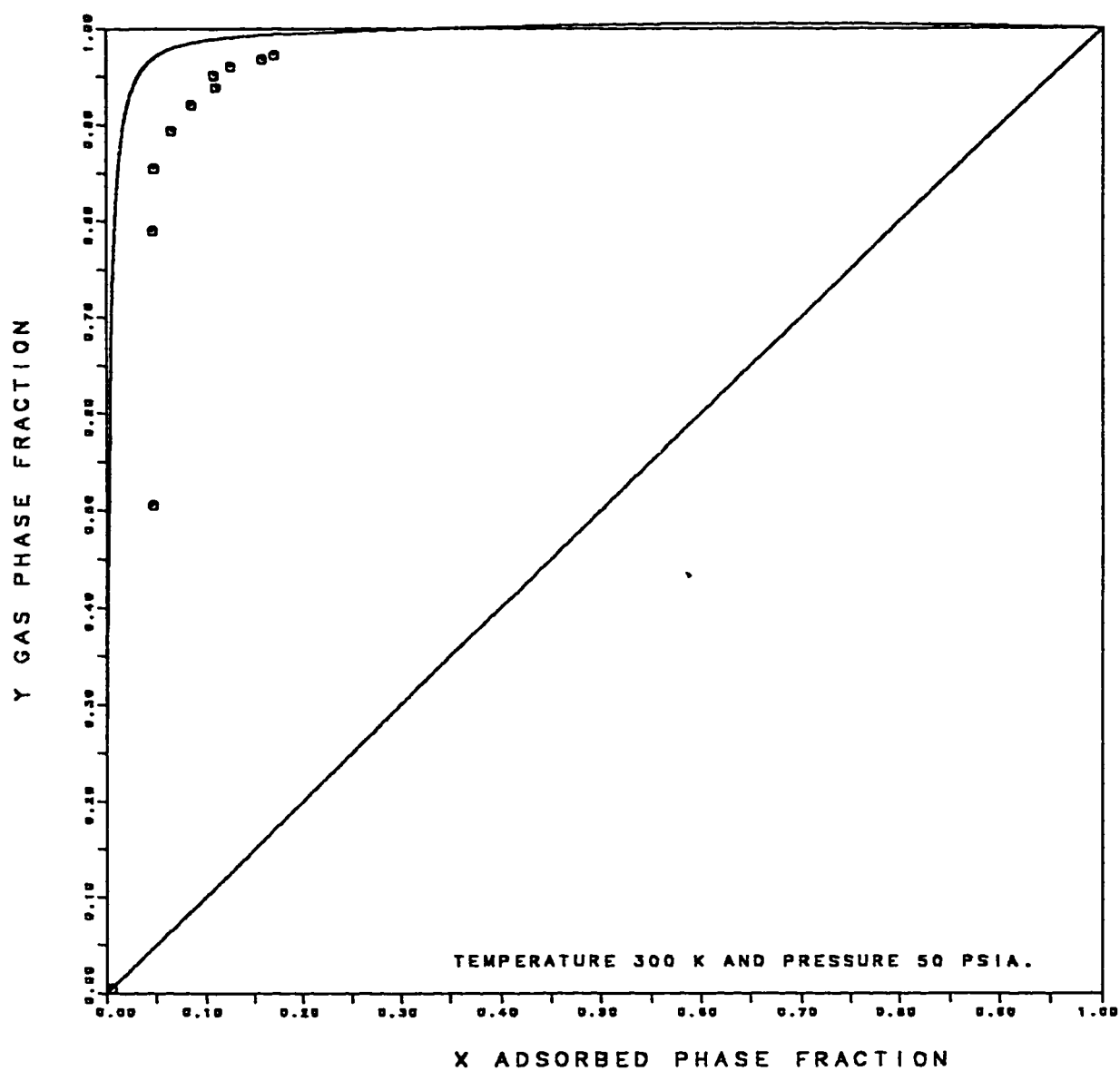


Fig. 5.61: X-Y Plot of Methane-n-Butane Binary on Linde S-115 Pellets:
Fit of Toth Model With Optimized N_0 and Intrinsic K .

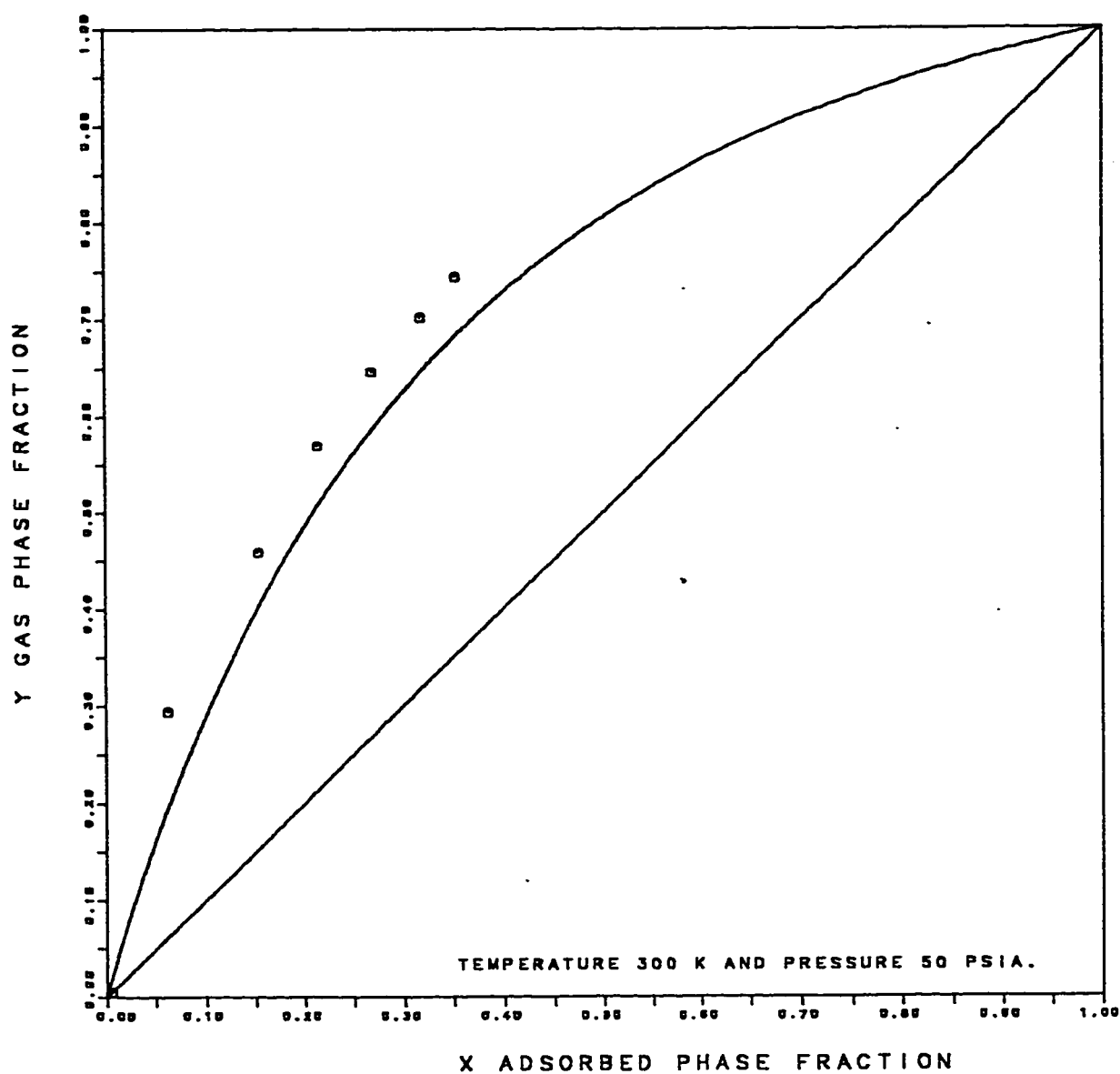


Fig. 5.62: X-Y Plot of Ethane-Propane Binary on Linde S-115 Pellets: Fit of Toth Model With Optimized N_0 and Intrinsic K .

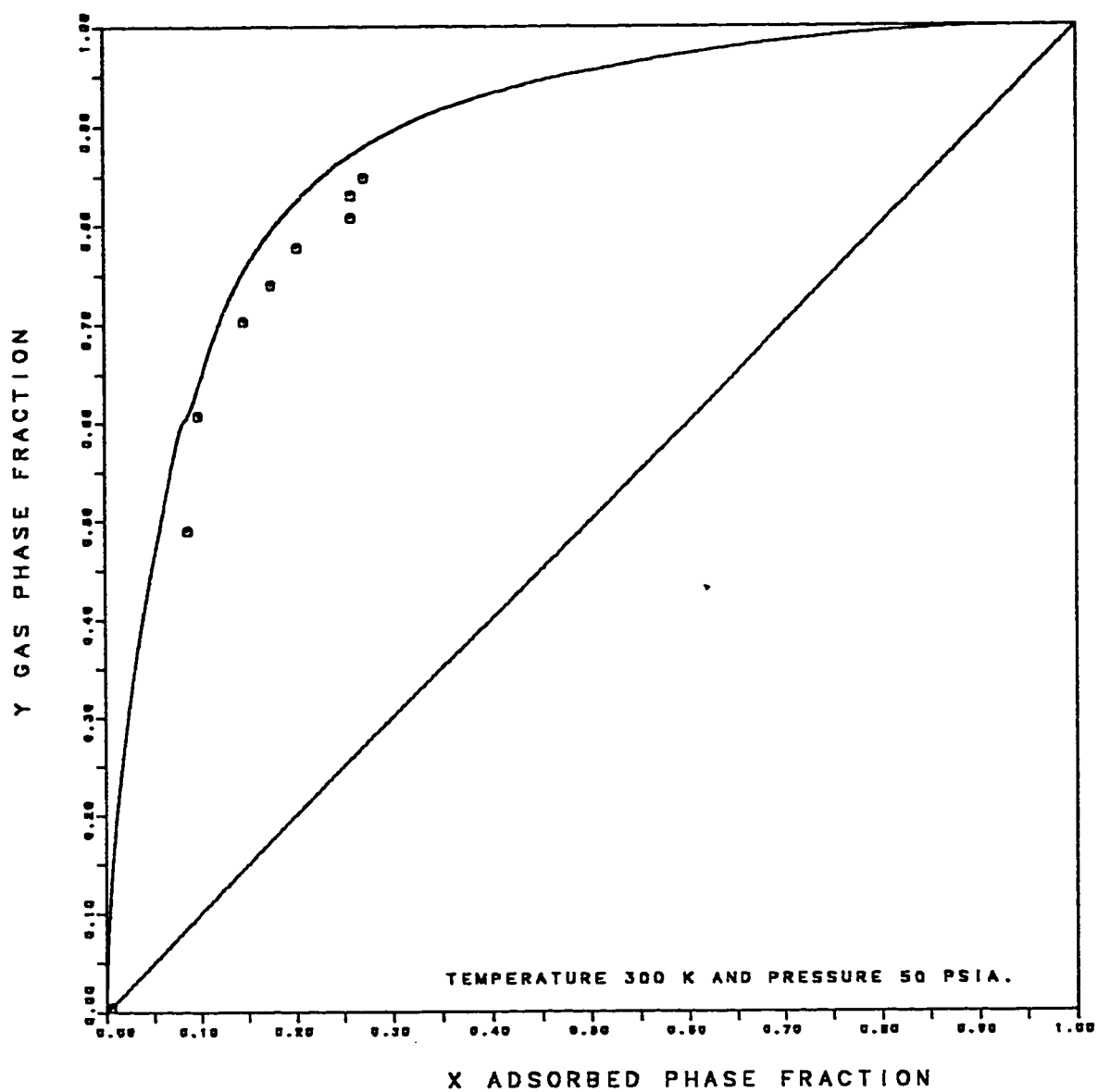


Fig. 5.63: X-Y Plot of Methane-Ethane Binary on Linde S-115 Pellets: Fit of Toth Model With Optimized N_0 and K .

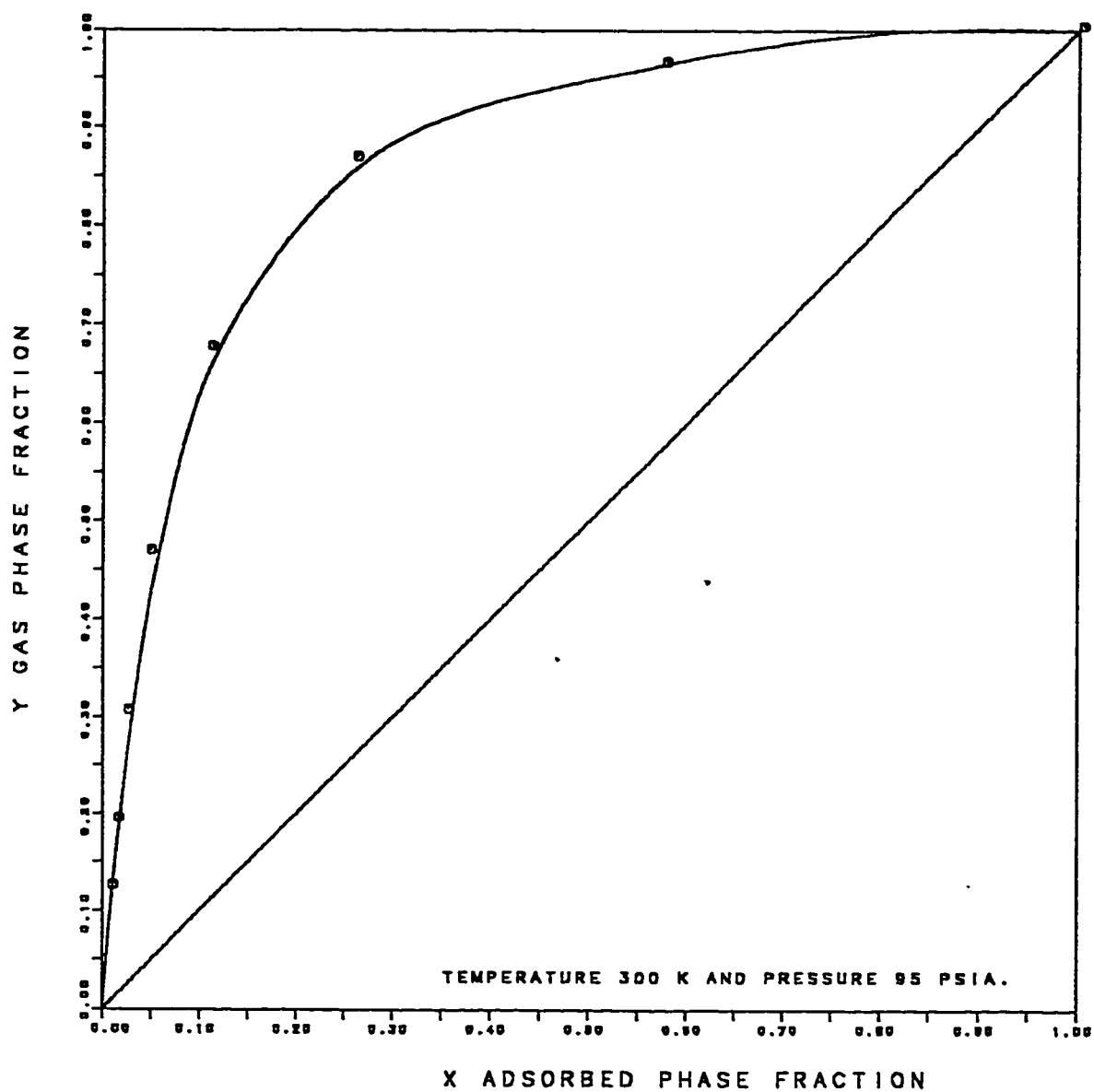


Fig. 5.64: X-Y Plot of Methane-Ethane Binary on Linde S-115 Pellets: Fit of Toth Model With Optimized N_0 and K .

CHAPTER 6

PURE AND MULTICOMPONENT EQUILIBRIUM RESULTS ON LINDE 13X PELLETS.

Pure component equilibrium adsorption data was measured for methane (up to 200 psia) and propane (up to 50 psia) at 275, 300, 325 and 350 °K. No pure component measurements were made for ethane and n-butane as the gas cylinders had been expended.

The data was analysed using the Soave-Redlich-Kwong equation of state and the intrinsic Henry constants determined using Barrer and Lee's virial equation by plotting $\ln(f/C)$ versus C as in Figures 6.1 and 6.2, respectively. The heat of adsorption ($-\Delta U$) and the pre-exponential factor (K'_0) were calculated from the Van't Hoff plot (Figure 6.3), and the results are presented in Table 6.1. The data is thermodynamically consistent, since all the isotherms when plotted as $d\ln C/d\ln f$ approaches 1 as f approaches zero. Also plotted in Figure 6.3 and tabulated in Table 6.1 are values reported in the literature for these sorbates and for ethane and n-butane where available. Note that in Table 6.1 the saturation concentration is calculated using the equation

$$N_o = 0.296 \times 0.8 \times p_{\text{adsorbate}} \quad (6.1)$$

where 0.296 is the large void fraction of the zeolite crystal.

6.1: Fit of the LRC Model For Linde 13X pellets:

Regression analysis for the three parameters K , N_o and n for the LRC model was performed for four cases:

- a) Using intrinsic K , theoretical N_o and optimising n only. Analysis results are reported in Table 6.2.
- b) Using intrinsic K and optimizing N_o and n only. Analysis results are reported in Table 6.3.
- c) Using theoretical N_o and optimising K and n only. Analysis results are reported in Table 6.4. and
- d) Optimizing K , N_o , and n . Analysis results are reported in Table 6.5.

From a study of the sum of least squares in each Table, only case (d) was good for both methane and propane. However the optimized K values for propane are approximately twice the intrinsic values and for methane there appears to be a curious interaction between the parameters N_o and n , i.e. when N_o is high (≈ 4.6), n is high (≈ 1.03) but when N_o is low (≈ 3.7), n is low (≈ 0.95). This effect is not observed for case (c) for methane where the sum of least squares is

still acceptable, the fit is good (see Figure 6.4) and the optimized Equilibrium constants are close to the intrinsic values. It is recommended that these values be used for methane. For propane however this case is not acceptable (see Figure 6.5). Accordingly it is recommended that case (d) values be employed i.e optimized K , N_0 and n , even though the optimized K values are twice the intrinsic and optimized N_0 values are approximately 80% of theoretical value. The fit is shown in Figure 6.6. The difference of optimized to intrinsic Equilibrium constant for propane suggests that the LRC model is not a good representation for this system.

6.2: Fit of The Toth Model to Linde 13X pellets:

Regression was performed for the Toth model for cases a, b, c and d as reported for the LRC model in section 6.1. The results of the regression analysis are presented in Tables 6.6 to 6.9 inclusive.

Excluding the 275 °K isotherm the fit for the methane isotherms was reasonable in all cases but was best for cases (c) and (d). As there is negligible difference between the fits in these two cases, it is recommended that the data be modeled using theoretical N_0 values and optimized K and n values. The optimized K values are approximately 10% higher than the intrinsic K with the exception of the 275 °K isotherm

where the optimized values is 46% higher. The fit for methane is shown in Figure 6.7.

However the fit for propane was only reasonable for case (d) i.e. when K , N_0 and n are all optimized, the results of which are presented in Table 6.9 and shown in Figure 6.8. As for the LRC model the optimized K values are double the intrinsic, and the optimized N_0 values are approximately 80% of the theoretical. The large difference between intrinsic and optimised K suggests this model is not the best.

The parameter n for both methane and propane is approximately 0.9, which means that the energy distribution is towards the left-hand side.

6.3: *Fit of Mathews and Weber Model to Linde 13X Pellets:*

Regression was performed for the Mathews and Weber model for cases a, b, c and d as reported for the LRC model in section 6.1. The results of the regression analysis are presented in Tables 6.10 to 6.13 inclusive.

The fit of the methane isotherm was reasonable for the four cases. Accordingly it is recommended that the model be calculated using intrinsic K , theoretical N_0 and optimised n the values for which are pre-

sented in Table 6.10. The isotherms fit for this case is shown in Figure 6.9. The results indicate that n may be slightly temperature increasing as the temperature increases.

Again however the fit for propane data was only reasonable for case (d) i.e. when K , N_0 and n are all optimized, the results of which are presented in Table 6.13 and shown in Figure 6.10. The optimized Henry constant K values are approximately 225% of the intrinsic, those for N_0 approximately 73% of theoretical, and the parameter n is approximately 1.02. The greater differences of K and N_0 in this model, in comparison to the LRC or Toth models for propane suggests that this model is the least attractive of the three looked at for this system. Conversely for methane it appears to be the best.

6.4: Fit of Jaroniec Model to Linde 13X Pellets:

This is a four parameter model (K , N_0 , n and m) in comparison to the three previous models which all involved three parameters only (K , N_0 and n). A similar four case regression was performed as for the other models, the results of which are presented in Tables 6.14 to 6.17 inclusive. The fit for the methane isotherms was reasonable for all four cases. Accordingly it is recommended that the model be calculated using intrinsic K , theoretical N_0 and optimized n and m , the values for

which are presented in Table 6.14. The isotherm fit for this case is shown in Figure 6.11. The results indicate that the parameters n and m may be slightly temperature dependent.

The fit for propane is clearly best using case (d) in which all four parameters (K , N_0 , n and m) are optimized as may be observed in Figure 6.13. However the optimized K values are 14 times greater than the intrinsic K and this is unacceptable. Case (c) where K is also optimized behaves in a similar manner. This strongly suggests that the parameters n and m are affecting the value of K . Accordingly it is recommended that this isotherm be calculated using intrinsic K values only. The remaining parameters can be optimized. The best results are achieved for case (b) (intrinsic K , optimized N_0 , m and n), the results of which are given in Table 6.15, and are shown in Figure 6.12. The fit is obviously not as good as in Figure 6.13 but the values used are more soundly physically based. The optimized N_0 values are approximately 80% of theoretical, and the parameters n and m are approximately 1.08 and 0.71 respectively.

The use of a 4th parameter does not appear to improve the fit in comparison to the three parameter models (LRC, Toth and Mathews & Weber) and hence its use does not appear warranted.

6.5: Fit of Ruthven Model To Linde 13X pellets:

The Ruthven model was applied to the data using theoretical β and intrinsic K' , but was found not to fit both methane and propane satisfactorily. In order to fit the model the K' was optimized using theoretical β and the fit of the model was somewhat reasonable for propane (see Figure 6.14) but the value of optimized K' was almost three times greater than the intrinsic value. For methane the fit was not satisfactory as may be observed from the sum of least squares in Table 5.18.

When both the parameters β and K' are optimized the fit of the model was good for methane and also reasonable for propane. The value of β was 97% of theoretical value for propane and for methane it is about 73% of theoretical value. But the value of optimized K' was again almost three times that of the intrinsic value for propane and for methane it is about 10% higher than the intrinsic value. For propane it can be observed from Figure 6.16 that because of the higher value of K' the fit of the model was not good at lower concentrations. Hence this model is not good for propane.

6.6: Fit of Multicomponent Ruthven Model To Linde 13X pellets:

The multicomponent Ruthven model described in section (4.7) is used to fit the multicomponent data, using intrinsic Henry constant and theoretical β . Since we did not measure the ethane and n-butane isot-

herm, the intrinsic Henry constant is used from literature for these two sorbates (1,2). It was found that with the intrinsic Henry constant the model does not fit the data as observed from the binary plots (Figures 6.16 to 6.20)

Hence it was decided to use the optimized Henry constant obtained from the regression of pure component data for methane, ethane, and propane and for n-butane it is obtained from the regression of multi-component data. The binary data analysed using these values are plotted in Figures 6.16 to 6.20 and are given in Tables 6.20 to 6.23.

The ternary and quarternary data are analysed using the optimized Henry constant and are given in Tables 6.24 to 6.31. It may be observed from these Tables that the fit of the model was good for methane-ethane binary and methane-ethane-propane ternary, and satisfactory for methane-propane binary and other ternary and quarternary equilibrium adsorption data.

Table 6.1 : Intrinsic Henry Constant (K'), Theoretical Saturation Concentration (N_O), Pre-exponential Factor (K'_O) And Heat Of Adsorption ($-\Delta U_O$) For Linde 13X Pellets.

Component	T Degrees Kelvin	N_O mmoles/gm pellet	K' (mmoles/gm pellet/psia)	K'_O	$-\Delta U_O$ Kcal/mole
Methane	275.00(a)	4.874	0.0758	4.266×10^{-5}	4.020
	300.00(a)	4.708	0.0377		
	325.00(a)	4.551	0.0227		
	350.00(a)	4.405	0.0258		
Ethane	323.00(b)		0.1786	4.242×10^{-5}	5.374
	373.00(b)		0.0629		
	423.00(b)		0.0245		
Propane	275.00(a)	3.009	22.6200	1.211×10^{-5}	7.860
	300.00(a)	2.952	5.7700		
	325.00(a)	2.898	2.3200		
	350.00(a)	2.845	1.0160		
	348.00(c)		1.5336	2.238×10^{-5}	7.696
	423.00(c)		0.2106		
	498.00(c)		0.0526		
n-Butane	348.00(c)		15.8332	3.620×10^{-6}	10.612
	423.00(c)		1.2473		
	498.00(c)		0.1517		

(a) This work, (b) Reference (2) and (c) Reference (1)

Table 6.2 : Optimised Parameters Of LRC Model (Intrinsic K & Theoretical N_O) For Linde 13X Pellets.

Component	T Temperature Degrees Kelvin	Saturation mmoles/gm pellet	N_O Conc mmoles/gm pellet	K Equilibrium Constant (1/(psia))	n Parameter	Sum of Least Squares
Methane	275.00	4.874		0.0155	1.1908	0.6025
	300.00	4.708		0.0080	1.0357	0.0336
	325.00	4.551		0.0050	1.0196	0.0078
	350.00	4.405		0.0036	1.0214	0.0109
Propane	275.00	3.009		7.5164	2.0587	0.7559
	300.00	2.952		1.9543	1.8794	0.6783
	325.00	2.898		0.8006	1.6681	0.4096
	350.00	2.845		0.3571	1.7564	0.5388

Table 6.3 : Optimised Parameters Of LRC Model (Intrinsic K) For Linde 13X Pellets.

Component	T Temperature Degrees Kelvin	Saturation mmoles/gm pellet	N_O Conc mmoles/gm pellet	K Equilibrium Constant (1/(psia))	n Parameter	Sum of Least Squares
Methane	275.00	4.399		0.0155	1.1069	0.2034
	300.00	4.607		0.0080	1.0405	0.0040
	325.00	4.376		0.0050	1.0264	0.0268
	350.00	4.327		0.0036	1.0194	0.0016
Propane	275.00	2.799		7.5164	1.6244	0.5599
	300.00	2.626		1.9543	1.4135	0.3807
	325.00	2.620		0.8006	1.4869	0.2060
	350.00	2.491		0.3571	1.4398	0.1128

Table 6.4 : Optimised Parameters Of LRC Model (Theoretical N_o) For Linde 13X Pellets.

Component	T Temperature Degrees Kelvin	N_o Saturation mmoles/gm pellet	K Equilibrium Constant (1/(psia))	n Parameter	Sum of Least Squares
Methane	275.00	4.874	0.0132	1.2112	0.1553
	300.00	4.708	0.0077	1.0537	0.0041
	325.00	4.551	0.0049	1.0404	0.0039
	350.00	4.405	0.0034	1.0254	0.0014
Propane	275.00	3.009	7.7970	1.8860	0.7991
	300.00	2.952	1.5004	1.8936	0.5559
	325.00	2.898	0.6125	1.7556	0.2744
	350.00	2.845	0.2331	1.8032	0.1966

Table 6.5 : Optimised Parameters (N_o , K & n) Of LRC Model For Linde 13X Pellets.

Component	T Temperature Degrees Kelvin	N_o Saturation mmoles/gm pellet	K Equilibrium Constant (1/(psia))	n Parameter	Sum of Least Squares
Methane	275.00	3.687	0.0257	0.8818	0.0139
	300.00	4.623	0.0080	1.0427	0.0039
	325.00	3.793	0.0069	0.9563	0.0008
	350.00	4.476	0.0034	1.0304	0.0014
Propane	275.00	2.546	14.4950	1.0339	0.1512
	300.00	2.417	3.6600	1.0432	0.0703
	325.00	2.218	1.6410	0.9817	0.0255
	350.00	2.197	0.6190	1.0700	0.0167

Table 6.6 : Optimised Parameters Of Toth Model (Intrinsic K & Theoretical N_0) For Linde 13X Pellets.

Component	T Temperature Degrees Kelvin	N_0 Saturation Conc mmoles/gm pellet	K Equilibrium Constant (1/(psia))	n Parameter	Sum of Least Squares
Methane	275.00	4.874	0.0155	0.8885	0.3016
	300.00	4.708	0.0080	0.9739	0.0144
	325.00	4.551	0.0050	0.9929	0.0102
	350.00	4.405	0.0036	0.9819	0.0022
Propane	275.00	3.009	7.5164	0.9104	2.0480
	300.00	2.952	1.9543	0.7531	1.7011
	325.00	2.898	0.8006	0.7830	1.0228
	350.00	2.845	0.3571	0.7113	0.8155

Table 6.7 : Optimised Parameters Of Toth Model (Intrinsic K) For Linde 13X Pellets.

Component	T Temperature Degrees Kelvin	N_0 Saturation Conc mmoles/gm pellet	K Equilibrium Constant (1/(psia))	n Parameter	Sum of Least Squares
Methane	275.00	4.484	0.0155	1.0000	0.2702
	300.00	4.708	0.0080	0.9736	0.0144
	325.00	4.551	0.0050	0.9930	0.0102
	350.00	4.405	0.0036	0.9817	0.0022
Propane	275.00	2.529	7.5164	1.6050	0.5538
	300.00	2.384	1.9543	1.5360	0.4446
	325.00	2.182	0.8006	1.7670	0.3502
	350.00	2.116	0.3571	1.5190	0.2295

Table 6.8 : Optimised Parameters Of Toth Model (Theoretical N_0) For Linde 13X Pellets.

Component	T Temperature Degrees Kelvin	N_0 Saturation mmoles/gm pellet	K Equilibrium Constant (1/(psia))	n Parameter	Sum of Least Squares
Methane	275.00	4.874	0.0227	0.7392	0.1102
	300.00	4.708	0.0088	0.9126	0.0038
	325.00	4.551	0.0055	0.9167	0.0024
	350.00	4.405	0.0037	0.9469	0.0015
Propane	275.00	3.009	94.6900	0.4201	0.5662
	300.00	2.952	14.8511	0.4514	0.3924
	325.00	2.898	4.3980	0.4826	0.1883
	350.00	2.845	1.9292	0.4682	0.1228

Table 6.9 : Optimised Parameters (N_0 , K & n) Of Toth Model For Linde 13X Pellets.

Component	T Temperature Degrees Kelvin	N_0 Saturation mmoles/gm pellet	K Equilibrium Constant (1/(psia))	n Parameter	Sum of Least Squares
Methane	275.00	4.500	0.0221	0.8284	0.0789
	300.00	4.988	0.0086	0.8577	0.0035
	325.00	4.500	0.0055	0.9256	0.0023
	350.00	4.567	0.0036	0.9221	0.0015
Propane	275.00	2.559	16.6520	0.9050	0.1458
	300.00	2.433	4.2270	0.8996	0.0652
	325.00	2.236	1.6520	0.9812	0.0256
	350.00	2.222	0.7495	0.8730	0.0141

Table 6.10: Optimised Parameters Of Mathews And Weber Model (Intrinsic K & Theoretical N_0) For Linde 13X Pellets.

Component	T Temperature Degrees Kelvin	N_0 Saturation Conc mmoles/gm pellet	K Equilibrium Constant (1/(psia))	n Parameter	Sum of Least Squares
Methane	275.00	4.874	0.0155	0.8523	0.0653
	300.00	4.708	0.0080	0.9443	0.0286
	325.00	4.551	0.0050	0.9699	0.0100
	350.00	4.405	0.0036	1.0430	0.0030
Propane	275.00	3.009	7.5164	0.9872	1.1748
	300.00	2.952	1.9543	0.9732	0.8091
	325.00	2.898	0.8006	0.9395	0.3410
	350.00	2.845	0.3571	0.9332	0.3629

Table 6.11: Optimised Parameters Of Mathews And Weber Model (Intrinsic K) For Linde 13X Pellets.

Component	T Temperature Degrees Kelvin	N_0 Saturation Conc mmoles/gm pellet	K Equilibrium Constant (1/(psia))	n Parameter	Sum of Least Squares
Methane	275.00	4.702	0.0155	0.8788	0.0167
	300.00	4.624	0.0080	0.9414	0.0094
	325.00	4.406	0.0050	0.8274	0.0025
	350.00	4.282	0.0036	0.9211	0.0023
Propane	275.00	2.871	7.5164	0.9779	0.7528
	300.00	2.772	1.9543	0.9672	0.4834
	325.00	2.843	0.8006	0.9214	0.2433
	350.00	2.616	0.3571	0.9379	0.1708

Table 6.12: Optimised Parameters Of Mathews And Weber Model (Theoretical N_O) For Linde 13X Pellets.

Component	T Temperature Degrees Kelvin	N_O Saturation Conc mmoles/gm pellet	K Equilibrium Constant (1/(psia))	n Parameter	Sum of Least Squares
Methane	275.00	4.874	0.0147	0.8505	0.0189
	300.00	4.708	0.0079	0.9322	0.0168
	325.00	4.551	0.0048	0.8467	0.0061
	350.00	4.405	0.0036	1.0243	0.0029
Propane	275.00	3.009	10.4500	0.9716	0.4603
	300.00	2.952	2.3952	0.9510	0.3393
	325.00	2.898	0.9448	0.9147	0.1652
	350.00	2.845	0.3663	0.9101	0.1896

Table 6.13: Optimised Parameters (N_O , K & n) Of Mathews And Weber Model For Linde 13X Pellets.

Component	T Temperature Degrees Kelvin	N_O Saturation Conc mmoles/gm pellet	K Equilibrium Constant (1/(psia))	n Parameter	Sum of Least Squares
Methane	275.00	4.603	0.0165	0.8950	0.0132
	300.00	3.971	0.0106	1.0988	0.0033
	325.00	4.236	0.0055	0.9217	0.0010
	350.00	4.076	0.0040	1.0523	0.0016
Propane	275.00	2.258	18.9440	1.0233	0.0977
	300.00	2.177	4.6087	1.0239	0.0450
	325.00	2.114	1.8041	1.0166	0.0226
	350.00	1.938	0.8153	1.0347	0.0092

Table 6.14: Optimised Parameters Of Jaroniec Model (Intrinsic K & Theoretical N_0) For Linde 13X Pellets.

Component	T Temperature Degrees Kelvin	N_0 Saturation conc mmoles/gm pellet	K Equilibrium Constant (1/(psia))	n Parameters	m	Sum of least squares
Methane	275.00	4.874	0.0155	0.7954	0.8786	0.1374
	300.00	4.708	0.0080	0.9348	0.9657	0.0039
	325.00	4.551	0.0050	0.9478	0.9702	0.0033
	350.00	4.405	0.0036	0.9610	0.9869	0.0015
Propane	275.00	3.009	7.5164	0.4773	0.5018	0.7224
	300.00	2.952	1.9543	0.5156	0.5739	0.5270
	325.00	2.898	0.8006	0.5533	0.6185	0.2575
	350.00	2.845	0.3571	0.5323	0.6288	0.1758

Table 6.15: Optimised Parameters Of Jaroniec Model (Intrinsic K) For Linde 13X Pellets.

Component	T Temperature Degrees Kelvin	N_0 Saturation conc mmoles/gm pellet	K Equilibrium Constant (1/(psia))	n Parameters	m	Sum of least squares
Methane	275.00	4.400	0.0155	0.9277	0.8762	0.0949
	300.00	4.708	0.0080	0.9289	0.9692	0.0082
	325.00	4.400	0.0050	0.9848	0.9616	0.0031
	350.00	4.400	0.0036	0.9623	0.9866	0.0015
Propane	275.00	2.547	7.5164	1.0910	0.7041	0.1950
	300.00	2.414	1.9543	1.0815	0.7176	0.1061
	325.00	2.206	0.8006	1.2184	0.7130	0.0525
	350.00	2.180	0.3571	1.0651	0.7285	0.0293

Table 6.16: Optimised Parameters Of Jaroniec Model (Theoretical N_0) For Linde 13X Pellets.

Component	T Temperature Degrees Kelvin	N_0 Saturation conc mmoles/gm pellet	K Equilibrium Constant (1/(psia))	n Parameters	m Parameters	Sum of least squares
Methane	275.00	4.874	0.0226	0.7406	1.0000	0.1103
	300.00	4.708	0.0088	0.9104	1.0000	0.0037
	325.00	4.551	0.0055	0.9152	1.0000	0.0030
	350.00	4.405	0.0033	0.9931	0.9627	0.0014
Propane	275.00	3.009	94.2640	0.4200	1.0000	0.5660
	300.00	2.952	14.9160	0.4510	1.0000	0.3924
	325.00	2.898	4.3940	0.4827	1.0000	0.1883
	350.00	2.845	1.9372	0.4678	1.0000	0.1227

Table 6.17: Optimised Parameters (N_0 , K & n) Of Jaroniec Model For Linde 13X Pellets.

Component	T Temperature Degrees Kelvin	N_0 Saturation conc mmoles/gm pellet	K Equilibrium Constant (1/(psia))	n Parameters	m Parameters	Sum of least squares
Methane	275.00	3.508	0.0186	1.3972	0.9540	0.0106
	300.00	4.708	0.0090	0.9053	1.0087	0.0038
	325.00	4.060	0.0075	0.9409	1.0978	0.0008
	350.00	3.000	0.0038	1.6096	0.8889	0.0010
Propane	275.00	2.575	97.1122	0.7655	2.5000	0.0988
	300.00	2.469	28.4807	0.7296	2.5000	0.0327
	325.00	2.300	10.7477	0.7567	2.5000	0.0075
	350.00	2.299	5.8956	0.6793	2.5000	0.0043

Table 6.18: Optimised Parameter K' (Theoretical β) Of Ruthven Model For Linde 13X Pellets.

Sorbate	T Temperature °K	β Molecular Volume $A \frac{v_3}{\text{molecule}}$	K' Henry Constant (molecules/cavity/psia)	Sum of least squares
Methane	275.00	80.67	0.3027	0.6087
	300.00	83.53	0.1437	0.5890
	325.00	86.40	0.0780	0.2416
	350.00	89.27	0.0497	0.1131
Propane	275.00	130.65	153.4740	0.2763
	300.00	133.16	34.2640	0.1765
	325.00	135.67	12.8140	0.0949
	350.00	138.19	5.0201	0.4743

Table 6.19: Optimised Parameters (β and K') Of Ruthven Model For Linde 13X Pellets.

Sorbate	T Temperature °K	β Molecular Volume $A \frac{v_3}{\text{molecule}}$	K' Henry Constant (molecules/cavity/psia)	Sum of least squares
Methane	275.00	63.92	0.2016	0.0757
	300.00	60.00	0.0928	0.0229
	325.00	60.00	0.0542	0.0078
	350.00	60.00	0.0350	0.0109
	(a)288.00	58-60	0.1081	
	(a)298.00	58-60	0.0831	
	(a)308.00	60-62	0.0649	
Propane	275.00	126.74	140.9800	0.2309
	300.00	129.01	31.3300	0.1572
	325.00	132.52	11.9610	0.0869
	350.00	135.89	4.7214	0.0417

(a) Reference (3)

TABLE 6.20: BINARY ADSORPTION OF METHANE & ETHANE ON LINDE 13X PELLETS

AT 300.00 DEGREE KELVIN AND 50.00 PSIA TOTAL PRESSURE.

PARTIAL PRESSURES		ETHANE PSIA		ADSORB PHASE CONCENTRATION AND MOLE FRACTION		THEORETICAL METHANE MOLE FRACTION		THEORETICAL ETHANE MOLE FRACTION	
METHANE PSIA	ETHANE PSIA	EXPERIMENTAL METHANE MMOLE/GM PELLETT	ETHANE MMOLE/GM PELLETT	THEORETICAL METHANE MMOLE/GM PELLETT	ETHANE MMOLE/GM PELLETT	EXPERIMENTAL METHANE MOLE FRACTION	ETHANE MOLE FRACTION	THEORETICAL METHANE MOLE FRACTION	ETHANE MOLE FRACTION
13.5623	36.9677	0.0820	2.6290	0.0624	2.4005	0.0302	0.9698	0.0253	0.9747
21.5294	28.6206	0.0920	2.5190	0.1182	2.2882	0.0352	0.9648	0.0491	0.9509
26.7850	23.2150	0.1830	2.4180	0.1692	2.1891	0.0704	0.9296	0.0717	0.9283
30.4124	19.4276	0.2300	2.3240	0.2157	2.1001	0.0901	0.9099	0.0932	0.9068
33.0888	16.6912	0.2510	2.2360	0.2585	2.0204	0.1009	0.8991	0.1134	0.8866
35.4209	14.7290	0.3230	2.1560	0.2987	1.9503	0.1303	0.8697	0.1328	0.8672
37.0275	13.1725	0.3600	2.0820	0.3339	1.8873	0.1474	0.8526	0.1503	0.8497
37.9786	11.9014	0.3980	2.0140	0.3639	1.8309	0.1650	0.8350	0.1658	0.8342
39.1450	10.8550	0.4310	1.9500	0.3954	1.7764	0.1810	0.8190	0.1821	0.8179
39.9200	9.9800	0.4310	1.8890	0.4230	1.7271	0.1858	0.8142	0.1967	0.8033

OPTIMIZED HENRY CONSTANT
(MOLECULES/CAVITY/PSIA)

HK1 HK2 HK3 HK4
0.1746 3.9565 46.468 822.000

MOLECULAR VOLUME

CUBIC ANGSTROM/MOLECULE
BETA1 BETA2 BETA3 BETA4
83.5344 105.1899 133.1647 167.4126

TABLE 6.21: BINARY ADSORPTION OF METHANE & ETHANE ON LINDE 13X PELLETS

AT 300.00 DEGREE KELVIN AND 95.00 PSIA TOTAL PRESSURE.

PARTIAL PRESSURES		ETHANE PSIA		ADSORB PHASE CONCENTRATION AND MOLE FRACTION		THEORETICAL METHANE MOLE FRACTION		THEORETICAL ETHANE MOLE FRACTION	
METHANE PSIA	ETHANE PSIA	EXPERIMENTAL METHANE MMOLE/GM PELLETT	ETHANE MMOLE/GM PELLETT	THEORETICAL METHANE MMOLE/GM PELLETT	ETHANE MMOLE/GM PELLETT	EXPERIMENTAL METHANE MOLE FRACTION	ETHANE MOLE FRACTION	THEORETICAL METHANE MOLE FRACTION	ETHANE MOLE FRACTION
29.6358	65.5642	0.0670	2.6210	0.0875	2.5192	0.0249	0.9751	0.0336	0.9664
47.3386	48.1214	0.1440	2.4820	0.1735	2.3830	0.0548	0.9452	0.0679	0.9321
58.4263	36.8236	0.2350	2.3520	0.2563	2.2540	0.0908	0.9092	0.1021	0.8979
65.9492	29.3807	0.3140	2.2310	0.3347	2.1357	0.1234	0.8766	0.1355	0.8645
70.2216	24.3784	0.3570	2.1170	0.4008	2.0349	0.1443	0.8557	0.1645	0.8355
75.0034	20.8966	0.4550	2.0100	0.4688	1.9408	0.1846	0.8154	0.1945	0.8055
77.0609	18.0291	0.5160	1.9170	0.5256	1.8557	0.2121	0.7879	0.2207	0.7793
78.9721	15.8779	0.5730	1.8300	0.5790	1.7787	0.2385	0.7615	0.2456	0.7544
80.8920	14.2079	0.6310	1.7500	0.6299	1.7081	0.2650	0.7350	0.2694	0.7306

TABLE 6.22: BINARY ADSORPTION OF METHANE & PROPANE ON LINDE 13X PELLETS

AT 300.00 DEGREE KELVIN AND 50.00 PSIA TOTAL PRESSURE.

OPTIMIZED HENRY CONSTANT (MOLECULES/GAVITY/PSIA)			
HK1	HK2	HK3	HK4
0.1746	3.9565	46.468	822.000
MOLECULAR VOLUME			
CUBIC ANGSTROM/MOLECULE			
BETA1	BETA2	BETA3	BETA4
83.5344	105.1899	133.1647	167.4126
ADSORB PHASE CONCENTRATION AND MOLE FRACTION			
EXPERIMENTAL		THEORETICAL	
METHANE PSIA	PROPANE PSIA	METHANE MMOLE/GM PELLETT	PROPANE MMOLE/GM PELLETT
16.7150	33.4350	0.0250	2.5310
26.5565	23.4935	0.0440	2.3790
32.7754	17.3246	0.0800	2.3870
37.0168	13.2232	0.1550	2.3420
39.4896	10.4404	0.1960	2.2980
41.6129	8.5171	0.2390	2.2640
42.8471	7.1029	0.2890	2.2270
43.9990	6.0909	0.3190	2.1990
THEORETICAL		EXPERIMENTAL	
METHANE MMOLE/GM PELLETT	PROPANE MMOLE/GM PELLETT	METHANE MMOLE/GM PELLETT	PROPANE MMOLE/GM PELLETT
0.0183	2.2902	0.0098	0.9902
0.0380	2.2461	0.0182	0.9818
0.0590	2.1996	0.0324	0.9676
0.0811	2.1515	0.0621	0.9379
0.1023	2.1051	0.0786	0.9214
0.1239	2.0605	0.0955	0.9045
0.1440	2.0186	0.1149	0.8851
0.1635	1.9803	0.1267	0.8733
THEORETICAL		EXPERIMENTAL	
METHANE MOLE FRACTION	PROPANE MOLE FRACTION	METHANE MOLE FRACTION	PROPANE MOLE FRACTION
0.0079	0.9921	0.0167	0.9833
0.0261	0.9739	0.0363	0.9637
0.0463	0.9537	0.0567	0.9433
0.0666	0.9334	0.0763	0.9237

TABLE 6.23: BINARY ADSORPTION OF METHANE & PROPANE ON LINDE 13X PELLETS

AT 300.00 DEGREE KELVIN AND 95.00 PSIA TOTAL PRESSURE.

ADSORB PHASE CONCENTRATION AND MOLE FRACTION			
EXPERIMENTAL		THEORETICAL	
METHANE PSIA	PROPANE PSIA	METHANE MMOLE/GM PELLETT	PROPANE MMOLE/GM PELLETT
62.7050	32.2450	0.0410	2.3800
71.9299	23.1400	0.0760	2.3210
77.7512	17.4388	0.0990	2.2630
81.4309	13.4990	0.1190	2.2120
84.1940	10.7260	0.1690	2.1680
86.3740	8.6260	0.2750	2.1310
88.3858	7.3942	0.3210	2.0930
THEORETICAL		EXPERIMENTAL	
METHANE MMOLE/GM PELLETT	PROPANE MMOLE/GM PELLETT	METHANE MMOLE/GM PELLETT	PROPANE MMOLE/GM PELLETT
0.0715	2.2480	0.0169	0.9831
0.1050	2.1954	0.0317	0.9683
0.1392	2.1421	0.0419	0.9581
0.1744	2.0876	0.0511	0.9489
0.2107	2.0329	0.0723	0.9277
0.2495	1.9761	0.1143	0.8857
0.2816	1.9317	0.1330	0.8670
THEORETICAL		EXPERIMENTAL	
METHANE MOLE FRACTION	PROPANE MOLE FRACTION	METHANE MOLE FRACTION	PROPANE MOLE FRACTION
0.0308	0.9692	0.0456	0.9544
0.0610	0.9390	0.0771	0.9229
0.0939	0.9061	0.1121	0.8879
0.1272	0.8728		

TABLE 6.24 TERNARY ADSORPTION OF METHANE-ETHANE-& PROPANE ON LINDE 13X PELLETS

AT 300.00 DEGREE KELVIN AND 50.00 PSIA TOTAL PRESSURE.

OPTIMISED HENRY CONSTANT (MOLECULES/CAVITY/PSIA)			
HK1	HK2	HK3	HK4
0.1746	3.9565	46.468	822.000
MOLECULAR VOLUME CUBIC ANGSTROM/MOLECULE			
BETA1	BETA2	BETA3	BETA4
83.5344	105.1899	133.1647	167.4126

PARTIAL PRESSURES			ADSORB PHASE MOLE FRACTIONS			
METHANE PSIA	ETHANE PSIA	PROPANE PSIA	EXPERIMENTAL MOLE FRACTION		THEORETICAL MOLE FRACTION	
			METHANE	ETHANE	METHANE	ETHANE
15.7570	16.8335	17.4794	0.0710	0.2910	0.0266	0.3462
25.7373	11.8525	12.5902	0.0780	0.2640	0.0545	0.3192
31.9396	8.7012	9.5392	0.1020	0.2380	0.0820	0.2934
35.9460	6.6459	7.5280	0.0760	0.2140	0.1085	0.2706
38.7594	5.2559	6.1846	0.1260	0.1930	0.1336	0.2497
40.5457	4.2474	5.1769	0.1380	0.1740	0.1572	0.2314
41.9877	3.4844	4.4479	0.1510	0.1570	0.1799	0.2132
						1.9357
						1.9033
						1.8709
						1.8384
						1.8085
						1.7785
						1.7519

TABLE 6.25 TERNARY ADSORPTION OF METHANE-ETHANE & PROPANE ON LINDE 13X PELLETS

AT 300.00 DEGREE KELVIN AND 50.00 PSIA TOTAL PRESSURE.

PARTIAL PRESSURES			ADSORB PHASE CONCENTRATION			
METHANE PSIA	ETHANE PSIA	PROPANE PSIA	EXPERIMENTAL CONCENTRATION		THEORETICAL CONCENTRATION	
			METHANE (MILLIMOLES/GM PELLETS)	PROPANE (MILLIMOLES/GM PELLETS)	METHANE (MILLIMOLES/GM PELLETS)	PROPANE (MILLIMOLES/GM PELLETS)
15.7570	16.8335	17.4794	0.0287	0.1177	0.0115	0.1500
25.7373	11.8525	12.5902	0.0322	0.1091	0.0239	0.1402
31.9396	8.7012	9.5392	0.0428	0.0998	0.0365	0.1306
35.9460	6.6459	7.5280	0.0330	0.0929	0.0489	0.1220
38.7594	5.2559	6.1846	0.0547	0.0837	0.0609	0.1139
40.5457	4.2474	5.1769	0.0607	0.0766	0.0726	0.1068
41.9877	3.4844	4.4479	0.0673	0.0699	0.0839	0.0994
						0.8385
						0.8359
						0.8329
						0.8290
						0.8251
						0.8207
						0.8167

TABLE 6.26 TERNARY ADSORPTION OF METHANE-ETHANE-& N-BUTANE ON LINDE 13X PELLETS

AT 300.00 DEGREE KELVIN AND 50.00 PSIA TOTAL PRESSURE.

OPTIMISED HENRY CONSTANT (MOLECULES/CAVITY/PSIA)			
HK1	HK2	HK3	HK4
0.1746	3.9565	46.468	822.000

MOLECULAR VOLUME CUBIC ANGSTROM/MOLECULE			
BETA1	BETA2	BETA3	BETA4
83.5344	105.1899	133.1647	167.4126

PARTIAL PRESSURES		ADSORB PHASE MOLE FRACTIONS			
		EXPERIMENTAL MOLE FRACTION		THEORETICAL MOLE FRACTION	
METHANE PSIA	ETHANE PSIA	METHANE	ETHANE	METHANE	ETHANE
25.5965	17.0209	0.0105	0.0833	0.0101	0.0665
31.9300	12.2550	0.0152	0.0689	0.0141	0.0565
36.4850	8.9300	0.0174	0.0578	0.0181	0.0485
39.5228	6.6603	0.0252	0.0479	0.0219	0.0422
41.8917	5.0470	0.0345	0.0396	0.0258	0.0367
43.3532	3.9090	0.0390	0.0323	0.0296	0.0325
28.1050	17.9450	0.0217	0.1232	0.0162	0.1151
					0.8686

TABLE 6.27 TERNARY ADSORPTION OF METHANE-ETHANE-& N-BUTANE ON LINDE 13X PELLETS

AT 300.00 DEGREE KELVIN AND 50.00 PSIA TOTAL PRESSURE.

PARTIAL PRESSURES		ADSORB PHASE MOLE FRACTIONS			
		EXPERIMENTAL MOLE FRACTION		THEORETICAL MOLE FRACTION	
METHANE PSIA	ETHANE PSIA	METHANE	ETHANE	METHANE	ETHANE
25.5965	17.0209	0.0220	0.1740	0.0197	0.1291
31.9300	12.2550	0.0310	0.1410	0.0273	0.1092
36.4850	8.9300	0.0350	0.1160	0.0348	0.0932
39.5228	6.6603	0.0500	0.0950	0.0420	0.0808
41.8917	5.0470	0.0680	0.0780	0.0493	0.0701
43.3532	3.9090	0.0760	0.0630	0.0563	0.0617
28.1050	17.9450	0.0450	0.2550	0.0317	0.2253
					1.6996

TABLE 6.28 TERNARY ADSORPTION OF METHANE-PROPANE-& N-BUTANE ON LINDE 13X PELLETS
AT 300.00 DEGREE KELVIN AND 50.00 PSIA TOTAL PRESSURE.

OPTIMISED HENRY CONSTANT (MOLECULES/CAVITY/PSIA)			
HK1	HK2	HK3	HK4
0.1746	3.9565	46.468	822.000

MOLECULAR VOLUME CUBIC ANGSTROM/MOLECULE			
BETA1	BETA2	BETA3	BETA4
83.5344	105.1899	133.1647	167.4126

PARTIAL PRESSURES			ADSORB PHASE MOLE FRACTIONS			
METHANE PSIA	PROPANE PSIA	N-BUTANE PSIA	EXPERIMENTAL METHANE	PROPANE PROPANE	THEORETICAL METHANE	FRACTION PROPANE N-BUTANE
14.3540	21.4978	15.2482	0.0137	0.2455	0.0051	0.2135
23.5052	15.7489	11.0459	0.0061	0.2366	0.0093	0.1996
29.8732	11.6028	8.0240	0.0115	0.2258	0.0131	0.1893
35.7318	9.0398	6.1284	0.0166	0.2156	0.0173	0.1839
38.3065	7.0591	4.7344	0.0329	0.2040	0.0206	0.1783
40.7300	5.5900	3.6800	0.0218	0.1993	0.0245	0.1751
42.5300	4.5400	2.9300	0.0249	0.1923	0.0285	0.1732

TABLE 6.29 TERNARY ADSORPTION OF METHANE-PROPANE-& N-BUTANE ON LINDE 13X PELLETS
AT 300.00 DEGREE KELVIN AND 50.00 PSIA TOTAL PRESSURE.

PARTIAL PRESSURES			EXPERIMENTAL CONCENTRATION				THEORETICAL CONCENTRATION			
METHANE PSIA	PROPANE PSIA	N-BUTANE PSIA	EXPERIMENTAL METHANE (MILLIMOLES/GM PELLET)	PROPANE PROPANE (MILLIMOLES/GM PELLET)	N-BUTANE N-BUTANE (MILLIMOLES/GM PELLET)	THEORETICAL METHANE (MILLIMOLES/GM PELLET)	PROPANE PROPANE (MILLIMOLES/GM PELLET)	N-BUTANE N-BUTANE (MILLIMOLES/GM PELLET)	THEORETICAL METHANE (MILLIMOLES/GM PELLET)	N-BUTANE N-BUTANE (MILLIMOLES/GM PELLET)
14.3540	21.4978	15.2482	0.0330	0.5900	1.7800	0.0102	0.4237	1.5504	0.0102	0.4237
23.5052	15.7489	11.0459	0.0140	0.5470	1.7510	0.0183	0.3934	1.5595	0.0183	0.3934
29.8732	11.6028	8.0240	0.0260	0.5120	1.7290	0.0258	0.3711	1.5635	0.0258	0.3711
35.7318	9.0398	6.1284	0.0370	0.4800	1.7090	0.0339	0.3593	1.5605	0.0339	0.3593
38.3065	7.0591	4.7344	0.0730	0.4520	1.6910	0.0401	0.3470	1.5587	0.0401	0.3470
40.7300	5.5900	3.6800	0.0470	0.4290	1.6770	0.0474	0.3396	1.5519	0.0474	0.3396
42.5300	4.5400	2.9300	0.0530	0.4090	1.6650	0.0550	0.3347	1.5429	0.0550	0.3347

TABLE 6.30 QUATERNARY ADSORPTION OF METHANE-ETHANE-PROPANE- & N-BUTANE ON LINDE 13X PELLETS

AT 300.00 DEGREE KELVIN AND 50.00 PSIA TOTAL PRESSURE

OPTIMIZED HENRY CONSTANT
(MOLECULES/CAVITY/PSIA)

HK1	HK2	HK3	HK4
0.1746	3.9565	46.468	822.000

MOLECULAR VOLUME
(CUBIC ANGSTROM/MOLECULE)

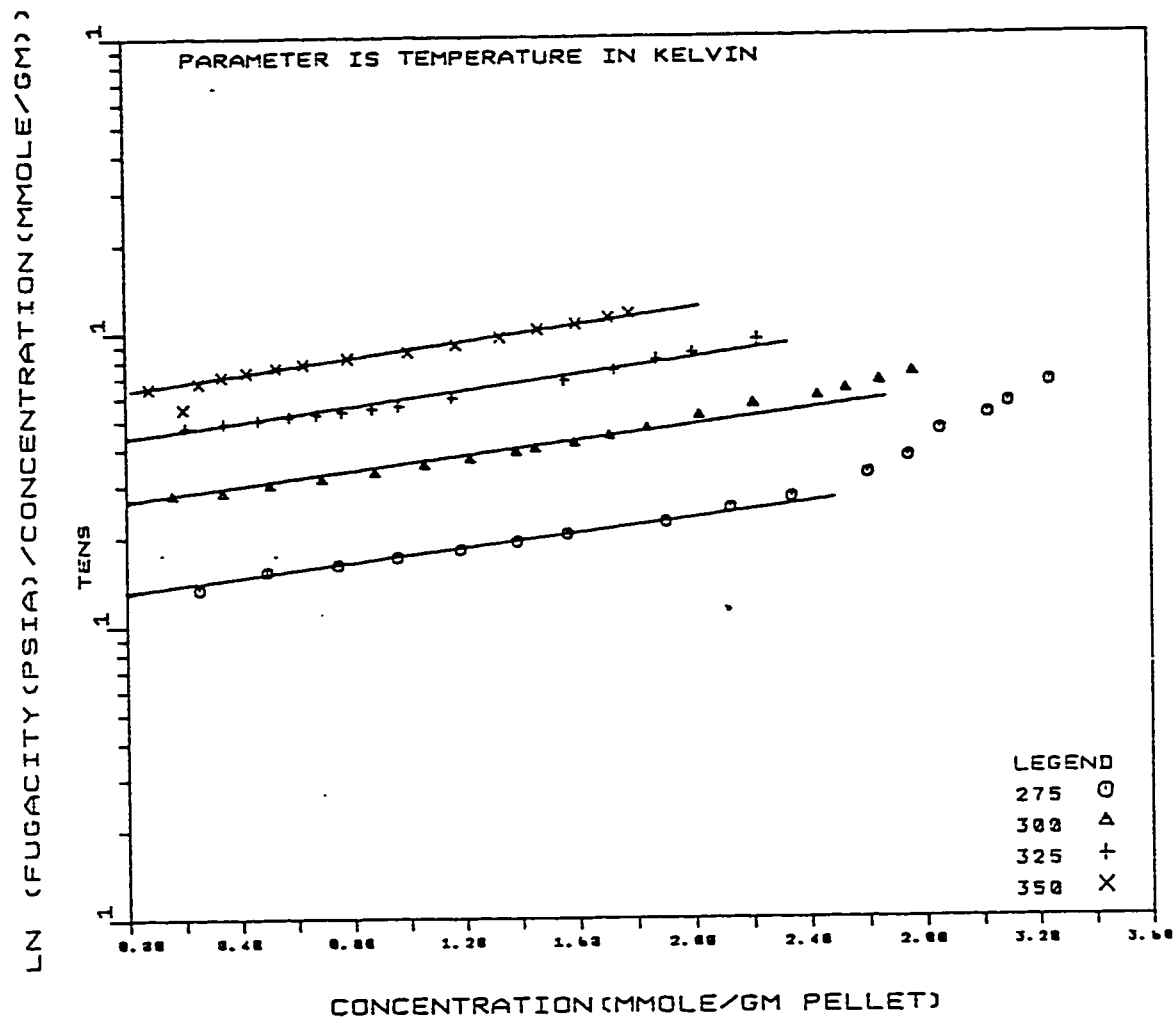
BETA1	BETA2	BETA3	BETA4
83.5344	105.1899	133.1647	167.4126

PARTIAL PRESSURES				ADSORB PHASE MOLE FRACTIONS				THEORETICAL MOLE FRACTION			
METHANE	ETHANE	PROPANE	N-BUTANE	METHANE	ETHANE	PROPANE	N-BUTANE	METHANE	ETHANE	PROPANE	N-BUTANE
PSIA	PSIA	PSIA	PSIA	PSIA	PSIA	PSIA	PSIA	PSIA	PSIA	PSIA	PSIA
15.0941	13.2412	12.2095	9.5352	0.0014	0.0474	0.1982	0.7530	0.0061	0.0496	0.1765	0.7678
25.2002	9.0659	8.9507	6.8432	0.0043	0.0409	0.1913	0.7634	0.0117	0.0407	0.1687	0.7790
31.8027	6.3876	6.7577	5.0720	0.0102	0.0345	0.1840	0.7714	0.0167	0.0341	0.1629	0.7863
36.2850	4.6150	5.2450	3.8550	0.0187	0.0290	0.1768	0.7755	0.0215	0.0291	0.1593	0.7901
39.4731	3.4252	4.2026	3.0491	0.0245	0.0240	0.1704	0.7811	0.0261	0.0251	0.1561	0.7926
41.6716	2.5776	3.4384	2.4524	0.0294	0.0197	0.1650	0.7859	0.0307	0.0219	0.1542	0.7931
43.1731	1.9920	2.8579	2.0270	0.0368	0.0163	0.1593	0.7876	0.0352	0.0193	0.1515	0.7939
27.9212	15.5762	3.5664	2.9562	0.0199	0.1111	0.1358	0.7333	0.0189	0.1185	0.1337	0.7289
17.6583	26.0809	3.7309	3.3599	0.0133	0.1637	0.1191	0.7040	0.0110	0.1803	0.1227	0.6860

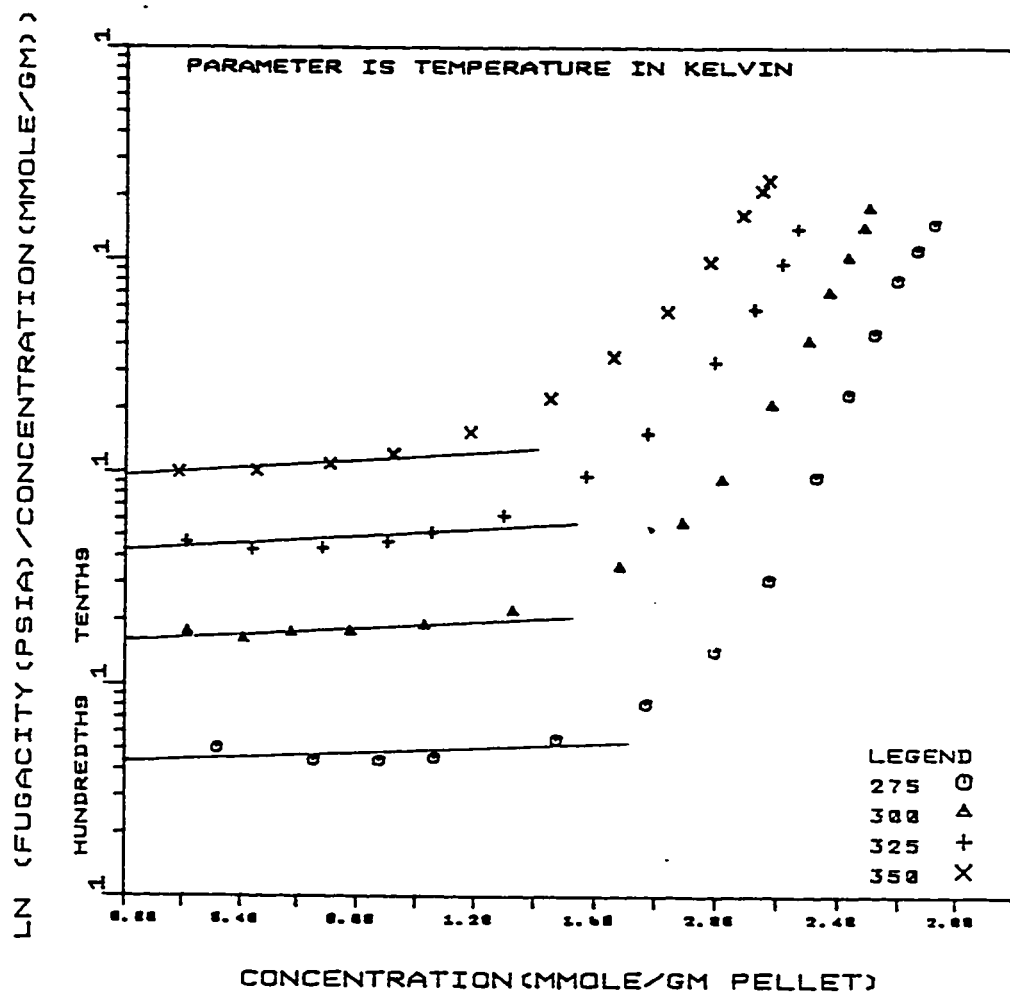
TABLE 6.31 QUATERNARY ADSORPTION OF METHANE-ETHANE-PROPANE- & N-BUTANE ON LINDE 13X PELLETS

AT 300.00 DEGREE KELVIN AND 50.00 PSIA TOTAL PRESSURE

PARTIAL PRESSURES				ADSORB PHASE CONCENTRATION				THEORETICAL FROM RUTHVEN MODEL			
METHANE	ETHANE	PROPANE	N-BUTANE	METHANE	ETHANE	PROPANE	N-BUTANE	METHANE	ETHANE	PROPANE	N-BUTANE
PSIA	PSIA	PSIA	PSIA	PSIA	PSIA	PSIA	PSIA	PSIA	PSIA	PSIA	PSIA
15.0941	13.2412	12.2095	9.5352	0.0030	0.1020	0.4270	1.6220	0.0123	0.0991	0.3530	1.5358
25.2002	9.0659	8.9507	6.8432	0.0090	0.0860	0.4020	1.6040	0.0231	0.0806	0.3342	1.5435
31.8027	6.3876	6.7577	5.0720	0.0210	0.0710	0.3790	1.5890	0.0328	0.0670	0.3204	1.5463
36.2850	4.6150	5.2450	3.8550	0.0380	0.0590	0.3590	1.5750	0.0420	0.0569	0.3114	1.5443
39.4731	3.4252	4.2026	3.0491	0.0490	0.0480	0.3410	1.5630	0.0507	0.0489	0.3036	1.5413
41.6716	2.5776	3.4384	2.4524	0.0580	0.0390	0.3260	1.5530	0.0595	0.0424	0.2985	1.5351
43.1731	1.9920	2.8579	2.0270	0.0720	0.0320	0.3120	1.5430	0.0679	0.0373	0.2920	1.5300
27.9212	15.5762	3.5664	2.9562	0.0410	0.2290	0.2800	1.5120	0.0378	0.2368	0.2673	1.4570
17.6583	26.0809	3.7309	3.3599	0.0280	0.3450	0.2510	1.4840	0.0225	0.3688	0.2510	1.4030



6.1: Virial Isotherm of Methane on Linde 13X Pellets.



6.2: Virial Isotherm of Propane on Linde 13X Pellets.

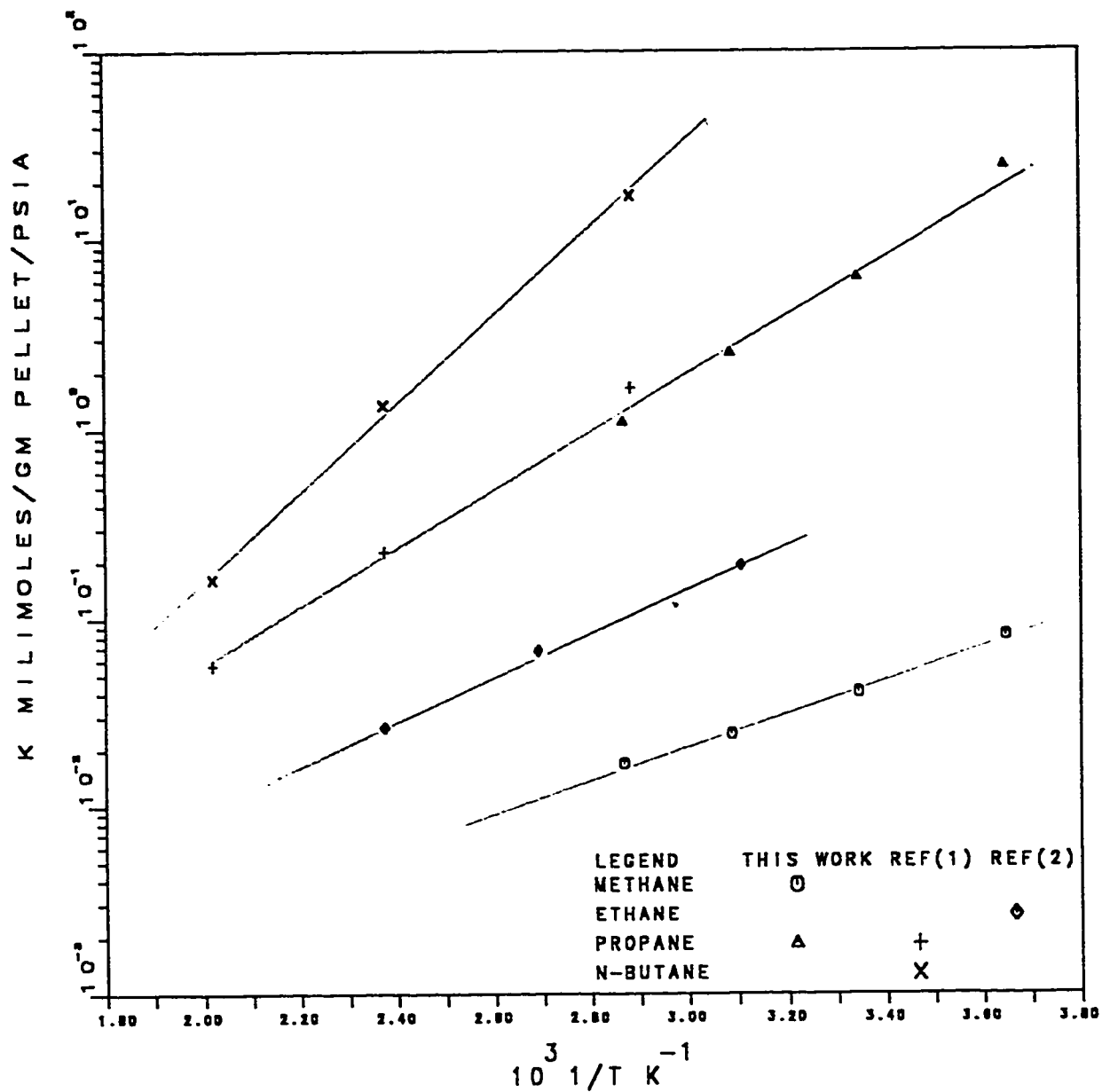
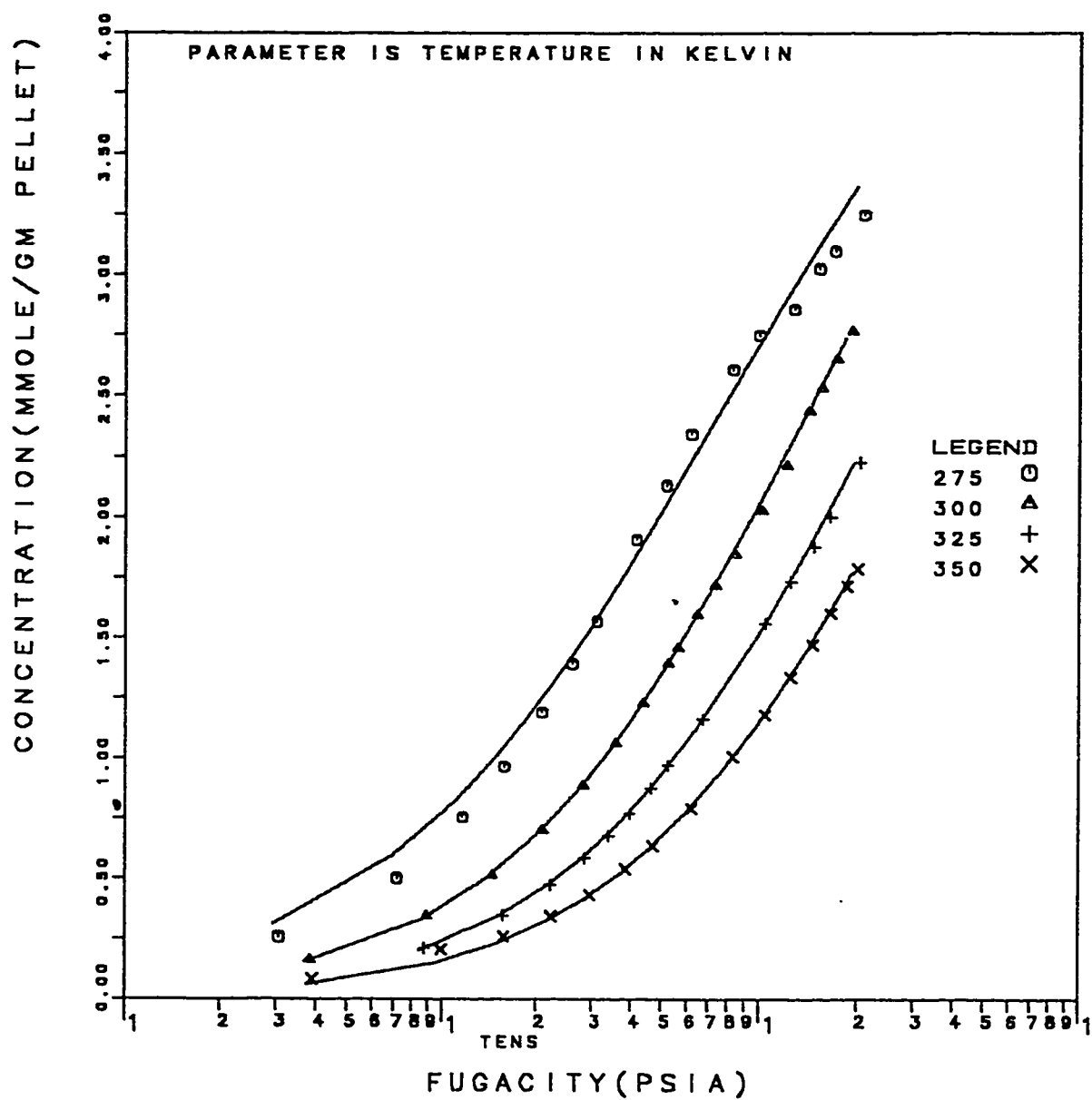
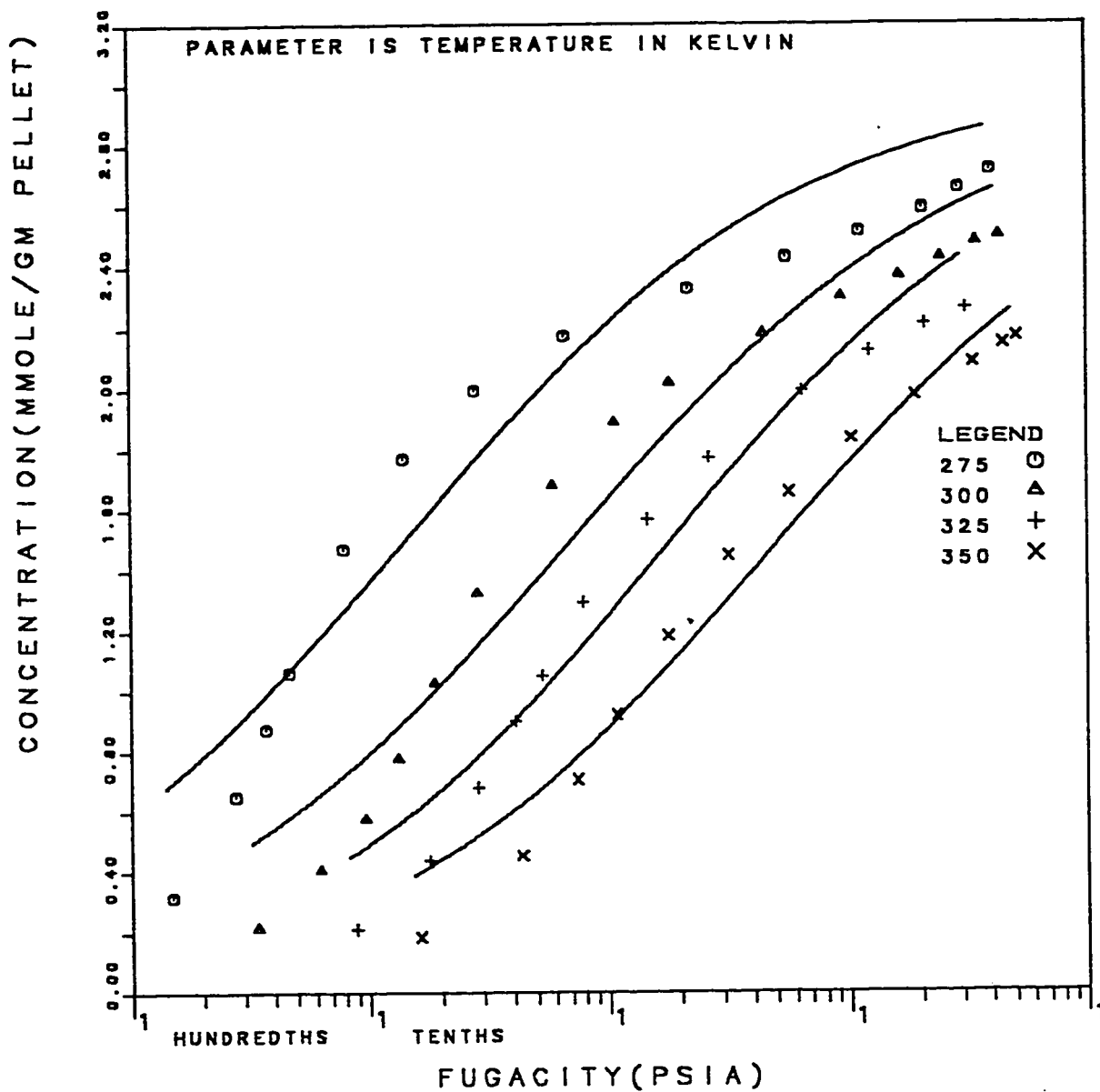


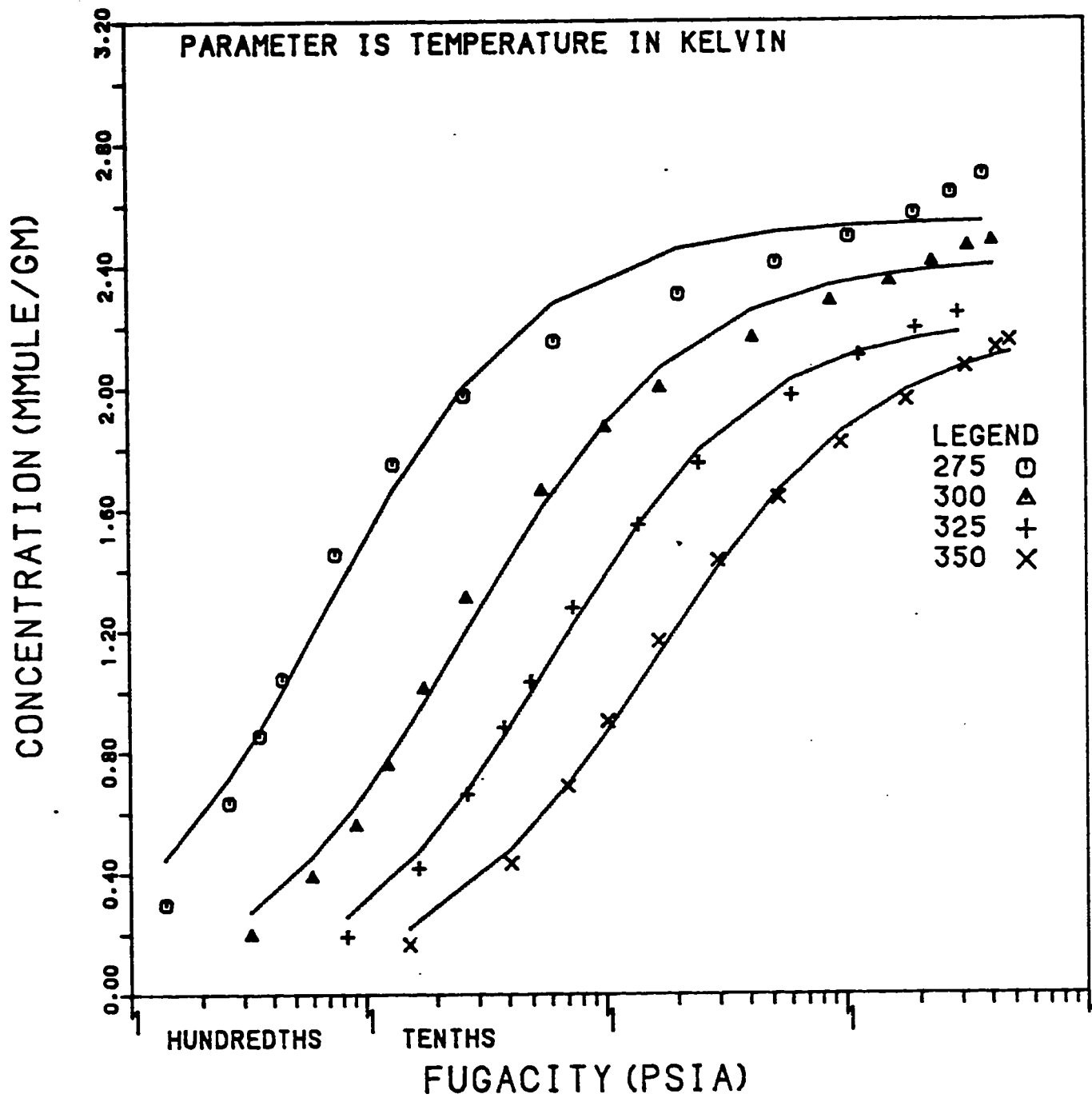
FIG. 6.3: VAN'T HOFF PLOT FOR LIGHT ALKANES ON LINDE 13X PELLETS.



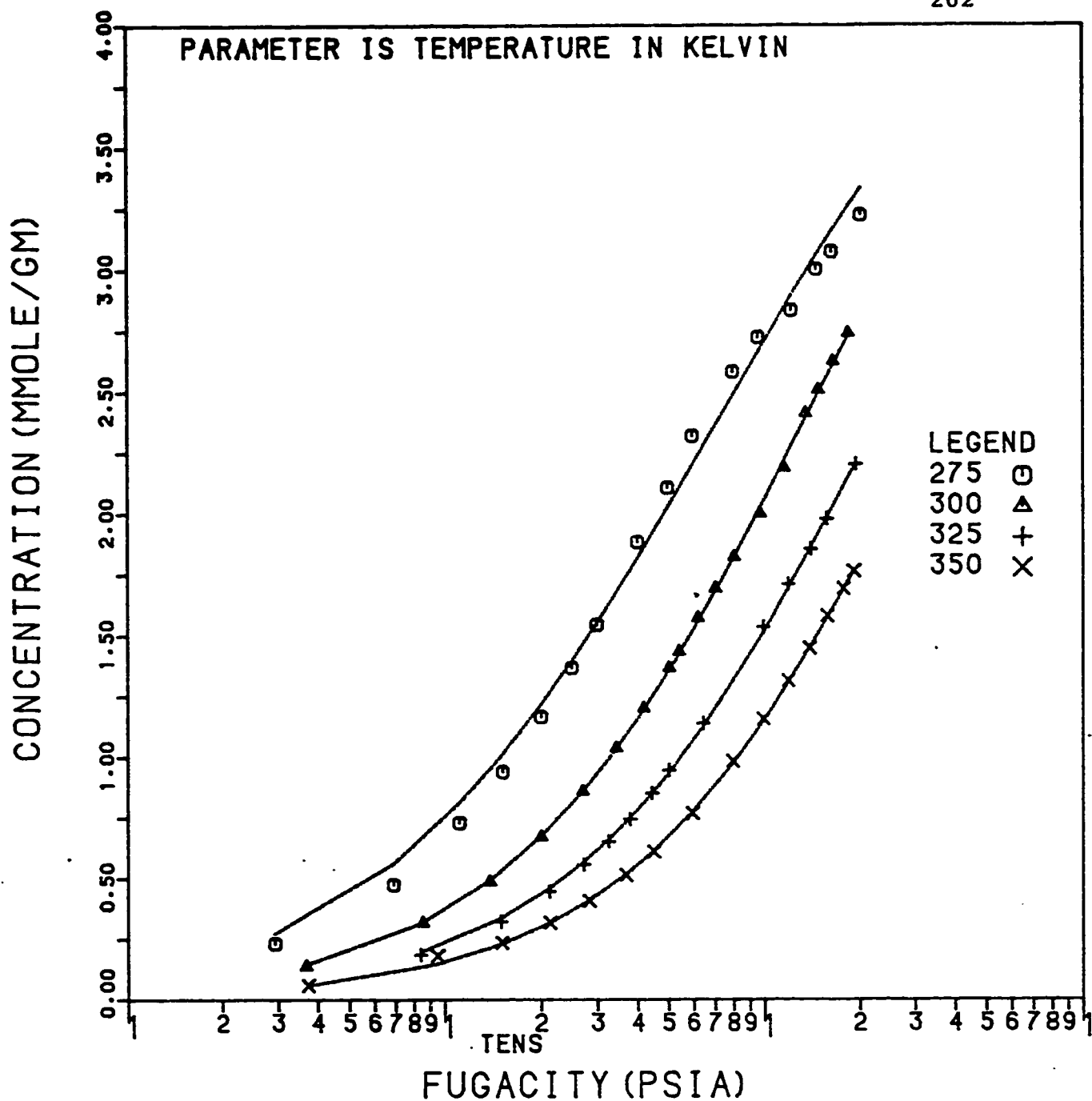
6.4: Methane Isotherms on Linde 13X Pellets: Fit of LRC Model With Theoretical N_0 and Optimized K.



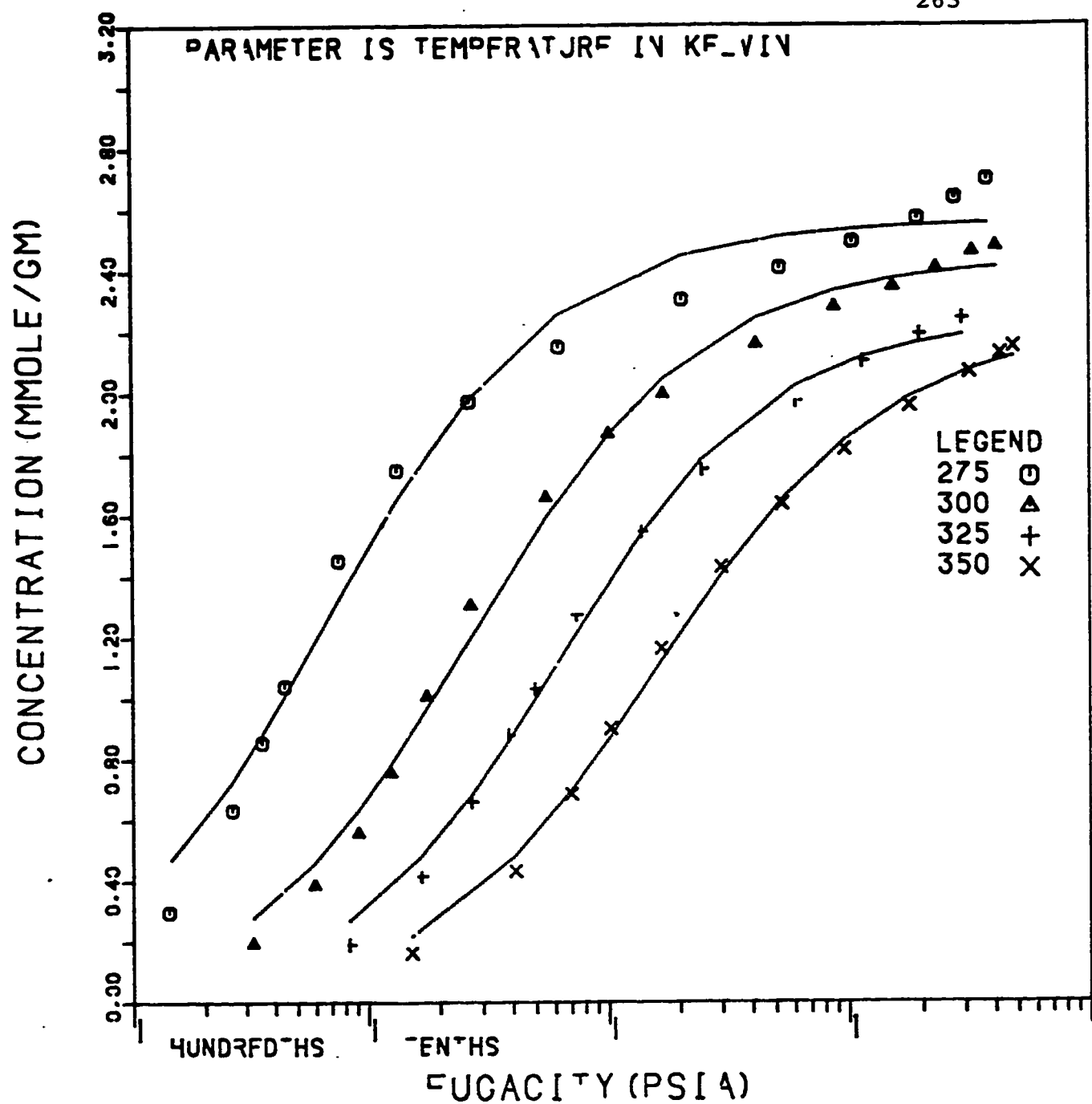
6.5: Propane Isotherms on Linde 13X Pellets: Fit of LRC Model With Theoretical N_0 and Optimized K.



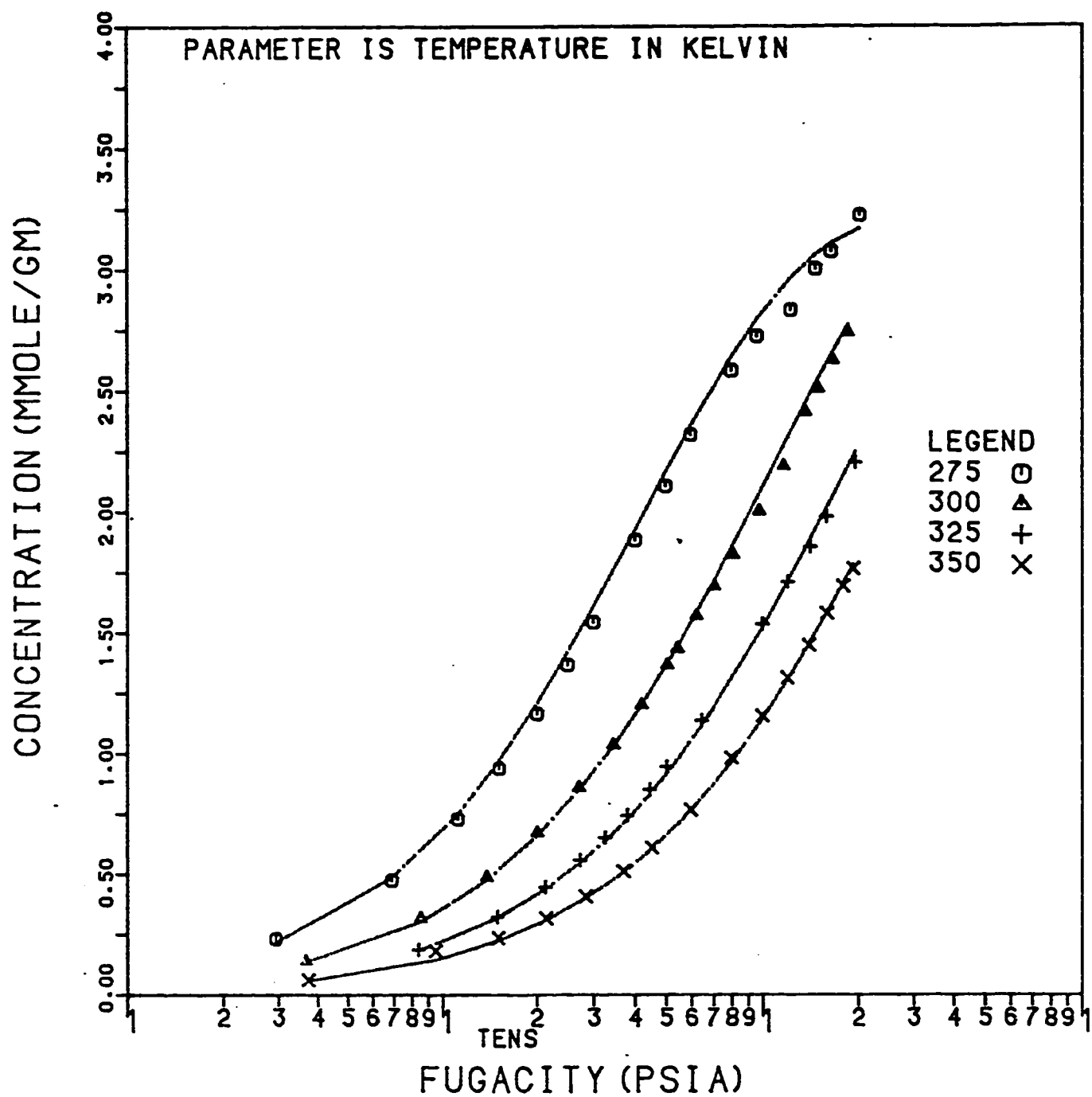
6.6: Propane Isotherms on Linde 13X Pellets: Fit of LRC Model Optimized N_0 and K .



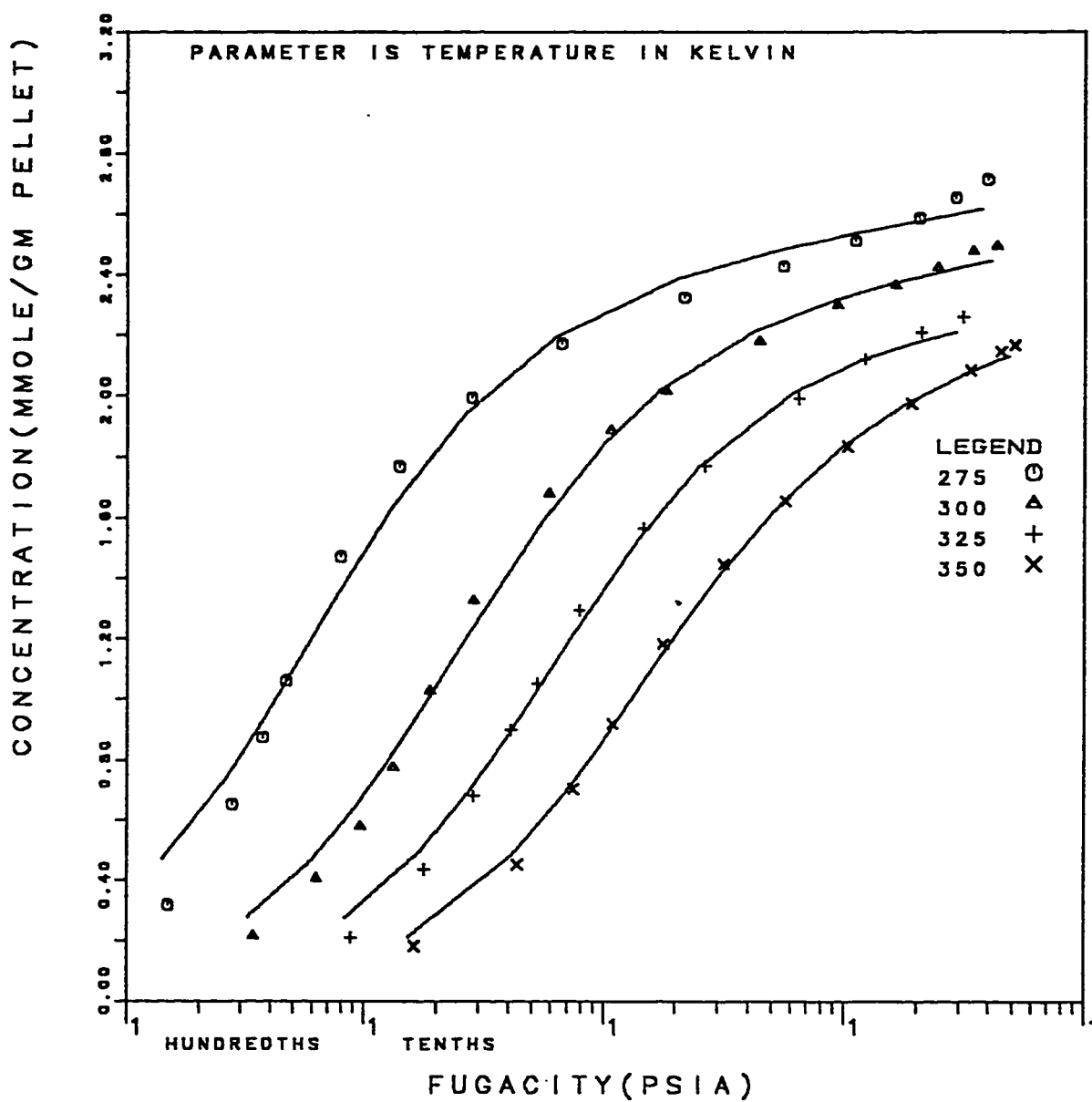
6.7: Methane Isotherms on Linde 13X Pellets: Fit of Toth Model With Theoretical N_0 and Optimized K .



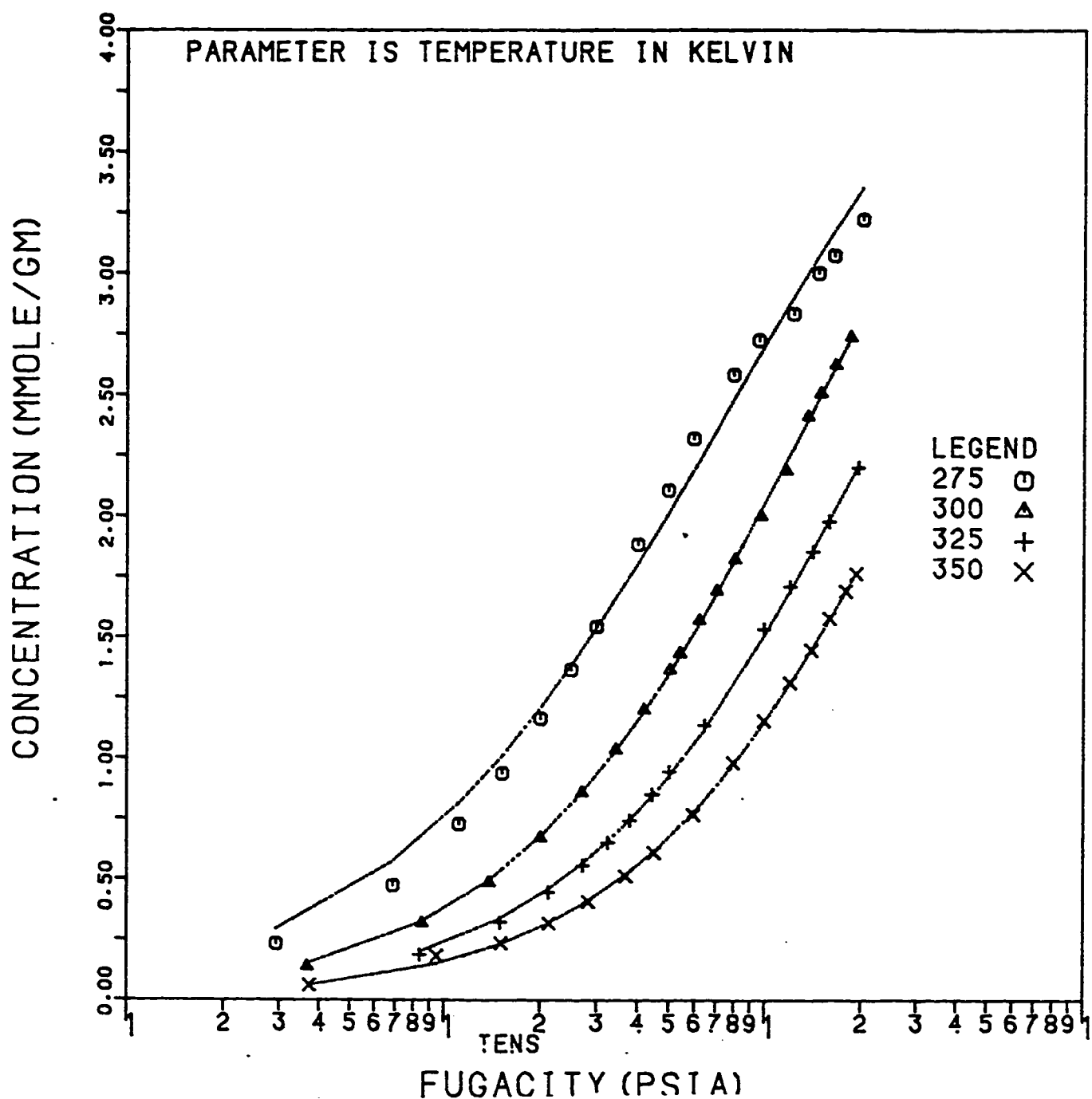
6.8: Propane Isotherms on Linde 13X Pellets: Fit of Toth Model Optimized N_0 and K .



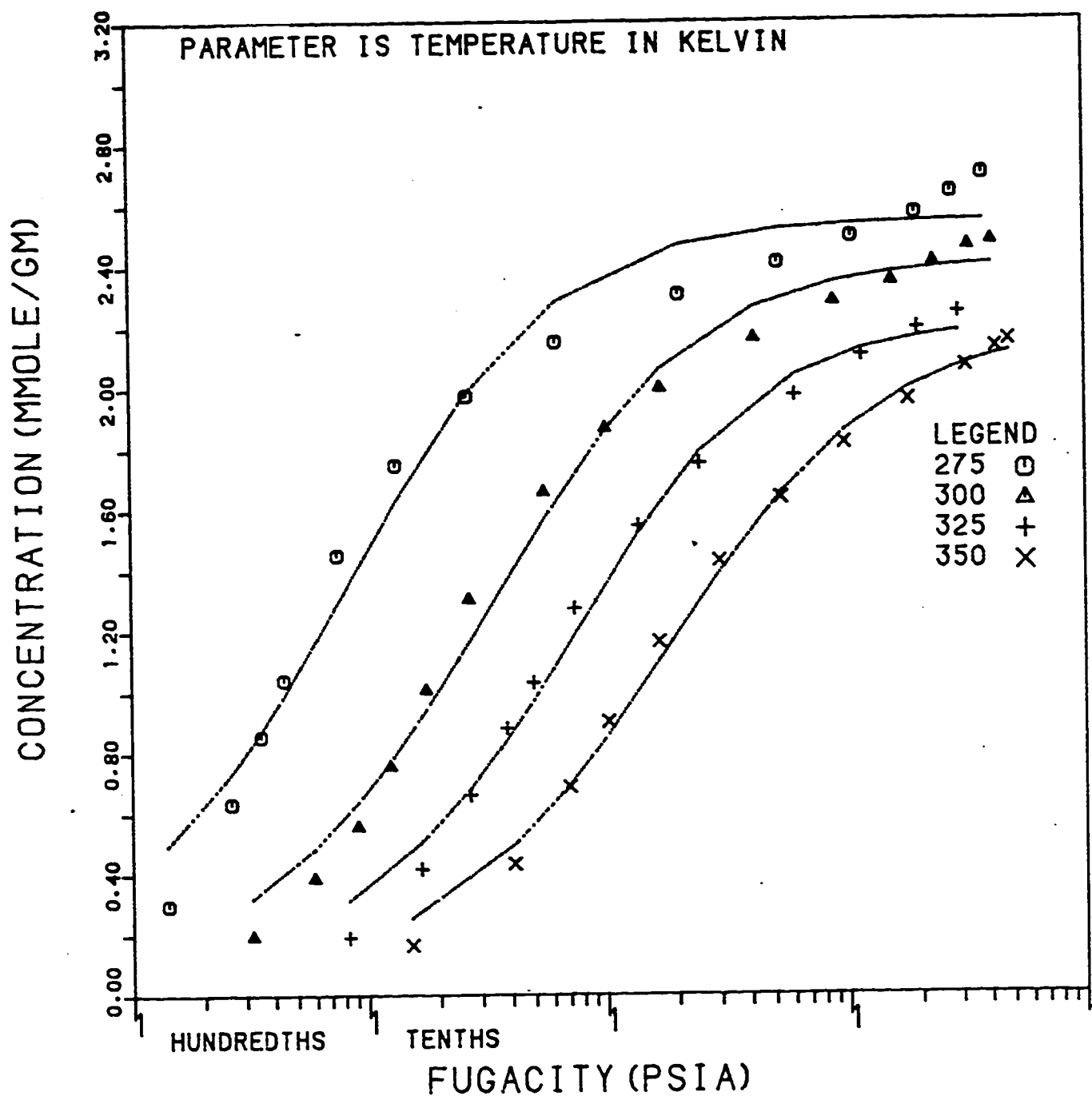
6.9: Methane Isotherms on Linde S-115 Pellets: Fit of Mathews and Weber Model With Optimized N_0 and Intrinsic K .



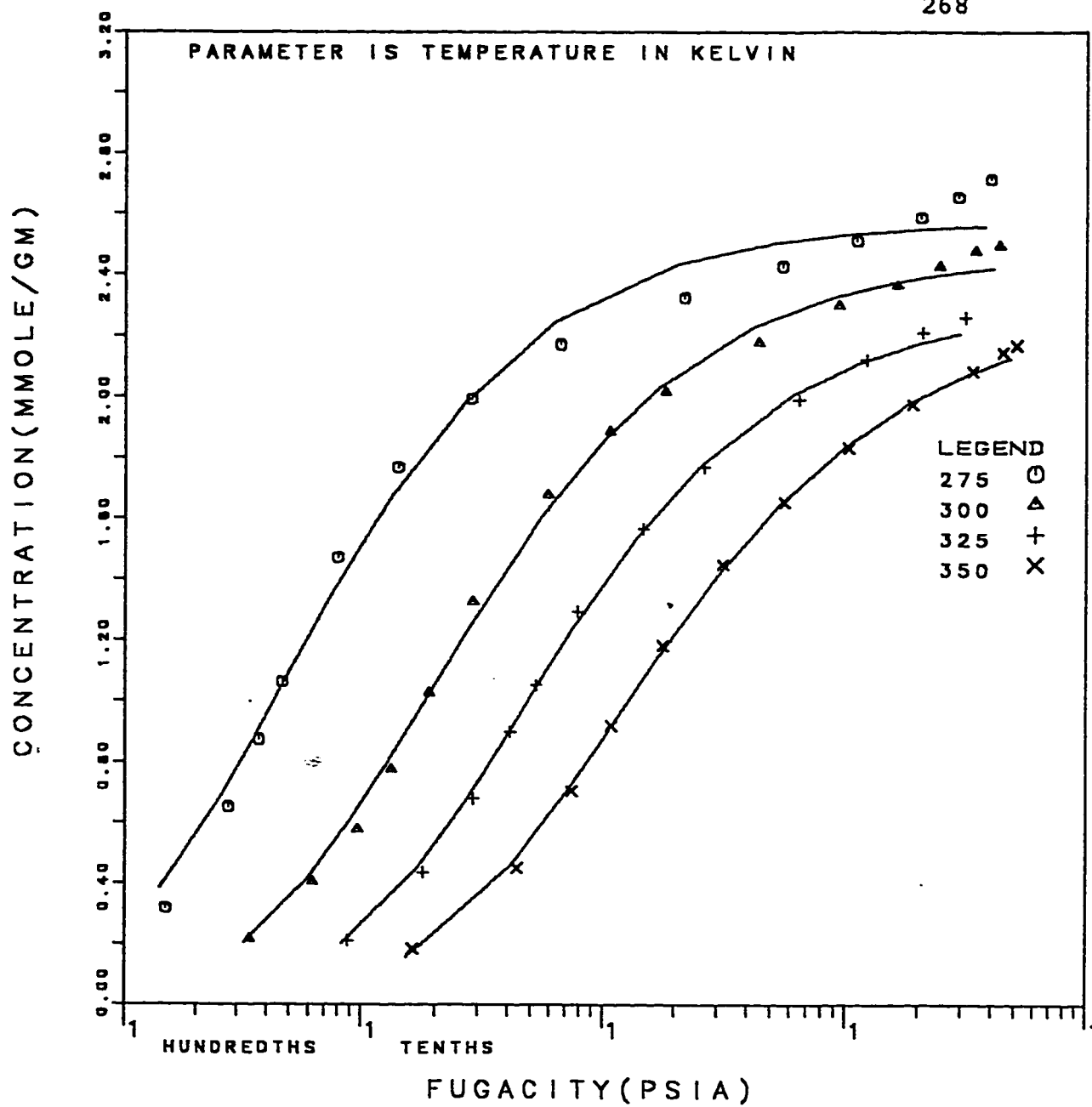
6.10: Propane Isotherms on Linde 13X Pellets: Fit of Mathews and Weber Model With Optimized N_0 and K .



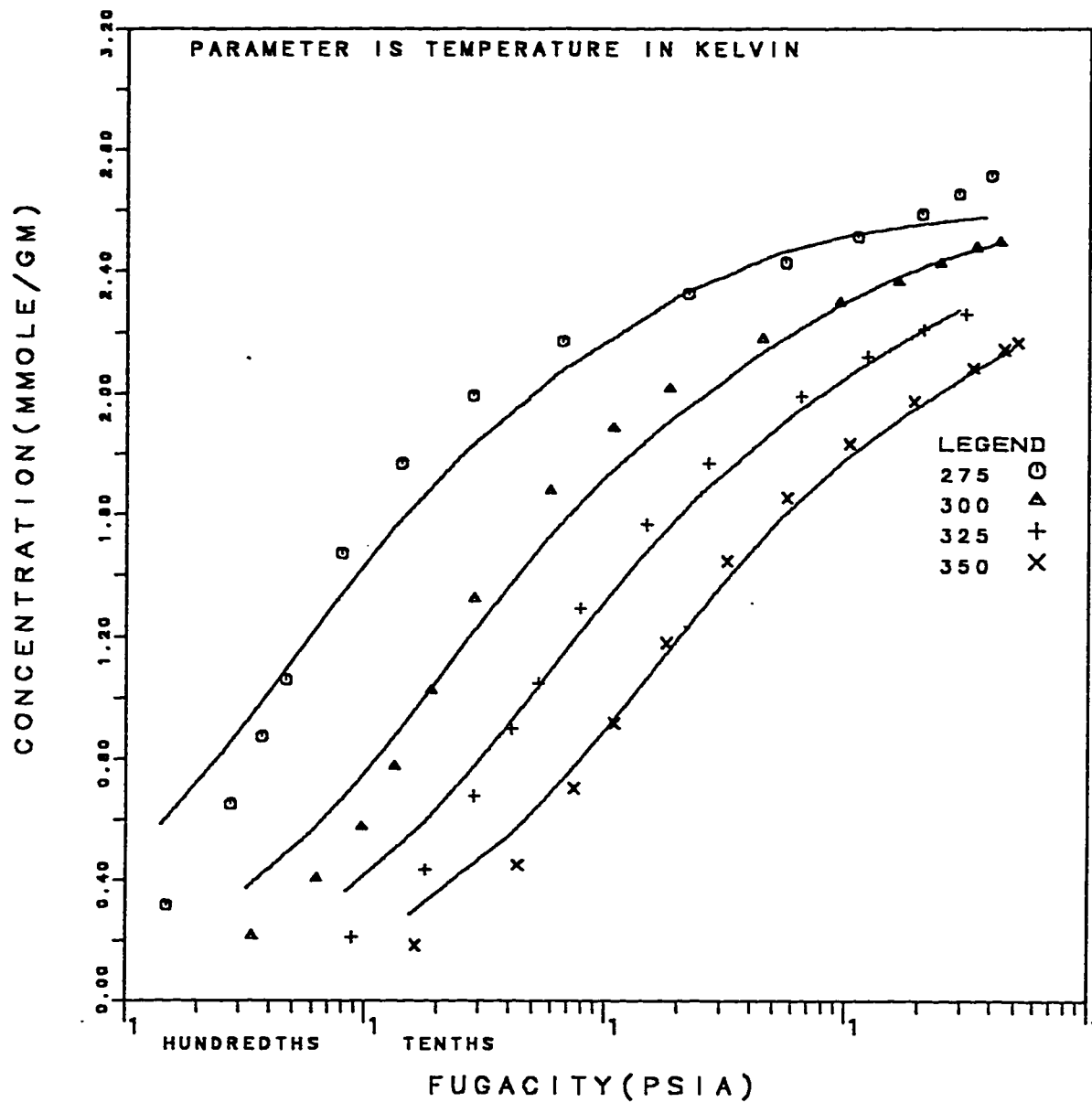
6.11: Methane Isotherms on Linde 13X Pellets: Fit of Jaroniec Model With Theoretical N_0 and Intrinsic K .



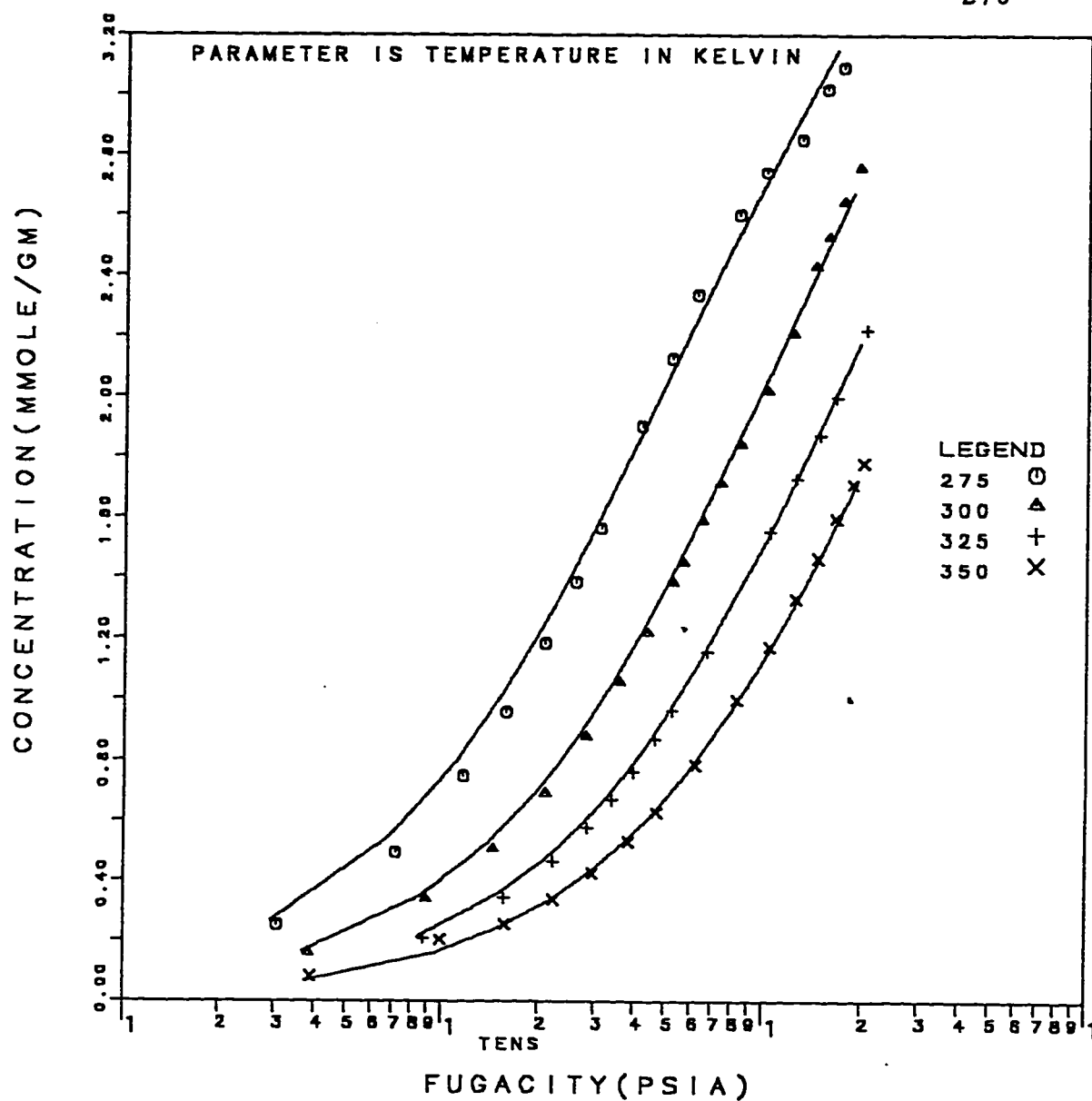
6.12: Propane Isotherms on Linde 13X Pellets: Fit of Jaroniec Model With Optimized N_0 and Intrinsic K .



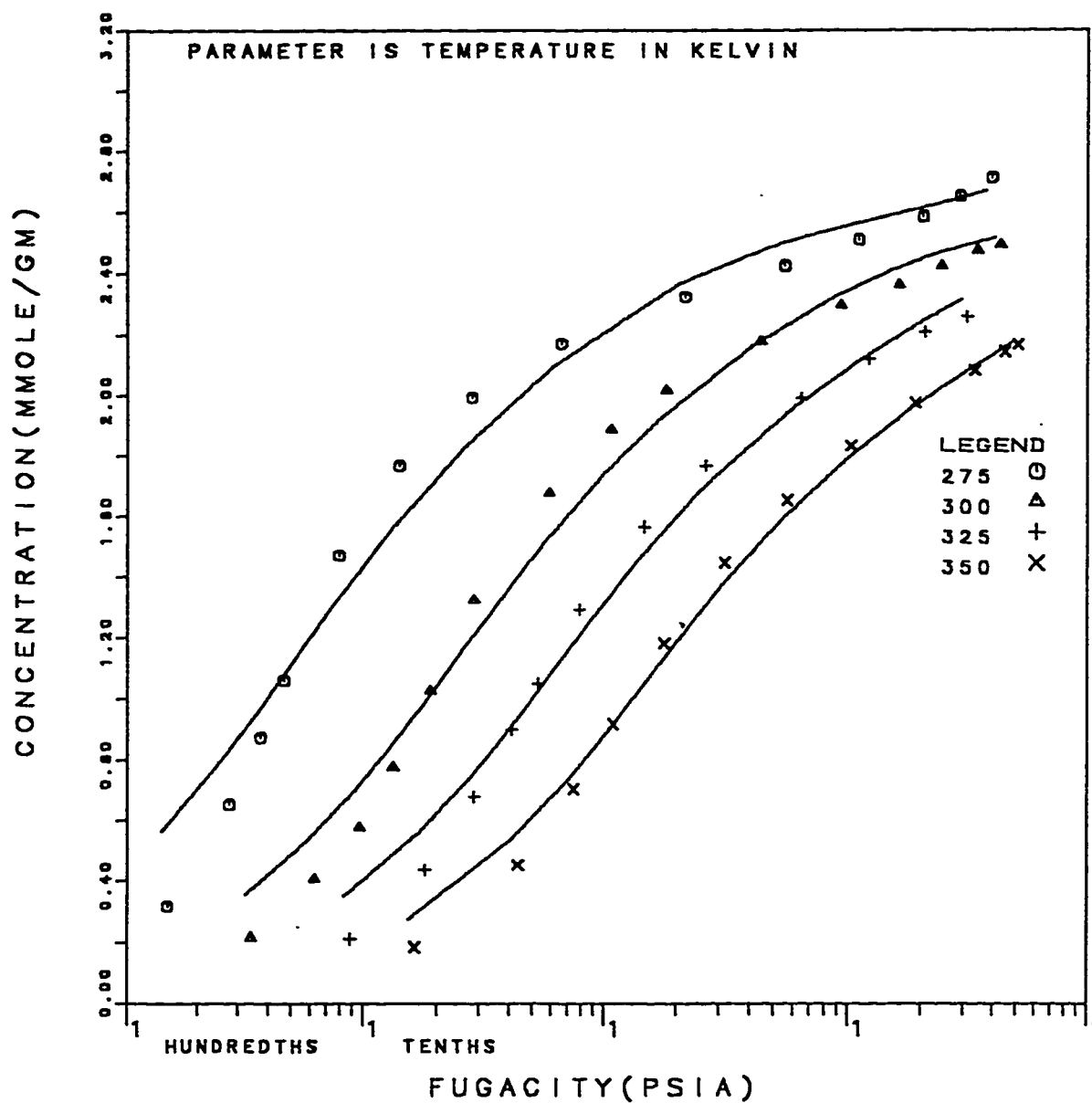
6.13: Propane Isotherms on Linde 13X Pellets: Fit of Jaroniec Model With Optimized N_0 and K .



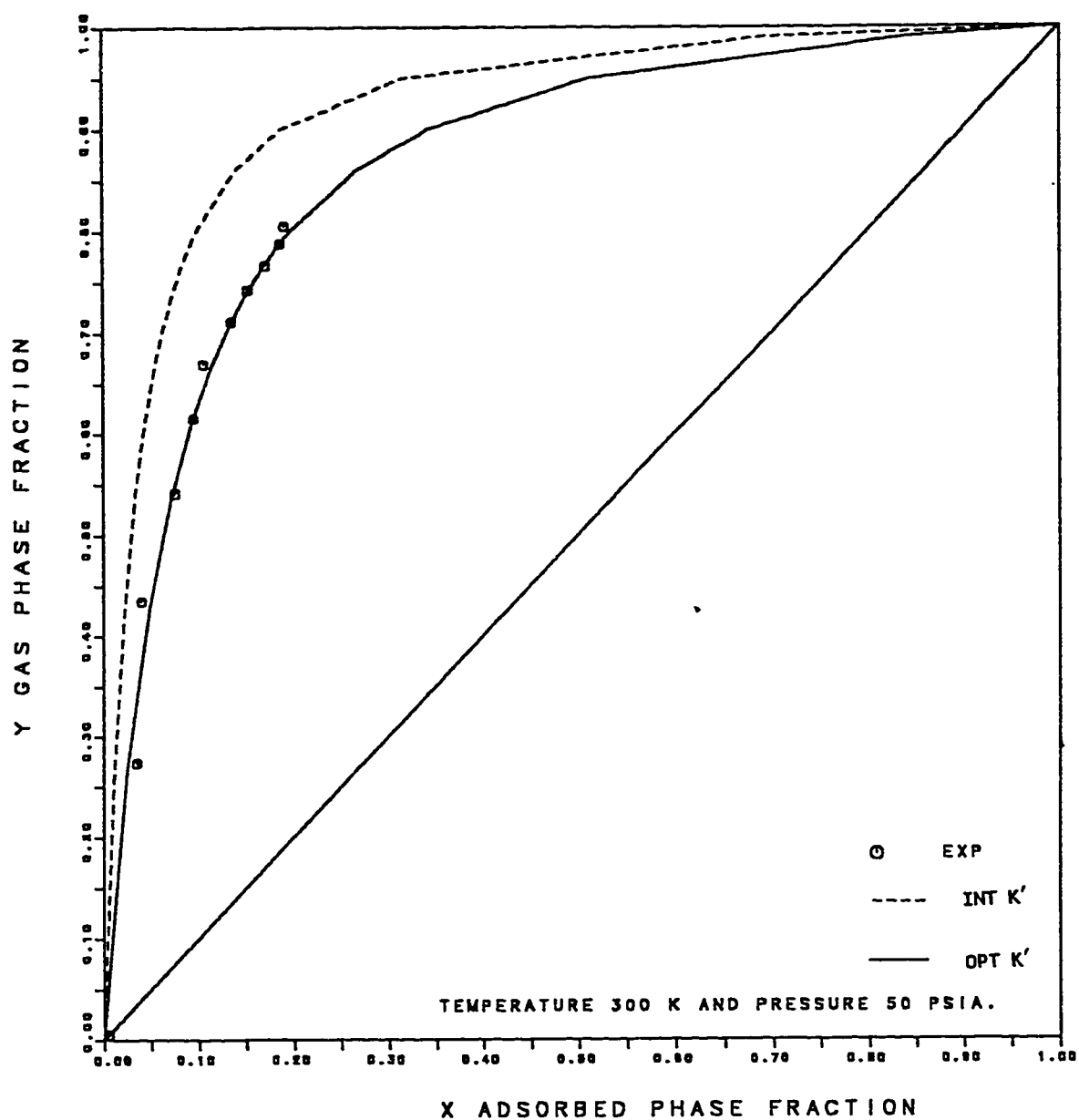
6.14: Propane Isotherms on 13X Pellets: Fit of Ruthven Model With Theoretical β and optimised Henry Constant.



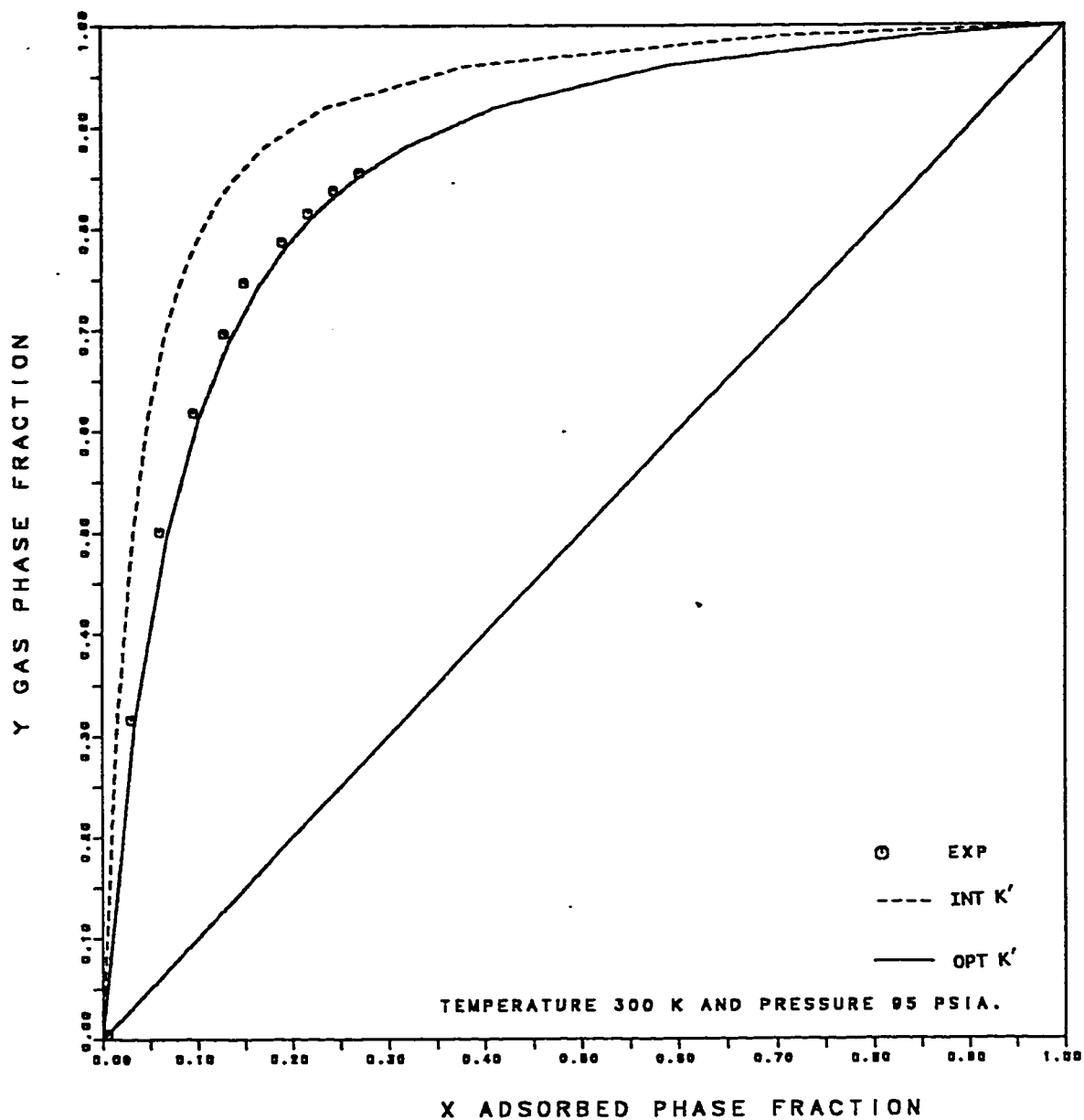
6.15: Methane Isotherms on 13X Pellets: Fit of Ruthven Model With Optimized β and Henry Constant.



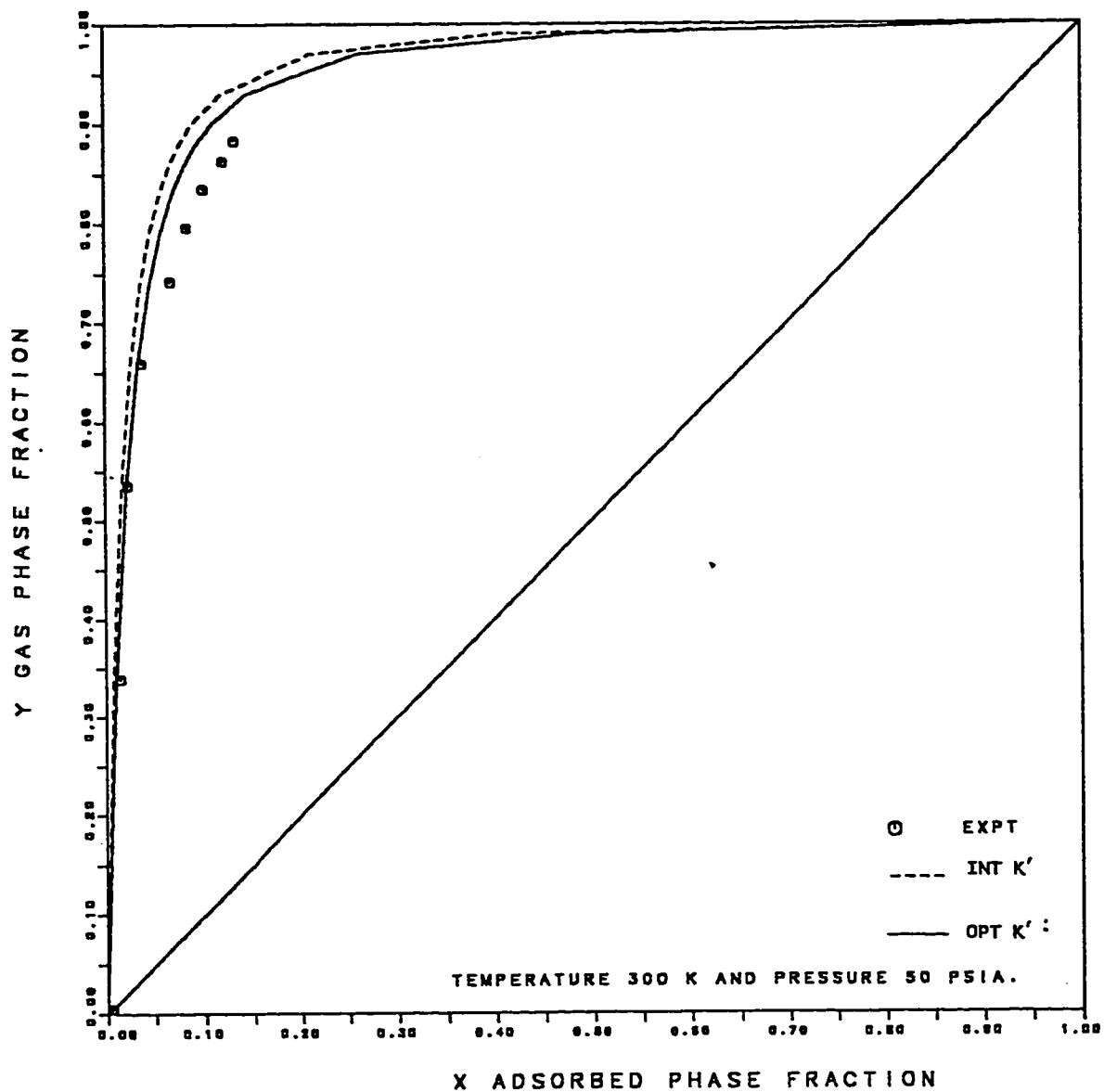
6.16: Propane Isotherms on 13X Pellets: Fit of Ruthven Model With Optimized β and Henry Constant.



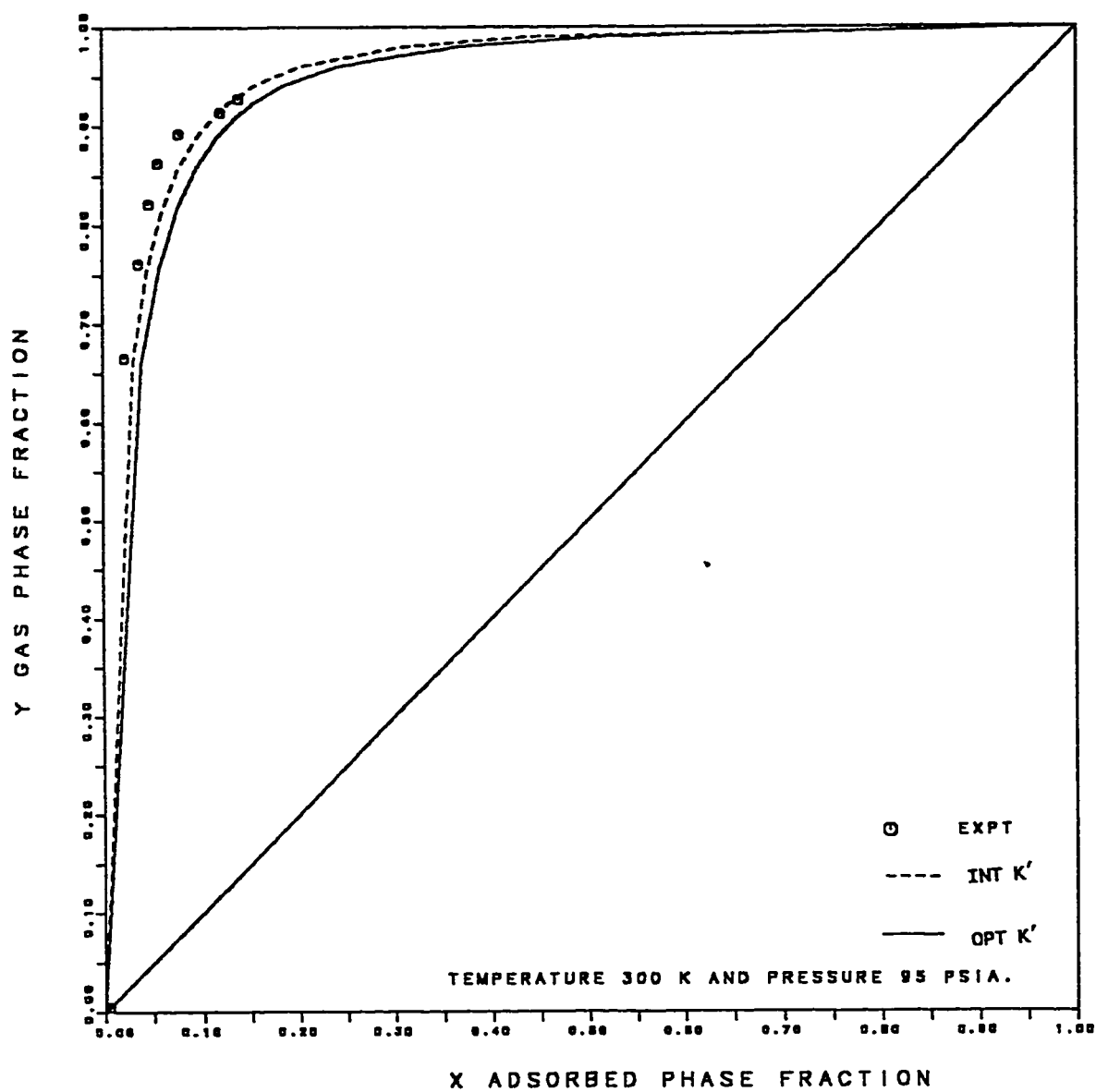
6.17: X-Y Plot of Methane-Ethane Binary on Linde 13X Pellets: Fit of Ruthven Model With Optimized and Intrinsic Henry Constant at 50 PSIA.



6.18: X-Y Plot of Methane-Ethane Binary on Linde 13X Pellets: Fit of Ruthven Model With Optimized and Intrinsic Henry Constant at 95 PSIA.



6.19: X-Y Plot of Methane-Propane Binary on Linde 13X Pellets: Fit of Ruthven Model With Optimized and Intrinsic Henry Constant at 50 PSIA.



6.20: X-Y Plot of Methane-Propane Binary on Linde 13X Pellets: Fit of Ruthven Model With Optimized and Intrinsic Henry Constant at 95 PSIA.

LITERATURE CITED

1. Hamad, E.D.K., "Comparision of Binary Adsorption of Propane and n-Butane on 5A and 13X Molecular sieves", M.S Thesis, KFUPM (1984).
2. Kaul, B.K., "A Modern Version of the Volumetric Apparatus for Measuring Gas Solid Equilibrium Data", Paper Presented at the AIChE Fall Meeting, San Francisco (1984).
3. Rolniak, P., and R. Kobayashi, "Adsorption of Methane and Several Mixtures", AIChE J., 26, 4, 616 (1980).
4. Hasanain, M.A. and K.F. Loughlin, "Demethanization of Natural Gas by Pressure Swing Adsorption", KACST Project No AR-6-147 Report # 4, April (1987).

CHAPTER 7

CONCLUSIONS AND RECOMMENDATION

7.1: Conclusions:

Pure and multicomponent equilibrium adsorption data for light n-alkanes on Linde 5A, S-115, and 13X adsorbents have been experimentally determined at 275, 300, 325 and 350°K up to pressures of 250 psia where possible. Six different pure component isotherm models have been used to analyse the data. Two multicomponent isotherms are used to model the multicomponent data.

The virial isotherm of Barrer and Lee (1) is used to determine the intrinsic Henry constant. With the exception of n-butane data, the intrinsic Henry constants derived from virial plots are comparable with reported literature values for 5A (2) and for 13X (3). The exception for n-butane is due to the high pressure apparatus. To measure the n-butane intrinsic Henry constant accurately, a high vacuum low pressure apparatus is required. Intrinsic Henry constants for silicalite have also been determined but no literature sources have been located for comparison purposes.

The heats of adsorption as determined from the intrinsic Henry constants and available literature data using the Van't Hoff plot are given

in Table 7.1 for all adsorbents. The values are comparable for each of the adsorbents, with the heat of adsorption of ethane, propane, and n-butane being the greatest on silicalite.

Table 7.1: Calculated Heats of Adsorption (Kcal/mole) for Light Alkanes on Different Adsorbents

Sorbate	5A	13X	S-115
Methane	5.41	4.02	4.87
Ethane	7.45	5.37(b)	7.83
Propane	7.60	7.86	9.52
n-Butane	10.28(a)	10.62(c)	11.53

(a) Ref (2), (b) Ref (3), (c) Ref (4)

Theoretical saturation concentrations N_0 were calculated for each of the adsorbents using the pore volume and the adsorbate density, considered as a highly compressed liquid. The formula provided by Dubinin (8) was used to evaluate the density by linear interpolation between the adsorbate density and the Van der waal's b . There is no indepth study of molar densities of adsorbates in adsorbents at present, and so it is difficult to state categorically that the N_0 values theoretically calculated are exact. However an estimate of their accuracy may be deduced

using Ruthven's isotherm which is a function of intrinsic Henry constant and molecular volume only. In chapter 4, the molecular volumes were optimized in the Ruthven's isotherm, the optimized values being comparable to the theoretical equation given by Dubinin with the exception of methane which was 36% lower. Similar results were reported by Rolniak and Kobayashi (6) for methane on 5A. The molar density and molar volume are related by the expression

$$\rho = \frac{1660}{\beta} \quad (7.1)$$

The saturation concentration N_o calculated using the optimized β are comparable to the theoretical N_o 's except for methane which is 36% lower. Hence we can conclude that the theoretically estimated N_o are reasonable with the possible exception of methane.

The pure component data was modelled using five different simple models:

- 1) Three 3 parameter models (LRC, Toth, and Mathews and Weber). The parameters were K , N_o and n .
- 2) One 4 parameter model (Jaroniec). The parameters were K , N_o , m and n .
- 3) One 2 parameter model (Ruthven). The parameters were K' , and β or (N_o).

For the 5A pellets, of the three parameter models the Mathews and Weber and the Toth models using optimized K , N_0 , and n values matched the data reasonably well. However, the optimized K and N_0 for the Toth model are in closer agreement with the intrinsic K and theoretical N_0 than those of the Mathews and Weber model, suggesting that the Toth model is the superior three parameter model. The four parameter Jaroniec model did not give any significant improvement over the Toth model and so its use is probably not justified. The more complex two parameter Ruthven model gave analogous results to the Toth model.

The four simple models (LRC, Toth, Mathews and Weber, Jaroniec) fitted the data for the light alkanes sorbing on S-115 silicalite quite well. However the more complex Ruthven model did not. This is probably a reflection of the fact that the Ruthven isotherm was derived for discrete cavities whereas the S-115 silicalite system consists of an inter-connecting chain of tubular cavities and as such does not fulfil one of the assumptions in the development of the Ruthven isotherm. It is difficult to discriminate between the four simple isotherms as to which gives the best fit. Considering only the least sum of squares criterion the Mathews and Weber isotherm is best. However, considering the intrinsic K , Theoretical N_0 and least sum of squares the use of the Toth isotherm with parameters as given in Table 5.7 appears the most appropriate.

Due to consumption of both ethane and n-butane cylinders only pure component measurements for methane and propane on Linde 13X zeolite were performed. All the simple models fitted the methane data quite reasonably but none fitted the propane data well. The most reasonable fits for propane were obtained with both the LRC and Toth models but even for both these models the optimized K value was at least twice the intrinsic and optimized N_0 value about 80% of theoretical. We conclude that the Toth model is the best of the simple models. The more complex Ruthven model was approximately equivalent to the simple models in that the value of optimized K was three times the intrinsic and the theoretical value of β was approached for propane.

To model the multicomponent data for 5A and 13X zeolite the multicomponent form of the Ruthven isotherm was developed. For S-115 silicalite the multicomponent form of the Toth isotherm was used.

Using the intrinsic K' value for 5A zeolite the binary data was satisfactorily modelled. However the ternary and quaternary data could only be satisfactorily modelled when the maximum permitted number of n-butane molecules was reduced from 4 to 3. This is probably a reflection of an excess volume limitation when three or four components are together. The optimized K' values were used to model the multicomponent data for 13X. The binary fit was again satisfactory but again the maximum number of molecules permitted in a cage had to be reduced for

the ternary and quaternary systems. The fit of the multicomponent Toth model to the S-115 data was excellent for both binary and ternary systems but low for the quaternary system.

From the analysis of multicomponent data the light alkanes can easily be separated using any of the adsorbents employed in this study. Considering equilibrium only the separation of methane is higher in S-115 than in either 13X or 5A.

7.2: Recommendations:

There should be a renewed equation for the liquid density for gases away above the critical temperature. The three parameter simple equations can be tested for other non-polar sorbate-sorbent systems and the four parameter Jaroniec model can be tested for polar sorbates.

The equipment design in this study can be used for the measurement of any high temperature and pressure, pure and multicomponent equilibrium adsorption data for other sorbates, as such data are in scarce in the literature (7). These data are necessary for the design of adsorption processes in the industrial gas separation.

More pure and multicomponent equilibrium and kinetic data are needed for other gases on the S-115 and 13X adsorbents. The separation of ethylene from ethane can be studied using S-115 pellets.

There is a need for compilation of the critically evaluated adsorption equilibrium data, which could be similar to DECHEMA Series for Vapor-Liquid equilibrium data used extensively for distillation calculations. Pennsylvania State University, is making such efforts under grants from the American Petroleum Institute (7).

LITERATURE CITED

1. Barrer, R.M., and J.A. Lee, *Surface Sci.*, 12, 354 (1968).
2. Ruthven, D.M., and K.F. Loughlin, *J. Chem. Soc., Faraday Trans. 1*, 68, 696 (1972).
3. Kaul, B.K., "A Modern Version of the Volumetric Apparatus for Measuring Gas Solid Equilibrium Data", Paper Presented at the AIChE Fall Meeting, San Francisco (1984).
4. Hamad, E.D.K., "Comparison of Binary Adsorption of Propane and n-Butane on 5A and 13X Molecular sieves", M.S Thesis, KFUPM (1984).
5. Stach, H., H. Thamm, J. Janchen, K. Fiedler and W. Schirmer, "Experimental and Theoretical Investigations of the Adsorption of n-Paraffins, n-Olefins and Aromatics on Silicalite", *Proceedings of the Sixth International Conference on Zeolites*,
6. Rolniak, P., and R. Kobayashi, "Adsorption of Methane and Several Mixtures of Methane and Carbon Dioxide at Elevated Pressures and Near Ambient Temperatures on 5A and 13X Molecular Sieves by Tracer Perturbation Chromatography", *AIChE J.*, 26, 4, 616 (1980).
7. Kaul, B.K. and N.H. Sweed, "Adsorption Equilibrium Data and Models Needs", *Fundamentals of Adsorption*, Edited by Myers, A.L. and G. Belfort, 239-248, published by AIChE, New York, (1984).
8. Dubinin, M.M., *Chem. Rev.*, 60, 235 (1960).

APPENDIX A

SOAVE-REDLICH-KWONG EQUATION OF STATE

The Soave-Redlich-Kwong (SRK) equation of state is given by

$$P = \frac{RT}{V - b} - \frac{a(T)}{V(V + b)} \quad (\text{A.1})$$

This can also be written in terms of compressibility as

$$Z^3 - Z^2 + (A - B - B^2)Z - AB = 0 \quad (\text{A.2})$$

$$\text{where } A = \frac{aP}{R^2T^2} \quad (\text{A.3})$$

$$\text{and } B = \frac{bP}{RT} \quad (\text{A.4})$$

At the critical point the usual restrictions for an inflection point apply
i.e.

$$\frac{\delta P}{\delta V} = \frac{\delta^2 P}{\delta^2 V} = 0$$

This leads to

$$a(T_c) = 0.42747 \frac{R^2 T_c^2}{P_c} \quad (A.5)$$

$$b(T_c) = 0.8664 \frac{RT_c}{P_c} \quad (A.6)$$

$$Z_c = \frac{1}{3} = 0.3333 \quad (A.7)$$

For other temperatures ($T \neq T_c$) Soave considered 'b' to be constant and for 'a' proposed an equation of the form

$$a(T) = a(T_c) \alpha(T) \quad (A.8)$$

where

$$\alpha(T) = \{1 + m[1 - \sqrt{T/T_c}]\}^2 \quad (A.9)$$

where m is correlated in terms of the acentric factor ω as

$$m = 0.480 + 1.574 \omega_i - 0.176 \omega_i^2 \quad (A.10)$$

The fugacity of a pure component (f_i) or of a component in a mixture (f_i) is given by

$$f_i = \phi_i P \quad (A.11)$$

$$f_i = \bar{\phi}_i P \quad (\text{A.12})$$

where ϕ_i is the fugacity coefficient for a pure component and $\bar{\phi}_i$ is the fugacity coefficient of a component in a mixture. These latter terms in the SRK equation are defined as

$$\ln \phi_i = (Z-1) - \ln(Z-B) - \frac{A}{B} \ln\left\{\frac{(Z+B)}{Z}\right\} \quad (\text{A.13})$$

and

$$\ln \bar{\phi}_i = \frac{B_i(Z-1)}{B} - \ln(Z-B) - \frac{A}{B} \left\{ A^* - \frac{B_i}{B} \right\} \ln\left\{\frac{(Z+B)}{Z}\right\} \quad (\text{A.14})$$

$$\text{where } A^* = 2\sqrt{A_i/A} \sum_{j=1}^N y_j \sqrt{A_j/A} \quad (\text{A.15})$$

and the mixing rules are

$$A = \sum_{i=1}^N \sum_{j=1}^N y_i y_j \sqrt{A_i A_j} \quad (\text{A.16})$$

$$B = \sum_{i=1}^N y_i B_i \quad (\text{A.17})$$

Using these equations the fugacity and molar density of the gas phase can be calculated to determine the moles adsorbed.

APPENDIX B

COMPUTER PROGRAMS FOR PURE AND MULTICOMPONENT DATA

The regression of pure component data is done on the CALCOMP plotter using subroutine BSOLVE which uses Marquadt's algorithm for the Optimization of non-linear parameters using a suitably chosen convergence criterion. The model Equation is given in the subroutine FUNC . The program for the LRC model is given here. The parameters are estimated by giving them minimum, maximum limits and some initial value. The input parameters are:

- KK = the number of parameters in the model
- B = initial guess of parameters (array)
- BMIN = minimum value of parameters (array)
- BMAX = maximum value of parameters (array)
- Y = an array of Y-axis (experimental conc)
- Z = an array of Z-axis (theoretical prediction)

Using the initial vector B, a function PH is calculated which is systematically reduced to a minimum value by varying B in the prescribed Marquadt method. At the minimum, the total sum of squares, and the experimental and theoretical profiles are plotted to indicate the agreement between theory and experiment.

The Conversion Factor for the Ruthven model are

For Linde 5A pellets:

1 millimoles/gm pellet = 2.22 molecules/cage

For Linde 13X pellets:

1 millimoles/gm pellet = 2.095 molecules/cage

```

C
C   ISOTHERM LOADING RATIO CORRELATION
C
C
C   ### DATA STRUCTURE SECTION ###
C
C   DIMENSION XARRAY(100),YARRAY(100),ZARRAY(100)
C   DIMENSION YY(6),A(2),B(2),WARRAY(100),ZZARRAY(100)
C   NUMBER OF DATA SETS
C   DATA INDEX1,INDEX2/4,4/
C   SCALING OF THE PLOT
C   DATA XDIST,YDIST,XCYCLE,YDVAL/16.,16.,3, 0.20/
C   DATA XFIRST,XLAST,YFIRST,YLAST/0.01,100.,0.0,3.2/
C   DATA A/-0.7,0.3/
C   DATA B/-0.4,0.2/
C   ### FORMAT STATEMENTS ###
C
C   5   FORMAT(22X,3(F10.5,1X))
C   10  FORMAT(F6.2,2X,I2)
C   11  FORMAT(F6.2,2X,I2)
C   15  FORMAT(2X,3(F10.4,2X))
C   16  FORMAT(9X,F10.4,2X)
C   20  FORMAT(55X,2(F10.5))
C
C   INITIALISE THE PLOTTER AND GIVE NUMBER FOR OUTPUT.
C
C   CALL PLOTS ( 0 , 0 , 1 )
C
C   MOVE THE PEN TO (5.0 , 5.0) , TO ENSURE THAT X=0 AND Y=0 ARE BOTH
C   5 CMS AWAY FROM THE LIMITS OF THE PLOT , AND RESET THE ORIGIN.
C   DRAW BOUNDARIES OF FIGURE.
C
C   CALL PLOT ( 3.0 , 8.0 , -3 )
C   CALL PLOT ( XDIST , 0.0 , 2)
C   CALL PLOT ( XDIST , YDIST , 2)
C   CALL PLOT ( 0.0 , YDIST , 2)
C   CALL PLOT ( 0.0 , 0.0 , 2)
C
C   ### SET UP SCALE FACTORS  FOR X AND Y AXIS ###
C
C   ### CARD SCALE IS NOT NECESSARY ONCE YARRAY(NP+1) & YARRAY(NP+2) ARE
C   DEFINED ###
C
C   NP=2
C   XARRAY(1)=XFIRST
C   XARRAY(2)=XLAST
C   CALL SCALG ( XARRAY(1),XDIST,NP, 1 )
C   XO=XARRAY(NP+1)
C   XS=XARRAY(NP+2)
C   YARRAY(1)=YFIRST
C   YARRAY(2)=YLAST
C   CALL SCALE(YARRAY(1),YDIST,NP,1)
C   YO=YARRAY(NP+1)

```

```

YS=YDVAL

C   YS=YARRAY(NP+2)
C
C   STARTING AT (0,0) , PLOT THE X-AXIS XDIST CMS LONG , AT 0 DEGREES ,
C   PLACING THE ANNOTAION ON THE CLOCKWISE SIDE OF THE AXIS , AND USING
C   THE VALUES CALCULATED BY 'SCALE' TO LABEL THE TICK MARKS
C
C   CALL LBAXS( 0.0 , 0.0 ,11H           , -11 ,XDIST,0.,XFIRST,XS)
C   POSX=XDIST/2.-3.0
C   CALL SYMBOL(POSX,-1.6,0.40,14HFUGACITY(Psia), 0.,14)
C
C   PLOT A SIMILAR Y-AXIS , YDIST CMS LONG , AT 90 DEGREES WITH THE
C   ANNOTATION ON THE COUNTER-CLOCKWISE SIDE.
C
C   CALL AXIS ( 0.0 , 0.0 , 11H           , 11 ,YDIST , 90. ,
C   +           YFIRST, YS)
C   +           YFIRST, YARRAY(NP+2))
C   POSY=YDIST/2.-4.0
C   CALL SYMBOL(-1.5,POSY,0.40,30HCONCENTRATION(MMOLE/GM PELLET),
C   +90.,30)
C
C   ### INPUT EXPERIMENTAL DATA POINTS ###
C
C   ### XARRAY IS THE EQUILIBRIUM PRESSURE
C   ### YARRAY IS THE EQUILIBRIUM ADSORBED PHASE CONCENTRATION
C   DO 1000 I2=1,INDEX1
C   READ(5,* )TEMP
C   I1=1
100  READ(5,5)XXX,YYY
C   IF(XXX.LT.0.0)GO TO 120
110  XARRAY(I1)=XXX
C   YARRAY(I1)=YYY
C   WRITE(6,15)XXX,YYY
C   I1=I1+1
C   GO TO 100
120  NP=I1-1
C   CALL MODEL(XARRAY,YARRAY,TEMP,NP,ZARRAY)
C   ### ZARRAY IS THE THEORETICAL ADSORBED PHASE CONCENTRATION
C   IF(I2.GT.1)GO TO 200
C
C   ### RESET NP+1 AND NP+2 POINTS SIMILAR FOR ALL SETS OF DATA ###
C
200  CONTINUE
C   XARRAY(NP+1)=XO
C   XARRAY(NP+2)=XS
C   YARRAY(NP+1)=YO
C   YARRAY(NP+2)=YS
C   ZARRAY(NP+1)=YO
C   ZARRAY(NP+2)=YS
C
C   ### PLOT DATA POINTS ###
C

```

```

      CALL LGLIN(XARRAY,YARRAY,NP,1,-1,I2,-1)
300  CONTINUE
C
C   ### RESET NP+1 & NP+2 POINTS SIMILAR FOR ALL SETS OF DATA ###
C
      XARRAY(NP+1)=XO
      XARRAY(NP+2)=XS
      ZARRAY(NP+1)=YO
      ZARRAY(NP+2)=YS
      DO 660 JK=1,NP
      WARRAY(JK)=ALOG10(XARRAY(JK))
660  CONTINUE
      WARRAY(NP+1)=ALOG10(XARRAY(NP+1))
      WARRAY(NP+2)=XS
C   ### PLOT THE THEORETICAL CURVES #####
C   CALL DOTTED(WARRAY,ZARRAY,NP,3)
      CALL FLINE (WARRAY,ZARRAY,-NP,1,0,3)
C
C   ### LABEL LEGENDS ETC ###
C
      CALL NUMBER(XDIST-2.5,YDIST-7.-0.5*I2,0.3,TEMP,0.0,-1)
      CALL SYMBOL(XDIST-1.0,YDIST-6.9-0.5*I2,0.3,I2,0.0,-1)
1000 CONTINUE
C
C   ### WRITE CHART NOTES ###
      CALL SYMBOL(XDIST-2.5,YDIST-7.,0.30,34HLEGEND
#           ,0.0,34)
      CALL SYMBOL(1.0, YDIST-0.5,      0.3,34HPARAMETER IS TEMPERATURE IN
# KELVIN,0.,34)
      CALL SYMBOL(-2.0,-2.5,0.30,70HFIG.6.5 PROPANE ISOTHERMS ON 13X PEL
#LETS FIT OF LRC MODEL              ,0.,70)
      CALL SYMBOL(-2.0,-3.2,0.30,70H      WITH THEORETICAL NO, AND OPT
#IMISED K.                          ,0.,70)
C
C   MOVE CARRIAGE , WITH PEN UP , TO (20,0) , RESET ORIGIN FOR THE
C   NEXT GRAPH , AND END LOOP.
C
C   ### CALL PLOT FOR CALCOPM PLOTTER
C   CALL PLOT ( 20.0 , -5.0 , 999 )
C   ### CALL CRPSEG FOR 3812 PAGE PRINTER
      CALL CRPSEG ('C3LRCOKA',70,70)
      CONTINUE
      STOP
      END
C
C   ### SUBROUTINE MODEL IS FOR CALCULATING THE THEORETICAL CURVES ###
C   ### BY OPTIMIZING THE PARAMETERS. ###
C
      SUBROUTINE MODEL(XX,YY,TT,NL,Z)
      DIMENSION P(200),A(20,20),AC(20,20),X(100),B(10),XX(100)
      *,YY(100),Z(100),Y(100),BV(10),BMIN(10),BMAX(10)
      *,PRE(100),C(100)
      REAL NO

```

```

COMMON X,TEMP,BETA
EXTERNAL FUNC

C
C   DATA FOR CALCULATING THEROTICAL SATURATION CONCENTRATION
C METHANE
C   DATA VM,TB,TC,VANB,ROHC/37.307,111.7,191.0,42.78,1.27/
C ETHANE
C   DATA VM,TB,TC,VANB,ROHC/53.693,184.6,305.4,63.80,1.27/
C PROPANE
C   DATA VM,TB,TC,VANB,ROHC/76.024,231.1,370.4,84.45,1.27/
C N-BUTANE
C   DATA VM,TB,TC,VANB,ROHC/96.066,272.7,425.1,122.6,1.27/
C   DO 1001 IN=1,4
C   R=1.987
C
C   TEMP=TT
C   NN=NL
C
C ### CALCULATE THE THEROTICAL SATURATION CONCENTRATION ###
C
C   LIQVOL = VM + (TEMP-TB)/(TC-TB)*(VANB-VM)
C   NO FOR 5A ZEOLITE.
C   NO = 216./LIQVOL
C   NO FOR S115 ZEOLITE.
C   NO = 152.0/LIQVOL
C   NO FOR 13X ZEOLITE.
C   NO = 236.8/LIQVOL
C   NUMBER OF PARAMETERS
C   KK=3
C
C
C ### HENRY'S CONSTANT FOR METHANE ON 5A.
C (IN MILLILOLES/GM PELLET)
C   IF (TT.EQ.275) HK = 0.09804
C   IF (TT.EQ.300) HK = 0.0474
C   IF (TT.EQ.325) HK = 0.0273
C   IF (TT.EQ.3100) HK = 0.01667
C
C   HENRY'S CONSTANT FOR ETHANE ON 5A.
C
C   IF (TT.EQ.275) HK = 1.2200
C   IF (TT.EQ.300) HK = 0.7692
C   IF (TT.EQ.325) HK = 0.2083
C   IF (TT.EQ.3100) HK = 0.0571
C
C   HENRY'S CONSTANT FOR PROPANE ON 5A.
C
C   IF (TT.EQ.275) HK = 35.088
C   IF (TT.EQ.300) HK = 6.667
C   IF (TT.EQ.325) HK = 3.922
C   IF (TT.EQ.3100) HK = 1.6667
C
C   HENRY'S CONSTANT FOR N-BUTANE ON 5A.

```

```

C
C IF (TT.EQ.275) HK = 7.143
C IF (TT.EQ.300) HK = 3.846
C IF (TT.EQ.325) HK =
C IF (TT.EQ.350) HK = 1.905
C
C HENRY'S CONSTANT FOR METHANE ON S115.
C
C IF (TT.EQ.275) HK = 0.14490
C IF (TT.EQ.300) HK = 0.064100
C IF (TT.EQ.325) HK = 0.03390
C IF (TT.EQ.350) HK = 0.02170
C
C HENRY'S CONSTANT FOR ETHANE ON S115.
C
C IF (TEMP.EQ.275) HK = 5.55556
C IF (TEMP.EQ.300) HK = 1.7240
C IF (TEMP.EQ.325) HK = 0.5230
C IF (TEMP.EQ.350) HK = 0.2780
C
C HENRY'S CONSTANT FOR PROPANE ON S115.
C
C IF (TT.EQ.275) HK =
C IF (TEMP.EQ.300) HK = 16.6667
C IF (TEMP.EQ.325) HK = 5.5556
C IF (TEMP.EQ.350) HK = 1.695
C
C HENRY'S CONSTANT FOR N-BUTANE ON S115.
C
C IF (TT.EQ.275) HK =
C IF (TEMP.EQ.300) HK = 90.9090
C IF (TEMP.EQ.325) HK = 28.570
C IF (TEMP.EQ.350) HK = 5.5556
C
C HENRY'S CONSTANT FOR METHANE ON 13X.
C
C IF (TT.EQ.275) HK = 0.07575
C IF (TT.EQ.300) HK = 0.037730
C IF (TT.EQ.325) HK = 0.02270
C IF (TT.EQ.350) HK = 0.01575
C
C HENRY'S CONSTANT FOR PROPANE ON 13X.
C
C IF (TT.EQ.275) HK = 22.620
C IF (TT.EQ.300) HK = 5.7700
C IF (TT.EQ.325) HK = 2.3200
C IF (TT.EQ.350) HK = 1.016
C ### READ INITIAL GUESSES OF PARAMETERS ###
C B(1)=NO
C B(2)=HK/NO
C B(3)=1.8
C

```


X

```
C    READ IN LIMITS ON PARAMETERS
C
    BMIN(1)=NO
    BMIN(2)=0.1
    BMIN(3)=1.6
    BMAX(1)=NO
    BMAX(2)=10
    BMAX(3)=1.90
C
    DO 110 I=1,NN
C
C    X(I) = INDEPENDENT VARIABLE PRESSURE IN PSIA
C
C    Y(I) = DEPENDENT VARIABLE CONCENTRATION IN MILIMOLES/GM PELLET
C
    X(I)=XX(I)
    Y(I)=YY(I)
110 CONTINUE
    FNU=0.0
    FLA=0.0
    TAU=0.0
    EPS=0.0
    PHMIN=0.0
    I=0
    KD=KK
    FV=0.0
    DV=0.
    DO 100 J=1,KK
    BV(J)=1
100 CONTINUE
    ICON=KK
    ITER=0
    WRITE(6,01)
01  FORMAT(10X,'COMPONENT USED IS N-BUTANE & ZEOLITE 5A  THEORETICAL
* NO AND OPTIMISED K. ')
    WRITE(6,02)
02  FORMAT(10X,'BSOLVE REGRESSION ALGORITHM')
C
200 CALL BSOLVE(KK,B,NN,Z,Y,PH,FNU,FLA,TAU,EPS,PHMIN,I,ICON,FV,DV,BV
*,BMIN,BMAX,P,FUNC,KD,A,AC,GAMM)
C
    ITER=ITER+1
    WRITE(6,03) ICON,PH,ITER
03  FORMAT(/,2X,'ICON=',I3,4X,'PH=',E15.8,4X,'ITERATION NO.=' ,I3)
    IF(ICON) 10,300,200
10  IF(ICON+1) 20,60,200
20  IF(ICON+2) 30,70,200
30  IF(ICON+3) 40,80,200
40  IF(ICON+4) 100,90,200
50  GO TO 95
60  WRITE(6,04)
04  FORMAT(/,2X,'NO FUNCTION IMPROVEMENT POSSIBLE')
    GO TO 300
```

```

70 WRITE(6,05)
05 FORMAT(//,2X,'MORE UNKNOWN THAN FUNCTIONS')
   GO TO 300
80 WRITE(6,06)
06 FORMAT(//,2X,'TOTAL VARIABLES ARE ZERO')
90 WRITE(6,07)
07 FORMAT(//,2X,'CORRECTIONS SATISFY CONVERGENCE REQUIREMENTS BUT
   *LAMDA FACTOR (FLA) STILL LARGE')
   GO TO 300
95 WRITE(6,08)
08 FORMAT(//,2X,'THIS IS NOT POSSIBLE')
   GO TO 300
300 WRITE(6,09)
09 FORMAT(//,2X,'SOLUTION OF THE EQUATION')
   DO 400 J=1, KK
   WRITE(6,11) J, B(J)
C   WRITE(7,11) J, B(J)
C   WRITE(8,11) J, B(J)
11 FORMAT(/,2X,'B(',I2,')=' ,E16.8)
400 CONTINUE
   WRITE(6,12) TEMP
12 FORMAT(//,9X,'ISOTHERM TEMPERATURE =' ,2X,F6.2,4X,'DEGREES KELVIN')
   WRITE(6,13)
13 FORMAT(//,10X,'B(1) IS SATURATION CONCENTRATION (QS) MMOLES/GM PEL
&LET',//,10X,'B(2) IS OPTIMISED HENRY"S CONSTANT /PSIA '
& //10X,'B(3) IS CONSTANT N ')
   WRITE(6,14)
14 FORMAT(15X,//,5X,
& //,5X,'FUGACITY',2X,'EXPT CONC',6X,'CALCULATED CONC',/
&,7X,'PSIA',3X,'MOLECULES/CAVITY',1X,'MOLECULES/CAVITY')
   WRITE(6,15) (X(JJ), Y(JJ), Z(JJ), JJ=1, NN)
15 FORMAT(//22X, //3(F10.5, 1X))
C 15 FORMAT(//1X, //(1X, 3F15.5))
C   WRITE(6,16) (Z(JJ), JJ=1, NN)
C 16 FORMAT(10X, 'Z(JJ)=' , F10.5)
C
1001 CONTINUE
1000 RETURN
   END
C
   SUBROUTINE FUNC(KK,B,NN,Z,FV)
C ### KK NUMBER OF PARAMETERS ###
C ### NN NUMBER OF DATA POINTS ###
C ### B PARAMETERS ARRAY ###
C ### Z THEORETICAL CONCENTRATION ARRAY ###
C
   DIMENSION X(100), Y(100), B(10), AKP(100), Z(100)
   COMMON X, TEMP, BETA
   DO 100 JJ=1, NN
   EK = B(2)
C   WRITE(6,*) EK
   AKP(JJ)=(EK*X(JJ))**(1/B(3))
C   -----

```

```

      Z(JJ)=B(1)*(AKP(JJ)/(1+AKP(JJ)))
C -----
100 CONTINUE
    RETURN
    END

C
C
C
    SUBROUTINE DERIV(KK,B,Z,P,FV,DV,J,JTEST)
    DIMENSION Z(5),P(10),DV(10),B(10)
    RETURN
    END

C
C
    SUBROUTINE BSOLVE(KK,B,NN,Z,Y,PH,FNU,FLA,TAU,EPS,PHMIN,I,ICON
*,FV,DV,BV,BMIN,BMAX,P,FUNC,KD,A,AC,GAMM)
C
    DIMENSION P(200),A(10,10),AC(10,10),X(100),B(10)
*,Z(100),Y(100),BV(10),BMIN(10),BMAX(10)
C
    K=KK
    N=NN
    KP1=K+1
    KP2=K+2
    KBI1=K*N
    KBI2=KBI1+K
    KZI=KBI2+K
    IF(FNU.LE.0.)FNU=10.0
    IF(FLA.LE.0.)FLA=0.01
    IF(TAU.LE.0.)TAU=0.001
    IF(EPS.LE.0.)EPS=0.00002
    IF(PHMIN.LE.0.)PHMIN=0.
120 KE=0
130 DO 160 I1=1,K
160 IF(BV(I1).NE.0.) KE=KE+1
    IF(KE.GT.0) GO TO 170
162 ICON=-3
163 GO TO 2120
170 IF(N.GE.KE) GO TO 500
180 ICON=-2
190 GO TO 2120
500 I1=1
530 IF(I.GT.0) GO TO 1530
550 DO 560 J1=1,K
    J2=KBI1+J1
    P(J2)=B(J1)
    J3=KBI2+J1
560 P(J3)=ABS(B(J1))+1.E-2
    GO TO 1030
590 IF(PHMIN.GT.PH.AND.I.GT.1)GO TO 625
    DO 620 J1=1,K
    N1=(J1-1)*N
    IF(BV(J1)) 601,620,605

```

```

601 CALL DERIV(K,B,N,Z,P(N1+1),FV,DV,J1,JTEST)
    IF(JTEST.NE.(-1)) GO TO 620
    BV(J1)=1.0
605 DO 606 J2=1,K
    J3=KBI1+J2
606 P(J3)=B(J2)
    J3=KBI1+J1
    J4=KBI2+J1
    DEN=0.001*AMAX1(P(J4),ABS(P(J3)))
    IF(P(J3)+DEN.LE.BMAX(J1)) GO TO 55
    P(J3)=P(J3)-DEN
    DEN=-DEN
    GO TO 56
55 P(J3)=P(J3)+DEN
56 CALL FUNC(K,P(KBI1+1),N,P(N1+1),FV)
    DO 610 J2=1,N
    JB=J2+N1
610 P(JB)=(P(JB)-Z(J2))/DEN
620 CONTINUE

```

C

C SET UP CORRECTION EQUATIONS

C

```

625 DO 725 J1=1,K
    N1=(J1-1)*N
    A(J1,KP1)=0.
    IF(BV(J1)) 630,692,630
630 DO 640 J2=1,N
    N2=N1+J2
640 A(J1,KP1)=A(J1,KP1)+P(N2)*(Y(J2)-Z(J2))
650 DO 680 J2=1,K
660 A(J1,J2)=0.
665 N2=(J2-1)*N
670 DO 680 J3=1,N
672 N3=N1+J3
674 N4=N2+J3
680 A(J1,J2)=A(J1,J2)+P(N3)*P(N4)
    IF(A(J1,J1).GT.1.E-20) GO TO 725
692 DO 694 J2=1,KP1
694 A(J1,J2)=0.
695 A(J1,J1)=1.0
725 CONTINUE
    GN=0.
    DO 729 J1=1,K
729 GN=GN+A(J1,KP1)**2

```

C

C SCALE CORRECTION EQUATIONS

```

    DO 726 J1=1,K
726 A(J1,KP2)=SQRT(A(J1,J1))
    DO 727 J1=1,K
    A(J1,KP1)=A(J1,KP1)/A(J1,KP2)
    DO 727 J2=1,K
727 A(J1,J2)=A(J1,J2)/(A(J1,KP2)*A(J2,KP2))
730 FL=FLA/FNU

```

```

      GO TO 810
800  FL=FNU*FL
810  DO 840 J1=1,K
820  DO 830 J2=1,KP1
830  AC(J1,J2)=A(J1,J2)
840  AC(J1,J1)=AC(J1,J1)+FL
C
C SOLVE CORRECTION EQUATIONS
      DO 930 L1=1,K
      L2=L1+1
      DO 910 L3=L2,KP1
910  AC(L1,L3)=AC(L1,L3)/AC(L1,L1)
      DO 930 L3=1,K
      IF(L1-L3)920,930,920
920  DO 925 L4=L2,KP1
925  AC(L3,L4)=AC(L3,L4)-AC(L1,L4)*AC(L3,L1)
930  CONTINUE
C
      DN=0.
      DG=0.
      DO 1028 J1=1,K
      AC(J1,KP2)=AC(J1,KP1)/A(J1,KP2)
      J2=KBI1+J1
      P(J2)=AMAX1(BMIN(J1),AMIN1(BMAX(J1),B(J1)+AC(J1,KP2)))
      DG=DG+AC(J1,KP2)*A(J1,KP1)*A(J1,KP2)
      DN=DN+AC(J1,KP2)*AC(J1,KP2)
1028 AC(J1,KP2)=P(J2)-B(J1)
      COSG=DG/SQRT(DN*GN)
      JGAM=0
      IF(COSG)1100,1110,1110
1100 JGAM=2
      COSG=-COSG
1110 CONTINUE
      COSG=AMIN1(COSG,1.0)
      GAMM=ARCOS(COSG)*180./(3.14159265)
      IF(JGAM.GT.0)GAMM=180.-GAMM
1030 CALL FUNC(K,P(KBI1+1),N,P(KZI+1),FV)
1500 PHI=0.
      DO 1520 J1=1,N
      J2=KZI+J1
1520 PHI=PHI+(P(J2)-Y(J1))**2
      IF(PHI.LT.1.E-10)GO TO 3000
      IF(I.GT.0)GO TO 1540
1521 ICON=K
      GO TO 2110
1540 IF(PHI.GE.PH)GO TO 1530
C
C EPSILON TEST
1200 ICON=0
      DO 1220 J1=1,K
      J2=KBI1+J1
1220 IF(ABS(AC(J1,KP2))/(TAU+ABS(P(J2))).GT.EPS) ICON=ICON+1
      IF(ICON.EQ.0)GO TO 1400

```

```

C
C   GAMMA LAMBDA TEST
C
    IF(FL.GT.1.0.AND.GAMM.GT.90.0) ICON=-1
    GO TO 2105
C
C   GAMMA EPSILON TEST
C
1400 IF(FL.GT.1.0.AND.GAMM.LE.45.0) ICON=-4
    GO TO 2105
C
1530 IF(I1-2) 1531,1531,2310
1531 I1=I1+1
    GO TO (530,590,800),I1
2310 IF(FL.LT.1.0E8)GO TO 800
1320 ICON=-1
C
2105 FLA=FL
    DO 2091 J2=1,K
        J3=KBI1+J2
2091 B(J2)=P(J3)
2110 DO 2050 J2=1,N
        J3=KZI+J2
2050 Z(J2)=P(J3)
        PH=PHI
        I=I+1
2120 RETURN
3000 ICON=0
    GO TO 2105
C
    END
C
C   SUBROUTINE DOTTED(X,Y,N,KODE)
C -----
C ----- SUBROUTINE TO DRAW DOTTED LINES OF ALL KINDS
C ----- THE ROUTINE IS SIMILAR TO THE CALCOMP ROUTINE DASHLN
C ----- EXCEPT THAT THE NATURE OF THE DOTTING IS SPECIFIED BY
C ----- THE USER IN THE PARAMETER KODE.
C ----- IF THE CODE IS POSITIVE, IT IS RESOLVED INTO ITS DECIMAL
C ----- DIGITS. THESE IN CYCLIC ORDER STARTING FROM THE MOST
C ----- SIGNIFICANT, SPECIFY THE LENGTHS OF THE SEGMENTS IN THE
C ----- LINE. THESE SEGMENTS ARE TRACED WITH THE PEN ALTERNATING
C ----- DOWN AND UP.
C ----- THE DIGITS SPECIFY THE LENGTHS AS FOLLOWS:
C ----- 1-- 0.01 INCH
C ----- 2-- 0.02 INCH
C ----- 3-- 0.03 INCH
C ----- 4-- 0.05 INCH
C ----- 5-- 0.10 INCH
C ----- 6-- 0.15 INCH
C ----- 7-- 0.20 INCH
C ----- 8-- 0.25 INCH

```

```

C ----- 9-- 0.35 INCH
C ----- ZERO DIGITS ARE IGNORED.
C -----
C -----
C -----
C -----
C -----
C ----- IF KODE IS NEGATIVE OR ZERO, IT SPECIFIES A STANDARD
C ----- LINE TYPE, AS FOLLOWS:
C --- 0 OR A SOLID LINE
C --- -1 OR 4 A DOTTED LINE
C --- -2 OR A DASHED LINE
C --- -3 OR 9424 DASH-DOT LINE
C --- -4 OR 13 CLOSELY SPACED DOTTS
C --- -5 OR 14 SMALL DOTS MODERATE SPACING
C --- -6 OR 55955924 LONG DASH ALTERNATES WITH DASH-DOT-DASH
C --- -7 OR 6424, A DOT-SHORT DASH LINE
C --- -8 OR 64259524 LONG DASH ALTERNATES WITH DOT-DASH-DOT
C --- -9 OR 64 LINE OF SHORT DASHES
C --- -10 OR 248424 DOUBLE DOTS WITH DASHES
C --- -11 OR 24249424 TRIPLE DOTS WITH DASHES.
C --- -12 OR 2 VERY CLOSELY SPACED DOTS, NOT-USABLE WITH LIQUID INK
C --- IF KODE IS OUT OF RANGE IT IS REPLACED BY (-1), I.E. A
C --- DOTTED LINE
C --- THE LENGTH SETTING CAN BE ALTERED BY INVOKING THE SUBROUTINE
C --- AT THE ALTERNATE ENTRY POINT SETDOT(CHLTH) WHERE CHLTH IS A
C --- REAL ARRAY OF DIMENSION 9 CONTAINING THE NEW LENGTHS.
C ---
C ---
C ---
C ---
C ---
C ---
C ---
C ---
C -----
C DIMENSION X(1),Y(1)
C DIMENSION CODE(9),SLTH(10),CHLTH(9),LTYPE(12)
C DATA NTYPES/12/
C DATA LTYPE/4,95,9424,13,14,55955424,6424,64259524,
2 64,248424,24249424,2/
C DATA CODE/0.01,0.02,0.03,0.05,0.10,0.15,0.20,0.25,0.35/
C ---
C --- CALCOMP SCALING CONVENTIONS.
C ---
C X0=X(N+1)
C Y0=Y(N+1)
C DELTAX=X(N+2)
C DELTAY=Y(N+2)
C ---
C --- SET INITIAL COORDINATES
C ---

```

```

      XT=(X(1)-X0)/DELTAX
      YT=(Y(1)-Y0)/DELTAY
C ----
C ---- SET N1 TO KODE (IFKODE>0) OR LTYPE(-KODE) (IF KODE<0)
C ---- OR BRANCH TO DRAW A SOLID LINE (IF KODE=0).
C ----
      IF(KODE.EQ.0) GO TO 270
      N1=KODE
      IF(N1.GT.0) GO TO 110
      N1=-N1
      IF(N1.GT.NTYPES) GO TO 100
      N1=LTYPE(N1)
      GO TO 110
100    N1=14
C ----
C ---- FIND THE SEGMENTS IN THE PATTERN
C ----
110    LIM=0
120    IF(N1.LE.0) GO TO 160
      N2=N1/10
      N0=N1-10*N2
      IF(N0.EQ.0) GO TO 140
      LIM=LIM+1
      SLTH(LIM)=CODE(N0)
140    N1=N2
      GO TO 120
160    I=1
      J=LIM
      STEP=SLTH(J)
      DS=0.0
      CALL PLOT(XT,YT,3)
      IUPDN=2
      GO TO 2100
C ----
C ---- MAIN LOOP. WILL THE STEP OVERSHOOT THE TARGET?
C ----
220    IF(STEP.GT.DS) GO TO 240
C ----
C ---- IF NO THEN TAKE THE STEP
C ----
      XC=STEP*COSN+XC
      YC=STEP*SINE+YC
      CALL PLOT(XC,YC,IUPDN)
      IUPDN=5-IUPDN
      J=J-1
      IF(J.LE.0) J=LIM
      DS=DS-STEP
      STEP=SLTH(J)
      GO TO 220
C ----
C ---- IF YES THE STEP OVERSHOOTS THE TARGET THEN GO TO TERGET.
C ----
240    CALL PLOT(XT,YT,IUPDN)

```



```
STEP=STEP-DS
2100  I=I+1
      IF(I.GT.N) GO TO 290
C  ----
C  ---- SET NEW TARGET.
C  ----
      XC=XT
      YC=YT
      XT=(X(I)-X0)/DELTAX
      YT=(Y(I)-Y0)/DELTAY
      DX=XT-XC
      DY=YT-YC
      DS=SQRT(DX*DX+DY*DY)
      IF(DS.EQ.0.0) GO TO 2100
      COSN=DX/DS
      SINE=DY/DS
      GO TO 220
270  CALL PLOT(XT,YT,3)
      DO 280 I=2,N
      XT=(X(I)-X0)/DELTAX
      YT=(Y(I)-Y0)/DELTAY
280  CALL PLOT(XT,YT,2)
290  RETURN
      ENTRY SETDOT(CHLTH)
      DO 320 I=1,9
320  CODE(I)=CHLTH(I)
      RETURN
      END
```

```

C
C ### MAIN PROGRAM TO CALCULATE THE CONCENTRATION IN THE ADSORBED PHASE
C ### FOR QUATERNARY ADSORPTION USING RUTHVEN'S MULTICOMPONENT MODEL
C
  DIMENSION XC1(50),XC2(50),XC3(50),QDNOMR(50),HKP1(50),HKP2(50)
  DIMENSION XC4(50),QNUMR1(50),QNUMR2(50),QNUMR3(50),QNUMR4(50)
  DIMENSION HKP3(50),HKP4(50),QDNR4(50),P1(50),P2(50),P3(50),P4(50)
  REAL I,J,K,L
C
C ### DATA FOR THE LINDE 5A PELLETS.
C   DATA VOLC,M,N,O,P,CF/776.0,9,7,5,3,2.22/
C   DATA TEMP,HK1,HK2,HK3,HK4/300.0,0.122,1.8200,34.95,1385.00/
C ### DATA OF LINDE 13X PELLETS INTRINSIC HENRY CONSTANT ###
C   DATA VOLC,M,N,O,P,CF/822.0,9,7,6,4,2.095/
C   DATA TEMP,HK1,HK2,HK3,HK4/300.0,0.0789,0.7628,&12.088,408.583/
C ### DATA OF LINDE 13X PELLETS OPTIMIZED HENRY CONSTANT ###
C   DATA TEMP,HK1,HK2,HK3,HK4/300.0,0.1746,3.9565,46.468,822.000/

  1  FORMAT (////8X,'HK1',6X,'HK2',6X,'HK3',6X,'HK4'
    ,///13X,'(MOLECULES/CAVITY PSIA)')
  2  FORMAT (/8X,'PC1',6X,'PC2',6X,'PC3',6X,'PC4'
    ,//7X,'PSIA',5X,'PSIA',5X,'PSIA',5X,'PSIA')
  3  FORMAT (/7X,'    PARTIAL PRESSURES (PSIA)                CALCULATED
1CONCENTRATION (MMOLES/GM PELLETT)',2X,/,7X,
2' METHANE    ETHANE    PROPANE    N-BUTANE    METHANE    ETHANE    PROP
3ANE    N-BUTANE')
10  FORMAT (5X,4F10.4)
11  FORMAT (////5X,'BETA1    BETA2    BETA3    BETA4'//5X,4F10.4)
15  FORMAT (5X,8F10.5)
C
C ### DUBININ EQUATIONS FOR CALCULATING THEORETICAL MOLECULAR VOLUME ###
C ### BETA = VM + ((TEMP-TB)/(TC-TB)*(VM-B)) ###
C ### VM = MOLAR VOLUME AT TB, TB = NORMAL BOILING POINT ###
C ### TC = CRITICAL TEMPERATURE, B = VAN DER WAAL'S SECOND COEFFICIENT #
  BETA1 = 61.95+ ((TEMP-111.7)/(191.-111.7)*(71.04-61.95))
  BETA2 = 89.16+ ((TEMP-184.6)/(305.4-184.6)*(105.94-89.16))
  BETA3 = 126.24+ ((TEMP-231.1)/(370.-231.1)*(140.2-126.24))
  BETA4 = 159.52+ ((TEMP-272.7)/(425.1-272.7)*(203.58-159.52))
C ### READ IN PRESSURE AND GAS PHASE COMPOSITION ###
  II = 1
110  READ (5,*) PRESS,Y1,Y2,Y3,Y4
  IF (PRESS.LT.0.0) GO TO 150
  P1(II) = PRESS*Y1/100
  P2(II) = PRESS*Y2/100
  P3(II) = PRESS*Y3/100
  P4(II) = PRESS*Y4/100
C   WRITE (6,10)P1(II),P2(II),P3(II),P4(II)
  II = II+1
  GO TO 110
150  NN = II-1
C   DO 1000 HK4 = HK4,HK4+200,50
C   HK3=HK4/FACTOR
  WRITE (6,1)
C   WRITE (6,*)'TEMP = ',TEMP

```

```

WRITE (6,10)HK1, HK2, HK3, HK4
WRITE (6,11)BETA1, BETA2, BETA3, BETA4
C   WRITE (6,2)
   WRITE (6,3)
   DO 100 JJ=1, NN
   HKP1(JJ)=HK1*P1(JJ)
   HKP2(JJ)=HK2*P2(JJ)
   HKP3(JJ)=HK3*P3(JJ)
   HKP4(JJ)=HK4*P4(JJ)
C   QNUMR(JJ)=HKP1(JJ)
   QNUMR1(JJ)=HKP1(JJ)
   QNUMR2(JJ)=HKP2(JJ)
   QNUMR3(JJ)=HKP3(JJ)
   QNUMR4(JJ)=HKP4(JJ)
   QDNOMR(JJ)=1. + HKP1(JJ) + HKP2(JJ) + HKP3(JJ) + HKP4(JJ)
   DO 200 L=0, P
   DO 200 K=0, O
   DO 200 J=0, N
   DO 200 I=0, M
   SIJKL = I+J+K+L
   IF (SIJKL.LT.2) GO TO 200
   PIJKL = GAMMA(I+1)*GAMMA(J+1)*GAMMA(K+1)*GAMMA(L+1)
   SBETA = I*BETA1 + J*BETA2 + K*BETA3 + L*BETA4
   IF (SBETA.GT.VOLC) GO TO 200
   PHKP = (HKP1(JJ)**I)*(HKP2(JJ)**J)*(HKP3(JJ)**K)*(HKP4(JJ)**L)
   TERM= PHKP/PIJKL*(1-(SBETA/VOLC))**SIJKL
   QNUMR1(JJ)=QNUMR1(JJ)+TERM*I
   QNUMR2(JJ)=QNUMR2(JJ)+TERM*J
   QNUMR3(JJ)=QNUMR3(JJ)+TERM*K
   QNUMR4(JJ)=QNUMR4(JJ)+TERM*L
   QDNOMR(JJ)=QDNOMR(JJ)+TERM
200  CONTINUE
C   -----
   XC1(JJ)=QNUMR1(JJ)/QDNOMR(JJ)
   XC2(JJ)=QNUMR2(JJ)/QDNOMR(JJ)
   XC3(JJ)=QNUMR3(JJ)/QDNOMR(JJ)
   XC4(JJ)=QNUMR4(JJ)/QDNOMR(JJ)
C   -----
   XC1(JJ) = XC1(JJ)/CF
   XC2(JJ) = XC2(JJ)/CF
   XC3(JJ) = XC3(JJ)/CF
   XC4(JJ) = XC4(JJ)/CF
   WRITE(6,15)P1(JJ), P2(JJ), P3(JJ), P4(JJ), XC1(JJ), XC2(JJ), XC3(JJ),
&XC4(JJ)
   WRITE(8,15) XC1(JJ), XC2(JJ), XC3(JJ), XC4(JJ)
100  CONTINUE
   CALL TABLE(P1, P2, P3, P4, XC1, XC2, XC3, XC4)
1000 CONTINUE
   STOP
   END
C
C   SUBROUTINE TABLE(PC1, PC2, PC3, PC4, CC1C, CC2C, CC3C, CC4C)
C
C ###   SUBROUTINE IS TO CALCULATE THE MOLE FRACTION AND ###

```

```

C ### WRITE THE CONCENTRATION AND MOLE FRACTION IN TABLES. ###
C
C   USING RUTHVEN'S MULTICOMPONENT MODEL.
C
      DIMENSION CC1E(50),CC2E(50),CC3E(50),CC4E(50),CC1C(50),CC2C(50)
      DIMENSION XC1E(50),XC2E(50),XC3E(50),XC4E(50),XC1C(50),XC2C(50)
      DIMENSION CC3C(50),CC4C(50),Z(50),PC1(50),PC2(50),PC3(50),PC4(50)
      DIMENSION XC3C(50),XC4C(50)
C ### FORMAT SECTION
  2  FORMAT (/8X,'PC1',6X,'PC2',6X,'PC3',6X,'PC4'
    ,//7X,'PSIA',5X,'PSIA',5X,'PSIA',5X,'PSIA')
  3  FORMAT (2X,'PRESSURE P1   CALCULATED CONCENTRATION',
    ,2X,/,3X,'PSIA      MMOLES/GM PELLET')
10  FORMAT (5X,4F10.4)
12  FORMAT (8X,2F10.5)
15  FORMAT (12F10.4)
25  FORMAT (12F10.4)
      WRITE (6,2)
      I1 = 1
C ### READ IN EXPERIMENTAL ADSORBED PHASE CONCENTRATIONS ###
110  READ (5,*) X1,X2,X3,X4
      IF (X1.LT.0.0) GO TO 150
      CC1E(I1) = X1
      CC2E(I1) = X2
      CC3E(I1) = X3
      CC4E(I1) = X4
      I1 = I1+1
      GO TO 110
150  II = I1 -1
      WRITE (6,3)
      DO 111 JJ = 1,II
      SUMCAL = CC1C(JJ) + CC2C(JJ) + CC3C(JJ) + CC4C(JJ)
      XC1C(JJ)= CC1C(JJ)/SUMCAL
      XC2C(JJ)= CC2C(JJ)/SUMCAL
      XC3C(JJ)= CC3C(JJ)/SUMCAL
      XC4C(JJ)= CC4C(JJ)/SUMCAL
      SUMEXP = CC1E(JJ) + CC2E(JJ) + CC3E(JJ) + CC4E(JJ)
      XC1E(JJ) = CC1E(JJ)/SUMEXP
      XC2E(JJ) = CC2E(JJ)/SUMEXP
      XC3E(JJ) = CC3E(JJ)/SUMEXP
      XC4E(JJ) = CC4E(JJ)/SUMEXP
111  CONTINUE
      WRITE(6,15)(PC1(JK),PC2(JK),PC3(JK),PC4(JK),XC1E(JK),XC2E(JK)
&,XC3E(JK),XC4E(JK),XC1C(JK),XC2C(JK),XC3C(JK),XC4C(JK),JK = 1,II)
      WRITE(6,25)(PC1(JL),PC2(JL),PC3(JL),PC4(JL),CC1E(JL),CC2E(JL)
&,CC3E(JL),CC4E(JL),CC1C(JL),CC2C(JL),CC3C(JL),CC4C(JL),JL = 1,II)
      RETURN
      END

```

```

C
C ### MAIN PROGRAM TO CALCULATE AND PLOT THE BINARY RUTHVEN MODEL
C
C ### CHANGE THE BETA AND HK FOR DIFFERENT SYSTEM
C
C ### DATA STRUCTURE SECTION ###

      DIMENSION XARRAY(50),YARRAY(50),ZARRAY(50),YEARAY(50)
      DIMENSION YY(6),A(2),B(2),WARRAY(50),ZZARAY(50),CLINE(10)
      DATA INDEX1,INDEX2/2,1/
      DATA W,L/25.,15./
      DATA XDIST,YDIST,XDVAL,XCYCLE,YDVAL/20.,20.,0.05,3,.05/
      DATA XFIRST,XLAST,YFIRST,YLAST/0.0,1.,0.0,1./

      DATA A/-0.7,0.3/
      DATA B/-0.4,0.2/
      INTEGER COPY(3)/0,1,1/
C
C ### FORMAT STATEMENTS ###
C
5   FORMAT(10X,2F10.4,40X,F10.4,10X,F10.4)
10  FORMAT(F6.2,2X,I2)
11  FORMAT(F6.2,2X,I2)
12  FORMAT(F8.5,2X)
15  FORMAT(2X,5(F10.4,2X))
16  FORMAT(9X,F10.4,2X)
20  FORMAT(55X,2(F10.5))
C
C INITIALISE THE PLOTTER AND GIVE NUMBER FOR OUTPUT.
C
      CALL PLOTS ( 0 , 0 , 1 )
C
C MOVE THE PEN TO (5.0 , 5.0) , TO ENSURE THAT X=0 AND Y=0 ARE BOTH
C 5 CMS AWAY FROM THE LIMITS OF THE PLOT , AND RESET THE ORIGIN.
C DRAW BOUNDARIES OF FIGURE.
C
      CALL PLOT ( 3.0 , 8.0 , -3 )
      CALL PLOT ( XDIST , 0.0 , 2)
      CALL PLOT ( XDIST , YDIST , 2)
      CALL PLOT ( 0.0 , YDIST , 2)
      CALL PLOT ( 0.0 , 0.0 , 2)
C
C ### SET UP SCALE FACTORS FOR X AND Y AXIS ###
C
C ### CARD SCALE IS NOT NECESSARY ONCE YARRAY(NP+1) & YARRAY(NP+2) ARE
C DEFINED ###
C
      NP=2
      XARRAY(1)=XFIRST
      XARRAY(2)=XLAST
      CALL SCALE ( XARRAY(1),XDIST,NP, 1 )
      XO=XARRAY(NP+1)
      XS=XDVAL

```

```

YARRAY(1)=YFIRST
YARRAY(2)=YLAST
CALL SCALE(YARRAY(1),YDIST,NP,1)
YO=YARRAY(NP+1)
YS=YDVAL

C
C   STARTING AT (0,0) , PLOT THE X-AXIS XDIST CMS LONG , AT 0 DEGREES ,
C   PLACING THE ANNOTAION ON THE CLOCKWISE SIDE OF THE AXIS , AND USING
C   THE VALUES CALCULATED BY 'SCALE' TO LABEL THE TICK MARKS
      CALL AXIS ( 0.0 , 0.0 , 11H           , -11 , XDIST , 0.0 ,
+               XFIRST, XS)
      POSX=XDIST/2.-3.0
      CALL SYMBOL(POSX,-1.6,0.40,26HX ADSORBED PHASE FRACTION , 0.,26)
C
C   PLOT A SIMILAR Y-AXIS , YDIST CMS LONG , AT 90 DEGREES WITH THE
C   ANNOTATION ON THE COUNTER-CLOCKWISE SIDE.
      CALL AXIS ( 0.0 , 0.0 , 11H           , 11 , YDIST , 90. ,
+               YFIRST, YS)
C   +               YFIRST, YARRAY(NP+2))
      POSY=YDIST/2.-4.0
      CALL SYMBOL(-1.5,POSY,0.40,20HY GAS PHASE FRACTION,90.,20)
C
C   ### INPUT EXPERIMENTAL DATA POINTS ###
C
      DO 500 I2=1,INDEX1
C   ### CALL SUBROUTINE RUTVEN TO PLOT
C   ### YARRAY IS THE GAS PHASE FRACTION
C   ### XARRAY IS THE EXPERIMENTAL SORBED PHASE FRACTION
C   ### ZARRAY IS THE THEORETICAL SORBED PHASE FRACTION
      CALL RUTVEN (NP,YARRAY,XARRAY,ZARRAY)
      DO 111 II = 1,NP
      WARRAY(II)= YARRAY(II)
111  WRITE(6,15)NP,YARRAY(II),WARRAY(II),XARRAY(II),ZARRAY(II)
C
C   ### RESET NP+1 AND NP+2 POINTS SIMILAR FOR ALL SETS OF DATA ###
C
C 200 CONTINUE
      XARRAY(NP-4)=XO
      XARRAY(NP-3)=XS
      YARRAY(NP-4)=YO
      YARRAY(NP-3)=YS
      ZARRAY(NP+1)=XO
      ZARRAY(NP+2)=XS
      CLINE(1) = 0.0
      CLINE(2) = 0.25
      CLINE(3) = 0.5
      CLINE(4) = 0.75
      CLINE(5) = 1.0
      CLINE(6) = XO
      CLINE(7) = XS
C   ### CALL DOTTED TO DRAW CENTRAL LINE

```

```

      CALL DOTTED(CLINE,CLINE,5,3)
C
C   ### PLOT DATA POINTS ###
C
C      CALL FLINE(CLINE,CLINE,2,1,-1,0)
      N=NP-5
      XARRAY(1) = 0.0
      YARRAY(1) = 0.0
      CALL FLINE(XARRAY,YARRAY,N,1,-1,I2)
      WARRAY(NP+1)=YO
      WARRAY(NP+2)=YS
      ZARRAY(1) = 0.0
      ZARRAY(NP) = 1.0
      WARRAY(1) = 0.0
      WARRAY(NP) = 1.0
      CALL FLINE(ZARRAY,WARRAY,-NP,1,0,3)
300  CONTINUE
C
C   ### RESET NP+1 & NP+2 POINTS SIMILAR FOR ALL SETS OF DATA ###
C
      YARRAY(NP+1)=YO
      YARRAY(NP+2)=YS
      ZARRAY(NP+1)=XO
      ZARRAY(NP+2)=XS
      XARRAY(NP+2)=XS
999  CONTINUE
500  CONTINUE
      CALL SYMBOL(7.0, YDIST-19.5,      0.3,40HTEMPERATURE 300 K AND PRESS
      #URE 50 PSIA.  ,0.0,40)

      CALL SYMBOL(0.0,-2.5,0.30,75HFIG.      BINARY ADSORPTION OF ETHANE A
      #ND N-BUTANE ON 5A PELLETS              ,0.,75)
      CALL SYMBOL(0.0,-3.2,0.30,75H          FIT OF RUTHVEN MODEL.
      #                                         ,0.,75)
C
C   MOVE CARRIAGE , WITH PEN UP , TO (20,0) , RESET ORIGIN FOR THE
C   NEXT GRAPH , AND END LOOP.
C
C      CALL PLOT (20.0 ,-5.0 ,999 )
      CALL CRPSEG('BINC13X2',70,70)
      CONTINUE
      STOP
      END
C
C
C   SUBROUTINE RUTHVEN TO CALCULATE THE CONCENTRATION IN THE
C   ADSORBED PHASE USING RUTHVEN'S BINARY MODEL.
C
C   SUBROUTINE RUTVEN (NN,Y,XC1E,XC1C)
C
      DIMENSION C1(50),C2(50),XC1E(50),QDNOMR(50),HKP1(50),HKP2(50),
      1XC2E(50),QNUMR1(50),QNUMR2(50),QNUMR3(50),QNUMR4(50),XC1C(50),

```

```

2XC2C(50), HKP3(50), HKP4(50), QDNR4(50), P1(50), P2(50), Y(50), P4(50)
REAL I, J
INTEGER M, N
C ### DATA FOR LINDE 5A PELLETS
DATA VOLC, M, N, O, P, CF/776.0, 12, 12, 5, 3, 2.22/
DATA TEMP, HKC1, HKC2, HKC3, HKC4/300.0, 0.122, 1.820, 34.95, 1385.00/
C ### DATA FOR LINDE 13X PELLETS INTRINSIC HENRY CONSTANT
C DATA VOLC, M, N, O, P, CF/822.0, 12, 12, 5, 3, 2.095/
C
C DATA TEMP, HKC1, HKC2, HKC3, HKC4/300.0, 0.0789, 0.7628, 12.088, 408.583/
C
C ### DATA FOR LINDE 13X PELLETS OPTIMIZED HENRY CONSTANT
C DATA TEMP, HKC1, HKC2, HKC3, HKC4/300.0, 0.1746, 1.8628, 46.468, 822.00/
c ### MOLECULAR VOLUMES BETA'S
DATA B1, B2, B3, B4/83.53, 105.19, 133.16, 167.41/
C
C GIVE VALUES OF BETA AND HK
C
BETA1 = B2
BETA2 = B4
HK1 = HKC2
HK2 = HKC4
C
1 FORMAT (////8X, 'HK1', 6X, 'HK2', 6X, 'HK3', 6X, 'HK4'
, //13X, ' (MOLECULES/CAVITY PSIA) ')
2 FORMAT (/8X, 'PC1', 6X, 'PC2', 6X, 'PC3', 6X, 'PC4'
, //7X, 'PSIA', 5X, 'PSIA', 5X, 'PSIA', 5X, 'PSIA')
3 FORMAT (/7X, ' PARTIAL PRESSURES (PSIA) CALCULATED
1CONCENTRATION (MMOLES/GM PELLETS)', 2X, //, 7X,
2' METHANE ETHANE PROPANE N-BUTANE METHANE ETHANE PROP
3ANE N-BUTANE')
10 FORMAT (5X, 6F10.4)
11 FORMAT (////5X, 'BETA1 BETA2 BETA3 BETA4'//5X, 4F10.4)
15 FORMAT (5X, 8F10.5)
II = 1
110 READ (5, *) PRESS, Y1, Y2
IF (PRESS.LT.0.0) GO TO 150
P1(II) = PRESS*Y1/100
P2(II) = PRESS*Y2/100
Y(II) = P1(II)/(P1(II)+P2(II))
C P4(II) = PRESS*Y4/100
WRITE (6, 10) PRESS, Y1, Y2, P1(II), P2(II)
II = II+1
GO TO 110
150 NN = II-1
C HK4 = 80
WRITE (6, 1)
WRITE (6, 10) HK1, HK2
WRITE (6, 11) BETA1, BETA2
WRITE (6, 3)
DO 100 JJ=1, NN
HKP1(JJ)=HK1*P1(JJ)
HKP2(JJ)=HK2*P2(JJ)

```



```

QNUMR1(JJ)=HKP1(JJ)
QNUMR2(JJ)=HKP2(JJ)
QDNOMR(JJ)=1.+ HKP1(JJ) + HKP2(JJ)
DO 200 I=0,7
DO 200 J=0,4
SIJ = I+J
IF (SIJ.LT.2) GO TO 200
PIJ = GAMMA(I+1)*GAMMA(J+1)
SBETA = I*BETA1 + J*BETA2
IF (SBETA.GT.VOLC) GO TO 200
PHKP = (HKP1(JJ)**I)*(HKP2(JJ)**J)
TERM= PHKP/PIJ*(1-(SBETA/VOLC))**SIJ
QNUMR1(JJ)=QNUMR1(JJ)+TERM*I
QNUMR2(JJ)=QNUMR2(JJ)+TERM*J
QDNOMR(JJ)=QDNOMR(JJ)+TERM
200 CONTINUE
C -----
C1(JJ)=QNUMR1(JJ)/QDNOMR(JJ)
C2(JJ)=QNUMR2(JJ)/QDNOMR(JJ)
C -----
C1(JJ) = C1(JJ)/CF
C2(JJ) = C2(JJ)/CF
WRITE(6,15)P1(JJ),P2(JJ),C1(JJ),C2(JJ)

100 CONTINUE
CALL TABLE (P1,P2,XC1,XC2,XC1E,XC2E,XC1C,XC2C)
1000 CONTINUE
RETURN
END

C
C
C SUBROUTINE TO CALCULATE THE MOLE FRACTION IN THE ADSORBED PHASE
C
C SUBROUTINE TABLE(PC1,PC2,CC1C,CC2C,XC1E,XC2E,XC1C,XC2C)
C
C USING RUTHVEN'S MULTICOMPONENT MODEL.
C
C DIMENSION CC1E(50),CC2E(50),CC3E(50),CC1C(50),CC2C(50)
C DIMENSION XC1E(50),XC2E(50),XC3E(50),XC1C(50),XC2C(50),XC3C(50)
C DIMENSION CC3C(50),Z(50),PC1(50),PC2(50),PC3(50),PC4(50)
C DATA VOLC,M,N,O,P/776.0,12,12,5,3/
C DATA TEMP,HK1,HK2,HK3,HK4/300.0,0.146,2.1906,51.095,1200.67/

C
1 FORMAT (/8X,'HK1',6X,'HK2',6X,'HK3',6X,'HK4'
, /13X,'MOLECULES/CAVITY PSIA')
2 FORMAT (/8X,'PC1',6X,'PC2',6X,'PC3',6X,'PC4'
, /7X,'PSIA',5X,'PSIA',5X,'PSIA',5X,'PSIA')
3 FORMAT (2X,'PRESSURE P1 CALCULATED CONCENTRATION',
, 2X,/,3X,'PSIA MMOLES/GM PELLET')
10 FORMAT (5X,4F10.4)
11 FORMAT (/5X,'BETA1 BETA2 BETA3 BETA4'/5X,4F10.4)
12 FORMAT (8X,2F10.5)
15 FORMAT (10X,10F10.4)

```

```

25  FORMAT (15X,9F10.4)
    BETA1 = 61.95+ ((TEMP-111.7)/(191.-111.7)*(71.04-61.95))
    BETA2 = 89.16+ ((TEMP-184.6)/(305.4-184.6)*(105.94-89.16))
    BETA3 = 126.24+ ((TEMP-231.1)/(370.-231.1)*(140.2-126.24))
    BETA4 = 159.52+ ((TEMP-272.7)/(425.1-272.7)*(203.58-159.52))
    WRITE (6,1)
    WRITE (6,10)HK1, HK2, HK3, HK4
    WRITE (6,11)BETA1, BETA2, BETA3, BETA4
    WRITE (6,2)
C   ### READ IN EXPERIMENTAL CONCENTRATIONS
    I1 = 1
110  READ (5,*) X1,X2
    WRITE (6,*)X1,X2
    IF (X1.LT.0.0) GO TO 150
    CC1E(I1) = X1
    CC2E(I1) = X2
    I1 = I1+1
    GO TO 110
150  II = I1 -1
    WRITE (6,3)
    DO 111 JJ = 1,II
    SUMCAL = CC1C(JJ) + CC2C(JJ)
    XC1C(JJ)= CC1C(JJ)/SUMCAL
    XC2C(JJ)= CC2C(JJ)/SUMCAL
    SUMEXP = CC1E(JJ) + CC2E(JJ)
    XC1E(JJ) = CC1E(JJ)/SUMEXP
    XC2E(JJ) = CC2E(JJ)/SUMEXP
111  CONTINUE
    WRITE(6,15)(PC1(JK),PC2(JK),CC1E(JK),CC2E(JK)
    &,CC1C(JK),CC2C(JK),XC1E(JK),XC2E(JK),XC1C(JK),XC2C(JK),JK = 1,II)
1000 CONTINUE
    RETURN
    END
C
      SUBROUTINE DOTTED(X,Y,N,KODE)
C -----
C ----- SUBROUTINE TO DRAW DOTTED LINES OF ALL KINDS
C ----- THE ROUTINE IS SIMILAR TO THE CALCOMP ROUTINE DASHLN
C ----- EXCEPT THAT THE NATURE OF THE DOTTING IS SPECIFIED BY
C ----- THE USER IN THE PARAMETER KODE.
C ----- IF THE CODE IS POSITIVE, IT IS RESOLVED INTO ITS DECIMAL
C ----- DIGITS. THESE IN CYCLIC ORDER STARTING FROM THE MOST
C ----- SIGNIFICANT, SPECIFY THE LENGTHS OF THE SEGMENTS IN THE
C ----- LINE. THESE SEGMENTS ARE TRACED WITH THE PEN ALTERNATING
C ----- DOWN AND UP.
C ----- THE DIGITS SPECIFY THE LENGTHS AS FOLLOWS:
C ----- 1-- 0.01 INCH
C ----- 2-- 0.02 INCH
C ----- 3-- 0.03 INCH
C ----- 4-- 0.05 INCH
C ----- 5-- 0.10 INCH
C ----- 6-- 0.15 INCH
C ----- 7-- 0.20 INCH

```

```

C ----- 8-- 0.25 INCH
C ----- 9-- 0.35 INCH
C ----- ZERO DIGITS ARE IGNORED.
C -----
C -----
C -----
C -----
C -----
C -----
C ----- IF KODE IS NEGATIVE OR ZERO, IT SPECIFIES A STANDARD
C ----- LINE TYPE, AS FOLLOWS:
C --- 0 OR A SOLID LINE
C --- -1 OR 4 A DOTTED LINE
C --- -2 OR A DASHED LINE
C --- -3 OR 9424 DASH-DOT LINE
C --- -4 OR 13 CLOSELY SPACED DOTTS
C --- -5 OR 14 SMALL DOTS MODERATE SPACING
C --- -6 OR 55955924 LONG DASH ALTERNATES WITH DASH-DOT-DASH
C --- -7 OR 6424, A DOT-SHORT DASH LINE
C --- -8 OR 64259524 LONG DASH ALTERNATES WITH DOT-DASH-DOT
C --- -9 OR 64 LINE OF SHORT DASHES
C --- -10 OR 248424 DOUBLE DOTS WITH DASHES
C --- -11 OR 24249424 TRIPLE DOTS WITH DASHES.
C --- -12 OR 2 VERY CLOSELY SPACED DOTS, NOT USABLE WITH LIQUID INK
C --- IF KODE IS OUT OF RANGE IT IS REPLACED BY (-1), I.E. A
C --- DOTTED LINE
C --- THE LENGTH SETTING CAN BE ALTERED BY INVOKING THE SUBROUTINE
C --- AT THE ALTERNATE ENTRY POINT SETDOT(CHLTH) WHERE CHLTH IS A
C --- REAL ARRAY OF DIMENSION 9 CONTAINING THE NEW LENGTHS.
C ---
C ---
C ---
C ---
C ---
C ---
C ---
C ---
C -----
C DIMENSION X(1),Y(1)
C DIMENSION CODE(9),SLTH(10),CHLTH(9),LTYPE(12)
C DATA NTYPES/12/
C DATA LTYPE/4,95,9424,13,14,55955424,6424,64259524,
2 64,248424,24249424,2/
C DATA CODE/0.01,0.02,0.03,0.05,0.10,0.15,0.20,0.25,0.35/
C ---
C --- CALCOMP SCALING CONVENTIONS.
C ---
C X0=X(N+1)
C Y0=Y(N+1)
C DELTAX=X(N+2)
C DELTAY=Y(N+2)
C ---
C --- SET INITIAL COORDINATES

```

```

C ----
      XT=(X(1)-X0)/DELTAX
      YT=(Y(1)-Y0)/DELTAY
C ----
C ---- SET N1 TO KODE (IFKODE>0) OR LTYPE(-KODE) (IF KODE<0)
C ---- OR BRANCH TO DRAW A SOLID LINE (IF KODE=0).
C ----
      IF(KODE.EQ.0) GO TO 270
      N1=KODE
      IF(N1.GT.0) GO TO 110
      N1=-N1
      IF(N1.GT.NTYPES) GO TO 100
      N1=LTYPE(N1)
      GO TO 110
100   N1=14
C ----
C ---- FIND THE SEGMENTS IN THE PATTERN
C ----
110   LIM=0
120   IF(N1.LE.0) GO TO 160
      N2=N1/10
      N0=N1-10*N2
      IF(N0.EQ.0) GO TO 140
      LIM=LIM+1
      SLTH(LIM)=CODE(N0)
140   N1=N2
      GO TO 120
160   I=1
      J=LIM
      STEP=SLTH(J)
      DS=0.0
      CALL PLOT(XT,YT,3)
      IUPDN=2
      GO TO 250
C ----
C ---- MAIN LOOP. WILL THE STEP OVERSHOOT THE TARGET?
C ----
220   IF(STEP.GT.DS) GO TO 240
C ----
C ---- IF NO THEN TAKE THE STEP
C ----
      XC=STEP*COSN+XC
      YC=STEP*SINE+YC
      CALL PLOT(XC,YC,IUPDN)
      IUPDN=5-IUPDN
      J=J-1
      IF(J.LE.0) J=LIM
      DS=DS-STEP
      STEP=SLTH(J)
      GO TO 220
C ----
C ---- IF YES THE STEP OVERSHOOTS THE TARGET THEN GO TO TARGET.
C ----

```

XXX

```
240  CALL PLOT(XT,YT,IUPDN)
      STEP=STEP-DS
250  I=I+1
      IF(I.GT.N) GO TO 290
C  ----
C  ---- SET NEW TARGET.
C  ----
      XC=XT
      YC=YT
      XT=(X(I)-X0)/DELTAX
      YT=(Y(I)-Y0)/DELTAY
      DX=XT-XC
      DY=YT-YC
      DS=SQRT(DX*DX+DY*DY)
      IF(DS.EQ.0.0) GO TO 250
      COSN=DX/DS
      SINE=DY/DS
      GO TO 220
270  CALL PLOT(XT,YT,3)
      DO 280 I=2,N
      XT=(X(I)-X0)/DELTAX
      YT=(Y(I)-Y0)/DELTAY
280  CALL PLOT(XT,YT,2)
290  RETURN
      ENTRY SETDOT(CHLTH)
      DO 320 I=1,9
320  CODE(I)=CHLTH(I)
      RETURN
      END
```

```

C
C
C
C
C
C
SUBROUTINE FUNC FOR THE RUTHVEN ISOTHERM MODEL
C
SUBROUTINE FUNC(KK,B,NN,Z,FV)
C
DIMENSION X(50),Y(50),B(10),QNUMR(50),QDNOMR(50),AKP(50),Z(50)
COMMON X,TEMP,BETA
C
DATA VOLC,CF/822.,2.095/
DATA VOLC,CF/776.,2.220/
DO 100 JJ=1,NN
BETA = B(2)
AKP(JJ)=B(1)*X(JJ)
QNUMR(JJ)=AKP(JJ)
M=10.0
FACT=1.0
DO 101 I=2,M
FACT=FACT*(I-1)
TERM=((AKP(JJ))**I*(1-(I*BETA/VOLC))**I/FACT)
QNUMR(JJ)=QNUMR(JJ)+TERM
101 CONTINUE
C
FACTD=1.0
QDNOMR(JJ)= 1+AKP(JJ)
DO 102 I=2,M
FACTD=FACTD*I
TERMD=((AKP(JJ))**I*(1-(I*BETA/VOLC))**I/FACTD)
QDNOMR(JJ)=QDNOMR(JJ)+TERMD
102 CONTINUE
C
DO 100 JJ=1,NN
C
-----
Z(JJ)=QNUMR(JJ)/QDNOMR(JJ)
Z(JJ)=Z(JJ)/CF
C
-----
100 CONTINUE
RETURN
END

```

V I T A

Name : HASSAN BIN ABDUL REHMAN

Family Name : BASHMAIL

Personal Data : Born on January 10, 1962;
Muslim; Indian.

Permanent Address : H. No 21-1-459, Ricab Gunj
Hyderabad 500 002, A.P, India.
Tel. (842) 521 511.

Schools Attended : Crescent High School
Hyderabad (1966 to 1975)

: Agarwal Boys High School
Hyderabad (1975 to 1977)

Colleges Attended : Agarwal Junior College
Hyderabad (1977 to 1979)

: College of Technology
Osmania University (B.Tech)
Hyderabad (1980 to 1984)

: King Fahd University of Petroleum & Minerals
Dhahran (1985 to 1988) (M.S)